SUBMERGED-MEMBRANE DISTILLATION AND CRYSTALLIZATION: SEAWATER REVERSE OSMOSIS BRINE TREATMENT AND RESOURCE RECOVERY

by

YOUNGKWON CHOI

A Thesis submitted in fulfilment for the degree of
Doctor of philosophy

School of Civil and Environmental Engineering
Faculty of Engineering and Information Technology
University of Technology Sydney (UTS)
New South Wales, Australia

December 2018

CERTIFICATION OF ORIGINAL AUTHORSHIP

I certify that the work in this thesis has not previously been submitted for degree nor has it been submitted as part of requirement for a degree except as fully acknowledge within the text.

I also certify that the thesis has been written by me. Any help that I have received in my research work and the preparation of the thesis itself has been acknowledged. In addition, I certify that all information source and literature used are indicated in the thesis.

This research is supported by the Australian Government Research Training Program (RTP).

Signature of Candidate

YOUNGKWON CHOI

Production Note:
Signature removed prior to publication.

ACKNOWLEDGEMENTS

I would like to express my deepest appreciation and gratitude to my supervisor, Prof. Saravanamuthus Vigneswaran, for providing me the opportunities to conduct research in University Technology Sydney. Without his concern and support, this work would not have been completed. I also appreciate to Dr. Gayathri Naidu who gave insightful comments and recommendation for this work.

Furthermore, I would like to offer special thanks to Prof. Sangho Lee and Prof. Eun Namkung. They have motivated me to challenge myself further and mentored me all through my professional and personal life. I am also grateful to my colleagues and friends for friendship, motivation and priceless support; Dr. Mohammed Johir, Yunchul Woo, Seongchul Ryu, Myoungjun Park, Jungeun Kim, Yonghyun Shin, and my great friends (Minsu Koo and Seungwan Yoo).

Last but not the least, my heartfelt appreciation goes out to my family, my father Changsuk Choi, mother Jeongja Park, brother Youngmin Choi, sister-in-law Haeyoung Kang, lovely niece Bom Choi who have been dedicated in believing me during my PhD. Especially, I would like to really appreciate my wife, Yunju Jo. I can entirely focus on my study because of her deepest belief and devoted love to me. I would also extend my gratitude to my daughter, Jiho Choi, for inspiring me and giving me strength to finish my PhD and be the father and husband that she can be proud of. You and Yunju have given me the greatest source of happiness, and you pushed me to do better in both being a PhD candidate and a father. My greatest wish is for you to know what you really want to do in the future and fulfill your dream. As your parents, your mother and I will be with you, beside you, in every step you take.

JOURNAL ARTICLE PUBLISHED OR SUBMITTED

1. ***Y. Choi**, G. Naidu, L.D. Nghiem, S. Lee, S. Vigneswaran, Membrane distillation crystallization for brine mining and zero liquid discharge: opportunities, challenges, and recent progress, Environ. Sci. Water Res. Technol., (**2019**).
2. ****Y. Jo, M.A.H. Johir, **Y. Choi**, G. Naidu, S.A. Rice, D. McDougald, J. Kandasamy, S. Vigneswaran, S. Sun, A comparative study on nitric oxide and hypochlorite as a membrane cleaning agent to minimise biofilm growth in a membrane bioreactor (MBR) process, Biochemical Engineering Journal, 148 (**2019**) 9-15.
3. ***Y. Choi**, G. Naidu, S. Lee and S. Vigneswaran, Effect of inorganic and organic compounds on the performance of fractional-submerged membrane distillation-crystallizer, Journal of Membrane Science, 582 (**2019**) 9-19.
4. ***Y. Choi**, S. Ryu, G. Naidu, S. Lee and S. Vigneswaran, Integrated submerged membrane distillation-adsorption system for rubidium recovery, Separation and Purification Technology, 218 (**2019**) 146-155.
5. ****G. Naidu, S. Ryu, R. Thiruvenkatachari, **Y. Choi**, S. Jeong and S. Vigneswaran, A critical review on remediation, reuse, and resource recovery from acid mine drainage, Environmental Pollution, 247 (**2019**) 1110-1124.
6. ****S. Ryu, G. Naidu, M.A. Hasan Johir, **Y. Choi**, S. Jeong, S. Vigneswaran, Acid mine drainage treatment by integrated submerged membrane distillation–sorption system, Chemosphere, 218 (**2019**) 955-965.
7. ***Y. Choi**, G. Naidu, S. Jeong, S. Lee, S. Vigneswaran, Fractional-submerged membrane distillation crystallizer (F-SMDC) for treatment of high salinity solution, Desalination, (**2018**).
8. ****G. Naidu, S. Jeong, **Y. Choi**, M.H. Song, U. Oyunchuluun, S. Vigneswaran, Valuable rubidium extraction from potassium reduced seawater brine, Journal of Cleaner Production, 174 (**2018**) 1079-1088.
9. ***Y. Choi**, G. Naidu, S. Jeong, S. Lee, S. Vigneswaran, Effect of chemical and physical factors on the crystallization of calcium sulfate in seawater reverse osmosis brine, Desalination, 426 (**2018**) 78-87.
10. ***Y. Choi**, G. Naidu, S. Jeong, S. Vigneswaran, S. Lee, R. Wang, A.G. Fane, Experimental comparison of submerged membrane distillation configurations for concentrated brine treatment, Desalination, 420 (**2017**) 54-62.

11. **G. Naidu, S. Jeong, **Y. Choi**, S. Vigneswaran, Membrane distillation for wastewater reverse osmosis concentrate treatment with water reuse potential, Journal of Membrane Science, 524 (**2017**) 565-575.
12. **G. Naidu, W.G. Shim, S. Jeong, **Y. Choi**, N. Ghaffour, S. Vigneswaran, Transport phenomena and fouling in vacuum enhanced direct contact membrane distillation: Experimental and modelling, Separation and Purification Technology, 172 (**2017**) 285-295.
13. ****Y. Choi**, S. Vigneswaran, S. Lee, Evaluation of fouling potential and power density in pressure retarded osmosis (PRO) by fouling index, Desalination, 389 (**2016**) 215-223.

*** Articles related to the Thesis**. ** Publications made during the PhD candidature including articles not entirely related to the Thesis.

CONFERENCE PAPERS AND PRESENTATIONS

1. ***Y. Choi**, G. Naidu, S. Lee, S. Vigneswaran, Fractional-submerged membrane distillation crystallizer (F-SMDC) for treatment of high salinity solution, 8th International Water Association (IWA) Membrane Technology Conference (IWA-MTC 2017), 5-8 September 2017, Oral Presentation.
2. ***Y. Choi**, G. Naidu, S. Lee, S. Vigneswaran, Fractional-membrane distillation integrated with crystallization (F-MDC) for reverse osmosis concentrate treatment and resource recovery, International Desalination Workshop 2017 (IDW 2017), 22-25 November 2017, Oral Presentation.
3. ***Y. Choi**, G. Naidu, Lee, S. Vigneswaran, Experimental comparison of submerged membrane distillation configurations for concentrated brine treatment, 2017 International Congress on Membrane and Membrane Processes, 29 July-4 August 2017, Poster Presentation.

Presentation made during the PhD candidature including proceedings, oral and poster presentations.

LIST OF ABBREVIATIONS

AGMD	Air gap membrane distillation
CG	Concentration gradient
CG ratio	Concentration gradient ratio (C_{Bottom}/C_{Top})
CI	Concentration increase (C_t/C_0)
CP	Concentration polarization
Cr	Crystallizer
CSD	Crystal size distribution
DCMD	Direct contact membrane distillation
DI	Deionized
DiPA	Diisopropylamine
DOC	Dissolved organic carbon
F-SMDC	Fractional-submerged membrane distillation crystallizer
GOR	Gain output ratio
HF	Hollow fiber
HOC	Hydrophobic organic compound
IP	Ionic production
KCuFC	Potassium copper hexacyanoferrate
LEP	Liquid entry pressure
LMW	Low molecular weight
MC	Membrane contactor
MD	Membrane distillation
MDC	Membrane distillation crystallization
MSF	Multi-stage flash
NF	Nanofiltration
OD	Osmotic membrane distillation
PAN	Polyacrylonitrile
PVDF	Polyvinylidene fluoride

PW	Produced water
R	Recovery ratio
RC	Reaction crystallization
RO	Reverse osmosis
SGMD	Sweep gas membrane distillation
SGPW	Shale gas produced water
SWRO	Seawater reverse osmosis
S-DCMD	Submerged-direct contact membrane distillation
S-MD	Submerged-membrane distillation
S-VMD	Submerged-vacuum membrane distillation
S-VDCMD	Submerged-vacuum enhanced direct contact membrane distillation
TG	Temperature gradient
TOC	Total organic carbon
TP	Temperature polarization
VCF	Volume concentration factor
VDCMD	Vacuum enhanced direct contact membrane distillation
VMD	Vacuum membrane distillation
VMDC	Vacuum membrane distillation crystallization
ZLD	Zero liquid discharge

LIST OF SYMBOLS

C	Concentration	
C_{Bottom}	Concentration at the bottom portion in F-SMDC	
C_f	Concentration at feed solution side	
C_{fm}	Concentration on membrane surface in feed side	
C_p	Concentration in permeate stream	
C_t	Concentration at specific time	
C_{Top}	Concentration at the top portion in F-SMDC	
C_0	Initial concentration	
J	Flux	$L/m^2 \cdot h$
J_t	Flux at specific time	$L/m^2 \cdot h$
J_0	Initial flux	$L/m^2 \cdot h$
K_{sp}	Solubility product constant	
m	Mass	mg
m_t	Mass at specific time	mg
m_0	Initial mass	mg
t	Time	
T	Temperature	°C
T_c	Temperature of coolant in condenser	°C
T_f	Temperature of feed solution	°C
T_{fm}	Temperature on membrane surface in feed side	°C
T_p	Temperature of permeate	°C
T_{pm}	Temperature on membrane surface in permeate side	°C
P_f	Hydraulic pressure of feed solution	bar
P_p	Hydraulic pressure of permeate	bar
Re	Reynolds number	
Q	Volumetric flow rate	m^3/s

v	Flow rate	m/s
v_p	Flow rate of permeate stream	m/s
$V_{Reactor}$	Volume of reactor	ml
$V_{Total,permeate}$	Total amount of permeate produced	ml
ΔP	Vapor pressure gradient	bar
Δt	Time difference	
ΔT	Temperature difference	°C

TABLE OF CONTENTS

LIST OF FIGURES

LIST OF TABLES

ABSTRACT

Seawater reverse osmosis (SWRO) brine management is an important component in sustainable desalination. Improving additional water production from brine with resource recovery can substantially enhance the overall efficiency of desalination process. SWRO plants generate a large amount of concentrated brine as the recovery rate from RO is still limited to 30-50%. Recently, membrane distillation (MD) has emerged as one of the alternative technologies for systematic reduction of the amount of brine as it leads to the additional production of high-quality water. MD process is driven by vapor pressure between high temperature feed solution and low temperature permeate stream. The vapor evaporated from the feed solution to permeate stream is transported through a porous hydrophobic membrane. MD can lead to the treatment of high concentration and zero liquid discharge (ZLD) as there is no hydraulic pressure restriction in MD. Other aspect of MD is the concentration of the feed solution, resulting to a supersaturation condition of salt present in SWRO brine. It enhances the potential of resource recovery in crystal form. MD can thus be combined with a crystallization technique known as membrane distillation-crystallization (MDC). In MDC process, there are two streams produced: the high-quality water and crystals as resource. MD concentrates the feed solution continuously via the production of clean water from feed solution. This makes a favorable condition for forming crystals. Also, the extraction of salt by crystallization from feed solution mitigates the adverse influence of high concentration on mass transfer in MD.

This research focused on the investigation of hybrid systems with submerged-membrane distillation (S-MD) for resource recovery and producing additional water recovery from SWRO brine. In this study, S-MD was coupled with other technologies such as crystallization and adsorption technologies to achieve resource recovery and volume minimization of SWRO brine.

A new concept of MDC named in this study as fractional-submerged membrane distillation crystallizer (F-SMDC) was investigated to improve the water recovery and resource recovery simultaneously.

Performance of S-MD with different configuration in treatment of SWRO brine

S-MD offers an additional advantage of a compact system compared to cross-flow MD. The performances of three different S-MD configurations were evaluated in this study, namely; submerged direct contact membrane distillation (S-DCMD), submerged vacuum direct contact membrane distillation (S-VDCMD) and submerged vacuum membrane distillation (S-VMD) for SWRO brine treatment. A 13-77% higher water flux was obtained by S-MDs with incorporation of vacuum (S-VMD and S-VDCMD) compared to S-DCMD due to higher driving force. Evaluation on the influence of feed concentration and permeate temperature revealed that S-MD with high vacuum was significantly affected by feed concentration. Meanwhile S-DCMD was severely affected by feed temperature losses, due to the membrane pore crystallization formation. Moreover, the crystallization on the membrane surface was influenced by the presence of vacuum pressure. A repeated cycle of S-DCMD with membrane air-backwashing was effective for flux recovery and to reduce membrane crystallization. This enabling to concentrate SWRO brine by 2.8 times of volume concentration factor (VCF).

Integrated SMD-adsorption system to recover the rubidium (Rb) and clean water

An integrated SMD with adsorption using granular potassium copper hexacyanoferrate (KCuFC) as adsorbent was evaluated for improving water recovery from brine while extracting valuable Rb. KCuFC showed good capacity for Rb extraction. The thermal S-MD process (55 °C) with a continuous supply of Rb-rich SWRO brine enabled Rb to be concentrated (99%

rejection) while producing additional fresh water. The thermal condition with concentrated Rb helped to improve the performance of granular KCuFC in Rb extraction. An optimum dose (0.24 g/L) KCuFC was identified based on 98% Rb adsorption (9.78 mg as Rb) from RbCl solution without a continuous supply of feed. The integrated submerged MD-adsorption system was able to achieve more than 85% water recovery and Rb extraction in continuous feed supply with two repeated cycles. The presence of Ca in SWRO brine resulted in $CaSO_4$ crystallization deposition onto the membrane and on the surface of the granular KCuFC submerged in the feed reactor. This led to a reduced recovery rate and Rb adsorption. Significantly better MD water recovery was obtained upon removal of Ca in SWRO brine while achieving a total of 6.65 mg of Rb extraction. A comparative study conducted on the performance of different KCuFC forms (granular, particle and powder) showed that the particle form of KCuFC exhibited 10–47% higher capacity in terms of Rb adsorption.

Resource recovery from high salinity solution using F-SMDC

MDC is an attractive process for high saline SWRO brine treatment. MDC produces additional fresh water while simultaneously recovering valuable resources. In this study, a novel approach of fractional-submerged MDC (F-SMDC) process was developed and tested. In this system, MD and crystallizer are integrated in a feed tank with a submerged membrane. F-SMDC principle is based on the presence of concentration/temperature gradient (CG/TG) in the feed reactor. The conditions provided at the top portion of the feed reactor (higher temperature and lower feed concentration) was well suited for MD operation, while the bottom portion of the reactor (lower temperature and higher concentration) was favorable for crystal growth. F-SMDC performance with direct contact MD to treat brine and produce sodium sulfate (Na_2SO_4) crystals showed positive results. The presence of CG/TG in F-SMDC enabled to achieve higher

water recovery for brine treatment with a VCF of over 3.5 compared to VCF of 2.9 with a conventional S-MDC set-up. Further, the high feed concentration and low temperature at the reactor bottom in F-SMDC enabled the formation of Na_2SO_4 crystals with narrow crystal size distribution.

Moreover, the reactor of F-SMDC contained the submerged hollow-fiber membrane. This enables water and salt recovery to occur simultaneously in a single reactor. The influence of inorganic and organic compounds present in brine solutions on the development and stability of CG/TG in F-SMDC was evaluated in detail. The results showed that properties of inorganic compounds (such as molecular weight and electronegativity) played a significant role in influencing CG/TG in F-SMDC. A high CG ratio (between 1.51 to 1.83 after crystallization) was observed when using feed solutions with inorganic compounds such as KCl, $MgSO_4$, and Na_2SO_4. However, only low CG ratio (between 0.94 to 1.46) was achieved in feed solutions containing lower molecular weight compounds, NH_4Cl and NaCl. High CG ratio with KCl resulted in the occurrence of salt crystallization at a faster rate (from VCF 2.4 onwards) compared to the predicted theoretical salt saturation point of VCF 3.0. On the other hand, Na_2SO_4 showed lower flux decline (12.56 % flux decline) compared to $MgSO_4$ (55.93 % flux decline). This is due to lower cation electronegativity of Na^+. The presence of CG in F-SMDC by concentrated inorganic compounds also enhanced organic compounds to gravitate downwards to the bottom of the reactor, potentially mitigating organic deposition on the membrane.

F-SMDC was used to recover Na_2SO_4 from simulated SWRO brine. CG and TG in the reactor enhanced the water recovery by MD and Na_2SO_4 crystallization by crystallizer. The crystals were not obtained at the bottom portion of F-SMDC due to deposition of calcium sulfate ($CaSO_4$) on the membrane surface and negative influence of low temperature-sensitivity

solubility slat such as NaCl. In order to obtain the higher degree of supersaturation of Na_2SO_4, sulfate-rich condition was created by adding salts such as Na_2SO_4, $MgSO_4$ and $(NH_4)_2SO_4$. In the case of addition of Na_2SO_4 and $MgSO_4$, the concentration increase at the top portion was observed, resulting in low CG ratio (around 1.7). On the other hand, the addition of $(NH_4)_2SO_4$ achieved faster Na_2SO_4 crystallization (VCF 1.42) at the bottom portion with higher CG ratio of over 2.0. Total water recovery ratio of 72 % and 223.73 g Na_2SO_4 crystals was achieved in the laboratory-scale F-SMDC unit used while treating simulated SWRO brine.

Tendency of $CaSO_4$ crystallization in high salinity solution

Discharge of brine back into the sea through submarine pipelines affects the marine ecosystem. MDC can produce additional amount of clean water with valuable resources recovery from the concentrated brine. The SWRO brine contains salts, which contributes to scaling development during the MDC operation. Hence, this research also investigated the crystallization tendency of calcium sulfate ($CaSO_4$) under high salinity and examined the effects of other inorganic and organic compounds in forming $CaSO_4$ crystallization. The crystallization tendency of $CaSO_4$ in SWRO brine was examined at different conditions such as: temperatures; changes in pH values; and in the presence of co-existing ions such as chemical agents, and organic matters. The results showed that the size and quantity of crystals formed increased with the increase in temperature. Furthermore, an increase in the pH values (from 5 to 9) increased the crystal size. At higher pH, the complexion of NaCl along with $CaSO_4$ was observed.

CHAPTER 1

INTRODUCTION

1.1. Introduction

Nowadays, the lack of the potable and fresh water is a serious challenge which threatens human life worldwide. Desalinated water is one of the solutions to obtain potable water. There are two main desalination technologies: membrane-based process, such as reverse osmosis (RO), and thermal-based process, such as multi-stage flash distillation (MSF) desalination. The seawater reverse osmosis (SWRO) technology is widely used because of its low-energy requirement compared to conventional thermal desalination (evaporation) technology (Choi et al. 2017; Quist-Jensen, Macedonio, et al. 2016). The SWRO process produces two streams: freshwater and wastewater (called brine, retentate, or concentrate (hereafter referred to as SWRO brine). Conventional treatment/disposal methods for SWRO brine pose environmental and ecological issues because of the large amount of wastewater produced by low water recovery capacity of SWRO (30 – 50 %) (Choi et al. 2016; Ji et al. 2010; Naidu et al. 2018; Naidu, Jeong, Choi, et al. 2017; Roberts et al. 2010; Voutchkov 2011; Younos 2005). The brine from SWRO plant is commonly discarded back to the sea or is treated by using conventional treatment methods. Its discharge and treatment methods are determined depending on the geographical position of SWRO plant. In coastal desalination plants, the brine is mostly discharged directly to the sea, which could adversely affect the marine ecosystem. In inland RO plant, the brine is treated or disposed by conventional methods, such as discharging into wastewater plant, deep well injection, and evaporation ponds. However, these lead to additional cost and hazardous potentials on microorganisms in wastewater plants and contamination of ground water.

In reality, the salt concentration of wastewater stream from SWRO is not exactly high, it is merely within the range of 1.4 - 2.0 times compared to seawater; however, the toxicity of chemicals (which are used during the operation of SWRO) and huge amount of wastes adversely affect the eco-system (Gryta 2002; Voutchkov 2011). Chemicals used in pre-

treatment of SWRO plant, such as coagulation and filtration, cause serious problems in brine treatment because wastewater generated by a RO plant is commonly discharged together with brine. To control these problems caused by conventional brine treatment methods, further concentration of brine and valuable resource recovery with a suitable post-treatment would be necessary because the chemical is present affect the performance of post-treatment of brine. Furthermore, the scaling issue caused by calcium sulfate ($CaSO_4$) in SWRO brine treatment limits the process efficiency of both processes. Formation of $CaSO_4$ crystallization causes performance degradation in SWRO brine treatment because of its low solubility. It leads to an additional removal step and, thus, low brine recovery.

Membrane Distillation: In this context, membrane distillation (MD) process has received attention as a promising technology for treatment of SWRO brine because of its reliability. MD is a mechanically and thermally driven desalination process which is operated by vapor pressure difference between feed solution at high temperature and permeate solution at low temperature flowing across a microporous hydrophobic membrane. MD is a promising technology for treating SWRO brine since it increases SWRO recovery ratio (producing additional high quality water) while systemically reduces brine volume, potentially achieving near zero liquid discharge in desalination plants (Gryta 2016). Thus, the effect of solution concentration (hydraulic pressure restriction) on permeate flux is less compared to other pressure-driven membrane processes, such as RO and nanofiltration (NF) (Curcio & Drioli 2005; Edwie & Chung 2012). In addition, MD offers more advantages compared to other desalination processes including high rejection of non-volatile components, lower operational pressure (compared to RO), lower operating temperature and smaller footprints (compared to thermal evaporation desalination process) (Lawson & Lloyd 1997; Naidu, Jeong, Choi, et al.

2017; Naidu, Shim, et al. 2017). This is because the mass (vapor) transfer in MD occurs through the membrane as a function of the difference of vapor pressure between the hot feed solution stream and cold permeate stream (Chen et al. 2014; Edwie & Chung 2013; Gryta 2002). Hence, MD has a higher capacity in the treatment of high concentration feed solution with high rejection ratio (over 99 %) for non-volatile components (Naidu, Shim, et al. 2017; Quist-Jensen, Sørensen, et al. 2017).

Despite its advantages, there are several drawbacks such as polarization phenomena (concentration and temperature polarization), scaling, and high energy consumption for temperature control in both solution (feed and permeate stream) which lead to the decrease in process performance of MD (Bouchrit et al. 2015). The high energy consumption in MD is a major issue which presents its application in desalination. The bulk feed solution temperature reduces as the feed solution is channeled into the membrane module. The heat loss in MD accelerates at higher feed flow rate requiring rapid reheating to maintain a constant feed solution temperature (Cath et al. 2004; Li & Sirkar 2017). In this context, MD in submerged module (S-MD) can be used to mitigate the energy consumption caused by heat loss in feed solution circulation. S-MD eliminates the need for feed recirculation, resulting in minimal heat loss (Julian et al. 2016). Additionally, S-MD configuration can make the MD process more compact because the reactor plays a dual role of membrane reactor and feed tank. It leads to process simplification and better operational efficiency in terms of improvement of brine recovery.

SMD-adsorption system in resource recovery: There is a high potential of valuable resource recovery from SWRO brine as it contains many valuable resources at high concentration. Brine treatment with valuable resources recovery leads to new economic resources which is

otherwise considered as waste. Furthermore, water reuse is considered as an economical and environmental-friendly solution along with desalination, resulting in zero liquid discharge (ZLD) and zero discharge (ZD) (Kim, Kim, et al. 2017; Liu et al. 2012; Pérez-González et al. 2012; Tong & Elimelech 2016). In the concept of ZLD and ZD, SWRO brine disposal is reduced, and the water production is enhanced by production of only two streams: fresh water and valuable mineral resource (Quist-Jensen, Macedonio, et al. 2016). In this context, an integrated SMD with adsorption system and membrane distillation crystallization (MDC) process have received attention as promising technologies in the treatment of SWRO brine.

Simultaneous brine treatment (clean water recovery) with extraction of valuable resources offsets the treatment costs compared to the conventional treatment methods. The operational advantage and conditions of S-MD can offer the valuable resource recovery with additional technologies such as adsorption and crystallization. Extraction of valuable resource by adsorption is effective because of its selectivity and reusability. Economically-valuable metals, such as lithium (Li), cesium (Cs), rubidium (Rb), and other heavy metals are present in the SWRO brine. The recovery of valuable Rb from SWRO brine can lead to the economic benefits, potentially offsetting brine treatment cost because of the substantially high economic price of Rb. However, the concentration of (Rb) in SWRO brine is low (0.11 – 0.30 ppm), and not economical to be removed by adsorption (Bolter et al. 1964; Jeppesen et al. 2009; Naidu, Jeong, Johir, et al. 2017). The maintenance of relatively high concentration of Rb in the solution may achieve stable adsorption capacity of adsorption. It can be obtained by combining of MD and adsorption, as well as improving brine recovery simultaneously. In MD, Rb in the solution can be concentrated by recovering additional clean water from the feed solution, resulting in a mitigation of Rb concentration reduction. In addition, the thermal condition (high temperature) of feed solution in MD leads to high adsorption capacity. The operating conditions of S-MD further offer favorable conditions to enhance the adsorption of Rb.

Membrane Distillation-crystallization: Crystallization is one of the liquid-solid separation and purification technique, which is widely used in the chemical, pharmaceutical and food industries (Chabanon et al. 2016; Kim, Kim, et al. 2017). It is based on the control of solubility, in which a pure solid crystal is extracted from the liquid (Lu et al. 2017). For continuous crystallization, the maintenance of supersaturated condition is essential, especially for solutions with low concentration of ions (Adler et al. 2000; Chabanon et al. 2016). The combination of both MD and crystallizer can offer favorable conditions for extraction of salt crystals from the feed solution.

Membrane distillation crystallization (MDC) process which is the combination of MD and crystallization processes is one of the promising potential technologies for simultaneous recovery of clean water and crystals form SWRO brine (Edwie & Chung 2013; Julian et al. 2016; Macedonio & Drioli 2010; Meng, Ye, et al. 2015; Tun et al. 2005). It take into the advantages of both processes simultaneously from high salinity solutions: high quality fresh water and extracting valuable resources (Julian et al. 2016). MDC controls saturation rate well, and lead to a faster nucleation rate and reduction of induction time compared to traditional crystallization processes (Quist-Jensen, Macedonio, et al. 2017). Moreover, the ability to concentrate solution up to a supersaturation with minimal flux decline is an additional advantage of MDC (Ali et al. 2013; Alkhudhiri et al. 2012; Naidu, Shim, et al. 2017). These advantages offer the potential of continuous crystallization in SWRO brine. Currently, cooling crystallization technique is widely used in MDC due to its ease of control (Lu et al. 2017). A typical MD crystallizer system is a continuous in-line set-up (Curcio et al. 2001; Curcio, Ji, Quazi, et al. 2010). However, one of the major limitations is the significant energy consumption due to re-heating and re-cooling of each process in same line. This results in a degradation of

total process efficiency (Chen et al. 2014; Edwie & Chung 2013; Kim, Kim, et al. 2017; Kim et al. 2016). Additionally, in an in-line circulation of feed solution, the short contact time of the feed solution in the crystallizer and direct contact of the supersaturated feed solution with the membrane is inevitable, resulting in deposition of crystals on the membrane surface. This makes the process impractical to achieve high water recovery.

Fractional-submerged membrane distillation crystallizer: In this regard, one should work on a process which can mitigate these limitations in conventional in-line MDC. Fractional submerged MDC (F-SMDC) concept should thus be investigated. F-SMDC is based on the principle of formation of feed concentration gradient (CG) and feed temperature gradient (TG) in a single reactor with submerged-MD. The single reactor helps to mitigate the energy losses through circulation and the short contact time (Choi et al.). Moreover, CG and TG in the feed reactor influence both MD and crystallization positively. Maintenance of lower feed concentration and high temperature at the top portion of the reactor, where the submerged membrane is located, is suitable for MD operation. Simultaneously, at the bottom portion of the reactor, high feed concentration with low feed temperature enhances crystallization. During F-SMDC operation, this leads to the formation of a high saturation state leading to continuous crystal formation at the bottom portion with minimized flux decline. This setting potentially promises higher water recovery with reduced crystal deposition issues on the membrane surface. Furthermore, the continuous formation of crystal at the bottom is expected to reduce the salt content in feed solution with continuous extraction of clean water (Julian et al. 2016).

1.2. Objective and motivation of this research

The conventional treatment methods currently used such as direct discharge into seawater, discharge into wastewater treatment plant, evaporation pond, and deep well injection lead to negative effects on eco-system as well as process limitations. Therefore, the MD and MDC processes are being researched as alternative processes for SWRO brine treatment because of their high performance in treating high concentration solutions and potential simultaneous recovery of water and valuable resources from SWRO brine. MDC process can achieve near zero discharge from desalination process due to simultaneous production of clean water and valuable resources as crystals. However, high energy consumption in the conventional MDC process using cooling crystallization technique remains an issue because of requirement of re-heating and re-cooling. Hence, detailed investigation is required on MDC and MD-adsorption hybrid systems to effectively manage SWRO brine. In this context, this thesis presents the innovative finding of treatment of SWRO brine using MD-based processes, such as S-MD and MDC. This research focused on three major areas.

First, the performance of S-MD process for SWRO brine treatment and valuable resource recovery was evaluated. Experimental and practical applications of S-MD technologies for treatment of SWRO brine were examined. The aims of the S-MD study were (a) to observe tendency of scaling on the membrane, (b) to find optimal configuration type for treating high concentration solutions and suitable configuration for new MDC approach, and (c) to examine the effectiveness of membrane cleaning for scaling and polarization effect mitigation. For these purposes, submerged vacuum membrane distillation (S-VMD), submerged direct contact membrane distillation (S-DCMD) and submerged vacuum direct contact membrane distillation (S-VDCMD) were operated with synthetic concentrated brines of varying concentrations as feed solutions. Additionally, the integrated submerged MD with adsorption process was

evaluated for recovering Rb from SWRO brine.

Secondly, the fractional-submerged membrane distillation crystallizer (F-SMDC), which is the new approach of membrane distillation crystallizer (MDC) process was investigated to develop a process with lower heat energy consumption, and it was optimized for concentrated brine treatment and resource recovery. The main goals of the study were (a) to investigate feasibility of MDC for brine treatment, (b) to optimise the MDC process in terms of stability and energy efficiency, and (c) maximizing resource recovery and additional clean water production. In F-SMDC, submerged hollow-fiber membrane module was used as DCMD. The reactor played three roles: feed tank, reactor of submerged membrane, and a combined feed tank and reactor in F-SMDC process, which leads to a more compact process, and has a better performance than conventional MDC process because of the advantages posed by both S-MD and crystallization process.

Thirdly, detailed analysis was carried out on the tendency of crystallization of calcium sulfate ($CaSO_4$) in the SWRO brine at different physical and chemical conditions such as temperature, pH and presence of inorganic and organic compounds. The exact understanding of $CaSO_4$ crystallization in SWRO brine treatment using MD and MDC is important for stable and better performance because of high potential of $CaSO_4$ crystallization as a scalant.

1.3. Structure of the study

This study is composed of ten chapters. Six chapters (from chapter 4 to 9) highlights the main findings of the studies. A brief explanation of each chapter is presented below:

- Chapter 1 (Introduction)

  The research background and main objectives are presented. The topics such as treatment of seawater reverse osmosis (SWRO) brine using membrane distillation (MD) and membrane distillation and crystallization (MDC) process are introduced. This chapter also shows the novelty and the relevance of this thesis.

- Chapter 2 (Literature review)

  The current research situation and the underlying issues of the MDC process is discussed, along with theoretical background on MD and crystallization processes. The specific information on MD, crystallization, by-product recovery using MDC, scaling and fouling control is discussed.

- Chaper 3 (Materials and methods)

  The materials and methods in this research are provided in detail.

Chapter 4 to 9 presents the experimental results with detailed discussion. Chapters 4 and 5 discuss on the MD-based processes and their application in SWRO brine treatment and resource recovery from SWRO brine.

- Chapter 4: Different configurations of submerged-MD were compared experimentally in treatment of SWRO brine. Furthermore, air-back washing method was evaluated for mitigation of inorganic compounds fouling in submerged-MD.

- Chapter 5: Integrated submerged MD-adsorption system was evaluated for simultaneous recovery of clean water and rubidium.

Chapters 6 to 8, highlights the new approach for MDC for treating a hypersaline solution. Its feasibility in recovering of resources from SWRO brine was also examined.

- Chapter 6: A new approach of MDC process, terms in study as fractional-submerged membrane distillation crystallizer (F-SMDC) was been investigated for high salinity solution treatment.

- Chapter 7: The effect of inorganic and organic compounds present in SWRO brine on F-SMDC was examined.

- Chapter 8: The feasibility of recovering Na_2SO_4 from SWRO brine was examined by creating a sulfate-rich condition in the reactor of F-SMDC.

The performance degradation of S-MD and F-SMDC processes by calcium sulfate ($CaSO_4$) crystallization was compared. For better understanding of scaling phenomenon during SWRO treatment, a research on $CaSO_4$ crystallization was conducted. It is presented in Chapter 9.

- Chapter 9: The tendency of $CaSO_4$ crystallization in treatment of SWRO brine is examined in various chemical and physical situations.

Chapter 10 summarizes all the key findings and important takeaways from the experimental and analysical results. Further consideration and ideas for future research in treatment of SWRO brine are also presented in Chapter 10.

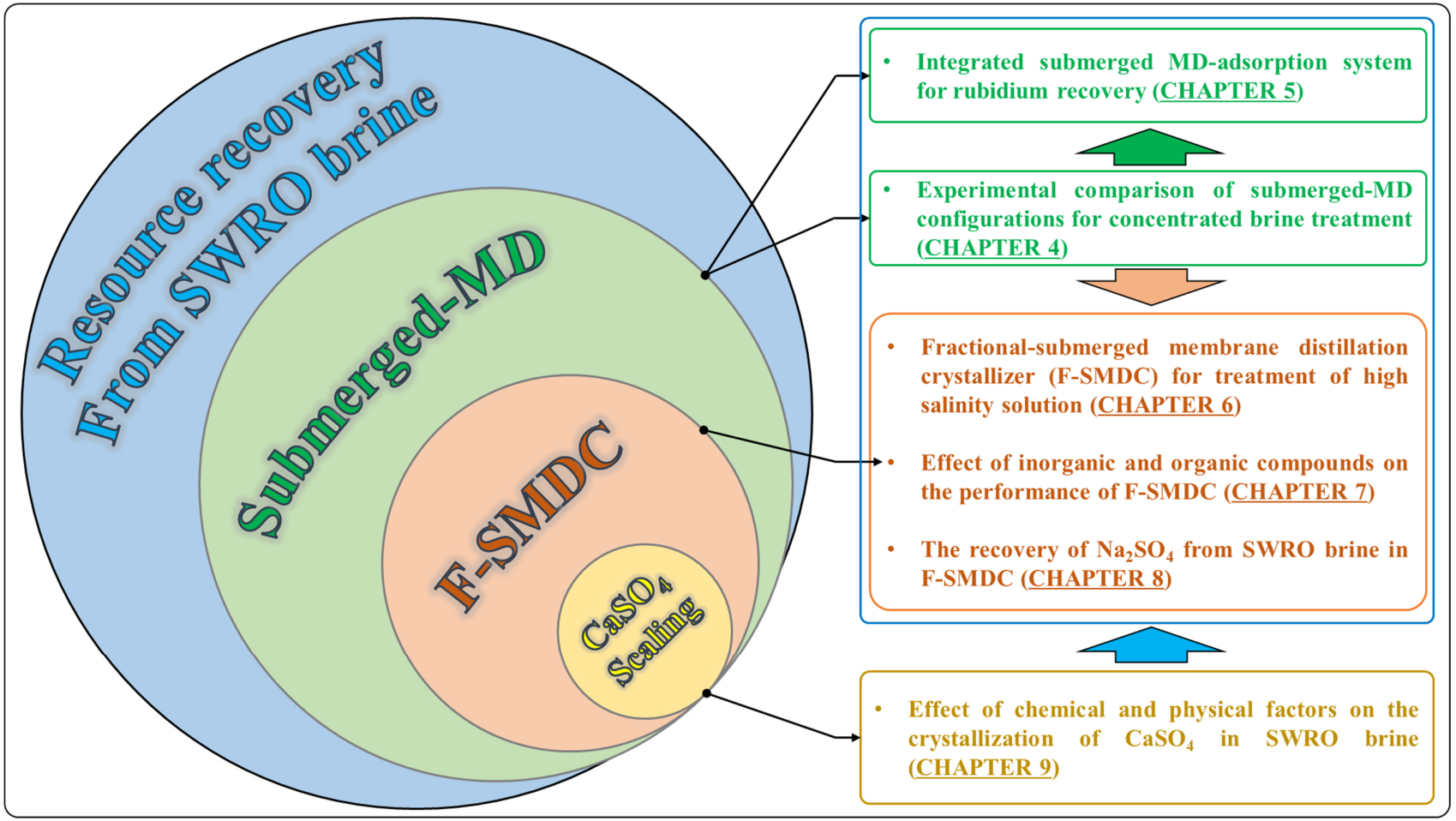

Figure 1-1. Structure of this study.

CHAPTER 2

LITERATURE REVIEW

2.1. Introduction

Fresh water shortage and the depletion of finite minerals are some of the most vexing issues of our time, especially with recent rapid improvement in economic development worldwide and thus demand for these resources (Quist-Jensen, Ali, et al. 2016). Membrane technology plays a major role in addressing the above issues. Specific additional treatments are required for improving water recovery strategies, operational costs, quality of water produced and overcoming the impact of brine (i.e. concentrate) and how much of it is disposed into the eco-system (Drioli et al. 2006). Brine from seawater reverse osmosis (SWRO) plants and wastewater streams from oil, shale gas and coal seam gas production plants are some examples of challenging water treatment and discharge scenarios. These methods consist of high concentrations of various inorganic, organic and toxic components which can seriously endanger human and environmental health.

For this reason, it is essential to find and implement the best treatment and disposal methods (Ali et al. 2017; Ali et al. 2015; Creusen et al. 2013; Drioli et al. 2012; Kim, Kwon, et al. 2017). For example, in SWRO process the water recovery factor ranges from 30 to 50% in seawater reverse osmosis plants, resulting in the generation of a huge amount of concentrate (brine) (Guan et al. 2012; Ji et al. 2010). This is one of the biggest challenges in SWRO desalination process. The extraction of oil and shale gas using hydraulic fracturing generates a volume of wastewater often known as produced water (PW). The major components of produced water are the high concentration of inorganic salt, organic compounds, heavy metal, oil, grease and production chemical compounds (Fakhru'l-Razi et al. 2009; Kim, Kwon, et al. 2017). The volume of produced water stream is nearby 70% of the total wastewater stream generated, and this amount is several times larger than the volume of recovered oil or gas (Çakmakce et al.

2008).

Membrane distillation (MD) is a promising option to treat brine and produced water (Ali et al. 2017; Bouchrit et al. 2015; Bush et al. 2016; Choi et al. 2017; Edwie & Chung 2012; Gryta 2016; Kim, Kwon, et al. 2017; Li & Sirkar 2005; Meng, Hsu, et al. 2015). In the pressure-driven membrane process, the high concentration (high salt (inorganic) content in the solution) suppresses the mass transfer (i.e. driven force of water flux) across the membrane. In the MD process, however, the effect of concentration on the mass transfer is not important because the driving force of MD is induced by vapor pressure difference between the hot feed stream and cold permeate stream. Thus, it is sufficient to have a lower operating pressure. Moreover, the nonvolatile solution can be completely rejected because only vapor is transferred throughout the hydrophobic membrane, resulting in high quality/purity permeate water being produced (Choi et al. 2017; Creusen et al. 2013; Lawson & Lloyd 1997). As a result, MD has much potential for the treatment of high concentration solution.

Crystallization technology presents a good option for the treatment of high concentration and complex solutions, i.e. challenging solutions. Basically, the main idea behind crystallization technology is to control the saturation level utilizing specific methods such as reduced temperature and the removal of solvent. The crystallization process is a basic unit-operation for separation and purification of chemical matter in the aqueous solution, and in fact, one of the most effective and powerful ways to product valuable crystal from the parent solution. This is a solid-fluid separation process in which crystals are formed from the parent solution, and it has been employed in many industries such as the chemical, petrochemical, pharmaceutical and food sectors. The reason why this is the case is that crystallization enjoys a wide-ranging applicability (Jiang et al. 2016; Zuoliang et al. 2013). More than 70% of pharmaceutical and

chemical production processes involve crystallization (Hash & Okorafor 2008). In particular, the batch cooling crystallization process is a widely used method for recovering valuable resources in the pharmaceutical industry (Abu Bakar et al. 2009; Holaň et al. 2015). The crystallization technology has certain advantages such as high recovery ratio of resources and the recovery of high quality water (Lu et al. 2017). Although crystallization is widely used for purification and separation, the design and operation of crystallizer still face many limitations (Curcio & Drioli 2005; Drioli et al. 2012). These include, for example, poor reproducibility in final crystals characteristics, limited supersaturation control and less ability to modulate the supersaturation generation rate.

Membrane distillation crystallization (MDC) process has the potential to solve the above issues. MD employed in the MDC process can remove/produce a solvent from an aqueous solution consisting of inorganic solute, resulting in supersaturation. Consequently, the recovery of fresh water and valuable resources can be obtained at the same time. Due to the operational properties of both MD and crystallization, the integration/combination of MD with the crystallization process (MD) has high potential for the treatment of high salinity solution without additional post-treatment (Guan et al. 2012). The MDC will result in enhanced water recovery ratio, a reduced brine disposal problem, faster crystallization rate and curtailment of crystals' induction time (Macedonio et al. 2007; Quist-Jensen, Macedonio, et al. 2017). MDC has been successfully applied for the recovery of fresh water and valuable resources from challenging solutions (Ali et al. 2015; Çakmakce et al. 2008; Chen et al. 2014; Creusen et al. 2013; Creusen et al. 2012; Edwie & Chung 2013; Guan et al. 2012; Ji et al. 2010; Kim, Kim, et al. 2017; Quist-Jensen, Macedonio, et al. 2016). The interesting aspect of this process is that: firstly, crystallization may require less energy compared to conventional evaporation crystallization;

secondly, it produces crystalline material from solution; and thirdly, clean water is recovered. Moreover, the MD as part of MDC can improve the limited supersaturation control of crystallization due to continuous solvent removal.

This review reports and critically reviews the research conducted on membrane distillation crystallization (MDC) process up to the present day. The potential and feasibility of MDC in treatment of challenging solutions is discussed. This review also addresses the operational problems such as crystal deposition/formation (scale) on the membrane, wetting phenomenon and economic implications (energy consumption and operational costs). Other applicable crystallization techniques such as drowning-out crystallization and reaction crystallization technologies are noted here.

2.2. Seawater reverse osmosis (SWRO) brine

In the desalination, reverse osmosis (RO) technology is widely used (called as seawater reverse osmosis (SWRO)). In RO, a semi-permeable barrier (reverse osmosis membrane) facilitates the separation of a seawater into pure water and concentrated solution of seawater (namely SWRO brine). Seawater is pressured against RO membrane at a pressure higher than the osmotic pressure of the seawater in order to facilitate the passage of the water molecules the membrane while most of the salt is rejected. In order to prevent fouling trough in RO, pre-treatment processes are required such as screening, chlorination, filtration, addition of anti-scalant and anti-foulant (**Figure 2-1**).

The generation of large amount of brine is the major issue in SWRO plant due to the its low water recovery. Clean water recovery from seawater by RO process is determined by the water

quality of feed solution (seawater). Typically, water recovery of SWRO plant is 30-50%. This means that 50-70% of feed water volume remains as RO concentrate (brine). RO brine causes economic and environmental problems due to its huge amount, high salinity and toxicity. Higher water recovery can reduce the volume of brine, but results in the higher concentration of brine. Further, it is energy intensive. Moreover, the scaling caused by divalent ions (Ca^{2+} and Mg^{2+}) present at relative higher concentration in SWRO brine is a serious problem in SWRO desalination plant, leading to short lifespan of the RO membrane (Choi et al. 2016).

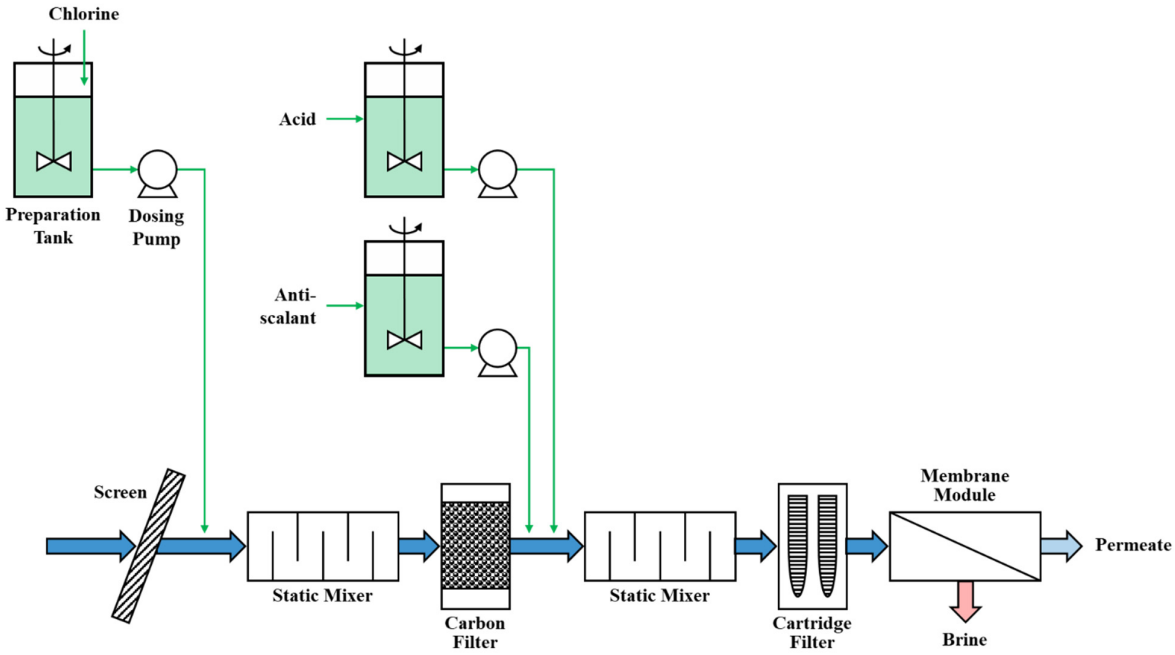

Figure 2-1. Schematic diagram of reverse osmosis (RO), adopted from literature ((El-Dessouky & Ettouney 2002)).

2.2.1. Influential factors on characteristics of brine

The water quality of SWRO brines depends on many factors such as (Chelme-Ayala et al. 2009; Greenlee et al. 2010; Pérez-González et al. 2012):

- Seawater desalination brine sources
- Pre-treatment process applied (chemicals added)
- Clean water recovery capacity (quality of water produced)
- Cleaning procedure

The quality of seawater is varied by geographical and climatological difference. It can influence the clean water recovery capacity of SWRO plant. The Ca^{2+} and Mg^{2+} concentration in SWRO brine is the important factor in determining the clean water recovery ratio due to their scaling potential. As a result, it influences the characteristics of SWRO brine in terms of salinity and density of brine. According to the water quality of seawater source, the suitability in treatment by SWRO process and suitable water recovery ratio can be determined. Water quality in Arabian Gulf is not suitable for RO desalination because of 4H: High salinity, High temperature, High turbidity and High marine life (Fath et al. 2013).

RO process requires appropriate pre-treatment, and insufficient pretreatment could result in frequent replacement of the membrane (short lifespan). Therefore, proper pretreatment is an essential. The pre-treatment for RO process usually consists of dual media filtration and precipitation steps for removal suspended particles as well as microorganism, and the addition of some chemicals for chlorination, de-chlorination, coagulation and flocculation. So, these chemicals added as pre-treatment are also include in SWRO brine. Thus, the pre/post treatment methods of SWRO plant can influence the chemical content of the SWRO brine: such as chlorine, coagulants, anti-scalant, acids used for pH adjustment, and cleaning chemicals.

2.2.2. Conventional brine management options

Evaporation ponds: Evaporation ponds are one of solar evaporation techniques to dispose the concentrate in areas whit warm climate and high evaporation rate (Ahmed et al. 2000). The brine from the SWRO plant is blended with seawater, and this stream is fed to a series of evaporation ponds. This technology has the limitations: 1) need for large land area, and 2) high potential for ground water contamination caused by leakage (Katzir et al. 2010; Pérez-González et al. 2012).

Discharge into wastewater treatment plant: Discharging into wastewater is a low-cost option with limited requirements for disposal of SWRO brine because the quality of brine influences the effluent quality of wastewater plant. The application of this method is dependent on two factors: 1) the distance between SWRO plant and wastewater plant, and 2) the influence of addition of brine on the increase of capacity wastewater plant (Mickley 2001). In addition, the enhanced dispersion should be applied because of high concentration of the wastewater effluent.

Land application: SWRO brine can be used in spray irrigation for plants (such as corps and grasses) which have tolerance for salinity (Kile & Ajy 2005; Mickley 2001). However, a careful monitoring should be required in subsurface water and solid in terms of salinity to prevent of contamination of subsurface water and accumulation of salt in soils (Chelme-Ayala et al. 2009).

Deep well injection: Deep well injection is a disposal option of liquid waste. The porous subsurface rock formation can be used in deep well injection. Liquid waste is injected into this formation. The depth of deep well ranges from a few hundred meters to a few thousand meters (300 to 2400m) (Chelme-Ayala et al. 2009; Saripalli et al. 2000). Its main purpose is

to prevent the movement and leakage of liquid waste into underground water source. So, geohydrological study should be conducted before the application for isolation of liquid waste in the well (Beltrán 1999).

Direct discharge into surface water: Direct discharge into surface water (lakes, river and sea) are the most common method for disposing brine (Giwa et al. 2017; Mezher et al. 2011). In coastal desalination plants, the common and lower-cost practice in management and handling of these great amount of brine is discharge back into the sea at the outfall of plant. However, there are several harmful environmental effects caused by this direct discharge. It could result in environmental impacts to organisms. It consists of highly concentrated salts and any un-reacted (or excess) pre-treatment chemicals and membrane cleaning agent. Moreover, when SWRO brine is discharged into the sea, more serious impact of brine can be induced by the higher density of brine compared to receiving seawater. The density difference between brine and receiving water induce the formation of a stratified system, with high concentration layer formed at a bottom of sea that will affect the benthic communities (Chelme-Ayala et al. 2009). The magnitude of this impact will depend on the characteristics of the brine, nature of the physical parameters (i.e., Bathymetry, hydrodynamics, etc.) and biological conditions of the receiving marine environment.

To avoid impacts from high-salinity brines, the desalination plant brine is used to be diluted with other waste streams, such as power plant cooling water and treated wastewater effluent or seawater available. Furthermore, the environmental impact of discharged brine streams can be further reduced with the use of more robust, environmentally-friendly pre-treatment methods that use less chemicals than conventional seawater pre-treatment. Effective pretreatment will

also reduce the fouling rate and frequency of chemical cleaning of RO.

The management strategies of brine consider the following: 1) improvement of direct disposal strategy, 2) volume minimization, and 3) reuse application of brine (Giwa et al. 2017). The wind-aided intensified evaporation (WAIV), brine concentrator, multi-effect distillation (MED) and membrane distillation (MD) are used for minimization of brine volume, and the precipitation, crystallization, adsorption and electrodialysis (ED) are used for reuse application of brine.

2.3. Crystallization/precipitation process

Crystallization/precipitation from solution is widely used by industries in their purification and solid-liquid separation processes (Mullin 2001; Tung et al. 2009). It is the basic unit operation in the production of crystalline commodity products (Profio et al. 2010). The basis of crystallization is to achieve supersaturation of the solute in solution; when it is exceeded, the crystallization and separation of crystals from the bulk solution occur. During the crystallization/precipitation process, it is important to control the solute's solubility so that the appropriate conditions to form crystals are facilitated. This is because the driving force of crystallization is the supersaturation of solute in solution. Factors such as decline in solution temperature, solvent removal, and chemical reaction between the solutes significantly affect the solubility of solute in solution, leading to higher crystallization. The following phenomena make this possible: cooling crystallization, evaporation crystallization, reaction and drowning-out crystallization, respectively (Lu et al. 2017; Tung et al. 2009).

Solubility of solute is a function of the solution temperature; the influence of temperature on solubility may be positive, negative, or neutral. **Figure 2-2** shows that the solubility is a

function of temperature. Positive temperature-solubility occurs when solubility increases as temperature increases (solute A), while negative temperature-solubility occurs when solubility decreases as temperature increases (solute C). Neutral temperature-solubility, on the other hand, has no definite variation of solubility when there is a change in temperature (solute B). The solubility of all solutes can be controlled by controlling of temperature and the supersaturation state is reached, resulting in a nucleation. However, the effect of temperature control on the difference of solubility is different as shown in **Figure 2-2**. In case of solute A and B, the supersaturation can be obtained by the decrease of temperature. According to the decrease of same temperature, the higher solubility difference can be obtained in solute A. Hence, in case of solute A, the cooling crystallization technique is the suitable to achieve the supersaturation. However, this cooling crystallization technique is not suitable for solutes B and C, as their solubilities do not decrease at lower temperatures. Therefore, other techniques such as evaporation, reaction and drowning-out crystallization are more suitable for these solutes (B and C). Evaporation crystallization decreases the solubility of the solute after reaching the supersaturation level once the solvent is evaporated and removed from solution. Drowning-out crystallization induces crystallization after an anti-solvent is added to the solution, thereby decreasing the overall solubility of the solute.

Based om the different solubility tendency with solution temperature, the temperature control can be used for salt separation from mixture (solution mining). For example, sylvinite, a sedimentary rock, is a mixture of sylvite and halite, which are KCl and NaCl, respectively. The concepts of crystallization may be exploited to extract KCl and NaCl separately from this mineral. Upon dissolution of sylvanite, K^+, Na^+, and Cl^- ions would be present in solution. Approximately 66% of sylvanite is constituted by NaCl (Garrett 1996), thus Na^+ would be

present in greater amount than K^+. Upon evaporation of the solution, NaCl (solute B in **Figure 2-2**) precipitates, leaving a solution containing mostly K^+ and Cl^- ions. Following the concepts of crystallization, KCl (solute A in **Figure 2-2**) can then be extracted from solution upon crystal formation after a marked decrease in temperature. The decrease in temperature will allow supersaturation of KCl in solution, and the subsequent crystallization.

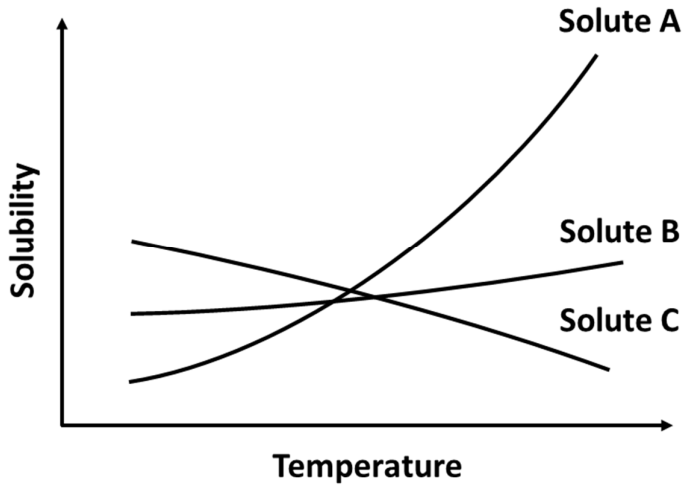

Figure 2-2. Different types of solubility curve of solutes in the solvent.

Based on the solubility product constant (K_{sp}) and ionic product (IP) of a substance, the potential of solute crystallization and precipitation can be predicted (Macedonio & Drioli 2010):

- When K_{sp} > IP, crystallization cannot occur since supersaturation is not reached;
- When K_{sp} = IP, the solution is saturated, but not enough for crystallization to occur;
- When K_{sp} < IP, crystallization occurs due to the solution being supersaturated.

Regardless of the crystallization technique employed, the crystals' formation and growth occur in the supersaturation zone. As depicted in **Figure 2-3**, the supersaturation zone includes metastable and unstable zones. Although crystals can be grown in the metastable zone,

nucleation does not occur. On the other hand, spontaneous nucleation occurs in the unstable zone. Stimulation and control of nucleation by control of solute solubility have been widely reported (Jiang et al. 2016; Narducci & Jones 2012; Phuong & Kwang-Joo 2011; Richard et al. 2011; Soare et al. 2011). All these studies aimed to introduce and establish suitable conditions for nucleation, and they included a reduction of the energy barrier of nucleation, resulting in nucleation (Ulrich & Frohberg 2013; Ulrich & Jones 2004). Seeding crystallization can be another option for the stimulation of crystallization without reaching supersaturation level. Seeding crystallization is commonly practiced in industrial crystallization processes. The presence of seed in the solution allows crystals to grow in the metastable zone.

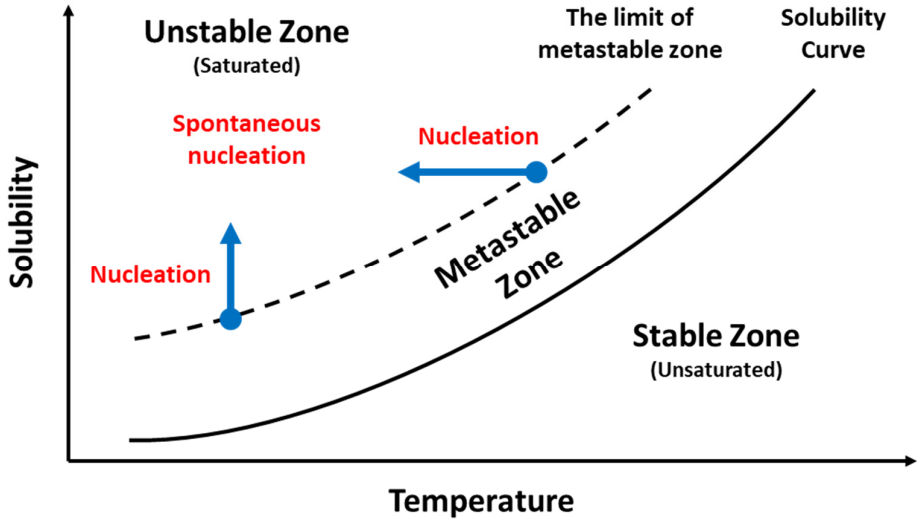

Figure 2-3. Liquid and solid phase variation as a function of temperature.

Current approaches to the crystallization process may be well-established and widely used in industries. There are, however, limitations which influence the quality of crystal produced and overall process efficiency. The main limitations are as follows (Drioli et al. 2012; S. 1989): (1) poor reproducibility of the produced crystals in terms of quality and characteristics, due to

inconsistent agitation and limited supersaturation level control, (2) reduction of supersaturation level after crystallization, which makes it difficult to continue operations without additional treatment, and (3) high energy consumption for heating in conventional evaporation crystallization. In this context, a new concept and approach in crystallization using a membrane technology is being investigated to overcome the limitations of conventional crystallization technologies.

2.4. Membrane distillation and crystallization process

2.4.1. Principles of MD/MDC

Membrane distillation (MD) process is a thermal separation strategy and it has various applications, including treatment of mine water, wastewater, radioactive waste water, brackish water, seawater and reverse osmosis (RO) brine (concentrate) (Naidu, Jeong, et al. 2016; Tijing et al. 2015). It is considered to be one of the most attractive technologies for seawater desalination applications. Normally, MD has some advantages including less hydraulic pressure than RO process, high rejection capacity of non-volatile elements, lower operation temperature and smaller footprint compared to conventional distillation processes (Lawson & Lloyd 1997). In MD process the membrane which is hydrophobic, is placed between a high temperature feed and a low temperature permeate. This hydrophobic property leads to only vapor molecules passing through the membrane (**Figure 2-4**).

Therefore, in the MD process the saline water and wastewater can be converted into high-quality water (permeate side) and a concentrate having the same components of mother liquid, but at a higher concentration (feed side). The main driving force for such separation is the vapor

pressure gradient ($\Delta P = P_f - P_p$) resulting from a temperature difference ($\Delta T = T_{fm} - T_{pm}$) between hot feed ($f$) and cold permeate ($p$) (Creusen et al. 2013). The conditions of temperature, concentration and hydraulic pressure in direct contact membrane distillation (DCMD) are illustrated in **Figure 2-4.** The concentration polarization (CP) and temperature polarization (TP) enables to differ the real concentration and temperature at the membrane surface between bulk solution and permeate (Chernyshov et al. 2003; Jiang et al. 2016; Srisurichan et al. 2006), resulting in a loss of driving force and mass transfer (El-Bourawi et al. 2006). The performance of MD is limited by CP/TP phenomena. These resist the heat and mass transfer at the boundary layer near the membrane. Hence, having a precise understanding of these phenomena is very important for appropriate operation of MD/MDC.

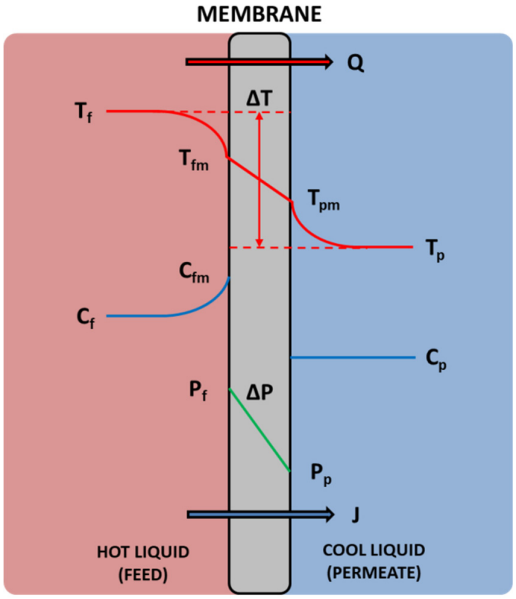

Figure 2-4. Concentration, temperature and vapor pressure profile over the membrane in the direct contact membrane distillation (MD) process (Image adapted from literature (Gryta 2002; Guan et al. 2014)). (T_f is the temperature in the feed solution, T_{fm} is the temperature on a membrane surface in the feed solution stream, T_p is the temperature in the permeate stream, T_{pm} is the temperature on the membrane surface in the permeate stream, C_f is the concentration in the feed solution stream, C_{fm} is the concentration on the membrane surface in the feed solution side, C_p is the concentration in the permeate stream, P_f is the hydraulic pressure of the feed solution, and P_p is the hydraulic pressure of permeate.)

In the MD process there are basic four configurations depending on the scenario on the permeate side (**Figure 2-5**): (a) direct contact membrane distillation (DCMD), (b) vacuum membrane distillation (VMD), (c) air gap membrane distillation (AGMD), and (d) sweep gas membrane distillation (SGMD). Each configuration has its own advantages and disadvantages, however, of the four types (Choi et al. 2017), DCMD is the most studied MD configuration. It has attracted more than half of all studies on MD due to its simple design and operation. Despite these advantages the DCMD does report the poorest energy efficiency for all configurations. In the VMD process, the permeate side of the membrane is operated under vacuum conditions or under low pressure. In VMD configuration, the higher water flux compared to other configurations can be achieved because of higher driving force and prevention of boundary layer formation near the membrane (Lawson & Lloyd 1997). However, more severe fouling problems are caused which in turn lead to the process performance becoming degraded (Choi et al. 2017). The AGMD configuration is considered to have the highest energy efficiency and is popular in commercial applications. The air gap width is usually in the 1 ~ 10 mm range, which is much larger than the membrane thickness (usually less than 300 μm). It influences the water flux of MD negatively because a membrane's thickness influences the mass transfer of MD. Although SGMD is similar to AGMD the gas is sweeping, and the vapor is condensed in an external condenser in SGMD. It has lower conduction heat loss than DCMD.

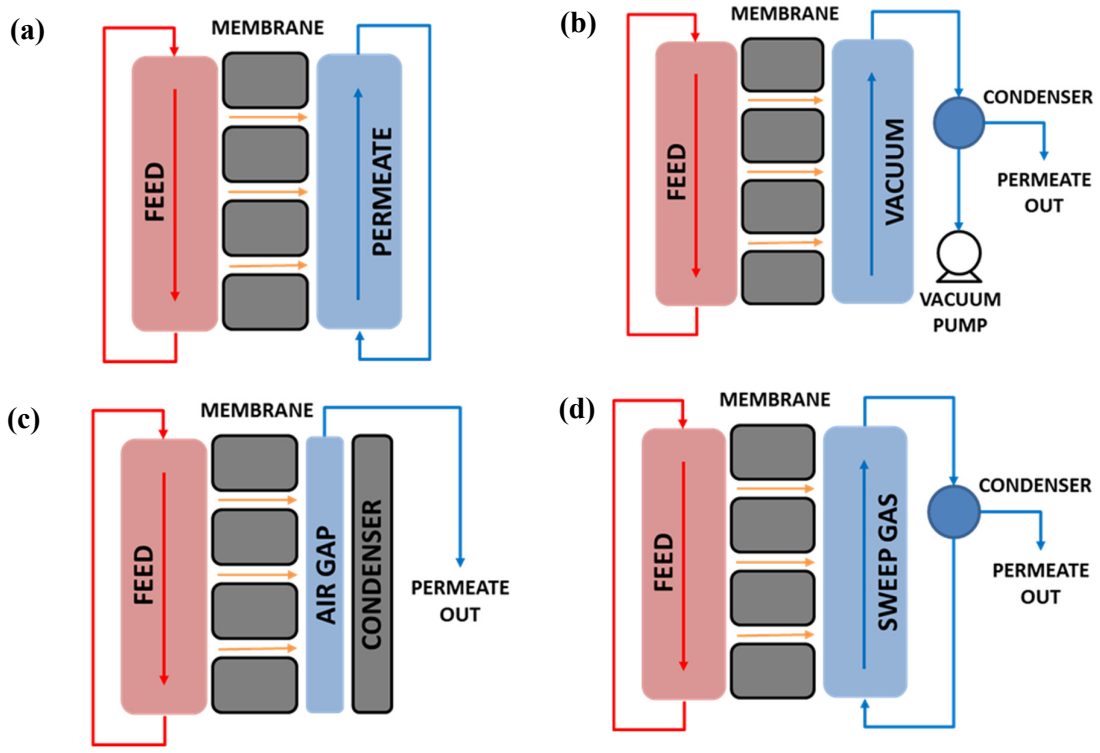

Figure 2-5. Different configurations of the membrane distillation process: (a) direct contact membrane distillation (DCMD), (b) vacuum membrane distillation (VMD), (c) air gap membrane distillation (AGMD) and (d) Sweep gas membrane distillation (SGMD).

One recent innovation known as membrane distillation-crystallization (MDC) has been investigated, thanks to the development of new membrane materials and membrane processes. MDC consists of both membrane distillation (MD) and crystallization in which high-quality water is produced in the MD process while the crystal form can be achieved as a solid from concentrated solution in a crystallizer (Creusen et al. 2013; Tun et al. 2005). These processes occur at the same stage which can help in the recovery of valuable products as well as for producing the fresh water from seawater desalination and treatment of reverse osmosis (RO) and nanofiltration (NF) brine. In high concentration wastewater treatment using the MDC process, valuable resources such as salt, lithium, and so on can be recovered because the

thermally driven operation concentrates an aqueous solution up to the supersaturation state.

The applicability of the crystallization process in the recovery of chemicals from feed solution was first reported in 1987 (Drioli et al. 1987). The MD process can be used to reach supersaturation by further concentration of solution. MD-crystallization process to recovery taurine in industrial wastewater treatment was examined (Wu et al. 1991). Their findings highlighted good prospects for the MD-crystallization process in treatment industrial wastewater. Both high quality water and crystals were obtained in their investigation. In these studies, the cooling crystallization technique was used in the individual crystallizer (**Figure 2-6 (a)**). In another study, an integrated MD-crystallization process was utilized for the treatment of concentrated sodium chloride solution in both batch and continuous modes (Gryta 2002). In this study, DCMD was used and furthermore, sodium chloride (NaCl) crystal of 100 $kg/m^2 \cdot d$ and permeate flux of 400 $L/m^2 \cdot d$ could be obtained when using an integrated MD and crystallization process. As shown in **Figure 2-6 (b)**, the feed tank was replaced by a crystallizer without applying the cooling crystallization technique (temperature of crystallizer: 323, 290, and 353 K, respectively).

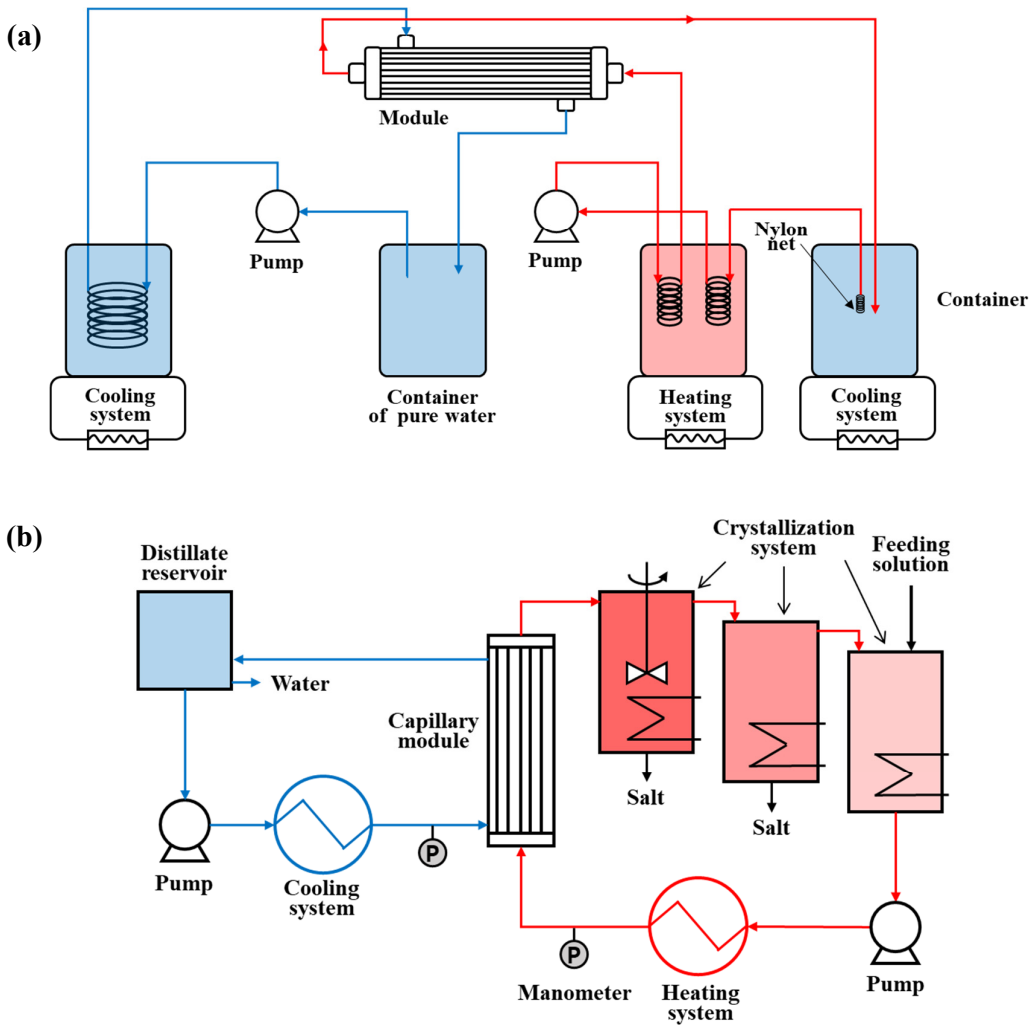

Figure 2-6. Experiment set-up for membrane distillation crystallization (MDC), adapted from literatures (a) (Wu et al. 1991), and (b) (Gryta 2002).

In the membrane crystallization technique, the membrane can be used as the tool and method for generating supersaturation. The membrane's function is different depending on the membrane material and design parameters. For the generation of supersaturation, the membrane can function in terms of heat transfer (heat exchanger), mass and heat transfer (membrane distillation, pervaporation), selective mass transfer (ultrafiltration, nanofiltration,

reverse osmosis, ions exchanger) or non-selective mass transfer for the purpose of mixing reactants (membrane contactor (MC)) (Chabanon et al. 2016). The functions of membrane in a membrane crystallizer is to remove solvent (Drioli et al. 2012). The membrane in this case does not act as a physical barrier for selective mass transport of specific components. Nonetheless the membrane can support the generation, maintenance and control of a supersaturation environment in which nucleation and growth of crystals occur. The uniform size and controlled morphology of crystals produced can be due to the supersaturation environment created by the membrane. This is because of the homogeneous nucleation of crystals at numerous points (pore of membrane) in which solvent removal occurs (Di Profio et al. 2005).

In MDC, which is one example of membrane crystallization technology, the membrane helps in the generation of supersaturation. This is made possible by the simultaneous effect of both the removal of solvent by evaporation and decline in the feed solution temperature. The solvent is continuously removed via solvent evaporation through the membrane from crystallizing liquid side to distillate side, resulting in supersaturation of crystallizing liquid. Moreover, the crystallizing liquid can be cooled down by the heat transferred from the cool liquid. Solubility of crystalline salt at a low temperature is lower than at a higher temperature, and this is referred to as negative-temperature solubility. For this reason, the decrease in temperature by the cool liquid enables the supersaturation condition to be reached. Furthermore, the extraction of salt crystallized from the feed solution leads to the maintenance of salt concentration near supersaturation degree while the solvent is continuously removed. **Section 2.4.3** discusses the status of current research with the relevant technical descriptions.

2.4.2. Theoretical background

The mass and heat transfer from the feed to permeate side take place due to the gradient of vapor pressure through the interface between liquid and the porous hydrophobic membrane. The trans-membrane flux caused by the mass transfer can be calculated by using the **Equation 2-1** (Ali et al. 2015; Quist-Jensen, Ali, et al. 2016):

$$\boldsymbol{J = B \cdot (P_{feed} - P_{permeate})} \qquad \textbf{Equation 2-1}$$

Where, J is the mass transfer flux (kg m^{-2} s^{-1}), and P_{feed} and $P_{permeate}$ refer to the vapor pressure corresponding to temperature of feed and permeate side (Pa) respectively. B is the membrane characteristic parameter, and it can be calculated by dust gas model (Alkhudhiri et al. 2012; Khayet 2011). According to the model, the mass transfer through the porous hydrophobic membrane is based on the Knudsen diffusion model, molecular diffusion model or transition model.

$$B = \left[\frac{3\tau\delta_m}{2\varepsilon r}\left(\frac{\pi RT}{8M}\right)^{1/2} + \frac{\tau\delta_m}{\varepsilon}\frac{P\alpha}{PD}\frac{RT}{M}\right]^{-1} \qquad \textbf{Equation 2-2}$$

Where, τ, δ_m, ε, r, R and M are tortuosity factor, membrane thickness, porosity, average membrane pore size, universal gas constant and molecular weight of water respectively. Antonie equation (**Equation 2-3**) states that the vapor pressure (P_{feed}, $P_{permeate}$) is exponentially related to the solutions temperature (Lawson & Lloyd 1997).

$$\boldsymbol{P = exp\left[A - \frac{B}{C+T}\right]}$$ **Equation 2-3**

Where, P is the partial vapor pressure (Pa), and A, B and C are the constants vary from substance (water: A = 23.1964, B = 3816.44 and C = -46.13) (Poling et al. 2001). It indicates that the driven force (vapor pressure) in DCMD increases with the increase in temperature difference between the feed and permeate sides. According to these equations, the trans-membrane flux in DCMD is influenced by membrane characteristics (τ, δ_m, ε, r), the temperature of both the feed and permeate fluids (T) and molecular weight of components (M) (Ding et al. 2010). Also, it is slightly varied by the experimental conditions (Mullin 2001; Tun et al. 2005)

The vapor pressure can be also influenced by the concentration of solute in the solution. At low concentration, the solute concentration does not significantly influence the vapor pressure on the feed side of the membrane. However, in high concentration (close to saturation level), the effect of solute concentration on the vapor pressure is significant (Chen et al. 2014). This correlation can be explained by **Equation 2-4** following:

$$J = C\,({P^0}_{fm} - {P^0}_{pm}) = C\,({P^0}_{fm}\,(1 - x_m)\,\gamma - {P^0}_{pm}) \quad \textbf{Equation 2-4}$$

$$\textit{Where, } \gamma = 1 - 0.5x_m - 10{x_m}^2$$

Where, C, ${P^0}_{fm}$, ${P^0}_{pm}$ and x_m refer to the overall mass transfer coefficient (kg m^{-2} s^{-1} Pa^{-1}), the saturated vapor pressure (Pa) near the surface of membrane in the feed and permeate side, and the solute mole fraction on the membrane surface in the feed side, respectively. γ is

the activity coefficient for salt solution (Gryta 2002; Schofield et al. 1990). The increase of solution mole fraction will lead to the decrease of vapor pressure and the flux (**Equation 2-5**). The concentration polarization coefficient (ξ) can be explained based on the film model (Tun et al. 2005).

$$\xi = \frac{c_w}{c_b} = exp\left(\frac{J}{\rho K}\right) \qquad \textbf{Equation 2-5}$$

Where, c_w and c_b are concentration at the membrane wall and in the bulk solution (mol L^{-1}), and K is the solute mass transfer coefficient (m s^{-1}).

As mentioned above, the temperature at both membrane surface (feed and permeate side) influences the vapor pressure at the feed and permeate side. For driving force in MD, it acts as a resistance caused by the temperature polarization, resulting in decrease of mass transfer. In order to understand the temperature at interface between liquid and membrane surface, the knowledge of heat transfer is important. Heat transfer coefficient (h, W m^{-2} K^{-1}) can be calculated by using the **Equation 2-6** following:

$$h = \frac{Nu\, k}{D} \qquad \textbf{Equation 2-6}$$

Where, Nu is the Nussel number, k is the thermal conductivity of fluid (W m^{-1} K^{-1}), and D is the hydraulic diameter of the channel (m). Nu can be calculated from **Equation 2-7** for laminar heat transfer (Tun et al. 2005).

$$Nu = 1.86 \left(Re\ Pr\ \frac{D}{l}\right)^{0.33} \left(\frac{\mu}{\mu_w}\right)^{0.14}$$ **Equation 2-7**

Temperature polarization coefficient (τ) can be described as (Schofield et al. 1987),

$$\tau = \frac{\Delta T_m}{T_f - T_p} = \frac{h}{h + h_c + h_v}$$ **Equation 2-8**

$$\textit{Where, } *\left(\Delta T_m = T_{fm} - T_{pm}\right)$$

Where, T_f and T_p represent the temperature of feed and permeate (°C), and T_{fm} and T_{pm} are the temperature of feed and permeate near the membrane wall (°C), respectively. T_m can be estimated by the experimental by using **Equation 2-9** and **2-10**.

$$T_{fm} = T_f - (T_f - T_p)\left[\frac{\frac{1}{h_f}}{\frac{1}{h_v + h_c} + \frac{1}{h_p} + \frac{1}{h_f}}\right]$$ **Equation 2-9**

$$T_{pm} = T_p + (T_f - T_p)\left[\frac{\frac{1}{h_p}}{\frac{1}{h_v + h_c} + \frac{1}{h_p} + \frac{1}{h_f}}\right]$$ **Equation 2-10**

Where, h_v and h_c refer to vapor heat transfer coefficient and membrane transfer coefficient (W m^{-2} K^{-1}) respectively. These can be calculated using equations following.

$$h_v = \frac{J\,\Delta H_v}{\Delta T_m}$$ **Equation 2-11**

$$h_c = \frac{k_m}{\delta}$$ **Equation 2-12**

Where, k_m is the thermal conductivity of the membrane (W m^{-1} K^{-1}). ΔH_v is the enthalpy at average membrane temperature (latent heat of vaporization, J kg^{-1}). It can be determined by **Equation 2-13**.

$$\Delta H_v = 1.7535 \left(\frac{T_{fm} + T_{pm}}{2}\right) + 2024.3$$ **Equation 2-13**

2.4.3. Current status

Although reverse osmosis (RO) for desalination and wastewater treatment is considered to be the most efficient process for solving the problem of lack of potable water, certain environmental and economic issues remain (Choi et al. 2018a; Ho et al. 2015; Morillo et al. 2014b; Roberts et al. 2010). Especially, the disposal of brine (i.e. RO concentrate) is the main drawback of RO process. The MDC process has attracted much interest as a new strategy for RO brine treatment (Choi et al. 2018b). Prior studies suggested that MDC process can contribute to a more integrated desalination strategy for water and mineral recovery from seawater, industrial wastewater and brine. In this respect, the treatment of RO brine using MDC process has been researched more and more. The number of publications on this topic has increased noticeably since 2010. The advantages of integrated MDC and NF/RO processes are: 1) the reduction in the large amount of disposed brine from NF/RO, 2) improved overall fresh water recovery and water quality, and 3) the recovery of valuable resources from brine, resulting in more economical MDC operation costs (Drioli et al. 2012).

In MDC, the persistence of a significant distillate flux can be achieved by the formation of crystals leaving the mother liquor (feed solution) even though it causes a reduction of supersaturation. A high total water recovery factor (88-89%) can be obtained in treatment of seawater brine by MDC (Ji et al. 2010). In addition, overall fresh water recovery of up to 92.8% can be obtained during RO brine treatment was demonstrated (Drioli et al. 2006). They also suggested that the MDC process leads to zero liquid discharge (ZLD) due to high water recovery being achieved. Integrated MDC has a clear advantage in reducing the amount of brine disposal and producing additional crystalline salt. The produced crystals and increase of water recovery can offset the entire operational costs. Subsequently, the adverse influence of brine on the environment - which is caused by its high concentration and chemical content - can be mitigated or eliminated by the continuous recovery of fresh water and resources in MDC (Choi et al. 2017; Naidu, Jeong, Choi, et al. 2017). By combining different membrane process, one can achieve better performance for seawater desalination (Macedonio et al. 2007). The much higher amount of water recovered (92%) can be achieved using a combination of NF, RO and MDC compared to a single RO unit (about 40%) and typical multi-stage flash (MSF) (about 10%).

The representative simultaneous MDC process designs are shown in **Figure 2-7** (Edwie & Chung 2012; Julian et al. 2016; Tun et al. 2005). The crystallizer placed in the retentate (feed) side of MD process serves as the feed tank as well. The retentate from the membrane module of MD is transferred to the crystallizer which increases the saturation level in it, resulting in crystallization (**Figure 2-7 (a)** and **(b)**). In these studies, MDC process behaved as though it was a batch-type evaporation crystallizer. When the state of supersaturation was attained, crystallization occurred in the crystallizer with no further evaporation and solvent being

removed by MD (Tun et al. 2005). There are different functions of crystallization, which increase the saturation level of retentate in the MDC process design: (1) the removal of solvent by evaporation (non-control of temperature) (**Figure 2-7 (a)** and **(c)**); and (2) the decrease of temperature in the crystallizer with solvent being removed (**Figure 2-7 (b)**).

However, in the case of the latter, the supersaturation level can be reached faster when the solubility of the target component is influenced by temperature. For example, the solubility of Na_2SO_4, KCl and $MgCl_2$ is significantly influenced by temperature. Their solubility is low at a lower temperature of solution than at a high temperature, and this is termed negative temperature-solubility correlation. The application of cooling (decrease of temperature) in a crystallizer (cooling crystallization technique) is a suitable application in this case for stimulating crystallization (Choi et al. 2018b). The DCMD process has been widely used in MDC because it is easy to operate. However, the feasibility of different MD configurations such as vacuum membrane distillation (VMD) and osmotic membrane distillation (OD) in the MDC process have been investigated (Jia et al. 2017; Julian et al. 2016; Luis et al. 2013; Quist-Jensen, Ali, et al. 2016; You et al. 2015). The submerged VMD-crystallization process for inland brine water treatment was examined, and found that the need to reheat the feed solution (which transferred from crystallizer) and heat loss due to circulation of the feed solution can be eliminated and avoided altogether by using a submerged membrane module (Julian et al. 2016). VMD also has higher mass transfer as compared to cross-flow DCMD. MDC process has been researched for recovery water and resource in challenging solutions such as SWRO brine, produced water from oil field (shale gas production), and industrial wastewater. The status of current research on MDC is summarized in **Table 2-1**.

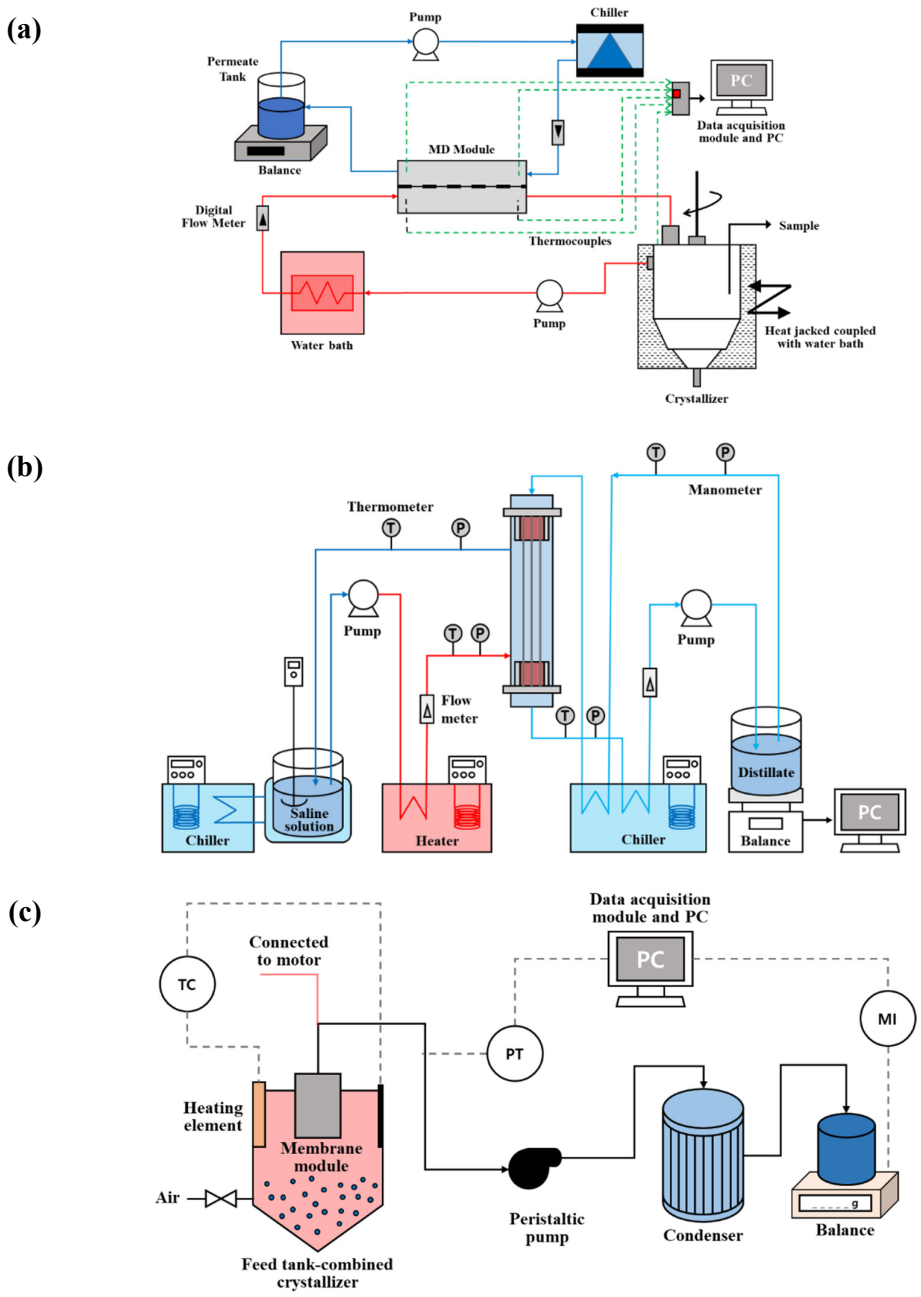

Figure 2-7. Schematic diagrams of MDC with different membrane module configurations (figures adapted from previous literature): (a) with DCMD-flat sheet membrane module (Tun et al. 2005), (b) with DCMD (Edwie & Chung 2012), and (c) with hollow fiber submerged VMD (Julian et al. 2016).

Table 2-1. MDC research on the treatment of challenging solutions.

Source		Feed solution[a]	MDC configuration[b]	Crystallization technique[c]	Operative Temperature (°C)			Crystallizer location[d]	Recovered mineral	Ref
					Feed	Permeate	Crystallizer			
Single component solution	Synthetic	NaCl solution	DCMD-Cr (HF)	Evaporation & Cooling	60.0 - 85.0	20.0 - 55.0	20.0	Batch-type or Feed line (= feed tank)	NaCl	(Gryta 2002)
		Na_2SO_4 solution (2.0 M)	DCMD-Cr (Flat sheet)	Evaporation	60.0	20.0	70.0 ± 2.0	Feed line (= feed tank)	Na_2SO_4	(Tun et al. 2005)
		NF brine (raw feed: 60g/L Na_2SO_4, R = 50%)	DCMD-Cr (HF)	Evaporation or Cooling	30.0 40.0	25.0 28.0	35.0	Additional continuous line	Na_2SO_4	(Curcio, Ji, Quazi, et al. 2010)
		NaCl solution (24.0 wt%)	DCMD-Cr (HF)	Evaporation & Cooling	60.0 ± 0.1 80.0 ± 0.1	17.0 ± 0.1	-	Feed line (= feed tank)	NaCl	(Edwie & Chung 2012)
		NaCl solution (70.0 g/L)	DCMD-Cr (HF)	Evaporation & Cooling	60.0 - 80.0	30.0 - 50.0	30.0	Feed line (= feed tank)	NaCl	(Guan et al. 2012)
		NaCl solution (26.4 wt%)	DCMD-Cr (HF)	Evaporation & Cooling	40.0 ± 0.1 70.0 ± 0.1	17.0 ± 0.1	25.0 ± 0.1	Feed line (= feed tank)	NaCl	(Edwie & Chung 2013)
		NaCl solution $CaCO_3$ solution	MD OD	Evaporative Osmotic					-	(Creusen et al. 2013)
		NaCl solution (26.7 wt%)	DCMD-Cr (HF)	Evaporation & Cooling	64.9	29.9	<64.9	Feed line	NaCl	(Chen et al. 2014)
		KNO_3 solution	DCMD-Cr (HF)		45.0 – 70.0	20.0 & 30.0	25.0	Feed line (= feed tank	KNO_3	(Jiang et al. 2016)
		NH_4Cl solution (20.0%) NH_4SO_4 solution (34.0%)	VMD-Cr (Flat-sheet)	Evaporation & Cooling	60.0	-	10.0	Batch type (after MD)	NH_4Cl NH_4SO_4	(You et al. 2015)
		LiCl solution (6.0, 7.0, 8.0 M)	DCMD-Cr OMD-Cr VMD	Evaporation & Cooling, Osmotic	52.0 52.0 40.0 - 60.0	20.0 20.0 -	30.0 - 60.0	Feed line (= feed tank)	LiCl	(Quist-Jensen, Ali, et al. 2016)

		Na_2SO_4 solution (0.8 M)	Submerged-DCMD-Cr (HF)	Evaporation & Cooling	50.0 ± 1.3	16.5 ± 0.2	20.0 ± 1.5	Feed line (= feed tank)	Na_2SO_4	(Choi et al. 2018b)
Brine (from desalination process)	**Modeled**	NF brine	DCMD-Cr (HF)	Evaporation & Cooling	35.0 ±1.5	15.0 ± 1.0	25.0	Feed line (= feed tank)	$MgSO_4 \cdot 7H_2O$ NaCl	(Drioli et al. 2004)
		NF/RO brine	DCMD-Cr (HF)	Evaporation & Cooling	34.0 ± 1.0	16.0 ± 2.0	25.0	Feed line (= feed tank)	NaCl	(Macedonio & Drioli 2010)
		SWRO brine	DCMD-Cr (HF)	Evaporation & Cooling	40.0	20.0	30.0	Feed line (= feed tank)	NaCl	(Ji et al. 2010)
		SWRO brine (R = 51%)	DCMD-Cr (HF)	Evaporation	38.6 ± 0.4	21.3 ± 0.1	38.6 ± 0.4	Feed line (= feed tank)	NaCl	(Macedonio et al. 2013)
		Seawater SWRO brine (R = 51%)	DCMD-Cr (HF)	Evaporation	36.1 ± 1.4	24.7 ±2.0	36.1 ± 1.4	Feed line (= feed tank)	$MgSO_4 \cdot 7H_2O$	(Quist-Jensen, Macedonio, et al. 2016)
		Sea salt solution (65 g/L)	DCMD-Cr (HF)	Evaporation	60.0	20.0	60.0	Feed line (= feed tank)	NaCl	(Shin & Sohn 2016)
		Inland brine	Submerged-VMD-Cr (HF)	Evaporation & Cooling	70.0 ± 0.5	-	<70.0 ± 0.5	Feed line (= low part of feed tank)	-	(Julian et al. 2016)
	Real	Concentrated seawater (RO brine, R=30%)	DCMD-Cr (HF)	Evaporation & Cooling	40.0	20.0	30.0	Feed line (= feed tank)	NaCl	(Ji et al. 2010)
Produce water	**Modeled**	Produced water	DCMD-Cr	Cooling	38.0	25.0	15.0	-		(Ali et al. 2017)
		Shale gas produced water	DCMD-Cr (Flat-sheet)	Evaporation & Cooling	60.0 ± 0.5	20.0 ± 0.5	40.0 ± 1.0	Feed line (= feed tank)	$BaCl_2$ $CaCO_3$ NaCl	(Kim, Kwon, et al. 2017)
	Real	Oilfield produced water	DCMD-Cr (HF)	Evaporation	35.0, 45.0, 55.0	10.0	-	Feed line (=feed tank)	NaCl	(Ali et al. 2015)
		Shale gas produced water	DCMD-Cr (HF)	Evaporation & Cooling	60.0 ± 1.0	20.0 ± 1.0	30.0	Feed line (= feed tank)	$CaCO_3$ NaCl	(Kim, Kim, et al. 2017)

Wastewater	**Modeled**	Radioactive wastewater	VMD-Cr (HF)	Evaporation & Cooling	28.3 – 35.2	-	20.0	Feed line (=feed tank)	Boric acid	(Jia et al. 2017)
	Real	Wastewater	DCMD-Cr (HF)	Evaporative & Seeding ($MgCl_2$)	45.0 – 65.0	-	-	Feed line (=feed tank)	$MgNH_4PO_4 \cdot H_2O$	(Quist-Jensen, Sørensen, et al. 2017)
		Industrial wastewater (NF brine)	DCMD-Cr (HF)	Evaporation or Cooling	30.8 - 51.4	16.5 - 44.9	37.0	Feed line (= feed tank)	Na_2SO_4	(Quist-Jensen, Macedonio, et al. 2017)
Carbon dioxide		Na_2CO_3 solution (150 and 200g/L)	OD-Cr (HF)	Evaporation & Concentration (Osmotic)	-	-	-	Feed line (=feed tank)	$Na_2CO_3 \cdot 10H_2O$	(Luis et al. 2013)

[a] SWRO = sea water reverse osmosis, RO = reverse osmosis, NF = nanofiltration, R= water recovery factor

[b] DCMD = direct contact membrane distillation, VMD = vacuum membrane distillation, OMD = osmotic membrane distillation, Cr = crystallization, HF = hollow fiber membrane, OD = osmotic distillation

[c] "Evaporative" indicates that additional treatment (such as temperature control or chemical treatment) is not applied; only by concentration by MD process. "Cooling" indicates that the temperature in crystallizer was maintained below the temperature of bulk solution.

[d] This indicates the crystallizer installation location. There are two types; MD and crystallizer separately ("Batch-type") and combination both MD and crystallizer in one process ("Feed line" and "feed tank (crystallizer plays in role of feed tank)",).

2.4.3.1. Optimization of operation parameters in MDC

MDC has two key advantages in the treatment of high concentration solutions and these are: (1) the driving force (temperature gradient) in MD, and (2) continuous extraction of solute from solution in the form of crystals, resulting in a maintenance of total contents in crystallizing solution. In the crystallization phase, a high concentration of solution (supersaturation level) is essential to obtain crystals from the solution. If there is a high concentration of target material in the feed solution, it is then easier and faster to achieve the supersaturation level. In this context, the researchers have used a single component solution with high concentration as a feed solution in order to examine the feasibility of MDC for the treatment of brine from a desalination plant (NF and RO) (NaCl: (Chen et al. 2014; Creusen et al. 2013; Edwie & Chung 2012, 2013; Gryta 2002; Guan et al. 2012), Na_2SO_4: (Curcio, Ji, Quazi, et al. 2010; Julian et al. 2016; Tun et al. 2005)). Also investigated here was the effect of different operational parameters on the current performance of MDC.

The membrane's properties and materials are the critical factors in MDC because the membrane surface is in direct contact with a crystalline solution. Therefore the interaction between a solute and membrane is likely to occur depending on the fluid dynamics, morphology and chemical properties (Drioli et al. 2012). Membranes with increased water flux and low sensitivity to fouling can help achieve stable operation and superior performance. The effect of membrane material and design on the mass/heat transfer in SWRO brine was analyzed using three different membranes (single-layer polyvinylidene fluoride (PVDF), dual-layer hydrophobic-hydrophobic PVDF, and dual-layer hydrophobic-hydrophilic PVDF/polyacrylonitrile (PAN) hollow fiber membrane) (Edwie & Chung 2012). The authors noted the prominent membrane characteristics for stable DCMD performance when treating saturated feed solution were: (1) more compact mixed-matrix morphology under membrane surface; and (2) a membrane with a smaller pore size along with a macrovoid-free cellular structure.

In order to mitigate the effect of generation and deposition of crystals on the membrane surface, reduce membrane fouling, and to stimulate the occurrence of crystallization away from the membrane surface,

new concept of MDC process This was known as fractional-submerged membrane distillation crystallization (F-SMDC) was investigated (Choi et al. 2018b). The submerged DCMD membrane module was placed at the top portion of the reactor, and crystallization occurred at the bottom (lower) portion of reactor feed tank and crystallizer). This operation is based on concentration gradient (CG) and temperature gradient (TG) along the reactor depth. The higher temperature and lower concentration of feed solution were maintained at the top portion of reactor, which is suitable for MD operation while the lower temperature and higher concentration were maintained at the bottom portion of reactor, which favors crystallization. In the presence of CG/TG in the F-SMDC, higher water recovery (VCF 3.5) and less membrane scaling with a high rate of crystal formation was possible to be obtained.

2.4.3.2. MDC applications

2.4.3.2.1. Brine mining and zero liquid discharge

The majority of previous studies utilized synthetic seawater brine as a feed solution to study the effects of inorganic matter present in NF/RO brine. In this context, a detailed experimental study on SWRO brine to examine the impact of organic matter on crystallization conducted (Ji et al. 2010). They observed that the dissolved organic matter influenced crystallization kinetics, for instance the reduction of magma density, nucleation and growth ratio of crystals, as well as permeate flux. The appropriate pre-treatment of seawater brine is essential to mitigate the effects of dissolved organic matter on how well the MDC process performs. In this study more than 90% of water was recovered with a reduction in volumetric wastewater disposal.

Virtually all the elements in the periodic table exist in seawater. It provides the opportunity to recover valuable elements from seawater. Crystals of lithium chloride (LiCl) from a single component solution using the MDC process was obtained (Quist-Jensen, Ali, et al. 2016). In this study, three MD configurations were used with crystallization process. In a single DCMD test, a negative flux was observed due to osmotic effects which overcame the thermal effect on water flux. However, in the combination of DCMD and OD, the driving force was further enhanced by using different concentration and temperature gradient simultaneously. However, doing so was still not enough to overcome the high solubility of LiCl (15.6 mol/kg H_2O at 20 °C). When VMD was used, the saturation level of LiCl was reached due to the minimum temperature polarization and reduced resistance to vapor transport within the pores.

The integrated MDC process for treating brine was studied, and combination of membrane distillation (MD) and osmotic distillation (OD) with internal crystallization was used (Creusen et al. 2013). NaCl and $CaCO_3$ seeds were added to prevent crystals plugging the membrane (**Figure 2-8**). A rapid decline

in flux was observed after a saturated NaCl was crystallized. This was due to the deposition of NaCl and $CaCO_3$ on the membrane surface (either with or without NaCl seeds) in MD. In OD, the flux decline was reduced when NaCl and $CaCO_3$ seeds were added. High water recovery percentage (approximately 99.8%) with crystals being produced was obtained through the integrated MD and OD process.

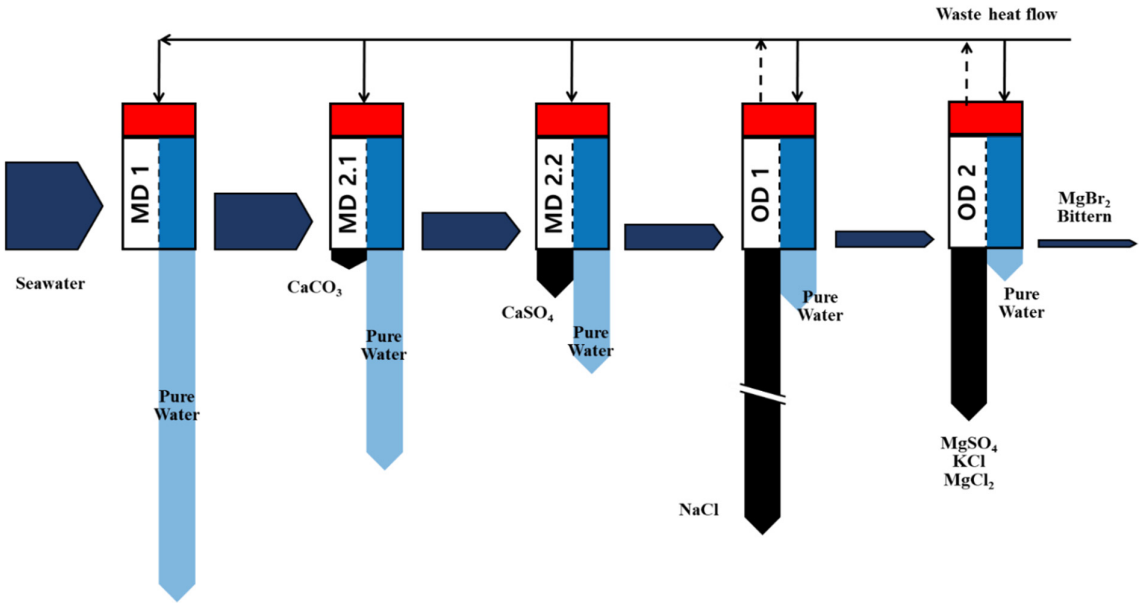

Figure 2-8. Proposed integrated MDC process for desalination of seawater, adapted from literature (Creusen et al. 2013).

2.4.3.2.2. Produced water treatment

Recently, the application of MDC has been extended to the phenomenon of produced water. The treatment and disposal of produced water (PW) from oil and gas has become a major worldwide issue due to the high demand for oil and natural gas. In oil and gas production processes, a large volume of wastewater is generated. Oilfield wastewater which is known as PW contains various inorganic and organic compounds as well as oil compounds, which can contaminate ground and underground water

and soil (Ali et al. 2015; Fakhru'l-Razi et al. 2009). The treatment of PW was studied using MDC process (Ali et al. 2017; Ali et al. 2015). It was demonstrated that MD/MDC emerged as a feasible technology for the treatment of PW as high quality NaCl crystals of 16.4 kg per cubic meter were separated at a water recovery factor of 37%.

Shale gas is an emerging energy source which can extend the duration of fossil fuel usage by several decades. The shale gas production industry generates a huge amount of produced water. In this scenario, the feasibility of the MDC (DCMD with flat-sheet or hollow fiber membrane module) process for the treatment of shale gas produced water was investigated (Kim, Kim, et al. 2017; Kim, Kwon, et al. 2017). A better stability of water flux and higher water recovery were observed in their study due to the reduction of ionic concentration by forced crystallization in a crystallizer. Calcium and barium influenced MDC performance because these can easily form scalant and foulant crystals on the membrane surface. As well, oil and grease caused a decrease of liquid entry pressure (LEP), resulting in the membrane being damaged. They affected the quality of the water produced and consequently, these components induced membrane wetting which was also triggered by organic matter present. They suggested that the pretreatment of oil, grease and multivalent ions (calcium and barium) prior to MDC application is essential for the treatment of shale gas produced water (Kim, Kim, et al. 2017; Kim, Kwon, et al. 2017). Furthermore, the optimization of operation conditions such as cross-flow velocity and temperature in the crystallizer can improve the energy efficiency of MDC, specifically improved water recovery and crystal production.

2.4.3.2.3. Resource recovery from wastewater

The wastewater or wastewater concentrate is also a suitable source for MDC to recover valuable resources since these wastewater streams contain high concentrations of organic and inorganic components. For example, these include ammonia, phosphorous, heavy metals, salts, polycyclic

aromatic hydrocarbons and proteins (Lu et al. 2017; Wang et al. 2011). The feasibility of MDC process for treating ammonium-rich wastewater (from fertilizer plant, intensive agriculture, and industrial activities) was investigated to recover ammonium salt (NH_4Cl and $(NH_4)_2SO_4$) (You et al. 2015). Recovered ammonium salt from wastewater is advantageous because it is widely used as a fertilizer in agriculture. However, in the absence of ammonium treatment, it leads to environmental contamination when it flows into groundwater (Effler et al. 1990; Li et al. 2010). The treatment of industrial wastewater containing large amounts of Na_2SO_4 by MDC process was studied (Quist-Jensen, Macedonio, et al. 2017).

Without pre-treatment, MDC produced the high crystals of Na_2SO_4 formed such as narrow crystal size distribution (CSD), constant growth rate and high purity although the high potential of scaling caused by bivalent ions and silica. However, with pre-concentrated feed solution made possible by NF, low purity Na_2SO_4 crystals were observed despite the fact that pre-concentration by NF can accelerate the saturation level. This situation was attributed to large concentrations of bivalent ions and silica being incorporated compared to the untreated solution. The potential of implementing MDC in wastewater treatment plants was noted for recovering phosphorus and ammonia in the form of struvite crystals ($MgNH_4PO_4 \cdot H_2O$) from the sludge dewatering process (Quist-Jensen, Sørensen, et al. 2017). Struvite has a practical application as a fertilizer. In this study, recovered phosphorous (60%) was obtained along with a high water recovery (~ 70%), which was 35% higher than without concentration when utilizing MD (Quist-Jensen, Sørensen, et al. 2017). The MD and MDC processes made it possible to transport volatile components (such as ammonia) to the permeate stream, resulting in it becoming ammonia-rich. It can directly be used as a fertilizer as well as struvite recovered in the form of crystals

The recovery of boric acid from simulated radioactive wastewater via MDC combined with VMD (VMDC) was investigated (Jia et al. 2017). The wastewater from nuclear power plants contains large amounts of boric acid (about 500 ppm) originating from the primary coolant of nuclear reactor (Wen

et al. 2016). The concentration factor of around 200 times was achieved with VMDC. In total, 96.0% of nuclides and 99.5% of boric acid rejection were obtained. Furthermore 50% of boric acid was successfully recovered from the feed solution when the temperature was 70 °C.

2.4.3.2.4. Carbon sequestration

Carbon dioxide (CO_2) causes the major greenhouse effect in earth. So, for this reason, it is important to capture it and reuse it. The MDC process was used for treatment of carbon dioxide originating from combustion technologies. CO_2 is typically captured using absorption with amines and water-based solutions such as sodium hydroxide (NaOH) because it is environmentally friendly. NaOH is used as an alkaline liquid absorbent, and CO_2 and hydroxyl ions react as follows (Drioli et al. 2004; Mansourizadeh et al. 2010):

$$CO_2 + OH^- \rightarrow HCO_3^- \quad \text{[React 1]}$$

$$HCO_3^- + OH^- \rightarrow {CO_3}^{2-} \quad \text{[React 2]}$$

Carbonate is formed in the solution. The main challenge that has to be solved is recovering the carbonate (as Na_2CO_3) and agent (NaOH) of alkaline liquid absorbent from solution which captures CO_2. MDC is an efficient technology for recovering carbonate in the form of Na_2CO_3 from liquid absorbent. Na_2CO_3 crystallization can be achieved by osmotic distillation crystallization technology (Luis et al. 2013; Ruiz Salmón et al. 2017). The concentration of osmotic solution is a key factor to obtain a viable operation efficiency based on the energy consumption.

2.4.4. Challenges of MDC

The advantages and feasibility of MDC for treating challenging solutions such as SWRO brine and produced water (the wastewater stream generated in oil and gas industries e.g. shale gas) have been demonstrated in various experimental and theoretical research studies (**section 2.4.3.2**). However,

there are issues which can seriously undermine performance of MDC. To enable its stable and efficient operation, certain adverse issues should be solved through additional experimental and theoretical studies. Some of these issues are described in more detail in the following subs-sections.

2.4.4.1. Membrane scaling

It is worth noting here that the following two types of research use the same framework but have two very different aims: (1) induction of crystallization; and (2) prevention of fouling caused by crystallization. In the MDC process, the membrane plays a role in supporting crystallization, making the preferential nucleation mechanism possible. When crystals are formed near the surface of the membrane, they are transferred to the crystallizer (bulk solution) via hydrodynamic transport (flow of solution). This helps to form seed of crystal or nuclei (called the seeding effect), and it results in accelerating crystallization in the bulk solution (Kim, Kim, et al. 2017; Shin & Sohn 2016). Homogeneous nucleation in the bulk solution and then the growth of crystals will occur when supersaturation is reached. After that, prediction of grown crystals leads to reduction of feed concentration which is caused by reduction of salt content in the bulk solution. This results in the reduction of concentration polarization in the membrane.

On the other hand, this crystallization phenomenon has an adverse effect on membrane processes. The role of membrane as a support for crystallization in MDC can lead to the membrane's degradation and a less effective operational performance. Previous studies have widely reported that water flux decline in MD and MDC was mainly caused by crystals' deposition on the membrane surface (Curcio & Drioli 2005; Kim, Kim, et al. 2017; Kimura et al. 1987; Lokare et al. 2017; Shin & Sohn 2016). There are two explanations regarding how flux is decreased by scale formation in the membrane process (Lee et al. 1999). Scale formation by inorganic compounds in membrane systems occurred due to crystallization on the surface (heterogeneous) and in bulk solution (homogeneous) (Oh et al. 2009).

Scale formation is caused by crystallization and hydrodynamic transport mechanisms (Kim, Kim, et al. 2017; Lokare et al. 2017; Shin & Sohn 2016). Crystallization on the membrane surface blocks it because the deposited scale grew laterally on the surface. This results in the phenomenon of flux decline. In the case of bulk crystallization, the nucleated crystal particles derived from the bulk solution can trigger flux decline because they are deposited on the membrane surface. The fine crystal particles transferred from bulk solution (crystallizer) cause secondary nucleation on the membrane surface. **Figure 2-9** illustrates all three scale formation mechanisms in the membrane process. Scale formation is also affected by membrane properties and process condition.

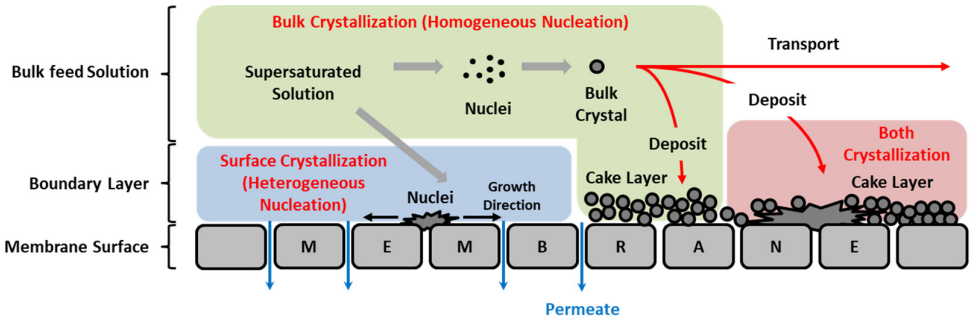

Figure 2-9. Schematic diagram of scale formation in membrane process, adapted from literature (Lee et al. 1999).

2.4.4.1.1. Factors of membrane scaling

The prevention of crystals' formation (and growth)/deposition on the membrane, which is stimulated by the concentration and temperature polarization remains a notable challenge in the MDC process (Creusen et al. 2013). Moreover, the concentration of feed solution influences water flux tendency in MD although the impact of feed solution concentration in the MD process is much less than in other membrane processes, at least theoretically. Previous MD studies convincingly established that water flux tendency in MD is also affected by feed concentration although the influence is smaller than in

other membrane processes. It leads to more severe nucleation and growth of crystals on the membrane surface (Naidu, Jeong, et al. 2016; Sanmartino et al. 2016). If the feed concentration in MD is relatively high, the saturation level is reached much more quickly, resulting in the increase of fouling potential , which is caused by crystals being deposited on the membrane surface (plugging/clogging) (Guan et al. 2012; Naidu, Jeong, et al. 2016). In MDC process, this phenomenon is more serious compared to single MD process. However, fouling by crystallization can be controlled by recovering the crystals produced (Macedonio & Drioli 2010). The potential of fouling and effect of feed concentration increases as the feed solution becomes saturated in the effort to obtain crystals from the bulk solution.

Moreover, the membrane's topographical and chemical properties influence the formation of crystals on the membrane surface. Its porous structure acts as a heterogeneous nucleation support mechanism. The solute molecules are entrapped on the rough morphology surface of the polymeric membrane. Then they lead to the interaction with the chemical functionalities located on the membrane's polymeric chain, resulting in more heterogeneous nucleation. It induces supersaturation of the solute at the boundary layer of the membrane. The concentration polarization in which high concentration layer near membrane surface causes crystal deposition on the membrane As a result, the lower energy barrier for heterogeneous nucleation near the membrane surface is induced by the presence of the membrane and concentration polarization with homogeneous nucleation caused in the bulk solution (Julian et al. 2016; Tun et al. 2005). The effect of membrane material and morphology on scaling formation was demonstrated (Ali et al. 2015). A cavity-like structure on the outside of the membrane (PP) can cause severe scale formation on the membrane's surface because it acts as an anchoring point for crystals to adhere and deposit. The PVDF membrane has a low surface roughness but also higher resistance to scale formation.

The degree of membrane crystallization also depends on the operation conditions and other factors such as flow rate and solution temperature. Fouling caused by generation/deposition of crystals on the

membrane surface can be controlled by optimizing the operational factors (Macedonio & Drioli 2010). The effect of flow rate on scale formation between surface crystallization and bulk crystallization is ambiguous (Shin & Sohn 2016). Surface crystallization decreases with an increase in the flow rate. Bulk crystallization increases with an increase in the flow rate because of secondary nucleation. Also, the feed solution's low flow rate creates a greater temperature gradient along the membrane module (Edwie & Chung 2012), resulting in crystallization occurring on the membrane. Therefore, it is important for the operations to have an appropriate flow rate to reduce the fouling problem.

Studies conducted using real wastewater and SWRO brine treatment show that the water flux of MD was significantly reduced by inorganic scaling such as calcium-based compounds (deposition on the membrane surface) (Choi et al. 2018a; Choi et al. 2017; Creusen et al. 2013; Drioli et al. 2012). This is difficult to manage and control. This scaling problem still remains as a precursor of fouling, resulting in the decline of water flux and recovery ratio. The sparingly soluble salts' crystal deposition and formation is a severe obstacle to improved water recovery ratio. In desalination and concentrate treatment processes, crystallization on the membrane surface caused by calcium-based crystalline compounds such as calcium carbonate ($CaCO_3$) and calcium sulfate ($CaSO_4$) occurs early. This is because of their lower solubility when compared to other crystalline compounds (such as NaCl, Na_2SO_4, $MgCl_2$, $MgSO_4$ and KCl) present in seawater and concentrate (Choi et al. 2018a; Choi et al. 2017; Julian et al. 2016; Lee et al. 2009; Naidu, Jeong & Vigneswaran 2014).

2.4.4.1.2. Mitigation strategies

The fine crystals generated on the membrane surface cannot be removed easily by membrane surface washing with pure water (Chen et al. 2014; Choi et al. 2017). Air backwashing as an alternative method for removing crystals that formed on the membrane surface (Choi et al. 2017; Julian et al. 2018). This strategy is suitable for hydrophobic membranes. They observed that every method cannot remove the

crystals existing on a membrane surface. Hence, the appropriate control of entrapped solute on the membrane is very significant both for: firstly, prevention of membrane fouling caused by crystallization deposition; and secondly, enhancing the formation of crystals in the bulk solution.

In order to avoid $CaSO_4$ and $CaCO_3$ precipitation during the concentration of the NF/RO brine, a conventional lime and soda-ash treatment can serve as a pre-treatment of the NF/RO desalination process. This method reduces calcium and magnesium hardness of the RO concentrates and thus limits the scaling problem (Ji et al. 2010; Masindi et al. 2017; Mohammadesmaeili et al. 2010). Adding Na_2CO_3 into the feed solution was done to remove Ca^{2+} ions (Macedonio & Drioli 2010; Quist-Jensen, Macedonio, et al. 2016). Ca^{2+} ions have been precipitated as $CaCO_3$ through reactive precipitation with anhydrous sodium carbonate (Macedonio et al. 2013). 98% of Ca^{2+} ions have been precipitated when Na_2CO_3 was added at a molar ratio of Ca^{2+} /CO_2 $^{3-}$ of 1:1.05. The seeding of $CaCO_3$ to some extent mitigated $CaCO_3$ scaling in MD (Creusen et al. 2013). The results indicated that fouling on the membrane surface caused by crystallization of $CaCO_3$ declined by adding $CaCO_3$ seeds in the MD process. This resulted in a sustainable flux of 6 L/m^2·h for a long period of time.

The injection of CO_2 gas into bulk solution can also remove Ca^{2+} as $CaCO_3$ precipitation (Drioli et al. 2004). In order to remove Ca^{2+} in the feed solution, a membrane contactor was used with carbon dioxide (CO_2) gas injection prior to MDC operation. Reactive precipitation was achieved by the addition of $NaHCO_3$/Na_2CO_3 aqueous solution into the membrane contactor and NF retentate solution (1:1 molar of Ca^{2+}/CO_3^{2-} ratio). These steps made it possible to remove Ca^{2+} as $CaCO_3$ precipitation. For stable operation and higher recovery factor in MDC, the management of scaling problem is the essential, and it can be achieved by the appropriate pre-treatment of feed solution.

2.4.4.2. Membrane wetting

In MD operation, fouling deposition on the membrane surface aggravates the phenomenon of

membrane wetting (Gryta 2002, 2005; Gryta & Barancewicz 2010; Naidu, Jeong, et al. 2016). Penetration of liquid through the hydrophobic membrane should be avoided because it degrades the quality of produced water and damages the membrane, causing ions to be rejected. Difference in high bulk temperature may increase membrane wetting (Tun et al. 2005). Also, the feed solution's supersaturation state around the membrane surface causes membrane wetting. Membrane wetted cannot be used further in the MD process for producing freshwater from feed that has high salinity. Membrane wetting seriously compromises the MD process and the quality of water produced (permeate) is undermined by crystallization on the membrane surface. It is associated with the solubility of substances such as salt and scalants, which depend on the temperature of the bulk solution. Temperature control is thus very important. Moreover, The all membrane pores can be filled by the feed solution under these conditions and wetting phenomenon occurs (**Figure 2-10**) (Gryta 2002). As a result, diffusive transport of solute through wetted pores occur, specifically from the feed solution to the permeate side due to the feed and membrane interaction. In turn this causes the permeate water to be contaminated.

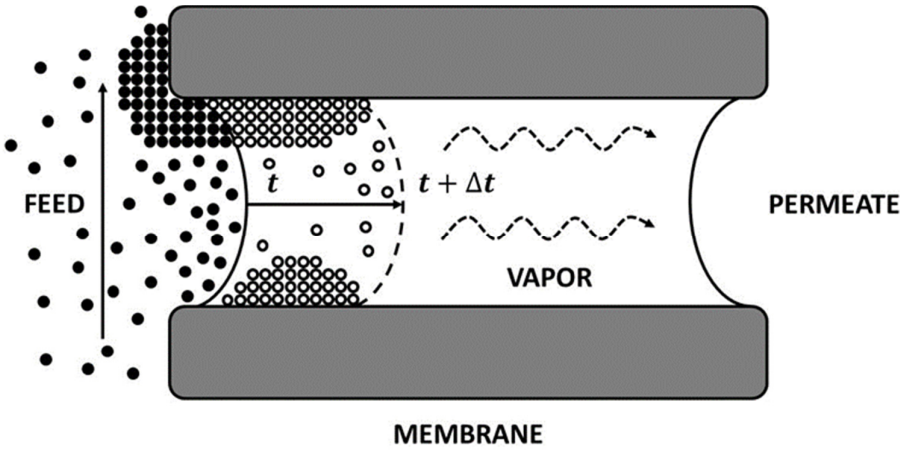

-

Figure 2-10. Model of membrane wetting phenomenon (Initial solute: ●, Solute after Δt: ○) (image adapted from literature ((Gryta 2002).

The deposition of organic components on the hydrophobic membrane leads to decreasing membrane hydrophobicity in the MD/MDC process, resulting in wetting phenomenon as well as organic fouling (Naidu, Jeong, Choi, et al. 2017). Specific components in the feed solution cause the solute to penetrate the membrane pores. For example, in the treatment of shale gas produced water (SGPW), membrane wetting caused by organic, inorganic components and oil matter, resulted in a relative low recovery (from 20–25%) of MDC (Kim, Kwon, et al. 2017). The authors suggested that pretreatment should thus be adopted to remove organic and oil components prior to the application of MDC. Like the scaling problem, the removal of causative substance in the feed solution is the necessary.

2.4.4.3. Energy efficiency

In most previous membrane distillation crystallization research, cooling crystallization has been used as a method to control the degree of saturation of solution (concentration of feed solution) because of its convenience. When it is combined with the MD process the operational costs will increase significantly because higher temperature requirement for MD operation, than the cooling crystallization process (Chen et al. 2014; Creusen et al. 2013; Edwie & Chung 2012; Julian et al. 2016). After cooling crystallization, the feed solution should be reheated for MD operation, and the feed solution is cooled again in a cooling crystallizer to increase the degree of saturation of solute. These two processes are repeated continuously. The consequence is that a large amount of energy is consumed and wasted, resulting in an increase of total operation cost.

The consumption of energy in the MDC process was evaluated (Guan et al. 2012). The effect of heat recovery unit was also investigated using the gain output ratio (GOR) which is a factor commonly used to assess energy efficiency in the evaporation process. They noted that the heat requirement in MDC causes high energy consumption (You et al. 2015), which amounted to 97.8% of the total operation energy. Energy consumption in crystallization is less than 0.5%. Moreover, they suggested that

optimized operational conditions of feed stream temperature can ensure that energy is consumed more effectively in MDC.

The economic efficiency of the desalination process using two desalination hybrid systems was compared, namely, NF/RO and NF/RO/MDC (Drioli et al. 2002). The thermal energy demand in the latter hybrid system can be offset by improving water recovery (100%), removing disposed brine and recovering valuable resources However, as mentioned above, when the cooling crystallization method is being implemented in the MDC process, it will result in serious economic problems. In order to improve the energy efficiency of MDC, further research on low energy/cost consumption crystallization methods is critical. Research on other adoptive crystallization methods (for example, cooling) are needed in combination with the MD process in order to improve the MDC process.

2.4.5. Recommended crystallization techniques for MDC

The application of adaptive crystallization techniques is one of options to address the adverse issues in MDC. The application of crystallization technique, which do not use an additional heat source for heating and cooling on crystallization, can improve the energy efficiency in MDC compared to conventional MDC with cooling crystallization technique. In MDC process, recently, the cooling crystallization technique has been widely studied. However, the combination of MD and cooling crystallization technique such as solute crystallization, freeze crystallization and eutectic freeze crystallization leads to high energy consumption. The crystallization techniques which require lower temperature of feed solution for crystallization are not sustainable for the MDC process because this feed solution needs to be heated again. As a separate MDC process, the cooling crystallization technique functions as two different processes. However, a simultaneous MDC process, i.e. where the crystallizer is placed along the feed flow channel, there will consequently be additional heat loss due

to reheating of the cooled feed solution that was transferred from the crystallizer. The cooling crystallization technique has limitations in recovering negative temperature-solubility solute because reaching the supersaturation level of negative temperature-solubility solute in solution cannot be stimulated by the decrease of temperature.

Additionally, the deployment of appropriate crystallization technique in MDC can mitigate the membrane scaling and wetting issues. Membrane scaling and wetting issues are caused by the nucleation and deposition of crystals on the membrane surface. The crystals transferred from crystallizer contributes to make these issues serious. If the crystals transfer is prevented and the crystallization occurrence is controlled in only crystallizer, the negative issues caused by the crystals on the membrane surface can be reduced. In the following two sub-sections, two possible crystallization technologies that can be adopted for solving the challenges in MDC are discussed.

2.4.5.1. Reaction crystallization

In reaction crystallization (RC), a reaction between a gas and a solution is used to generate sparingly soluble or insoluble components so that the separation of solutes from the solution can be facilitated (Huang et al. 2014). A reactant is used to reduce the solubility of the crystallizing component in the solution by chemical reaction (Å & C. 1992). This technique is commonly used in the recovery and separation of inorganic components and heavy metal ions (Rahman et al. 2014; Rubio & Tessele 1997; Suzuki et al. 2002; Tait et al. 2009). Heavy metals ions can be removed/precipitated by converting them into hydroxide, sulfide or carbonate precipitants. The common method is to add alkaline chemicals (Lu et al. 2017). Hydroxide precipitation is widely used because of its simplicity and low cost. However, this technique does experience some drawbacks such as low precipitation rate and difficulty in treating lime effluent. The sulphide precipitation method has been employed to remove a wide range of heavy metals, for example Sr^{4+}, Ni^{2+}, Mn^{2+}, Zn^{2+}, Ag^{+}, Cu^{2+}, Pb^{2+} and Hg^{2+} and by using various sulfide sources such as Na_2S, NaHS, FeS, H_2S and CaS (Veeken et al. 2003). The recovery of

NH_4^+ and PO_4^{3-} can be obtained by struvite reaction crystallization ($MgNH_4PO_4 \cdot 6H_2O$) from a wide range of wastewaters such as fertilizer plant wastewater, swine wastewater and leather tanning wastewater (Rahman et al. 2011; Rahman et al. 2014; Tünay et al. 1997; Yu et al. 2013). Crystalline struvite can serve as a mineral fertilizer in agriculture (Hutnik et al. 2013). A novel process for simultaneously recovering NH_4^+ and PO_4^{3-} from swine wastewater. Was reported (Huang et al. 2014). They did this by using modified zeolite as an adsorbent and magnesium source for recovering ammonia and nitrogen.

The reaction crystallization discussed above occurs at a relatively high supersaturation level because homogeneous nucleation occurs prior to heterogeneous nucleation. The energy barrier for heterogeneous seeded nucleation is lower compared to homogeneous nucleation. As a result, heterogeneous nucleation occurs at a lower supersaturation level than the homogeneous process (Sluys et al. 1996). In order to reduce the energy required for nucleation in the solution, seed crystals in the supersaturated solution are usually used to initiate crystallization. Here, seed crystals act as the nuclei of crystals (Wendt et al. 2015). Addition of seed crystals into the supersaturated solution leads to their spontaneous growth although the solution concentration is only reached to metastable zone (nucleation does not occur in the metastable zone). This results in reduction of reaction time. The inducting the crystallization was investigated by using fluorapatite/calcite as seed crystals for the removal of fluoride (Deng et al. 2016). The same concept has also been applied for the recovery of magnesium, ammonium and phosphate from wastewater (Ohlinger et al. 2000; Wu & Bishop 2004; Zhang et al. 2009).

2.4.5.2. Drowning-out crystallization

Drowning-out crystallization is the separation of salt from solution by adding an extraneous component, which is a gas, solid, supercritical fluid or liquid (Berry et al. 1997). Gas or solid drowning-out agents should be soluble in the original solvent, and the liquid drowning-out agent should be miscible with

the original solvent (Gianluca et al. 2009). It is also important to select the drowning-out agent accordingly as it influences the morphology and structure of crystal formed (Barata & Serrano 1998; Holmbäck & Rasmuson 1999). This component is often referred to as the drowning-out agent, antisolvent, precipitant, salting-out agent, solventing-out agent or watering-out agent. In this process through the addition of an extraneous component, the solubility of a targeted component will decrease and supersaturation level will be reached, resulting in crystallization (Lu et al. 2017). Controlling the level of solubility with the appropriate agents does influence crystal morphology, structure and yield.

The feasibility of a drowning-out separation process using ethanol to recover polyphenols from olive mill wastewater was investigated (Dammak et al. 2016). The concentration of polyphenol increased considerably after the addition of ethanol to the wastewater, resulting in highly-concentrated polyphenols isolate (up to 75% (w/w)). The ethanol used as the drowning-out agent was regenerated by batch evaporation. This method is an energy-saving alternative to cooling and evaporation crystallization (Mostafa Nowee et al. 2008). An energy cost reduction of 63% was obtained as compared to that of three-effect evaporation by the addition of diisopropylamine (DiPA) used as an antisolvent in producing NaCl and Na_2CO_3 (Weingaertner et al. 1991). In another study, the recovery of NaCl using antisolvent crystallization with DiPA was examined (Zijlema et al. 2000). The reduction in energy costs (29%) was achieved and favorably comparable to on-site integrated steam power plant.

On the other hand, the effect of a drowning-out agent on the characteristics of membranes used in the MDC process should be considered because the decrease in liquid entry pressure (LEP) of a membrane degrades its ion rejection ability, resulting in decreased quality of produced water. It strongly depends on the type and concentration of alcohol (García-Payo et al. 2000). Ethanol has been widely used as a drowning-out agent. Increasing the ethanol concentration in the solution causes a linear decrease in the membrane's LEP (Gostoli & Sarti 1989).

2.5. Conclusion

Membrane distillation crystallization (MDC) is a promising technology, that can simultaneously recover clean water and valuable resources in crystal form, for treating various challenging hypersaline solutions (seawater reverse osmosis (SWRO) brine, produced water from oil fields and wastewater). It leads to resource recovery and additional water recovery, resulting in near zero liquid discharge theoretically. Previous and ongoing research clearly demonstrates the emerging attraction and feasibility of MDC technology for advanced wastewater treatment and desalination with resource recovery. However, there is still a lack of fundamental and practical research on MDC process for treatment of challenge solution in terms of recovery of both fresh water and valuable minerals.

This review discussed the theoretical background and state of current research on MDC process in terms of the treatment of these challenging water source. The challenges related to MDC performance and operations such as crystallization on the membrane surface, high energy consumption, membrane wetting and energy/cost efficiency were discussed. The following conclusions can be made:

- A substantial number of MDC research has been based on single component solution treatment such as NaCl, Na_2SO_4 and $CaCO_3$. It has set out to examine the feasibility of the MDC process in high concentration salt solution and the effect of operational conditions on MDC performance.

- The MDC process can potentially treat challenging solutions (simulated and raw solut ions) such as SWRO brine, produced water from oil fields and wastewater, and lead to the recovery of resources from the feed solution.

- There are some adverse issues in the MDC process that need to be ameliorated, such as crystallization on the membrane surface, membrane wetting and high energy cons umption. These were aggravated by the high concentration of inorganic contents and

specific contents of feed solution (e.g. oil in produced water; organic matter in waste water). The appropriate application of pre-treatment strategies should be considered to generate stable performance and prevent such problems.

- Cooling crystallization has been widely employed in the MDC process to intentionally induce supersaturation. However, this leads to the consumption of high energy because the feed solution should be reheated when the feed solution is transferred from cooling crystallizer to membrane module.

- Applying other crystallization techniques that have no effect on the temperature (i.e. no decrease in the temperature of the feed solution) and adverse phenomena (e.g. crystallization on the membrane surface and membrane wetting), may improve energy and cost considerations in real and practical scenarios. In order to dispel any concerns with the MDC process, further research on energy consumption and adverse phenomena are pertinent.

- The MDC researches have been conducted in the lab-scale. In order to apply it in real filed, the pilot-scale research is necessary. However, the experimental and theoretical information for MDC operation is not enough for scale-up. Hence, the further piratical research and theoretical analysis should be conducted.

CHAPTER 3

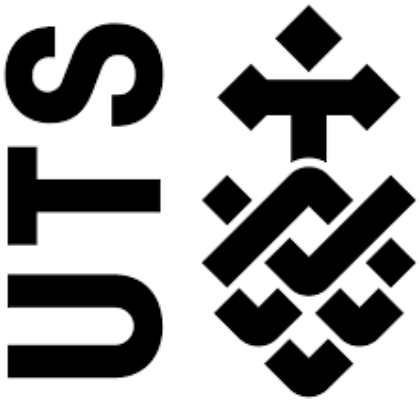

MATERIALS AND METHODS

3.1. Introduction

In this thesis, the feasibility of resource recovery and improving of brine recovery from SWRO brine was investigated by using S-MD, integrated submerged MD-adsorption and F-SMDC process. The experimental studies were conducted with the view of improving efficiency of different configuration of S-MD and S-Md hybrid systems. The methodologies adopted in this study are presented in this chapter.

3.2. Experimental procedure

3.2.1. Feed solution

3.2.1.1. Simulated SWRO brine

Simulated SWRO brine representing 50% recovery was used as a feed solution in S-MD and F-SMDC processes. The constituents in simulated SWRO brine is present in **Table 3-1**. Prior to the use of SWRO brine as a feed solution, the deionized (DI) water was used as a feed solution to evaluate the consistency/stability of S-MD and F-SMDC processes. The simulated SWRO brine contains only major components of SWRO brine such as Na^+, Mg^{2+}, K^+, Ca^{2+}, Cl^- and SO_4^{2-}. It was prepared with reagent grade salts (Sigma-Aldrich): sodium chloride (NaCl), calcium chloride dihydrate ($CaCl_2 \cdot 2H_2O$, magnesium chloride ($MgSO_4$), sodium sulfate (Na_2SO_4) and potassium chloride (KCl).

Table 3-1. Composition of simulated seawater reverse osmosis (SWRO) (50 % recovery).

Ion contents	Concentration (mg/L)
Sodium (Na^+)	24,433 – 24,641
Magnesium (Mg^{2+})	2,630 – 2,842
Potassium (K^+)	845 – 896
Calcium (Ca^{2+})	921-952 (0 for SWRO without Ca)
Chloride (Cl^-)	38,815 - 44,205
Sulfate (SO_4^{2-})	5,499 - 5,543

3.2.1.2. Feed solution for S-MD with different configurations

The consistency/stability of MD process performance and initial water flux were first evaluated with deionized (DI) water as feed solution. The MD performance was then investigated using a simulated solution representing 50% recovered SWRO brine (**Table 3-1**). Additional solutions/chemicals were used to investigate the specific phenomena in S-MD with different configurations. The effect of concentration polarization phenomenon on the performance of S-MD was examined in terms of permeate flux in S-MD using high concentration of NaCl (100 - 300 g/L) and Na_2SO_4 (400 g/L) single component solution.

3.2.1.3. Feed solution for integrated submerged MD with adsorption

The adsorption capacity of adsorbent and suitability of integrated submerged MD-adsorption process were evaluated with single rubidium (Rb^+) solution (5 mg Rb^+/L). The performance of integrated submerged MD-adsorption process was then investigated with a simulated SWRO brine (50 % recovery, R=50 %) (**Table 3-1**). Here, granular KCuFC was used as adsorbent. The concentration of other ions in SWRO brine was similar, however, 5 mg/L of Rb^+ was added into SWRO brine. Rubidium

chloride (Sigma-Aldrich) was used to spike Rb^+ concentration to 5 mg/L. The effect of $CaSO_4$ crystallization in integrated submerged MD-adsorption process was examined using two types of simulated SWRO brines: with Ca^{2+} and without Ca^{2+} in SWRO brine. The simulated SWRO brine without Ca^{2+} was considered as pretreated SWRO brine solution.

3.2.1.4. Feed solution for F-SMDC

The performance of F-SMDC process was investigated using Na_2SO_4 solution of 120 g/L. The solution containing sodium sulfate and sodium chloride was used to examine the effect of salinity and low temperature-sensitivity solubility component in F-SMDC (**Table 3-2**).

Table 3-2. Composition of model solution used in the F-SMDC.

Ions	Concentration (mg/L)
Sodium (Na^+)	58,320
Sulfate (SO_4^{2-})	81,150
Chloride (Cl^-)	30,020

Moreover, in order to examine the effect of different components (present in seawater brine) on the CG/TG formation in F-SMDC, different feed solutions were used individually; sodium chloride (NaCl), potassium chloride (KCl), ammonium chloride (NH_4Cl), sodium sulfate (Na_2SO_4), and magnesium sulfate ($MgSO_4$). NaCl is the representative material which has medium solubility variation with respect to solution temperature. The molecular weight of NaCl is medium. It is also the major compound in seawater brine. KCl was chosen as a representative material of relatively high MW. It has medium solubility variation with solution temperature. NH_4Cl has relatively low MW and high solubility variation with respect to solution temperature. All the three compounds are chloride ion (Cl^-)

based solutions, they enable the examination on the effect of electronegativity of cations on CG/TG formation. In order to compare the effect of anion's electronegativity on CG/TG, sulfate ion (SO_4^-) based solutions (Na_2SO_4 and $MgSO_4$) were used. The electronegativity values of the ions used in this study are shown in **Table 3-3**. In order to examine the induction time of crystals, the concentration of each compound in the feed solution was determined as the saturation concentration is reached at VCF 3 (at 20°C). The tendency of the movement of organic compound in F-SMDC was also examined using three representative model organic compounds namely; alginic acid (AA) (A7003, CAS NO. 9005-32-7, Sigma-Aldrich, St. Louis, MO), humic acid (HA) (53680, CAS No. 1415-93-6, Sigma-Aldrich, St. Louis, MO), and bovine serum albumin (BSA) (A2135, CAS No. 9048-46-8, Sigma-Aldrich, St. Louis, MO). They represent polysaccharides, humics, and proteins, respectively. The organic compound concentration of feed solution was 20 mg/L. It was filtered using GF/C (glass microfiber filters, Whatman) before the usage. The components of feed solution are shown in **Table 3-4**.

Table 3-3. The electronegativity of anion and cation (Allred 1961).

Cations	Electronegativity	Anions	Electronegativity
K^+	0.82	Cl^-	2.16
Na^+	0.93	H^-	2.20
Mg^{2+}	1.31	S^-	2.58
N^+	3.04	O^-	3.44

Table 3-4. Component of feed solution used to study the effect of inorganic and organic compounds.

Component	Concentration (ppm)
Sodium sulfate (Na_2SO_4)	71,020
Dissolved organic carbon (DOC)	12.41
→ HOC (Hydrophobic)	1.85
→ CDOC (Hydrophilic)	10.56
→ Bio-polymer	0.09
→ Humic subst. (HS) + Building blocks	8.90
→ LMW	2.57

In Na_2SO_4 recovery from simulated SWRO brine, the feasibility of F-SMDC was examined using three SWRO brine solutions: (1) real SWRO brine (**Table 3-5**), (2) simulated SWRO brine (50% recovered) and (3) simulated SWRO brine (50% recovered (R = 50%)) without Ca^{2+}. And, an influence of low temperature-sensitivity solubility component in F-SMDC was studied using single 1M sodium chloride solution.

Table 3-5. Composition of real SWRO brine from a seawater desalination plant.

Ion contents	**Concentration (mg/L)**
Sodium (Na^+)	22,150
Magnesium (Mg^{2+})	2,500
Potassium (K^+)	770
Calcium (Ca^{2+})	880
Chloride (Cl^-)	41,300
Sulfate (SO_4^{2-})	8,120

3.2.1.5. Feed solution for the tendency of $CaSO_4$ in high salinity solution

The tendency of $CaSO_4$ crystallization in high salinity solution was evaluated using synthetic standard feed solution containing Ca^{2+}, Na^{+}, Cl^{-} and SO_4^{2-}. Their concentration were twice higher as seawater (to represent 50% recovered SWRO brine). It was prepared using calcium chloride dihydrate, sodium chloride and sodium sulfate. The composition is presented in **Table 3-6**.

Table 3-6. Composition of the standard feed solution for the $CaSO_4$ crystallization experiment.

Ions	**Concentration (mg/L)**
Calcium (Ca^{2+})	1,620
Sodium (Na^{+})	51,460
Chloride (Cl^{-})	73,770
Sulfate (SO_4^{2-})	11,520

3.2.2. Membrane and submerged membrane module

In this research, polyvinylidene fluoride (PVDF) hollow fiber membrane supplied by Econity (Republic of Korea) was used in S-MD, integrated submerged MD-adsorption and F-SMDC processes. This membrane has an inner and outer diameter of 0.7 mm and 1.2 mm, respectively, a nominal pore size of 0.1 μm, wall thickness of 250 μm, contact angle of 106° ± 2, and liquid entry pressure (LEP) of 2.0 - 2.3 bar. The membrane module consisted of 18 fibers potted on both sides (each fiber of 0.2 m length) with the effective membrane area was 0.0136 m^2.

3.2.3. Experimental methods and lab-scale experimental set-up

3.2.3.1. Submerged-membrane distillation (S-MD)

3.2.3.1.1. Lab-scale S-MD set-up

Three different S-MD configurations were used in this study: submerged-direct contact MD (S-DCMD), submerged-vacuum MD (S-VMD) and submerged vacuum enhanced DCMD (S-VDCMD) (**Figure 3-1**). All experiments with different configurations were conducted in same feed solution temperature (55 °C), and it was maintained using heater. The temperature was monitored by temperature sensor which is placed in the feed tank to measure the temperature of feed solution in real time. The feed solution was stirred at 200 rpm (Reynolds number (R_e) over 90,000) for turbulent flow in the feed tank. In S-DCMD and S-VDCMD, the temperature and flow rate of the permeate stream was set at 20 °C and 0.5 L/min, respectively. The temperature of the permeate stream was monitored by temperature sensor which is placed upstream of membrane module, and it was maintained using cooling water bath with circulator. In S-VMDC and S-VDCMD, the vacuum pump was applied in the permeate tank. The permeate vapor coming from feed solution through the membrane was condensed by a glass condenser placed in the permeate side. The details of experiment conditions are explained in chapter 4.

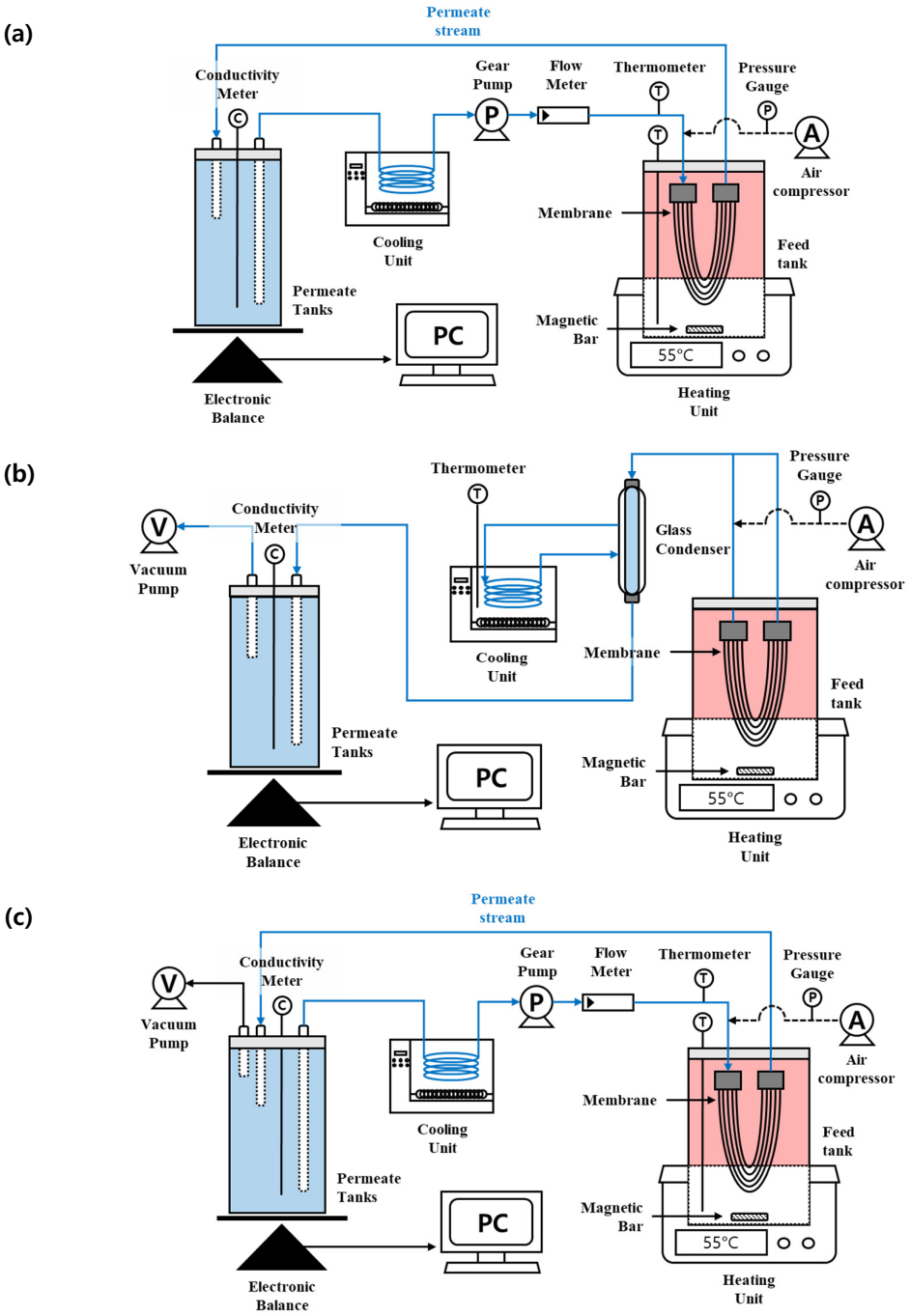

Figure 3-1. Schematics of lab-scale S-MD set-up with different configuration: (a) submerged-direct contact membrane distillation (S-DCMD), (b) submerged-vacuum membrane distillation (S-VMD) and (c) submerged-vacuum enhanced direct contact membrane distillation (S-VDCMD).

3.2.3.1.2. Air-back washing

The air backwashing methods was used to recover the performance of MD caused by the fouling and scaling in the membrane (on the surface and in the pores of membrane). The basic mechanism is same as the water backwashing of hydrophilic membrane. However, the high hydrophobicity of membrane is essential for high rejection in MD. The backwashing using water leads to reduction of the membrane hydrophobicity. In air backwashing, the air (gas phase) was used instead of liquid phase (**Figure 3-2**). Determination of pressure applied is important because of potential of wetting by water remaining inside membrane. The pressure applied should not lead to the water penetration through the pores of membrane. So, lower pressure than liquid entry pressure (LEP) was directly applied in lumen side of membrane by the air compressor (LEP of the membrane used in this study: 2.3 bar) (**Figure 3-1**). In this study, the air was applied through the inside to out of membrane for 2 mins at a pressure of 2 bar. It was conducted after the operation of MD operation.

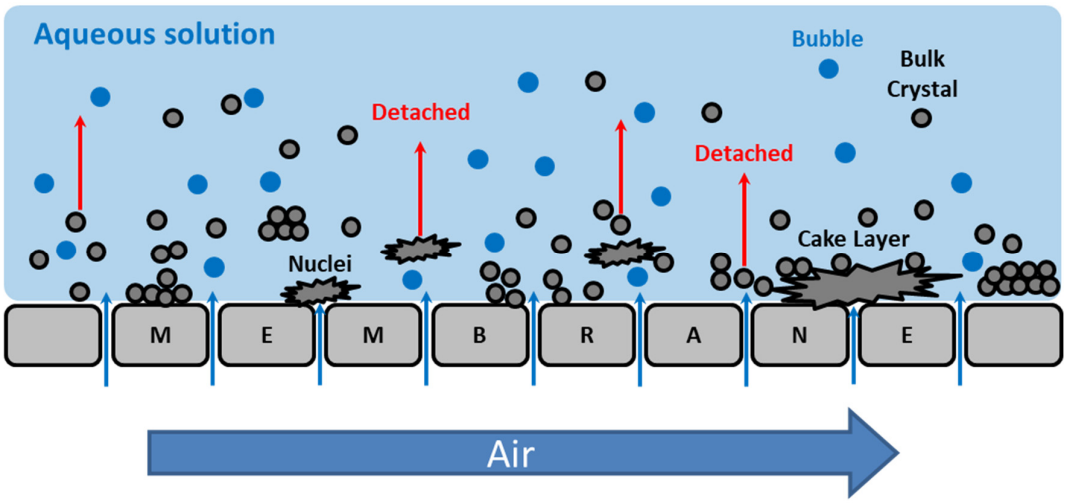

Figure 3-2. Mechanism of fouling and scaling removal from the membrane with air backwashing.

3.2.3.2. Integrated submerged MD-adsorption

3.2.3.2.1. Lab-scale integrated submerged MD-adsorption set-up

The integrated submerged MD-adsorption system was used for simultaneous recovery of rubidium and clean water from SWRO brine. The membrane module used was the same as the one used in S-MD. The submerged membrane module and adsorbent was placed in double jacked reactor (**Figure 3-3**). The single reactor played a role of membrane and adsorption reactor. This study was conducted at same experimental conditions as that of S-DCMD experiment. The raw feed solution was continuously supplied from a reservoir to the reactor. The supply rate to the feed solution from the feed reservoir to the reactor was dependent on the permeate flux. The permeate water quality was monitored in real time in terms of conductivity using potable conductivity meter (HQ40d multi, Hach). The details of experiment are discussed in chapter 5.

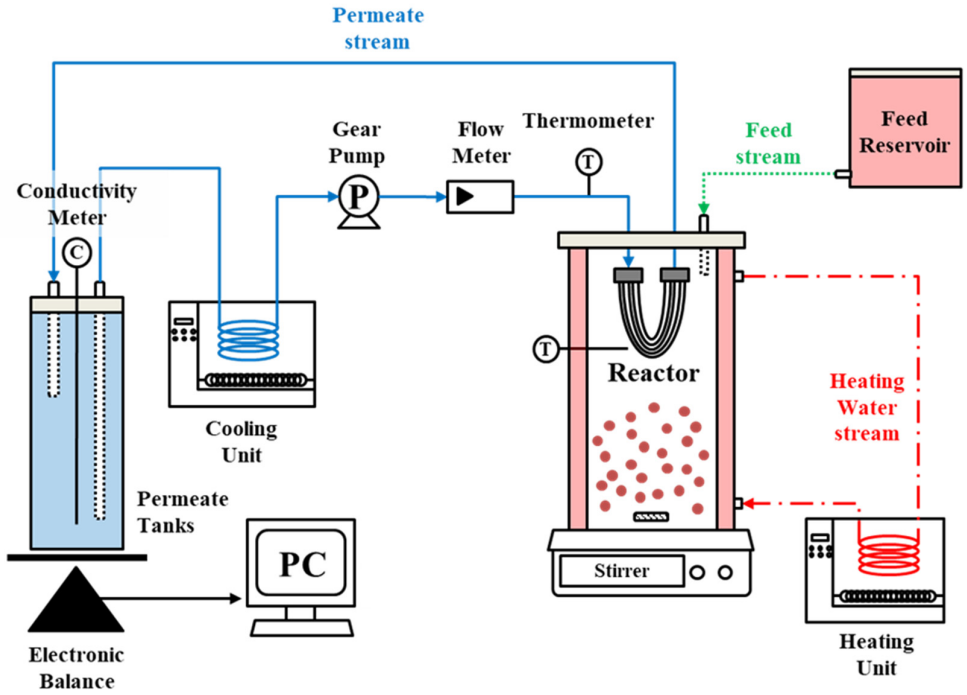

Figure 3-3. Schematic of lab-scale set-up of integrated submerged MD-adsorption system.

3.2.3.2.2. KCuFC adsorbent

The granular potassium copper hexacyanoferrate (KCuFC) encapsulated by polyacrylonitrile (PAN) was used as adsorbent in the integrated submerged MD-adsorption system. The performance of three different KCuFC adsorbents namely powder form (< 100 μm), particle form (mean size: 0.45 mm) and granular form (mean size: 2.42 mm) was evaluated. The size of adsorbent was measured using microscopy with image analyzer (ImagePro 7). The detailed preparation method of KCuFC adsorbents is presented in our previous research (Naidu et al. 2018; Naidu, Loganathan, et al. 2016).

3.2.3.2.3. Rb adsorption equilibrium

Equilibrium adsorption experiments of different sizes of KCuFC adsorbents were conducted using batch equilibrium adsorption test to evaluate the difference of adsorption capacity of different form/size adsorbents. KCuFC adsorbents were dosed in the range of 0.06 to 0.65 g/L. The feed solution was 70 mg/L of Rb^+. The pH_{eq} and temperature were kept at 7.0 ± 0.8 and 55 °C.

3.2.3.3. Fractional-submerged membrane distillation crystallizer (F-SMDC)

3.2.3.3.1. Lab-scale set-up of F-SMDC

F-SMDC process with S-DCMD configuration is based on the formation of concentration gradient (CG) and temperature gradient (TG) in the reactor along the height of reactor. This enhances the performance of both S-MD and crystallization processes. The membrane module was placed at the top portion of the reactor (**Figure 3-4**). The reactor is equipped with double wall to enable the control of TG as the temperature control of feed solution is essential in the reactor (**Figure 3-5**). The partition in the shape of funnel (length = 25 mm, and hole diameter = 20 mm) was installed between the top and bottom portion. F-SMDC reactor consisted of three cylindrical cells. The total reactor volume is 1,740

mL. The top portion consisted of two cylindrical cells, and the bottom portion consisted of one cylindrical cell. A funnel-shaped partition was placed between the top and bottom portions. It acts as a barrier/trap which minimizes mixing of solution through convection caused by temperature control. The temperature of feed solution at the top and at the bottom portions of the reactor was maintained at 50.0 ± 1.2 °C and 20.0 ± 1.3 °C, respectively. The temperature at the top and bottom portions was controlled using water bath with circulator (heating and cooling). The temperature of feed solution at each portion was measured by temperature sensors placed along the reactor. The raw feed solution was provided continuously/automatically from feed reservoir by gravity to the top portion of the reactor. Temperature of the feed solution in the reservoir and permeate stream was maintained at room temperature (23.2 ± 0.3 °C) and 16.5 ± 0.3 °C, respectively. The permeate temperature was measured using temperature sensors placed prior to the membrane module. A constant permeate flow rate of 0.5 L/min was maintained using a gear-pump. The water quality of permeate in terms of conductivity was monitored using a potable conductivity meter (HQ40d multi, Hach) in real-time. Feed samples were collected regularly from the top and bottom portions separately. External crystallizer was used to extract the crystals from the bulk solution remained at the top portion during the last stage of F-SMDC operation. The Details on the operation of external crystallizer is explained in chapter 6.

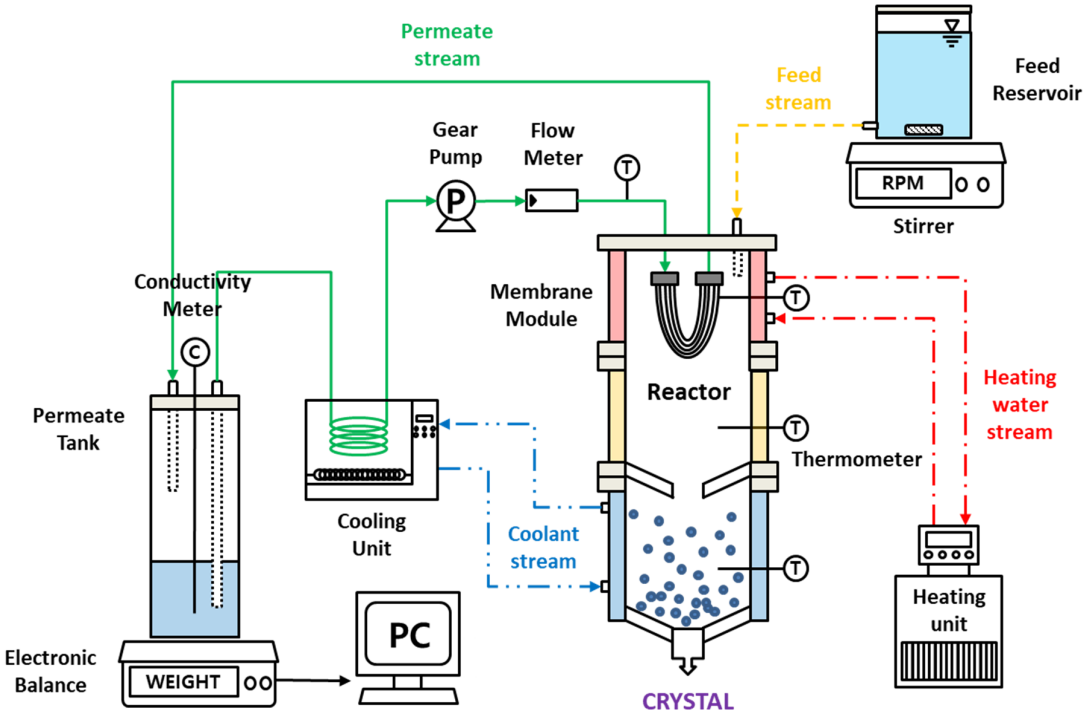

Figure 3-4. Fractional submerged membrane distillation-crystallization (F-SMDC) set-up: the permeate stream (——), the stream of continuous feeding to the reactor (from feed reservoir) (——), the stream of heating water (—·—), the coolant stream (—··—).

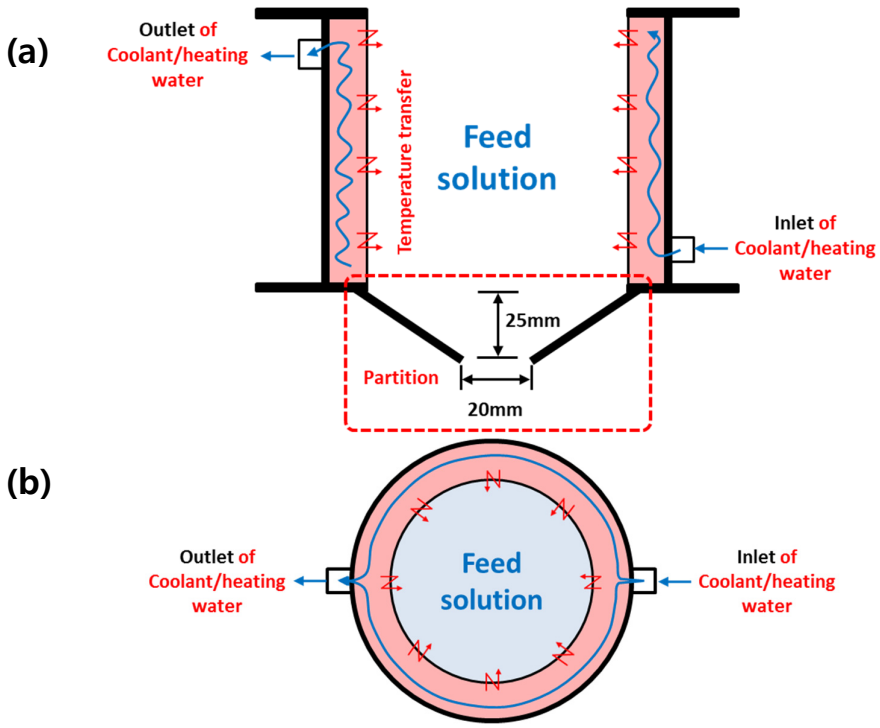

Figure 3-5. Details of F-SMDC reactor showing the double wall feature for generating temperature gradient (heating in the top portion of the reactor and cooling at the bottom portion of the reactor): (a) Cross-sectional view, and (b) Aerial view.

3.2.3.3.2. Membrane washing

Calcium sulfate ($CaSO_4$) crystals deposited on the membrane surface and in the pores of membrane was removed by air back-washing for 3 mins at a pressure of 2 bar (under LEP of the membrane used in this study). In the experiment with ammonium sulfate, the membrane was washed using deionized water. A stirring at 250 rpm was provided for 5 mins.

3.2.3.3.3. Masking a sulfate-rich condition

The sodium sulfate (Na_2SO_4), magnesium sulfate trihydrate ($MgSO_4 \cdot 3H_2O$) and ammonium sulfate ($(NH_4)_2SO_4$) were used to make a sulfate-rich condition of SWRO brine in the reactor. In case of addition of Na_2SO_4, 120 g/L Na_2SO_4 was used as feed solution from beginning (VCF 1) to VCF 2.5 to create sulfate-rich condition and well formation of CG in the reactor prior to the feeding of simulated

SWRO brine (without further addition of Na_2SO_4). From VCF 2.5 to the end of operation, only SWRO brine was fed as feed solution.

In the case of addition of $MgSO_4 \cdot 3H_2O$ and $(NH_4)_2SO_4$, a same concentration of 200 g/L was added into the simulated SWRO brine solution, and the reactor was filled up with the sulfate-rich SWRO brine. After that, the simulated SWRO brine was used as feed solution without any further addition of $MgSO_4 \cdot 3H_2O$ and $(NH_4)_2SO_4$.

3.2.3.4. Calcium sulfate ($CaSO_4$) crystallization

3.2.3.4.1. Batch crystallization

The tendency of $CaSO_4$ crystallization in the concentrated brine was examined using batch experiments (heating temperature: 60 °C, pH 7.0, and stirring speeds: 200 and 50 rpm). The effect of temperature, pH, other ions concentration (inorganic components), organic components and mixing intensity on $CaSO_4$ crystallization was examined. The feed was NaCl, Na_2SO_4, and $CaCl_2 \cdot 2H_2O$.

A 500 mL feed solution was first prepared in a beaker with pH adjusted using 0.1M HCl and 0.1M NaOH (pH 7.0). In order to examine the effect of temperature on $CaSO_4$ crystallization, feed solutions were heated in a water bath. The feed solutions were heated to 50 °C, 60 °C, and 80 °C in a water bath to examine the effect of temperature on $CaSO_4$ crystallization. When studying the influence of inorganic and organic components, pre-determined component was added into the feed solution at standard condition. After that, the feed solutions were mixed in a jar-tester at a high speed (200 rpm) for 2 min to achieve complete mixing and then allowed to stand for 24 h at a room temperature with a low speed stirring (50 rpm). Slow mixing is provided to facilitate crystallization. Subsequently, after 24 h, the crystals formed were separated from the solution by using a glass microfiber filter (Whatman,

Grade GF/C, pore: 1.2 μm). The effect of mixing (intensity) on the $CaSO_4$ crystallization tendency was also evaluated. The mixing was applied in a jar tester at different speeds (0 rpm, 20 rpm, and 150 rpm) following a high-speed mixing (200 rpm for 2 min). The procedure of batch crystallization experiment is depicted in **Figure 3-6**.

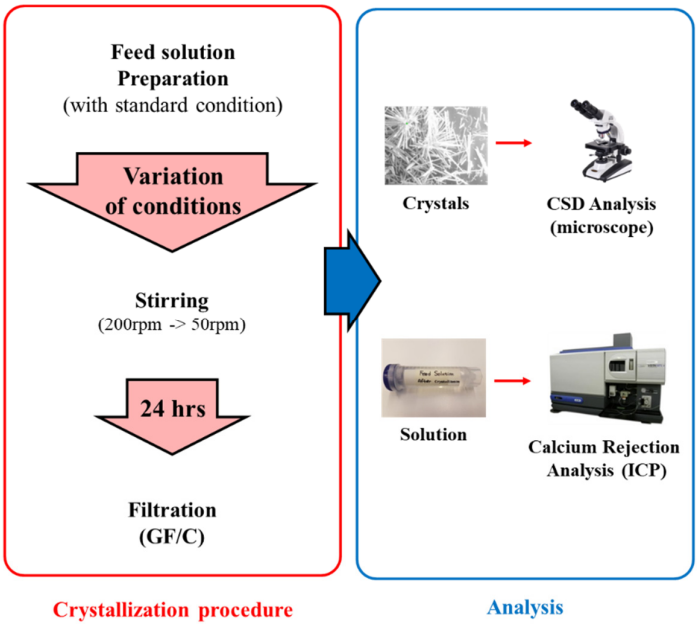

Figure 3-6. Schematic diagram of batch crystallization procedure and analysis.

3.2.3.4.2. Chemicals

The characteristics of SWRO brine depend on the seawater quality, the recovery ratio of the SWRO plant, the pre-treatment methods, and the chemical cleaning methods of the membrane used in the SWRO plant (Chelme-Ayala et al. 2009; Greenlee et al. 2011; Pérez-González et al. 2012; Squire et al. 1997). This SWRO brine contains various ions in addition to the chemical components that are used in the pre-treatment processes and chemical cleaning of RO membrane. Additionally, brine contain organic components at higher concentration compared to seawater. In order to examine the influence of them, the chemical and organic components were mixed into the standard feed solution. The

additives used are presented in **Table 3-7**.

Table 3-7. The additives in the standard feed solution.

Means in SWRO		**Chemicals**
Other ions in brine	HCO_3^-	Sodium bicarbonate ($NaHCO_3$)
	Mg^{2+}	Magnesium chloride hexahydrate ($MgCl_2 \cdot 6H_2O$)
	K^+	Potassium chloride (KCl)
Chemical washing agent		Ethylene diamine tetraacetic acid (EDTA, $C_{10}H_{16}N_2O_8$)
Coagulant		Ferrous sulfate ($FeSO_4$) Ferric chloride ($FeCl_3$)
Organic component		Model organic compounds • Alginate (AA) (to represent polysaccharides) • Humic acid (HA) (to represent humics) • Bovine serum albumin (BSA) (to represent proteins)

3.2.3.4.3. Physical factors

Both in water treatment and crystallization processes, the mixing (physical mixing and aeration) are used to maintain a homogeneous condition without any precipitation and polarization in the reactor and mitigate the membrane fouling of membrane in the water treatment process. The application of physical devices generates kinetic energy and affects the formation and growth of $CaSO_4$ crystals in the solution (Akrap et al. 2010). In this study, the effect of agitation (mixing) was evaluated on the $CaSO_4$ crystallization tendency.

3.3. Analysis

3.3.1. Crystal analysis

The morphology and identifying the type of crystal formed in the membrane, bulk solution and adsorbent surface was characterized using a field emission scanning electron microscopy-energy dispersive X-ray (FESEM-EDX, Zeiss supra 55VP, Carl Zeiss AG). In case of the crystals formed in the membrane, a cross-sectional membrane samples were also observed to examine the crystallization phenomenon in the pores of the membrane as well as on the surface of membrane. Prior to SEM analysis of crystals formed, the membrane surface was gently flushed with deionized (DI) water to remove crystals formed in the bulk solution.

Prior to the analysis of crystals (in terms of the size distribution and weight), the crystals in the solution was vacuum filtered using a glass microfiber filter (Whatman, Grade GF/C, pore = 1.2 μm). The crystals were then dried at room temperature (23.2±0.3 °C) for 120 h and the mass of crystals dried was measured using an electronic balance. The size distribution and morphology of crystals were analyzed using a microscopy method. In this method, at least 70 (range of 70 to 150) crystals were randomly selected, and size of each crystal was measured using microscope with an image analyzer (ImagePro7). The crystal sizes were then quantified with a crystal size distribution (CSD) procedure.

3.3.2. Water quality and concentration of solution

The water quality and concentration of salt were measured by two analyzers. The ion concentrations and contents of the model synthetic brine solution were characterized by using inductively coupled plasma optical emission spectrometry (ICP-OES (Optima7300DV- ICP-OES Perkin Elmer, USA) and ICP-MS (Agilent 7500, Agilent, USA)). In study of F-SMDC, the concentrated of feed solution was

measured using pre-calibrated conductivity curves made using different concentration of each chemical (NaCl, KCl, NH_4Cl, Na_2SO_4 and $MgSO_4$). The variation of water quality in the permeate was monitored using a potable water quality meter (HQ40d multi, Hach) in real time.

The concentration and content of organic compounds in the solution was characterized using total organic carbon (TOC) analyser (multi N/C 3100, analytik jena, Germany) and a dual column liquid chromatography organic carbon detector (LC-OCD). The detailed fractional variation of organic compounds was evaluated using a LC-OCD analyzer coupled with size exclusion chromatography column (Toyopearl TSK HW50S column (TOSOH Bioscience GmbH, Stuttgart, Germany)) (Jeong et al. 2016). In LC-OCD analysis, total dissolved organic carbon (DOC) is categorized into hydrophilic (bio-polymer, humic substance, building block, and low molecular weight (LMW) material) and hydrophobic (hydrophobic organic compound (HOC)) fraction (Naidu, Jeong, Kim, et al. 2014).

3.3.3. Numerical analysis

Volume concentration factor (VCF) can be calculated from the reactor volume and the amount of produced fresh water. The calculation of VCF is different for continuously supplying feed into reactor. In case of no continuous supply of feed water, the VCF value was calculated using the following equation:

$$\mathrm{VCF} = \frac{V_{reactor}}{V_{reactor} - V_{total,\ permeate}}$$

Where, $V_{Reactor}$ is the reactor volume, and $V_{total,permeate}$ is the total amount of permeate produced. In S-MD experiments, above calculation methods was used. In the study of F-SMDC and integrated submerged MD-adsorption, continuous supply of feed solution was provided at the same rate of produced fresh water. Thus, the feed solution concentration in the rector would increase while the total

volume of feed solution is maintained constant, if the rejection ratio of produced fresh water is 100% over time. In this context, the VCF value was calculated as:

$$\mathrm{VCF} = \frac{V_{reactor} + V_{total,\ permeate}}{V_{reactor}}$$

In F-SMDC, the formation of concentration gradient (CG) was evaluated based on concentration gradient ration (C_{Bottom}/C_{Top}) and normalized concentration increase (C_t/C_0). The capacity of the adsorbents was evaluated using adsorption rate of Rb (mg Rb/h), concentration variation ration compared to initial concentration (m_t/m_0) and cumulative mass of Rb adsorbed (mg). The m_t/m_0 is the ratio of adsorbed mass at time ($_t$) and zero ($_0$).

CHAPTER 4

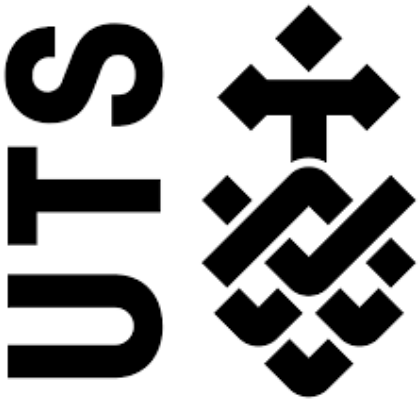

EXPERIMENTAL COMPARISON OF SUBMERGED MEMBRANE DISTILLATION CONFIGURATIONS FOR CONCETRATED BRINE TREATMENT

This chapter has been published as: **Y. Choi**, G. Naidu, S. Jeong, S. Vigneswaran, S. Lee, R. Wang, A.G. Fane, Experimental comparison of submerged membrane distillation configurations for concentrated brine treatment, Desalination, 420 (2017) 54-62.

4.1. Introduction

Membrane distillation (MD) is a promising technology for treating seawater reverse osmosis (SWRO) brine to increase SWRO recovery ratio (producing additional high quality water) while systematical reducing brine volume, potentially achieving near zero liquid discharge in desalination plants (Gryta 2016). MD is driven by a thermal gradient between the hot feed and cold permeate separated by a porous and hydrophobic membrane barrier. Water vapor evaporated from feed solution, is transported through the pores of the hydrophobic membrane, and condenses at the permeate side (Gryta 2002). The benefit of having no hydraulic pressure restriction and the possibility of obtaining high solute rejection have led to much attention on the application of MD for treating highly saline feed solutions (Chen et al. 2014; Creusen et al. 2013; Edwie & Chung 2013; Gryta 2002; Ji et al. 2010; Jiang et al. 2016; Julian et al. 2016; Meng, Ye, et al. 2015). Further, the MD process is able to concentrate feed water to a supersaturated state, forming salt crystals (Naidu, Jeong, Kim, et al. 2014). As such, apart from producing fresh water, the recovery of salts can be achieved using MD coupled with crystallization process (Chen et al. 2014; Creusen et al. 2013; Edwie & Chung 2013; Gryta 2002; Ji et al. 2010; Jiang et al. 2016; Julian et al. 2016; Meng, Ye, et al. 2015). However, MD has several drawbacks such as polarization effects (concentration and temperature polarizations), scaling, fouling and high thermal energy consumption as well as heat loss (Bouchrit et al. 2015). Polarization effect causes a decrease in MD driving force, and scaling and fouling development impairs the MD membrane (Naidu, Jeong, et al. 2016; Sanmartino et al. 2016). While the thermal consumption can be addressed with alternative energy sources (Duong, Cooper, et al. 2016; Shim et al. 2015), heat loss in a conventional cross flow MD set-up is inevitable. The bulk feed solution temperature tends to reduce as the feed solution is channeled out to the membrane module. The heat loss tendency in MD accelerates at higher feed flow rate requiring rapid reheating to maintain a constant feed solution temperature, invariably, compromising the efficiency of the MD operation (Cath et al. 2004; Li &

Sirkar 2017). For instance, a hollow fiber DCMD unit for desalination treatment was used and reported heat loss through the surface area as the solution was channelled from cooling/heating reservoirs to the membrane module (Li & Sirkar 2017). The study recommended approaches such as optimizing the design and insulating the equipment to minimize the heat loss.

In this context, a submerged MD (S-MD) in which the membrane module is submerged directly in the feed solution tank, eliminates the need for feed recirculation and reheating, thereby, potentially minimizing heat loss (Julian et al. 2016). The feasibility of S-MD has been explored in a few studies (Khaing et al. 2010; Phattaranawik et al. 2008; Phattaranawik et al. 2009; Tomaszewska & Białończyk 2013). However, these studies are primarily focused on the application of submerged MD bioreactors. Recently, the performance of a submerged direct contact MD (S-DCMD) was compared with a conventional cross flow DCMD system for seawater desalination, indicating the beneficial performance of S-DCMD (Francis et al. 2015). Nevertheless, a detailed investigation of S-MD system for SWRO brine treatment is still lacking, especially the aspect of scaling development. It must be acknowledged that directly submerging MD membrane modules into the SWRO brine feed containing high sparingly soluble salts could result in the occurrence of severe scaling on the membrane. Therefore, the scaling development and its reversibility are important factors to determine the feasibility of S-MD application for SWRO brine.

Moreover, most previous studies have been focusing on the S-DCMD configuration. Apart from S-DCMD, the potential of different S-MD configurations with the application of vacuum (submerged vacuum DCMD; S-VDCMD and submerged vacuum MD; S-VMD) should be examined. Particularly, the influence of feed temperature and concentration may vary in different S-MD configurations affecting the overall performance in treating SWRO brine (Duong, Duke, et al. 2016). Moreover, several studies to improve the performance of MD process have also reported on mitigation methods

to these effects. For instance, the effect of transverse vibration on polarization effects with air backwashing and aeration was compared (Meng, Hsu, et al. 2015). In another study, the effect of bubbling and hydrodynamic on the fouling reduction to control fouling in submerged membrane process as a fouling mitigation mechanism was investigated (Ndinisa et al. 2006).

Therefore, the results presented in this chapter compares the performance of three different S-MD configurations (S-DCMD, S-VDCMD and S-VMD) for the treating of SWRO brine. The most suitable S-MD configuration for treating SWRO brine was identified based on the evaluation of baseline permeate flux (deionized water as feed solution), influence of feed concentration (sodium chloride as feed solution) and feed temperature (sodium sulfate as feed solution). The performance of the most suitable S-MD configuration for SWRO brine was evaluated in a continuous operation with air backwashing as a membrane cleaning mitigating to reverse scaling and restore the flux.

4.2. Materials and Methods

The experiments were carried out with S-VMD, S-DCMD and SVDCMD configurations. The effective area of the membrane was 0.0136 m^2 for all the configurations. The feed solution temperature (T_f) was maintained at 55°C by using a heater. A temperature sensor was placed in the feed tank to measure the temperature in real-time. The feed solution was stirred at 200 rpm, enabling to achieve a turbulent flow with a Reynolds number (*Re*) over 90,000. In the case of both S-DCMD and S-VDCMD (**Figure 3-1 (a)** and **(c)**, respectively), the permeate flow rate was set at 0.5 L/min. Permeate temperature (T_p) was maintained at 20 °C by using a chiller, and it was measured using a temperature sensor in the permeate line prior to the membrane module. For S-VMD, a glass condenser was placed on the permeate side to condense the vapor from the membrane (**Figure 3-1 (b)**). The cooling water temperature (T_c) for condensing the vapor was 10 °C. To apply vacuum pressure for S-VMD and S-VDCMD, a vacuum

pump was installed in the permeate tank. The vacuum pressure applied on S-VMD was 50 mbar. The S-VMD was set at an average 50 mbar based on numerous VMD studies that have applied vacuum from a range of 20 mbar up to 100 mbar (Julian et al. 2016; Li & Sirkar 2017; Mericq et al. 2010; Zuo et al. 2017). S-VDCMD was tested with two different vacuum pressures (500 mbar and 700 mbar) by applying partial vacuum to the permeate tank. The permeate flux was calculated based on the weight difference with time using an electronic balance. All the experiments were repeated to ensure the reproducibility.

The method of air backwashing was adopted to study the reversibility of scaling and fouling on the membrane surface and in the pores of the S-DCMD membrane. Upon the occurrence of flux decline, the S-DMCD operation was stopped and air backwashing was separately carried out for duration of 2mins with 2 bar pressure. This pressure was chosen to ensure lower pressure than the membrane LEP (2.3 bar) to avoid the possibility of water penetration due to membrane wetting and prevent membrane damage while trying to achieve maximum force for effectively detaching the deposited crystals.

4.3. Results and discussion

4.3.1. Baseline performance (DI water as feed solution)

In this study, a baseline test was carried out to compare the performance of the three S-MD configurations (S-DCMD, S-VMD and S-VDCMD) using the same module and experimental conditions (T_f = 55 °C, T_p = 20 °C, T_c = 10 °C and v_p = 0.66 m/s) with the exception of varying permeate pressure in the presence of vacuum for S-DCMD (500 and 700 mbar) and S-VMD (50 mbar). DI water was used as the feed solution to compare the permeate flux trends without the effect of concentration polarization (CP).

An initial permeate flux of 7.94±0.54 L/(m^2·h) (LMH) was obtained with S-DCMD. Comparatively,

an increased permeate flux was observed with S-VMD (77%) and S-VDCMD configurations (13-26%) (**Figure 4-1**). A lowered permeate pressure (increased vacuum pressure) in S-VDCMD resulted in the increase of permeate flux, from 8.93±0.50 LMH at 700 mbar to 10.08±0.59 LMH at 500 mbar. The higher permeate flux in S-VMD (50 mbar) compared to S-DCMD and S-VDCMD (500 mbar and 700 mbar) was attributed to the higher driving force. In S-VDCMD, higher water flux was achieved than in S-DCMD due to combination of lower permeate pressure (application of vacuum in the permeate) and vapor pressure difference (temperature difference). The same observation was made in a previous study comparing the performance of DCMD and V-DCMD [32]. The presence of vacuum in S-VMD at 50 mbar resulted in 27% permeate flux increment compared to S-DCMD. It is well established in MD studies that a higher vacuum condition creates a higher driving force, resulting in higher permeate flux (Naidu, Shim, et al. 2017). Nevertheless, in spite of the high vacuum condition, the permeate flux increment in S-VMD (50 mbar) was only marginally higher to S-VDCMD (500 mbar). In this context, it is worth mentioning that at the end of the experiment, a pattern of increased wall thickness was observed on the used S-VMD membrane compared to the used S-DCMD and S-VDCMD membranes. The thicknesses of the used S-MD membrane were measured using SEM analysis of the membrane cross sections. The results (**Table 4-1**) confirmed the observation of increased membrane thickness under vacuum condition. It appears that the membrane structure could not be retained under high vacuum pressure applied in the lumen side of the membrane. The change of membrane structure may have increased the membrane resistance in S-VMD (50 mbar), resulting in only slightly higher permeate flux compared to S-VDCMD (500 mbar).

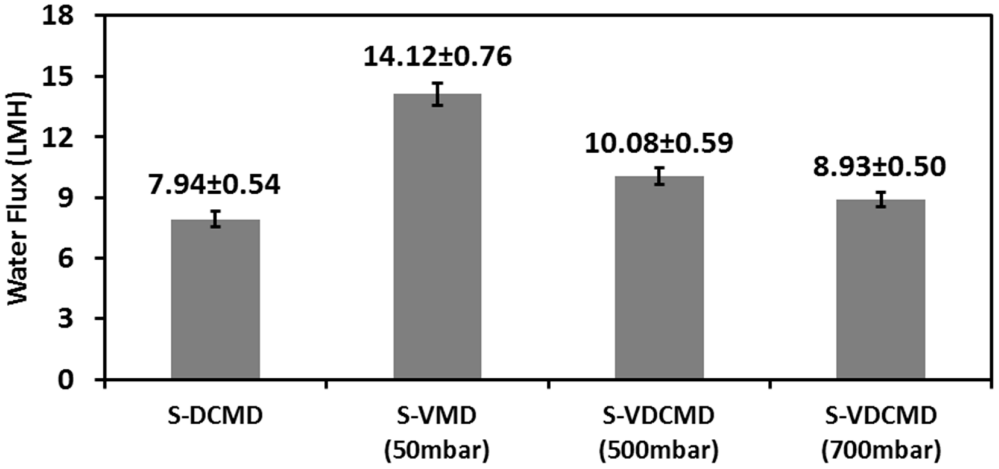

Figure 4-1. Base line test comparing the water flux of different S-MD configurations (feed solution = DI water, operating period = 1h, T_f = 55 °C, T_p = 20 °C, T_c = 10 °C and v_p = 0.66 m/s).

Table 4-1. The change of membrane wall thickness after operation in different configuration.

Membrane in each configuration	Wall Thickness of membrane (μm)
Virgin	240.07 ± 6.70
S-DCMD	246.53 ± 9.80
S-VMD (50 mbar)	286.81 ± 9.10
S-VDCMD (500 mbar)	267.80 ± 2.21
S-VDCMD (700 mbar)	265.97 ± 8.37

4.3.2. Influence of operating condition

A set of experiments were carried out to study the influence of operating conditions with different S-MD configurations. These experiments were carried out with high concentration NaCl and Na_2SO_4 solutions, to understand the influence of operating conditions, namely feed concentration and feed temperature on the S-MD configurations. Further, a simple energy/economic comparison between the different configurations was discussed.

4.3.2.1. Feed concentration

The concentration of feed solution plays an important role in determining the initial permeate flux that can be obtained with respect to vapor pressure reduction. In this study, the influence of feed concentration on S-MD performance was examined based on the pattern of permeate flux obtained using high concentration of NaCl (100-300 g/L) as feed solution. This observation was carried out using S-DCMD to represent the presence of vapor pressure, S-VMD (50 mbar) to represent the presence of high vacuum and S-VDCMD (500 mbar) to represent the presence of a combination of vapor pressure with vacuum.

In all three S-MD configurations, a similar pattern of flux decline with the increase of NaCl concentration was observed (**Figure 4-2**). However, the flux decline rate was significantly different in the three configurations. The flux decline rate was in the order of S-VMD (50 mbar) > S-VDCMD (500 mbar) > S-DCMD. The results indicated the higher sensitivity of S-VMD towards feed concentration compared to the other configurations. Similar observation was reported by other MD studies (Ali et al. 2013; Meng, Hsu, et al. 2015).

A highly concentrated feed solution tends to increase the resistance of ions at the membrane surface boundary layer. This can potentially interfere with vapor movement from feed to permeate side in the MD process. In S-DCMD, the mass transfer occurrence from feed to permeate solution would be minimally influence by the presence of these ions around the membrane boundary layer. This is because S-DCMD is driven by vapor pressure attributed to temperature difference (hot feed and cool permeate solution). However, in S-VMD, the main driving force is the interaction of applied vacuum pressure and vapor pressure (hot feed temperature). These indicated that the vacuum pressure (50 mbar) worked on mass transfer with stronger driving force than S-DCMD. In addition, it leaded to the attracting and holding the ions presented in the feed solution near the membrane surface, resulting in the faster and serious membrane crystallization (deposition and growth of crystals on the membrane

surface) (Meng, Ye, et al. 2015). As a result, higher concentration layer occurs on the S-VMD membrane boundary layer. The higher concentration layer interferes with mass transfer of vapor. In line with this, as shown in **Figure 4-2**, S-VMD was more sensitive to increase of feed concentration.

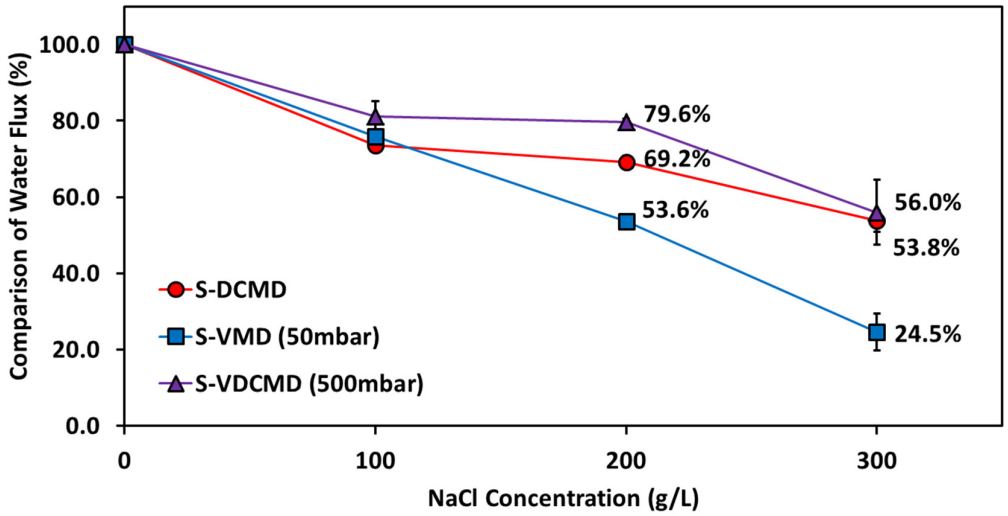

Figure 4-2. Comparison of permeate fluxes after one hour operated at different feed concentrations of NaCl (feed solution = NaCl solution, operating period = 1h, T_f = 55 °C, T_p = 20 °C, T_c = 10 °C and v_p = 0.66 m/s).

4.3.2.2. Solution temperature

The influence of feed temperature and potential temperature losses due to the contact with cold permeate solution in the S-MD was evaluated with concentrated Na_2SO_4 feed solution. Na_2SO_4 solution was chosen as a feed solution in view of temperature influences on its solubility. The solubility of Na_2SO_4 (g/100g) is 9.1 at 10 °C, 19.5 at 20 °C, 40.8 at 30 °C, 48.8 at 40 °C, and 45.3 at 60 °C. The effect of low temperature of permeate stream on the crystallization on the membrane distillation was examined using S-DCMDC and S-VMD in this study. S-VDCMD was not used because it is driven by the vapor pressure caused by both a temperature difference of two streams and vacuum pressure. As shown in **Figure 4-3**, crystals having different sizes were detected in the two different S-MD

processes (S-DCMD and S-VMD). Relatively large crystals (Length: over 1,000 μm, Width: over 300 μm) together with fine crystals were detected on the used S-DCMD membrane, while, only fine crystals were detected on the used S-VMD membrane. Moreover, the used S-DCMD membrane was completely covered with crystals while, the used S-VMD membrane was only partially covered with crystals. Theoretically, it is expected that the low temperature of permeate flow would cause a decrease of temperature on the membrane surface and boundary area. This in turn, it would decrease the solubility of crystalline solute especially at increased feed solution concentrations (Hou et al. 2015; Zuo et al. 2014).

In S-DCMD, the direct contact with cold permeate solution resulted in lower feed membrane surface temperature. This scenario lowered the solubility of concentrated Na_2SO_4 crystalline, resulting in dramatically high crystal formation on the membrane surface and the presence of pore crystallization on the S-DCMD membrane compared to the S-VMD. Hence the feed temperature on the membrane surface plays an important role in stimulating the generation and growth of crystals on membrane surfaces. This result suggested that S-DCMD was more susceptible to feed temperature losses than S-VMD (Hou et al. 2015; Zuo et al. 2014).

The cold condition of the permeate side causes a temperature difference between the membrane wall temperatures and the bulk feed temperatures. In S-DCMD, the saturation degree of crystals (with inverse temperature solubility properties) tend to be influenced by this large temperature difference. In addition, higher concentration layer is generated by concentrate around the membrane boundary layer. The effect of both concentration and temperature phenomena aggravates the crystallization phenomenon on the membrane surface. However, in the case of S-VMD, the effect of low permeate temperature is minimized, attributes to much lower temperature difference compared to S-DCMD. The pattern of pore crystallization development is dependent on the severity of temperature difference. The temperature of the outside (shell side) membrane wall in S-DCMD is much lower compared to S-VMD,

causing the decrease of crystal solubility. As a result, pore crystallization (toward shell side of wall) phenomenon tends to be more serious in S-DCMD.

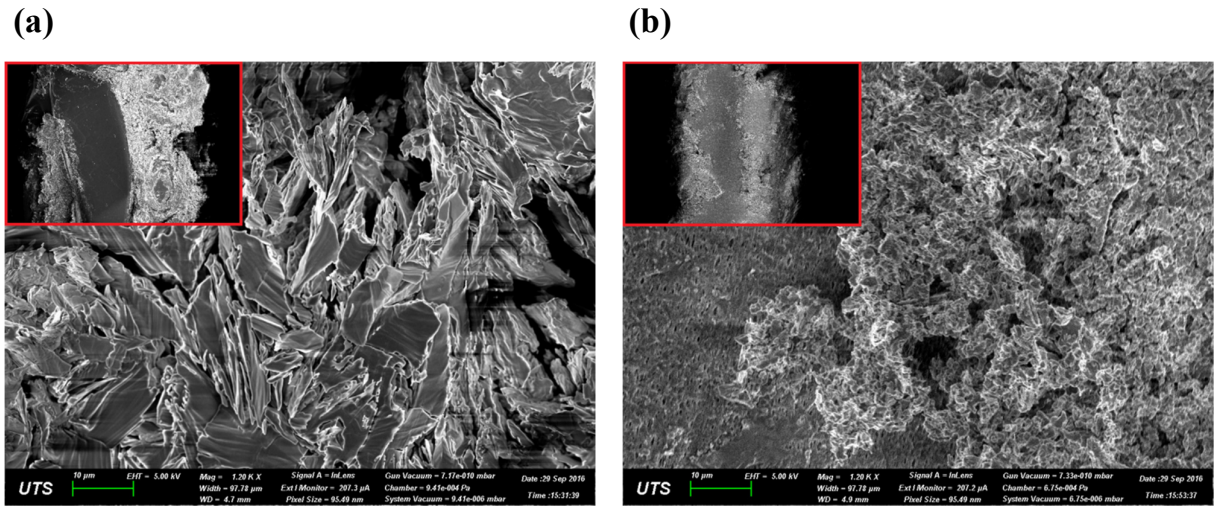

Figure 4-3. SEM images of used membrane surface and sodium sulfate crystals (Feed solution: 400g Na_2SO_4/L solution, and magnification: X100 and X1.2K) of (a) S-DCMD, and (b) S-VMD.

4.3.2.3. Economic/energy aspect

In MD, apart from permeate flux performance, the energy consumption varies with different MD configurations. The energy consumption is an important factor in choosing a suitable MD configuration. Generally, DCMD requires more energy to achieve the same amount of flux increase compared to VMD due to significant heat conduction losses (Duong, Cooper, et al. 2016; Guan et al. 2014). Nevertheless, in another study, the energy efficiency of different MD configurations based on gain output ratio was examined and reported the benefit of DCMD (Summers et al. 2012). It was highlighted that compared to VMD, DCMD has the potential to achieve high gain output ratio,if properly optimized in multi stage design, due to its configuration simplicity and capacity for heat transfer with heat recovery devices.

Overall, S-VMD has a number of advantages in terms of achieving higher permeate flux and energy

consumption. However, the performance of S-VMD was greatly affected by feed concentration. Further, in this study, a scenario of increased membrane wall thickness was observed for S-VMD (50 mbar) which could be related to a combination of issues including the unsuitability of this specific membrane type for the vacuum configuration setting. On the other hand, the S-DCMD and S-VDCMD (500mbar) showed much more promising results for high salinity solution. In view of this, evaluation with SWRO brine was carried out with only S-DCMD and S-VDCMD.

4.3.3. Performance for brine treatment (synthetic brine as feed solution)

The performance of S-MD configurations for SWRO brine treatment, permeate flux and permeate quality (in terms of conductivity) were compared with synthetic SWRO brine as feed solution (50% recovered brine,**Table 3-1**). Normalized flux was used to compare the performance of the S-MD configurations in view of the different initial baseline fluxes observed for different configurations. Experiments were conducted until the permeate fluxes were reduced to near zero level.

4.3.3.1. Permeate flux

The initial permeate fluxes of S-MDs with SWRO brine feed deceased by a factor of 2.9 to 35.7% in comparison to baseline flux with DI water. This flux decline could be attributed to the reduction of vapor pressure driving force at high feed concentration (Kezia et al. 2015). In comparing the initial SWRO brine permeate flux within the different configurations; the S-VDCMD maintained the pattern of obtaining higher flux values compared to S-DCMD.

As shown in **Figure 4-4** and **Table 4-2**, S- In S-DCMD, a VCF of 1.95 was achieved before flux decline was observed, reducing the flux to near zero at VCF 2.21. In all S-VDCMD experiments, almost similar final VCFs were observed (500 mbar: VCF 2.11, and 700 mbar: VCF 2.08). Overall, in terms of final VCF achieved, S-DCMD achieved the highest VCF.

4.3.3.2. Permeate quality

Overall, good quality conductivity with a rejection of 99.9% was achieved as shown in **Figure 4-4 (b)**. Nevertheless, a slight increase of permeate conductivity to 16.02-16.85 µS/cm was observed above VCF 1.5 for S-VDCMD while the permeate solution of S-DCMD remained low at 5.03 µS/cm. The results indicated the higher tendency of partial wetting in the presence of partial vacuum (S-VDCMD) compared to without vacuum (S-DCMD) for treating SWRO brine with the submerged configuration. However, an important factor in establishing the suitability of S-DCMD and S-VDMCD for brine treatment is to evaluate the crystallization formation on the membrane.

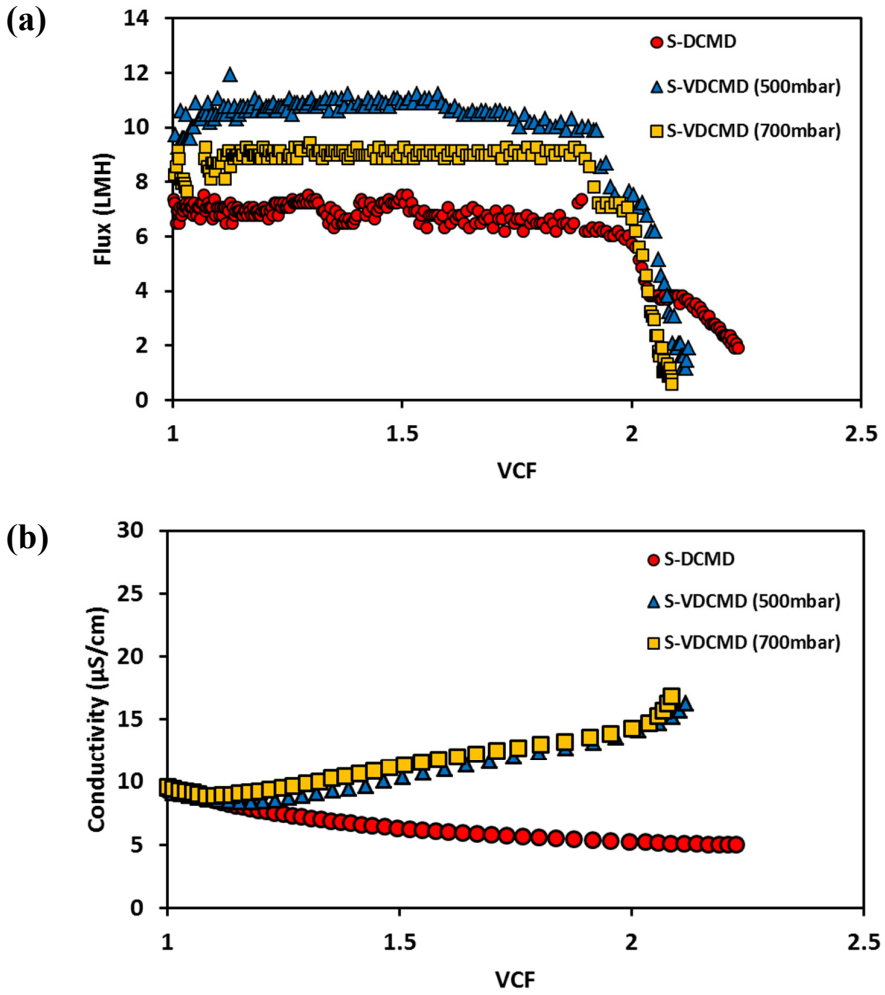

Figure 4-4. (a) Permeate flux and (b) quality (conductivity) of different S-MD configurations using 50% recovered brine as feed solution.

Table 4-2. Achieved VCF in different S-MD configurations.

S-MD configurations	Volume concentration factor (VCF)	
	Before rapid flux decline	Final
S-DCMD	1.95	2.21
S-VDCMD (500mbar)	1.89	2.11
S-VDCMD (700mbar)	1.88	2.08

4.3.3.3. Crystallization in membrane

The tendency of crystal formation on the membrane surface and pores was evaluated using SEM-EDX analysis. Synthetic brine solution used in this study contained sparingly soluble salts such as calcium scalant (i.e. calcium sulfate) (Naidu, Jeong, Choi, et al. 2017). Evidently, as shown in the EDX analysis, calcium-based crystals with sulphur ions were observed on the membrane surface in S-VDCMD (**Figure 4-5**).

The EDX analysis did not detect visible peaks of calcium and sulphur on the membrane surface of S-DCMD, suggesting the possibility of sparse and minimal crystal deposition on its surface. Moreover, crystal was not observed on the membrane surface of S-DCMD with the naked eye because they were removed by washing. This is because of the loosely deposited crystals in the absence of vacuum. It is also due to the hydrophobic characteristic of membrane (contact angle: 106 ± 2). Hence, strong calcium-based crystal formation on the membrane surface was most likely due to the vacuum pressure.

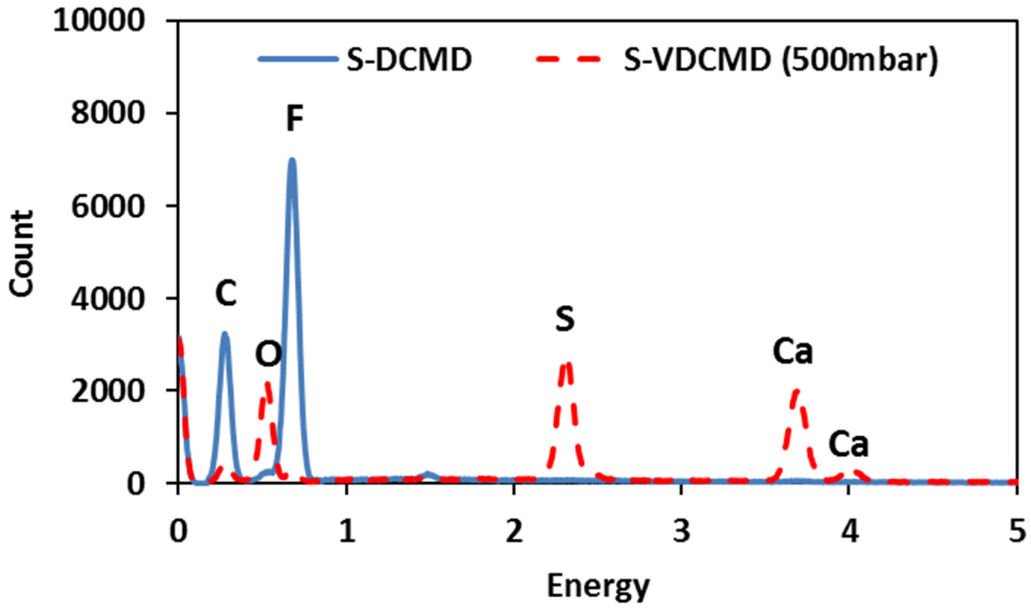

Figure 4-5. SEM-EDX results of the membrane surface in S-MD.

Pore crystallization The presence of fine crystals was observed in the pores of the used S-DCMD membrane as shown by the cross section image in **Figure 4-6 (c)**. Comparatively, the used S-VDCMD (500 mbar) membranes did not exhibit any pore crystallization and appeared similar to the virgin membrane (**Figure 4-6 (a)** and **(i)**). This could be because the presence of vacuum was a suitable condition for crystal formation on membrane surface. As crystals tend to deposit onto the membrane surface, crystal pore penetration reduced.

Membrane crystallization A different pattern of crystal deposition was observed on the membrane surface compared to membrane pore. On the surface of the used S-DCMD membrane, only fine crystals were present with some scatters of large crystals (**Figure 4-6 (d)**). In the case of used S-VDCMD (500 mbar) membranes, large crystal deposition was detected on the membrane surface (**Figure 4-6 (d)** and **(j)**).

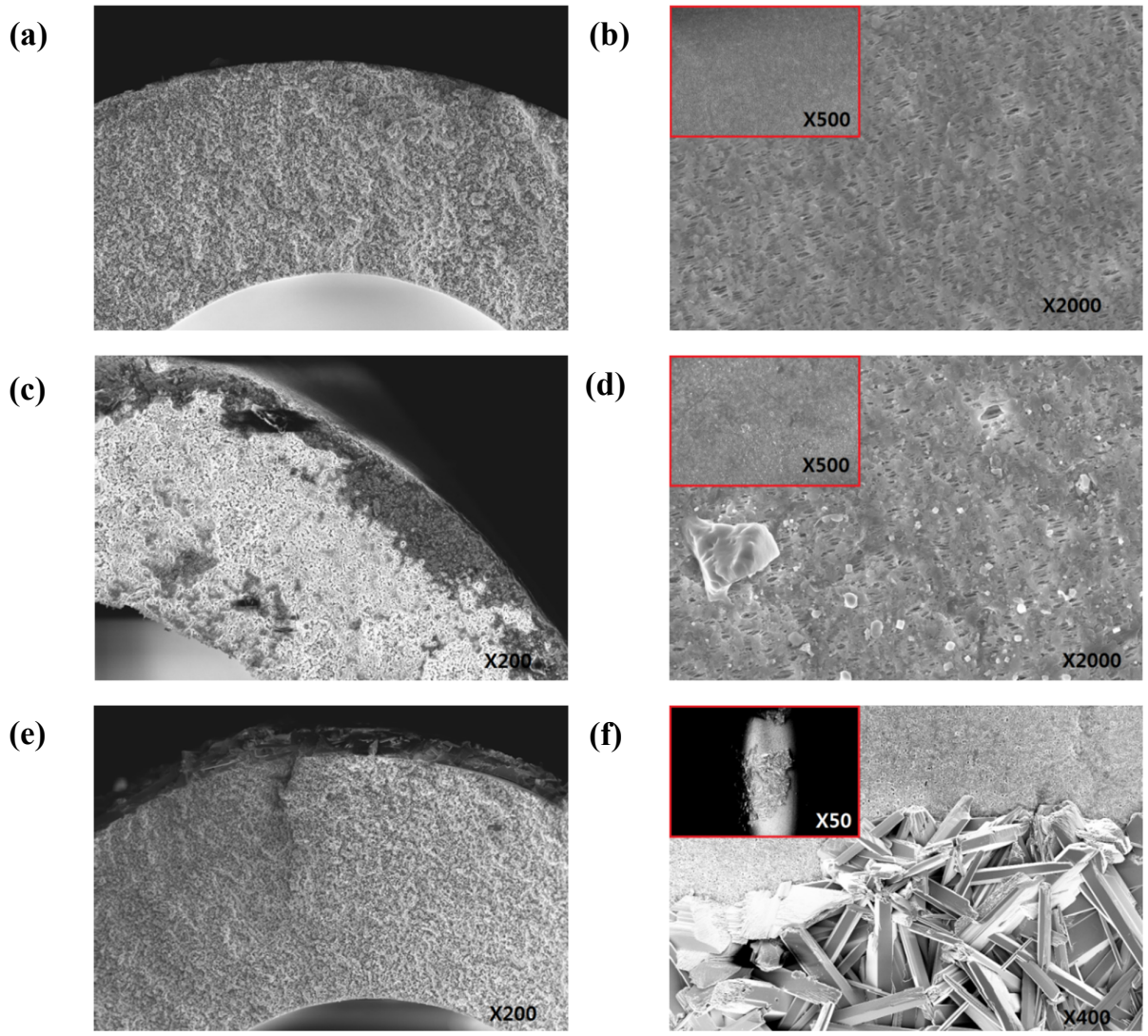

Figure 4-6. SEM images of used membrane for each S-MD configuration (feed solution: synthetic 50% recovered brine): (a) Virgin (Cross-section), (b) Virgin (Surface), (c) S-DCMD (Cross-section), (d) S-DCMD (Surface), (e) S-VDCMD (at 500mbar) (Cross-section), and (f) S-VDCMD (at 500mbar) (Surface).

Additionally, to study the effect of vacuum on the crystallization, the used S-VDCMD (500mabr), was compared with S-VDCMD (700 mbar). A pattern of increased crystal deposition on the membrane surface was observed at higher vacuum (**Figure 4-7**). For instance, in S-VDCMD (500 mbar) prevalent deposition layer of crystals was detected while almost no crystal deposition was observed on the used

S-VDCMD (700 mbar). A correlation of dominant presence of crystals on used S-MD membrane pores and surface areas was prevalent with vacuum addition. It was expected that when vacuum and vapor pressure are combined in S-MD process, both pressures could enhance crystal depositions on the membrane surface, and the crystals adhered strongly to the membrane surface. This phenomenon became more prevalent at the increased vacuum. The formation of large crystals on the membrane could be attributed to the higher driving force for water vapor permeation, and thus higher local salt concentration on the membrane surface, resulting in rapidly growth into larger crystals and stronger crystal deposition on the membrane surface. On the other hand, the S-VDCMD (700 mar) behaved similarly to the S-DCMD, where, minimal deposition of crystals occurred on the membrane surface. As a result, over time, the crystals were pulled into the membrane, resulting in deposition onto the membrane pores. The analysis of S-VDCMD performance with SWRO brine solution highlighted that a moderate vacuum condition was more suitable to maintain a stable flux and permeate quality as well as membrane crystallization formation.

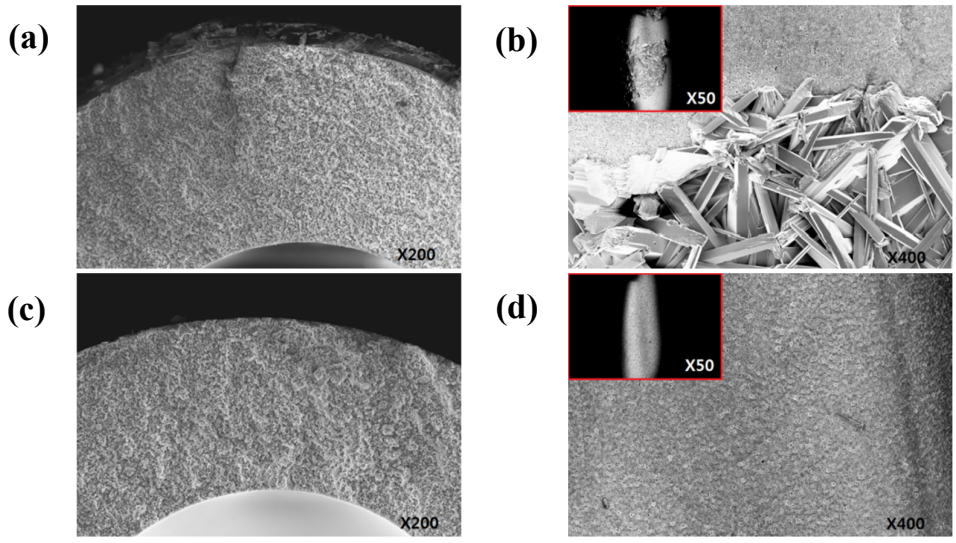

Figure 4-7. SEM images of used membrane for each S-VDCMD configuration (feed solution: synthetic 50% recovered brine): (a) S-VDCMD (at 500mbar) (Cross-section), (b) S-VDCMD (at 500mbar) (Surface), (c) S-VDCMD (at 700mbar) (Cross-section), and (d) S-VDCMD (at 700mbar) (Surface).

4.3.4. Air backwashing

In submerged modules, scaling phenomenon is a more significant issue than in cross-flow module because membrane module is submerged directly in feed solution. Moreover, when concentrated brine is used as feed solution, crystals cause more severe fouling if concentration of salts in feed solution is super-saturated. For instance, although the surface of all the used S-MD membranes were washed with DI water prior to SEM analysis, crystals deposition could still be detected as presented in the crystallization section, suggesting its prevalent deposition on the membrane. Moreover, in the S-DCMD, apart from the crystals on the membrane surface, crystals were also observed in the membrane pores. As such, it is important to evaluate the reversibility of the crystals and the recovery of permeate flux in repeated air washing cycles using the same membrane. Hence, the efficiency of air backwashing method was evaluated to mitigate the fouling and crystal formation and deposition on the membranes of S-DCMD.

As shown in **Figure 4-8**, S-DCMD operation was conducted until the flux approached zero in the first cycle, and then air backwashing was applied. During the first cycle, crystals were observed in feed solution (i.e. bulk crystallization) at around VCF 2.78, and then flux decreased to near zero. After the air backwashing, flux was recovered around 80.3% and VCF 2.67 was achieved before flux decline in the second cycle. Interestingly, in the third cycle, 113.8% flux recovery was achieved compared with the first cycle but shorter VCF was made (VCF 2.24, before flux decline). In the fourth cycle, a VCF of 2.26 (before flux decline) was achieved. A flux recovery of 118.3% was observed compared with the first cycle were achieved. As air backwashing was repeated, VCF achieved reduced and the flux recovery was higher than the first cycle flux. However, no obvious change of membrane structure was detected (**Figure 4-9**).

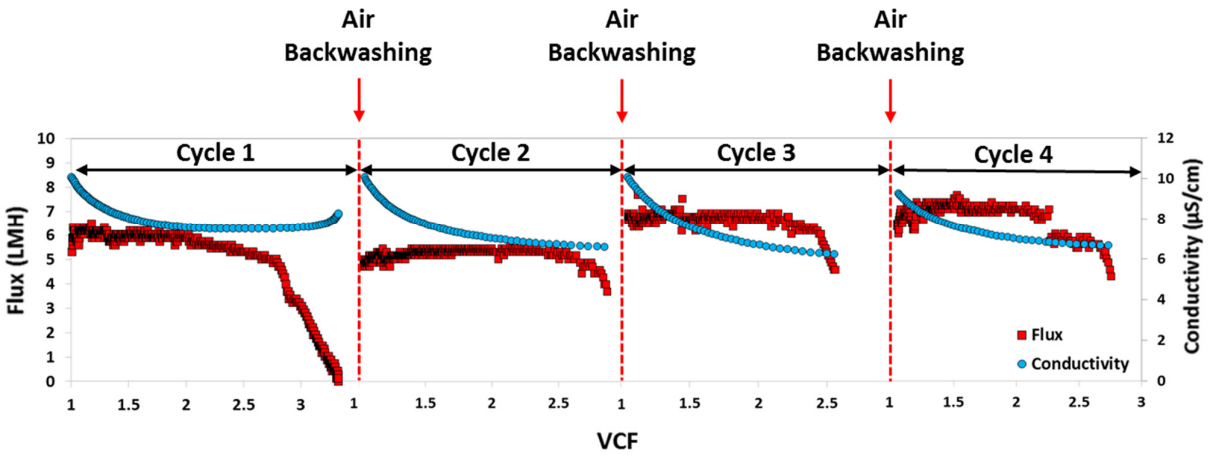

Figure 4-8. The variation of flux and conductivity with periodic air backwashing.

As shown in **Figure 4-6**, crystals were found on the membrane surface in S-DCMD. The crystallization effect in the used membrane could be alleviated by applying the air backwashing. Also, the decrease of permeate water quality caused by partial wetting in the membrane can also be reduced (**Figure 4-9**). After applying the air backwashing, permeate flux was recovered, and the conductivity in permeate side did not increase during operation of S-DCMD process. However, crystals on the membrane surface were not removed completely. It was expected that crystals remained on the surface may cause more crystallization and induce both polarization phenomena (Duong, Duke, et al. 2016). The environment condition, which crystals are generated and grown up easily, was made around crystals remained on the membrane surface, and then pore blocking by crystals progresses quickly. The air backwashing is an efficient method to mitigate the wetting phenomenon and to reduce crystallization on the membrane. Nevertheless, it could not overcome wetting and crystallization phenomenon completely.

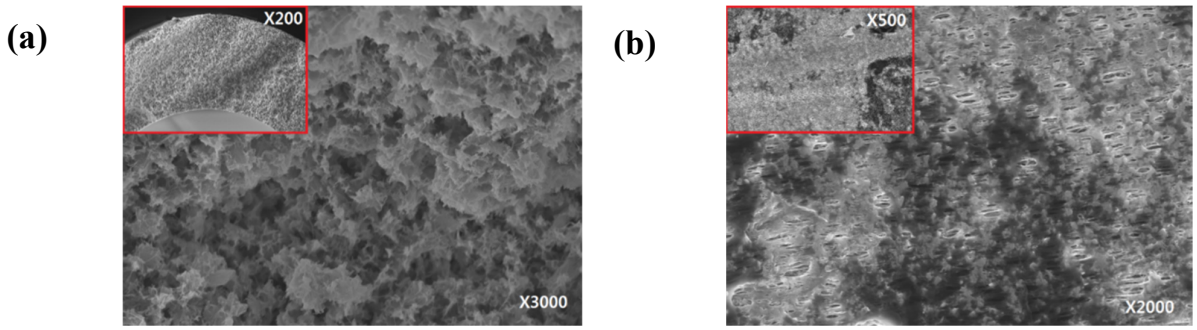

Figure 4-9. SEM images of used membrane ((a) cross-sectional and (b) surface) after fourth cycle of air backwashing.

4.4. Summary of this research

The performance of three different S-MD configurations (S-VMD, S-DCMD, and S-VDCMD) was evaluated for the treatment of concentrated brine from SWRO plant. From the investigations, following conclusions were made are as below:

- In the baseline test, the S-VMD (50 mbar) obtained 40-77% higher permeate flux compared to S-DCMD and S-VDCMD (500 mbar and 700 mbar) , attributed to the higher driving force
- The tendency of membrane crystallization in each S-MD configuration was different, which was associated to the varying influence of feed concentration and temperature in the different configurations.
- The feed concentration strongly influenced the S-VMD behaviour while the feed temperature played a strong role in S-DCMD.
- The S-VDMD and S-DCMD configurations enabled to concentrate brine solution to over 2.08 VCF.

- S-DCMD configuration is more suitable to treat concentrated brine (high salinity solution) due to higher permeate flux at high concentration. Also, a low potential of wetting phenomenon was observed in S-DCMD compared to S-VDCMD and S-VMD.
- By using the air backwashing method, permeate flux in S-DCMD was effectively recovered indicating that the air backwashing resulted in the alleviation of crystallization on the membrane and the reduction of wetting.

CHAPTER 5

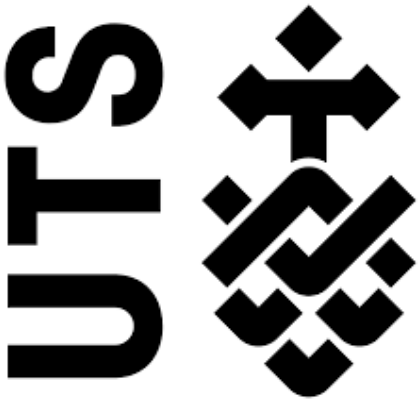

INTEGRATED SUBMERGED MEMBRANE DISTILLATION-ADSORPTION SYSTEM FOR RUBIDIUM RECOVERY

This chapter has been published as: **Y. Choi**, S. Ryu, G. Naidu, S. Lee and S. Vigneswaran, Integrated submerged membrane distillation-adsorption system for rubidium recovery, Separation and Purification Technology, 218 (2019) 146-155.

5.1. Introduction

Reducing seawater reverse osmosis (SWRO) brine can substantially improve the additional cost incurred and its related environmental issues. In this context, various treatment methods have been explored to minimize SWRO brine volume (Abdulwahab et al. 2013; Afrasiabi & Shahbazali 2011; Choi et al. 2018b; Choi et al. 2017; Naidu et al. 2018). Apart from brine volume minimization, in recent times, much focus is being placed on mining valuable resources from brine. This is because, seawater contains a variety of elements, and these elements exist at a higher concentration in the brine. In fact, the salt concentration of SWRO brine depends highly on the ratio of desalination plant recovery and seawater concentration (Lee et al. 2018). Some of the elements present in the seawater and SWRO are economically valuable metals, such as lithium, cesium, rubidium, and other heavy metals. At similar concentration levels (0.11-0.33 mg/L), the economic/market price of Rb is substantially high (11,180 US$/kg) compared to Li (13.9 US$/kg) (*U.S. Department of the Interior: U.S. Geological Survey. Mineral Commodity Summaries* ; Loganathan et al. 2017; Sodaye et al. 2009). Rb is known to be use in the laser industry, as well as atomic clocks and photocells. As such, the recovery of valuable Rb from SWRO brine can lead to the economic benefits, as it can potentially offset brine treatment cost.

Adsorption/ion exchange is a simple method for recovering and extracting valuable resources selectively from the solution, and the adsorbents can be regenerated after desorbing the adsorbed compounds. This makes this process a sustainable approach for resource recovery. Our previous studies have established the selective extraction capacity of potassium copper hexacyanoferrate (KCuFC), a potassium-based ion exchange adsorbent for recovery of Rb from seawater brine (Naidu et al. 2018; Naidu, Jeong, Johir, et al. 2017), The high selectivity of Rb with KCuFC is attributed to the exchangeability with structural potassium in the ion exchange adsorbent based on the similar unhydrated ionic radii (Naidu, Jeong, Johir, et al. 2017). Invariably, a significant competition will be

present between Rb and Cs due to the similar ionic radii mechanisms. However, giving the minimal presence of Cs in non-radioactive seawater (Rb: Cs molar ratio = 1: 0.001), Cs does not play a significant role in competing with Rb. Hence, KCuCF is able to maintain a high Rb selectively in seawater brine. Although KCuFC exhibits high Rb selectivity in SWRO brine, its performance capacity is challenged due to the low concentration of Rb in SWRO brine (0.11 – 0.30 ppm) compared to other major elements, for instance sodium, magnesium and, potassium (Bolter et al. 1964; Loganathan et al. 2017; Naidu, Jeong, Johir, et al. 2017). Increasing the concentration of Rb in SWRO brine through an integrated process will enable to enhance the performance of by KCuFC.

Using a highly-selective membrane, the target element can be concentrated by the extraction of only fresh water from the feed solution without its ion contents, thus the reduction of target element (Rb) concentration can be mitigated. Membrane distillation (MD) is a suitable technology which can achieve SWRO brine treatment (Choi et al. 2017; Gryta 2016). The SWRO brine comprises of major elements at high concentrations such as Na, Ca, Mg and K (Ho et al. 2015; Jeong et al. 2016) which adversely influence the membrane process's performance, causing permeate flux reduction (Choi et al. 2017). In MD, the effect of high concentration of feed solution (hydraulic pressure restriction) is lower compared to other pressure-driven membrane processes, such as reverse osmosis and nanofiltration. This is because the mass (vapor) transfer in MD occurs through the membrane as a function of vapor pressure difference between the hot feed solution stream and cold permeate stream (Chen et al. 2014; Edwie & Chung 2013). Hence, MD is favorable for treating brine concentrate while achieving high rejection ratio (over 99 %) for non-volatile elements (Naidu, Shim, et al. 2017; Quist-Jensen, Sørensen, et al. 2017).

The MD-adsorption integration was established to be beneficial as it provided a long contact time for encapsulated KCuFC to extract Rb compared to a conventional fixed bed column (Naidu, Jeong, Johir, et al. 2017). Meanwhile, the heat source of MD, which is applied to the feed solution for vapor transfer,

enhances adsorption capacity of KCuFC (without the need for an additional heat source). However, compared to conventional cross flow flat sheet MD, a submerged hollow fiber MD is advantageous in terms of heat consumption and process intensification/integration as recirculation of feed solution is not necessary in this set-up. While circulating the feed solution, heat losses occurs, requiring additional heating of the feed solution. Moreover, in a submerged MD set-up, KCuFC adsorbent can be added directly into the reactor tank, resulting in a compact system and the reactor plays the dual role of feed tank and membrane reactor. In this scenario, fresh feed solution can be continuously supplied into the reactor, resulting in Rb mass increment over time, which can effectively maximize KCuFC absorption capacity. In addition, during the adsorption phase, higher adsorption capacity was obtained when the solution was at a high temperature (Ding et al. 2013; Saffarionpour et al. 2019). For better adsorption efficiency, an additional heat source is required, resulting in additional operation cost (Naidu, Jeong, Johir, et al. 2017). However, in the integrated process of MD and adsorption, the heat source of MD, which is applied to the feed solution for vapor transfer, can also be used as the heat source for adsorption. Moreover, higher mass transfer in the submerged MD process compared to cross-flow MD has been established in the previous researches (Julian et al. 2016; Meng, Hsu, et al. 2015). However, it must be acknowledged that the susceptibility of scaling/crystallization in a submerged MD for brine treatment is inevitable and the effect of scaling on the overall performance of the integrated system must also be evaluated in detail.

In this study, an integrated submerged MD-adsorption process is investigated for improving fresh water recovery and Rb extraction from SWRO brine. In order to establish the feasibility of integrated submerged MD-adsorption, factors that influence the process such as continuous supply of fresh brine to increase Rb mass over time, crystal deposition on the membrane and reactor, KCuFC adsorbent size (powder, particle and granular) will be evaluated in detail.

5.2. Materials and Methods

Experiments were conducted with an integrated submerged MD-adsorption process consisting of submerged membrane and adsorption process in a single reactor (**Figure 3-3**). A known amount of KCuFC adsorbent was added into the membrane reactor at the start of the experiment. The double jacked reactor was used as submerged membrane reactor, adsorption reactor and feed solution tank. The temperature of feed solution was set at 55 °C by using heating water bath with water circulator. The temperature was monitored in real time by the temperature sensor placed inside the reactor. The feed solution was mixed at 250 rpm using magnetic stirrer. It provided a shear force for adsorbent with a Reynolds number (*Re*) over 32,860. The raw feed solution was continuously supplied from a reservoir to the reactor. The supply rate to the feed solution was dependent on the permeate flux. The temperature and flow rate of permeate stream were 20 °C and 0.5 L/min, respectively. The permeate temperature was controlled by a cooling water bath (chiller), and it was measured using a temperature sensor prior to the membrane module. The permeate water quality was monitored in real time in terms of conductivity.

Three different forms of KCuFC adsorbents were used to evaluate the effect of adsorbent size and form on the adsorption capacity. They were: powder form (Size: < 100 μm), particle form (mean size: 0.45 mm) and granular form (mean size: 2.42 mm). The capacity of the adsorbents was evaluated using adsorption rate of Rb (70 mg Rb/h), concentration variation ration compared to initial concentration (m_t/m_0) and cumulative mass of Rb adsorbed (mg). The m_t is the concentration with time, and m_0 is the initial concentration.

5.3. Results and discussion

5.3.1. Integrated submerged MD-adsorption process with granular KCuFC

High adsorption of Rb on granular KCuFC was demonstrated in previous researches, and it showed enhanced adsorption capacity at increased temperatures (Naidu et al. 2018; Naidu, Jeong, Johir, et al. 2017). For instance, Naidu et al., (Naidu, Jeong, Johir, et al. 2017) established the endothermic features of KCuFC that resulted in 10 to 15% higher Rb sorption as the solution temperature was increased from 25 C to 55C. The enhanced Rb extraction capacity of KCuFC in thermal condition lead to an integration with MD. They used a cross flow flat sheet MD set-up with KCuFC adsorbent placed in the feed tank and highlighted the beneficial potential to achieve both water recovery and enhanced Rb extraction at higher temperature. However, contrary to a cross flow flat sheet MD, in this study, a submerged MD (S-MD) process was applied with a hollow fiber membrane module. The application of S-MD was used as it enables to (a) attain a more compact design containing both the submerged hollow fiber membrane and KCuFC absorbent in a single reactor; (b) a continuous supply of fresh brine in long cycles, closely emulating a pilot scale operation. Moreover, via the application of S-MD, there is no need for circulation of the feed solution When the feed solution circulates, heat loss occurs, leading to more heat consumption for reheating of the feed solution. The focus of this study was to establish the capacity of Rb extraction with continuous cycles of fresh brine in S-MD setting. The influence of scaling/crystal development and its effect on S-MD performance and Rb extraction was evaluated in detail. For this reason, in this study, this process was studied with: (a) model Rb solution; and (b) model seawater reverse osmosis (SWRO) brine solution containing a predetermined amount of Rb.

5.3.1.1. Model single Rb solution

The integrated submerged MD-adsorption process with granular KCuFC adsorbent was first studied with 5 mg Rb/L feed solution at a feed temperature of 55 °C. Different doses of adsorbent were used to determine the optimum adsorbent dose for achieving a high Rb adsorption. In this study, three different doses were used (0.05, 0.13, and 0.24 g of adsorbent/L of water in the reactor). The initial volume of feed solution was 2.0 L, and additional feeding of feed solution was not applied in this experiment. The submerged MD-adsorption process lasted for 10 hours and a stable permeate flux of 8.28 ± 0.11 L/m^2·h was achieved. This corresponds to a volume concentration factor (VCF) of 2.25. The dosing of granular KCuFC in solution did not influence the permeate flux of MD and in fact, it was similar to the MD operation without the addition of granular KCuFC adsorbent (8.22 ± 0.11 L/m2·h). A high permeate quality was achieved (rejection: 99.99%).

Higher Rb rejection was observed when the adsorbent dose increased (**Figure 5-1**), as earlier studies have reported (Gupta et al. 2011; Sivaraj et al. 2001). The Rb mass adsorption of 9.78 mg (98% Rb extraction ratio) was obtained within 10 hours using 473.3 mg granular KCuFC adsorbent (0.24 g/L). Smaller doses (91.30 mg (0.05 g/L) and 249.50 mg (0.13 g/L)) led to less Rb being adsorbed, these amounts being 60 and 81%, respectively.

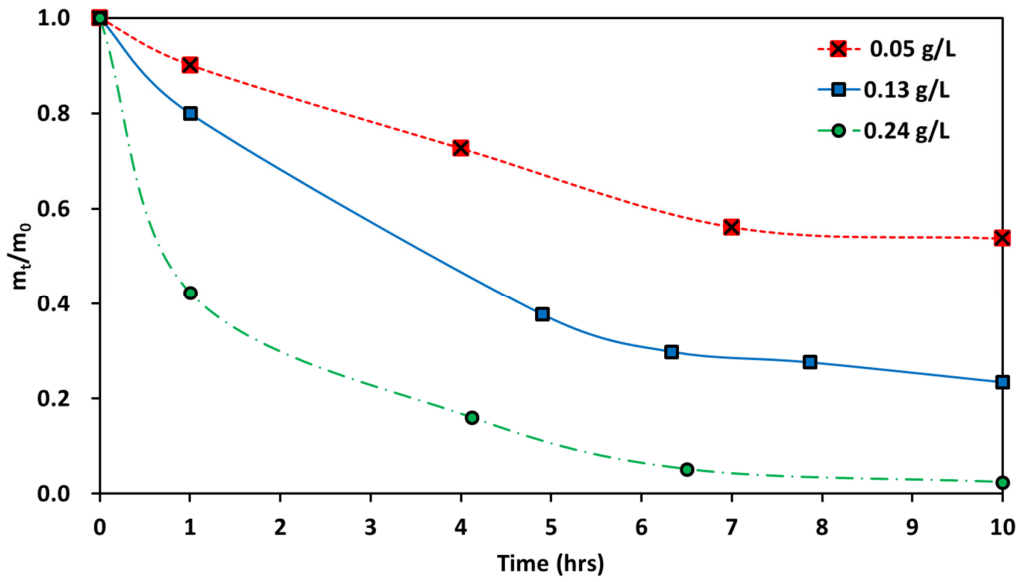

Figure 5-1. Comparison of Rb adsorption ratio over time in integrated submerged MD-adsorption with different granular KCuFC dose = 0.05, 0.13, 0.24 g/L) (T_f = 55 °C, T_p = 20 °C, 2 L feed solution = 5 mg Rb/L (2L)) (m_t and m_0 are the Rb concentration at given time and at the start of experiment, respectively).

The above experiments were conducted without a continuous supply of the feed solution. The adsorption efficiency and regeneration of granular KCuFC adsorbent were then studied with a continuous supply of feed solution containing Rb. When the concentration of Rb reached the initial concentration, the adsorbent was regenerated using 0.2M NH_4Cl solution (Naidu, Jeong, Johir, et al. 2017). The submerged MD-adsorption experiment was continued (second cycle) using the regenerated adsorbent and the same feed solution utilized in the first cycle experiment. The supply rate of Rb during both cycles was the same as the permeate flux of S-MD which was stable (**Figure 5-2**). The Rb supply rate was calculated based on the permeate flux and it was 0.318 ± 0.07 mg of Rb/h during the operation.

The adsorption rate of Rb during cycles 1 and 2 (2 hours after the experiment started) were 1.41 and 1.24 mg Rb/h, respectively (**Figure 5-2**). These were much higher than the supply rate and then the adsorption rate decreased rapidly. The higher adsorption rate led to the reduction of Rb concentration

in bulk solution although Rb ions were supplied continuously. The minimum concentration (1.5 ppm, rejection ratio: 70.2%) of Rb in the first cycle was observed at the final point where the adsorption rate was higher than the supply rate of Rb ions. After this point, the rate of reduction of adsorption rate decreased and the concentration of Rb in bulk solution increased. The cumulative Rb adsorptions were 53.4 and 33.3 mg/g for cycle 1 (27 hrs) and 2 (14 hrs), respectively. In both cycles, Rb adsorption was around 21.70 ± 0.034 mg/g without an increase in Rb concentration in the bulk solution (i.e. Rb adsorption rate by adsorbent > Rb supply rate by continuous feeding). Subsequently, the Rb ions were continuously adsorbed at a lower adsorption rate. Based on these results, the regeneration frequency of the adsorbent can be determined according to variations in the adsorption rate. It is better to maintain the adsorption rate above a specific rate for stable operation because a lower adsorption rate causes the Rb concentration in the solution to increase.

A total of 23.85 mg of Rb was extracted (total Rb extraction ratio: 80%) (14.69 mg Rb during cycle 1, 9.16 mg Rb during cycle 2) from both cycles (5.0 mg Rb/L initial solution concentration). Simultaneously, approximately 5.0 L of fresh water was produced (2.82 L during cycle 1, 2.03 L during cycle 2) from treating 6.0 L of Rb solution, achieving a water recovery of 81% (**Table 5-1**). The water recovery rate can be improved by further cycles of the integrated submerged MD-adsorption process. The result indicated the importance of the integrated submerged MD-adsorption process with granular KCuFC adsorbent to achieve Rb extraction while maintaining continuous fresh water production.

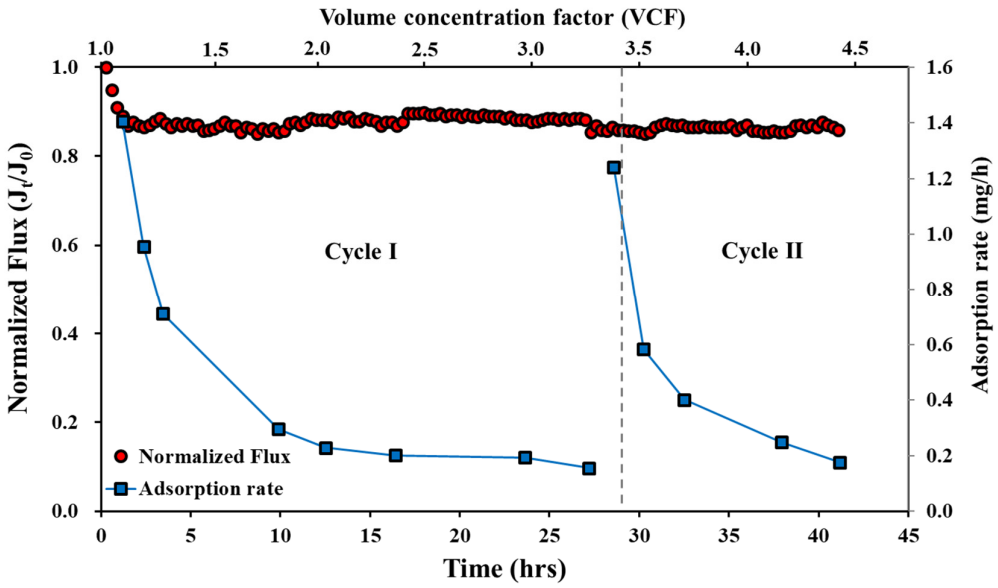

Figure 5-2. Normalized flux and adsorption rate as a function of time and VCF (T_f = 55 °C, T_p = 20 °C, feed solution = 5 mg Rb/L, adsorbent dosage = 0.24 g/L).

Table 5-1. Efficiency of Rb recovery and water production in integrated submerged MD-adsorption process (T_f = 55 °C, T_p = 20 °C, feed solution = 5.0 mg Rb/L (volume = 6 L), adsorbent dosage = 0.24 g/L).

Parameters	Value
Water production (L)	4.85 (recovery = 81 %)
Total adsorbed Rb (mg)	23.85 (recovery = 80 %)
Adsorption capacity per unit of adsorbent (mg/g)	86.75

5.3.1.2. Performance of integrated submerged MD-adsorption process with simulated SWRO brine

The selective Rb extraction capacity of granular KCuFC adsorbent in SWRO brine was examined using simulated SWRO brine containing 5.0 mg Rb/L. In real SWRO brine, Rb concentration is around 0.1 - 0.2 mg/L. However, in this study, a higher concentration of 5.0 mg Rb/L was used to compare with the results of model 5.0 mg Rb/L solution. In order to examine the performance of integrated submerged MD-adsorption system for SWRO brine, two types of simulated SWRO brines were used: (1) SWRO brine with Ca^{2+} and (2) SWRO brine without Ca^{2+}.

The integrated submerged MD-adsorption system with SWRO brine achieved an initial permeate flux of 7.24 ± 0.11 L/m^2·h. Over time, the permeate flux gradually reduced and by VCF 1.96, a 26 % flux decline occurred (at VCF of 1.96) (**Figure 5-3 (a)**). Thereafter the permeate flux decreased rapidly by 35–39%. Comparatively, the integrated submerged MD-adsorption system with a single Rb solution achieved 81% water recovery while maintaining a stable permeate flux throughout the operation. The significant flux decline with SWRO brine was attributed to the increase of resistance of inorganic ions at the membrane boundary layer at a higher ion concentration (Choi et al. 2017). At this point,

significant $CaSO_4$ deposition on the membrane surface was observed and the amount of crystals formed on the membrane surface increased, resulting in rapid flux decline. $CaSO_4$ caused a scaling problem when SWRO brine with Ca^{2+} was used and most of the crystals were detached/transferred from the membrane to the bulk solution (**Figure 5-4**).

Rb adsorption rate and total adsorbed Rb with SWRO brine were lower compared to the model single Rb solution. The adsorption rate at the 2-hour point after the operation began was 0.46 mg Rb/h, and then it was observed to be reduced. This is attributed to the decrease of vacant surface sites on the adsorbent with respect to time (Lian et al. 2009), thus reducing the adsorption rate. This corresponds to total adsorbed Rb per unit weight of adsorbent (3.35 mg/g) in the initial stage (2-hour point), and then the increase ratio reduced (**Figure 5-3 (b)**). As shown in **Figure 5-3 (b)**, the Rb concentration of bulk solution (m_t) increased gradually, leading to a lower adsorption rate than the feeding rate of Rb. However, the adsorption rate was higher than the supply rate during the initial period in the case of model Rb solution (0.237 g/L of adsorbent). Additionally, the Rb was adsorbed by the adsorbent despite the decreasing adsorption rate. In treating the SWRO brine with Ca, 2.32 mg Rb (recovery = 8%) was extracted (adsorption mass per unit adsorbent weight (g): 8.42 mg as Rb/g) and production of 1.1 L fresh water before rapid permeate flux decline, which corresponds to a water recovery rate of only 18% from the feed solution of 6 L.

Moreover, the present of salts (such as Na^+, Mg^{2+}, K^+ etc.) in SWRO brine does not affect the purity of Rb recovered. This is because a selective ion exchange occurs only between potassium in the inner structure of KCuFC and Rb from SWRO brine due to the similar ionic radius (Jeong et al. 2016). Due to the higher ionic radius, other salts such as Na^+, Ca^{2+} and Mg^{2+} cannot enter the inner surface. These salts deposit only onto the surface of KCuFC. During the desorption stage, washing the surface of the absorbent with DI water effectively removes these salts while chemical desorption (NH_4Cl) selectively elutes Rb from the inner lattice of KCuFC, resulting in high pure RbCl.

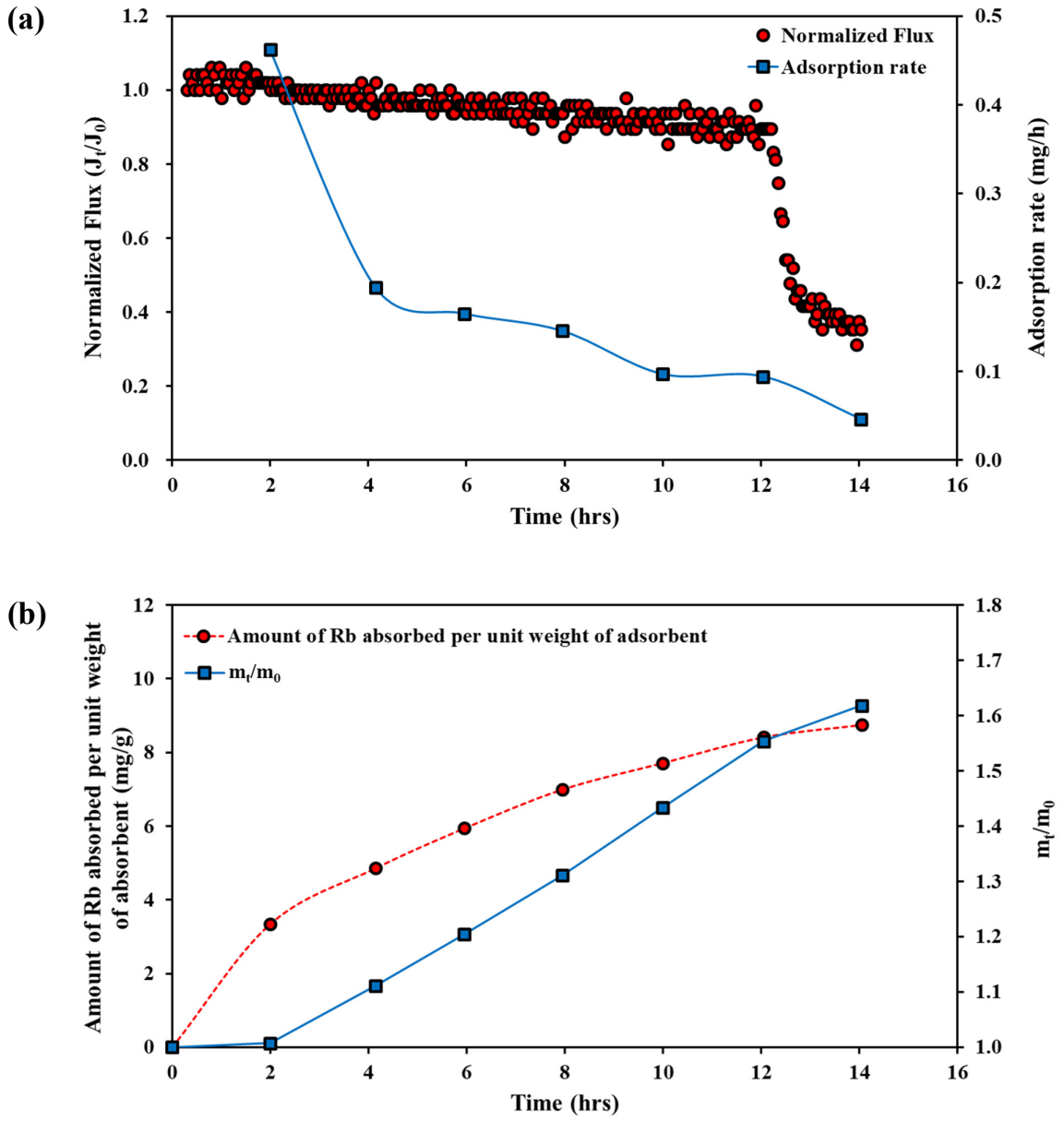

Figure 5-3. The adsorptive capacity of granular KCuFC in an integrated submerged MD-adsorption process: (a) normalized flux and adsorption rate, and (b) adsorption mass per unit time and Rb concentration variation (T_f = 55 °C, T_p = 20 °C, feed solution = simulated SWRO brine **with Ca^{2+}** (R = 50 %) (volume = 6 L), adsorbent dosage = **0.24 g/L**) (m_t and m_0 are the amount of Rb in the feed tank at the given time and initially).

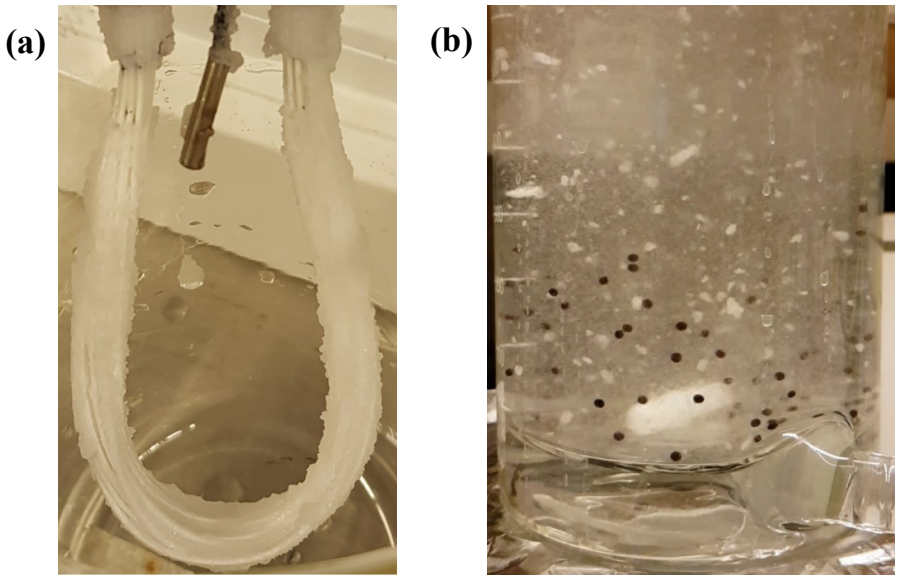

Figure 5-4. Crystal formation at the end of integrated submerged MD-adsorption operation (a) on the membrane surface, and (b) in the membrane reactor (feed tank).

Crystallization on the membrane surface and in the MD reactor impacted negatively on the process performance. Crystals were deposited on the membrane surface, resulting in the rapid permeate flux decline in MD (**Figure 5-4 (a)**). As shown in **Figure 5-5**, the crystal deposition on the adsorbent also occurred on the adsorbent surface, resulting in further reduction of a vacant surface sites of adsorbent. The crystals also detected in the reactor were mainly $CaSO_4$ crystals. The $CaSO_4$ crystals deposited on the adsorbent surface were not completely removed by simple washing using deionized water (**Figure 5-5 (b)**). This can lead to problems in adsorbent regeneration, during which, the $CaSO_4$ crystals deposited are dissolved in the desorption solution and result in contamination.

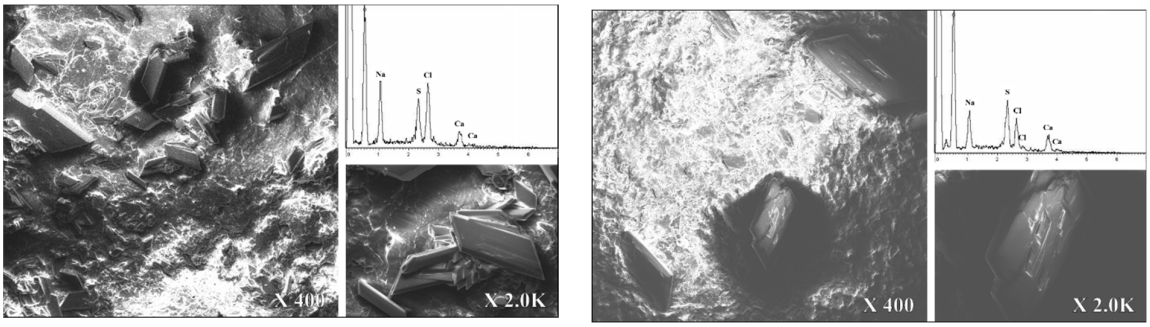

Figure 5-5. SEM-EDX result of KCuFC used at VCF 2.0 (a) without washing, (b) after washing using a deionized water.

In order to mitigate $CaSO_4$ crystallization, a simulated SWRO brine solution without Ca was used to mimic SWRO free from Ca. In MD, the presence of Ca affects permeate flux decline due to the occurrence of CaSO4 scaling on the membrane surface. Therefore, SWRO brine containing Ca results in significant flux decline by 12 hours (**Figure 5-3**). For this reason, Ca is commonly removed by softening techniques, such as lime-soda ash softening, prior to MD operation (Masindi et al. 2017; Mohammadesmaeili et al. 2010). As anticipated, SWRO brine without Ca enabled to maintain a stable flux (7.37 ± 0.15 $L/m^2 \cdot h$) by up to 20 hours (**Figure 5-6**). Two times higher MD operation duration was achieved using SWRO without Ca. In line with the higher operation duration, two times higher adsorbent dose (0.48 g/L) was used when operating MD using SWRO brine without Ca compared to the dose of 0.24 g/L used for SWRO brine containing Ca. The initial permeate flux (7.37 ± 0.15 $L/m^2 \cdot h$) was same for both simulated SWRO brine (i.e. with and without Ca) (**Figure 5-6**). However, in terms of flux decline trend a gradual decrease was observed without any rapid flux until around VCF 2.58 (i.e. after 20 hours operation). During this time, 1.8 L permeate was produced. Crystallization did not occur on the membrane surface or in the reactor. This indicated that the MD operation can be maintained with no significant reduction of the process's performance.

The adsorption rate and adsorption amounts (mg) of the SWRO brine without Ca were low compared

to model 5.0 mg Rb/L solution (**Figure 5-6** and **Table 5-1**). The performance with SWRO brine without Ca addition was also low even when a higher adsorbent dose was used. Initial adsorption rate of Rb (2 hours after the experiment began) was 0.95 mg Rb/h, which was slightly higher than the supply of Rb during continuous feeding. Following that, the adsorption rate became lower than supply rate, resulting in an increase in the Rb concentration in the solution. However, the Rb was continuously adsorbed even when the adsorption rate was lower. At VCF 2.58 (which marked the end of the experiment), the adsorption capacity was 34.33 mg as Rb/g of adsorbent (total adsorbed Rb: 9.48 mg) for SWRO without Ca^{2+}. In comparison to SWRO with Ca^{2+} addition at the same VCF (VCF 1.9), the adsorption capacity was 24.09 mg Rb/g adsorbent (total adsorbed Rb: 6.65 mg) (adsorption capacity: 8.42 mg as Rb/g, total absorbed Rb: 2.32 mg in SWRO brine with Ca). These results highlighted two significant outcomes: firstly, that the absence of Ca in SWRO brine prevented $CaSO_4$ crystallization (scaling) in the integrated submerged MD-adsorption process; and secondly, it improved Rb adsorption capacity and recovery ratio of permeate (fresh water).

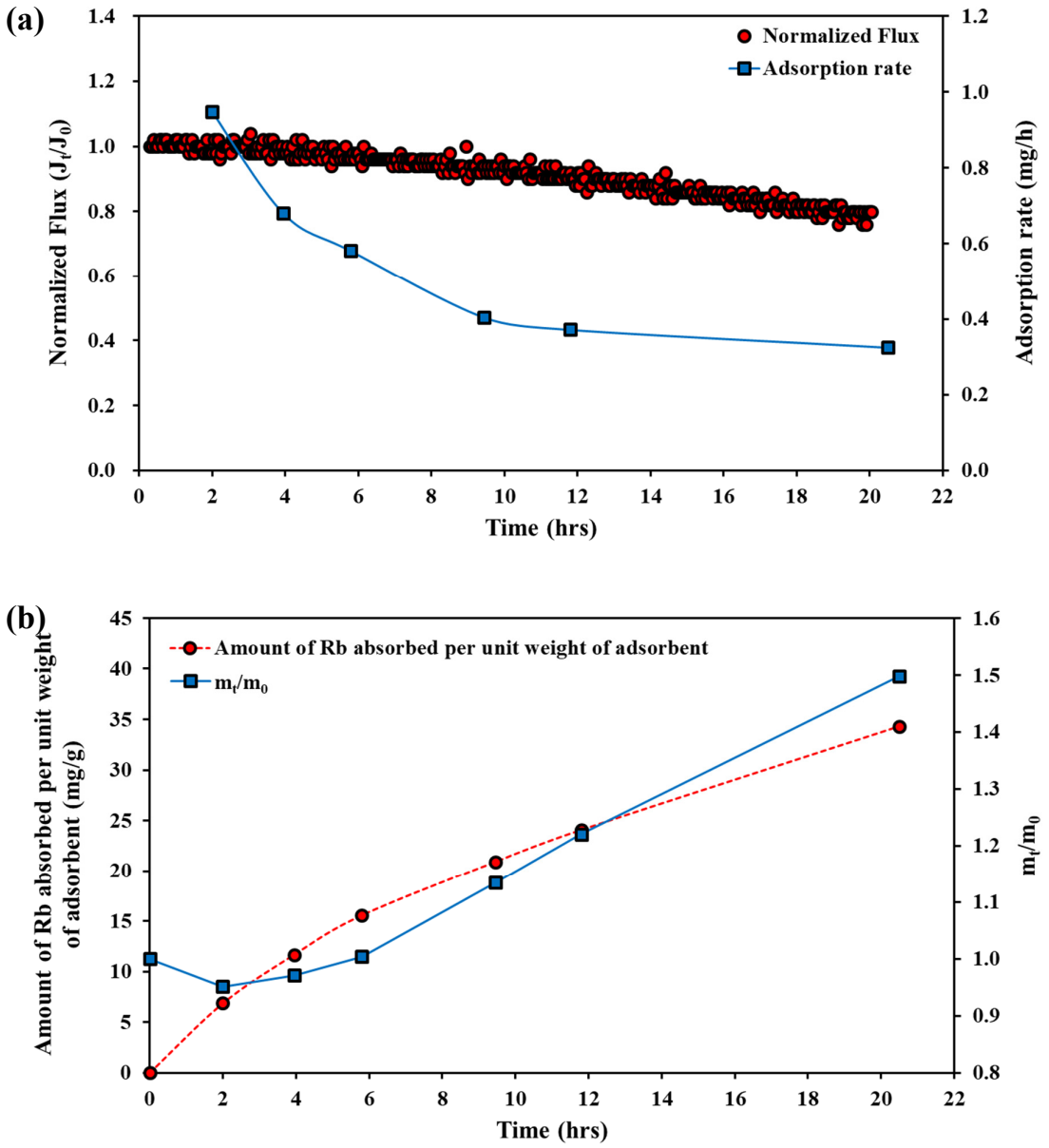

Figure 5-6. The efficiency of granular KCuFC in integrated submerged MD-adsorption process: (a) normalized flux and adsorption rate, and (b) adsorption mass (mg) per unit time and Rb mass variation in the solution (m_t/m_0) (T_f = 55 °C, T_p = 20 °C, feed solution = simulated SWRO brine **without Ca^{2+}** (R = 50 %), adsorbent dosage = **0.48 g/L**).

Table 5-2. Efficiency of integrated submerged MD-adsorption process at different adsorbent doses and in the presence/absence of Ca^{2+} in simulated SWRO brine (T_f = 55 °C, T_p = 20 °C, feed solution = simulated SWRO brine w/ Ca^{2+}, w/o Ca^{2+}, adsorbent dosage = 0.24, 0.48 g/L).

Parameters	With Ca^{2+} (0.238 g/L)	Without Ca^{2+} (0.477 g/L)
Water production (L)	1.10	1.84 <
Final VCF without rapid flux decline	1.96	2.58 <
Adsorption rate after 2 hours from beginning (mg/h)	0.46	0.95
Adsorption capacity per unit of adsorbent (mg/g)	8.42	24.09 (34.33 in the end)
Total adsorbed Rb (mg)	2.32	6.65 (9.48 in the end)

5.3.2. Comparing the adsorption capacity of different sized adsorbents (in integrated submerged MD-adsorption)

5.3.2.1. Adsorption equilibrium and adsorption rate

In order to examine the effect of adsorbent size, batch adsorption equilibrium experiments at 55°C in the reactor were performed with three different forms of KCuFC: powder form (size: < 100 μm), particle form (mean size: 0.45 mm) and granular form (mean size: 2.42 mm) (**Figure 5-7**). The highest adsorption capacity was obtained with KCuFC adsorbent in particle form (**Figure 5-8**). Adsorption capacity with particle form of KCuFC was 4–58% higher compared to powder form KCuFC, and 10–47% higher compared to granular form KCuFC. The maximum adsorption capacity (Q_{max}) values (based on Langmuir model) of powder and granular forms of KCuFC adsorbents were 135.32 and 164.15 mg/g, respectively. The particle form KCuFC adsorbent achieved 32–60% higher adsorption

capacity compared to powder and granular forms of KCuFC adsorbent with a Q_{max} of 216.17 mg/g.

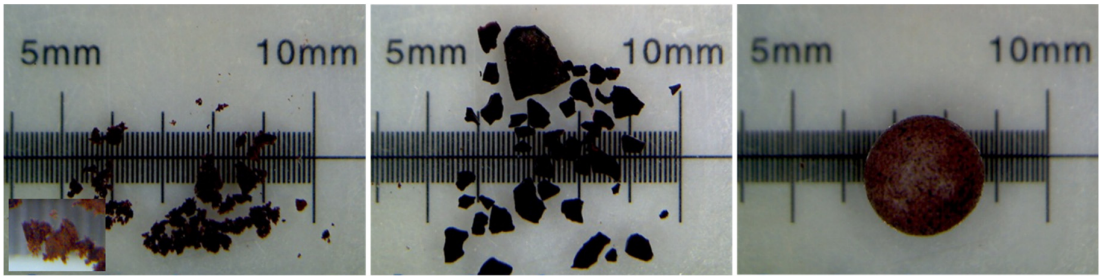

(a) Powder KCuFC **(b)** Particle KCuFC **(c)** Granular KCuFC

Figure 5-7. The different form and size KCuFC adsorbent used in this study.

The initial adsorption rate varied for different adsorbent forms (**Figure 5-8 (b)**), especially at higher doses. The initial adsorption rate of particle KCuFC was higher compared to other forms of KCuFC for different doses (1.65–6.32 mg Rb/h). Granular KCuFC adsorbent showed the lowest initial adsorption rate (0.88–3.10 mg Rb/h).

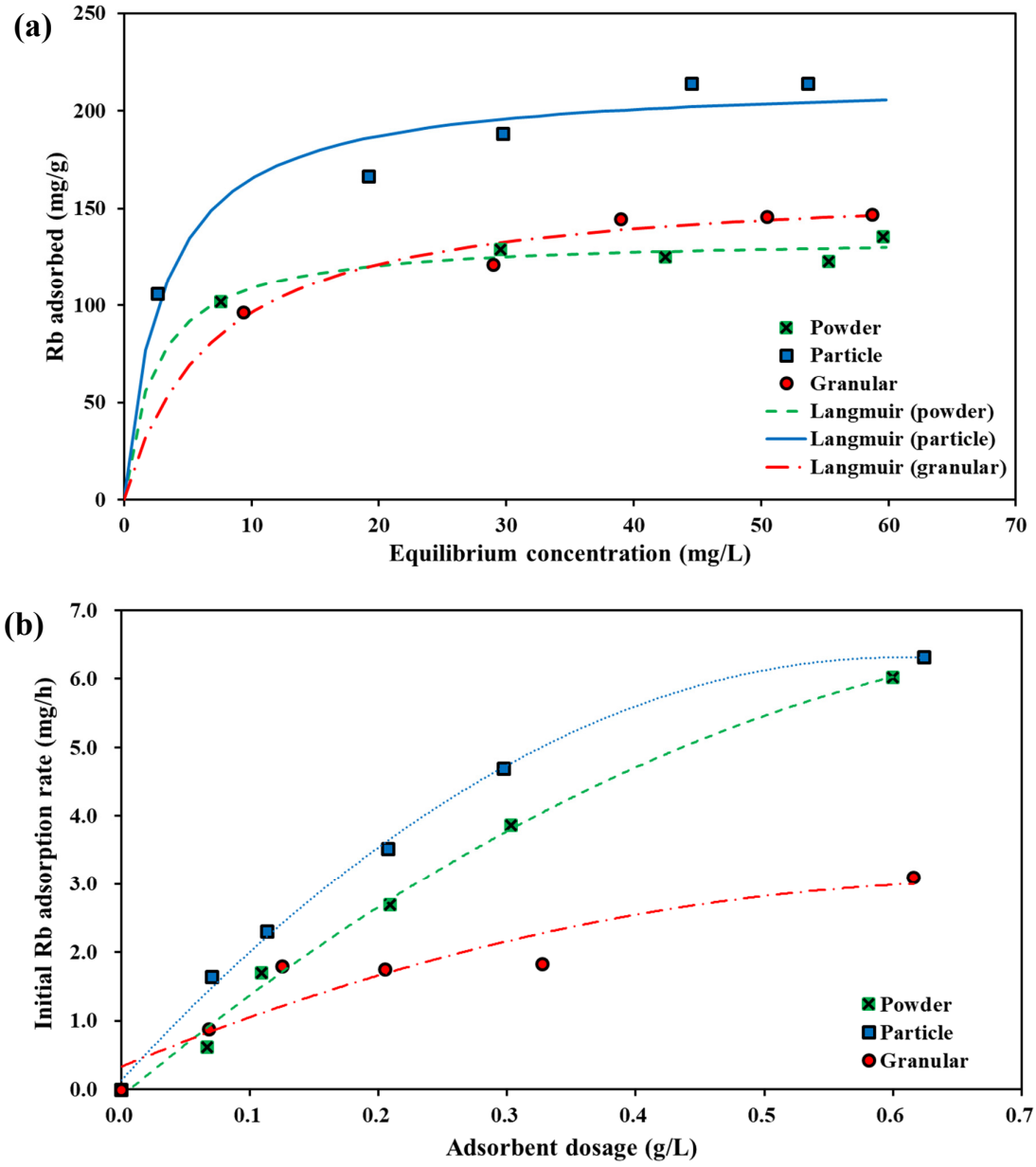

Figure 5-8. Batch Rb adsorption with different sizes of KCuFC adsorbents: (a) adsorption equilibrium with Langmuir model, and (b) initial adsorption rate (after 1 hour) (solution= 70 mg Rb/L, pH_{eq} = 7.0 ± 0.8, feed volume = 0.2 L, adsorbent dosage = from 0.06 to 0.65 g/L).

5.3.2.2. Submerged MD-adsorption with different sizes of adsorbent

The effect of adsorbent size was examined on the Rb extraction from model Rb solution in the integrated submerged MD-adsorption process. The powder and particle forms of KCuFC in suspension were used with continuous provision of model 5.0 mg Rb/L feed solution. The experiments were conducted using the same experimental conditions as that for the granular KCuFC adsorbent experiment (temperature of feed solution and permeate: 55 and 20 °C, flow rate of permeate: 0.8 L/min). The adsorption capacity was different for the two different sizes of adsorbent used (**Figure 5-9** and **Table 5-3**). The trend observed in the integrated submerged MD-adsorption process was similar to that of the batch test (**Figure 5-8 (a)**). The integrated submerged MD-adsorption process both with powder and particle KCuFC adsorbents gave rise to a stable permeate flux (8.44 ± 0.20 L/m^2·h for powder adsorbent; 8.49 ± 0.19 L/m^2·h for particle adsorbent). The experiment was run for 10 h with a VCF of 1.99. The permeate flux of the integrated submerged MD-adsorption process was not affected by dosing of powder and particle KCuFC adsorbent in solution, and high permeate quality was obtained. Two hours after the start, reductions of 85% and 97% of Rb concentration were obtained with powder and particle KCuFC, respectively. With both adsorbents, after approximately 4 hours from the start, the Rb concentration increased gradually. At this point, the adsorption rates were 0.54 and 0.66 mg Rb/h for powder and particle adsorbent, respectively. However, these values varied with time. The Rb concentrations in the reactor were 17% and 3% when powder and particle forms of adsorbents, respectively, were employed. The initial adsorption rate in the integrated submerged MD-adsorption process was similar with the batch adsorption results (particle (3.96 mg as Rb/h) > powder (2.99 mg as Rb/h) > granular (1.41 mg as Rb/h)). After 10 hours of operation, the adsorption rate was in the order of particle (0.63 mg as Rb/h), granular (0.40 mg as Rb/h) and powder (0.25 mg as Rb/h). The total amounts of Rb adsorbed were 9.23, 13.42 and 5.98 mg for powder, particle and granular KCuFC adsorbent, respectively. Here, the adsorbent dose was 0.237 g/L.

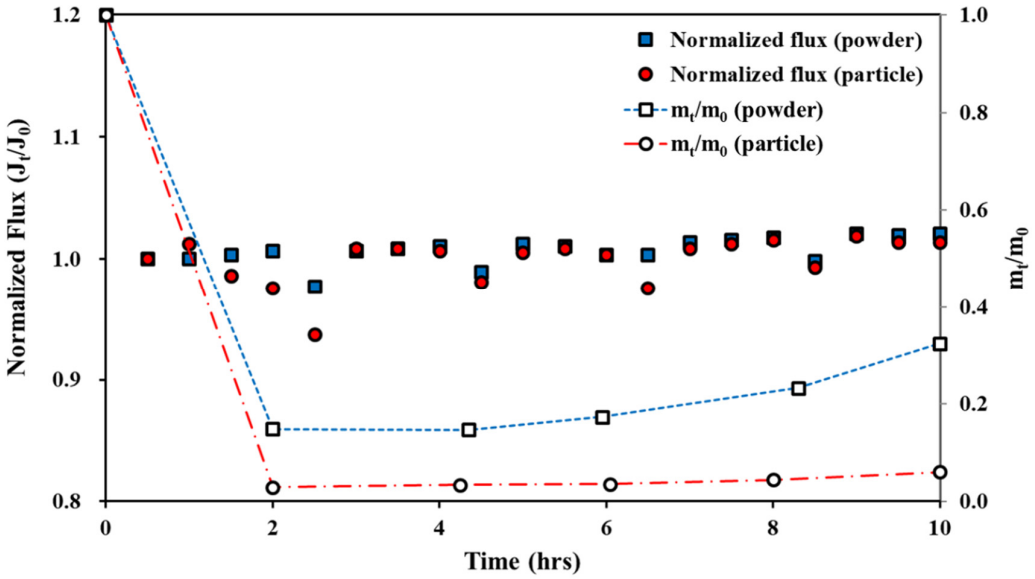

Figure 5-9. Variation of normalized flux and Rb concentration in solution for powder and particle adsorbents (T_f = 55 °C, T_p = 20 °C, feed solution = 5 mg Rb/L, adsorbent dosage = 0.24 g/L).

Table 5-3. The comparison of adsorption quantity for different sizes of adsorbent (powder, particle, and granular forms) (adsorbent dose = 0.24 g/L; operation duration 10 h, VCF 2.0)

Parameter	Powder	Particle	Granular (during cycle 1)
Adsorption rate after 2 hrs (mg/h)	2.91	3.96	1.41
Adsorption rate after 10 hrs (mg/h)	0.25	0.63	0.40
Total adsorption mass adsorbed (mg/g)	33.48	48.69	21.73
Total Rb adsorbed (mg)	9.23	13.42	5.98

The adsorbent's size influenced both the adsorption capacity and initial adsorption rate, which is due to the active surface area of the adsorbent. In general, smaller sized particles should have a higher active area for the contact of adsorbate (Min et al. 2000; Yamamoto 2001). However, in this study the

highest adsorption performance was not obtained for the adsorbent in powder form. This may be due to the adsorbent structure which may have been modified during the manufacturing process. Grinding of KCuFC particles into powder form may have reduced their adsorption ability due to the physical force although it should have a larger active area than particle KCuFC adsorbent. As well, the KCuFC powder may have been dissolved (although it does not have high solubility) and the small particles should have been dissolved more in the solution. In order to evaluate the stability of the different adsorbent forms, the concentrations of dissolved metals (Cu and Fe) released from the adsorbent into the feed solution were analyzed, because Rb adsorption by KCuFC adsorbent is driven by the force between transition ions (such as Cu) in KCuFC absorbent and Rb in the feed solution (Naeimi & Faghihian 2017). The suitability of the particle size over powder and granular were deduced based on adsorption capacity results that showed particle form KCuFC achieved higher adsorption capacity (48.69 mg/g) compared to power (33.48 mg/g) and granular (21.73 mg/g). In the case of granular form KCuFC, it is well established that polymer encapsulation of adsorbent compromises the availability of active ion exchange sites, resulting in substantially higher mechanical stability but lower adsorption capacity. The mechanical stability of granular form KCuFC is well reflected by the significantly lower dissolved metals (Cu and Fe) released from this adsorbent. For instance, the Fe release ratio by powder and particle KCuFC were, 1.57 and 1.37 times larger than that of granular KCuFC. In comparing the performance of powder and particle form KCuFC, Cu and Fe release ratio was 155 and 1.14 times higher with powder form KCuFC compared to particle form KCuFC. These results potentially suggest prevalent structure losses may have occurred with powder form KCuFC. This in turn, may have compromised the chemical structure of powder form KCuFC, resulting in lower absorption capacity compared to particle form KCuFC. Nevertheless, a more detail structural analysis should be carried out to substantially establish this observation.

The three forms of KCuFC adsorbents used in this study have certain advantages and disadvantages in

their application in the integrated submerged MD-adsorption. The powder and particle forms of KCuFC adsorbents have higher adsorption rate and capacity than granular KCuFC adsorbent. They do not, furthermore, influence the permeate flux. Subsequently, the powder and particle forms of KCuFC adsorbents are much more suitable for the integrated submerged MD-adsorption process for recovering Rb from the SWRO brine. However, the powder KCuFC adsorbent cannot be easily separated from bulk solution due to its small particle size. Also, it is deposited on the surface of the reactor, causing the mass loss of adsorbent. On the other hand, compared to the other two forms, the granular form can be easily separated from the solution. Nonetheless it does suffer from having the lowest adsorption capacity. The particle KCuFC adsorbent can mitigate the separation problem of adsorbent (this is a challenge with the powder form) while maintaining good adsorption capacity (compared to the granular form). However, the separation problem remains with the particle form. In order to solve these concerns, modified ways for preventing the mass loss and ease of separation of adsorbent from solution need to be considered for ensuring the integrated submerged MD-adsorption process performs at is most effective. A modified way is suggested for improving the performance of integrated submerged MD-adsorption process in this study. Specifically, this means using a cage for confining the adsorbent in a specific room. The material of the "cage" in which the adsorbent is confined should be a porous one, having smaller pores than adsorbent particle size. It should be able to allow the unconstrained water to flow so that a shear for adsorption is provided. This method can make the separation of adsorbent easy. Further, modification of KCuFC such as integrating with metal organic framework may also be favorable to kinetically enhance adsorption rate (Naeimi & Faghihian 2017). It is assumed that if the method is applied for particle, the possibility of having multiple cycle of integrated submerged MD-adsorption process can be improved with high adsorption capacity and ease of separating the adsorbent.

5.4. Summary of this research

The performance of integrated submerged membrane distillation (MD)- KCuFC adsorption for simultaneous water recovery and rubidium (Rb) extraction from seawater reverse osmosis (SWRO) brine was evaluated in detail. Based on the results, it was concluded that:

- Granular KCuFC adsorbent showed high affinity for Rb in thermal conditions (55 ° C). The adsorption capacity in terms of total adsorbed Rb mass was dependent on th e dose rate. Rb extraction rate increased from 59.9% at 0.05 g/L up to 97.5% at 0.2 4 g/L.

- Integrated submerged MD-adsorption with continuous supply of feed solution and adsorbent separation and regeneration successfully enhanced the performance of both MD and the adsorbent. This process can simultaneously recover high-quality fresh water (permeate conductivity of 1.25–1.98 μS/cm, rejection: 99.99%) and Rb as valuable resources.
- The multiple cycle operation of integrated submerged MD-adsorption with 5 mg Rb/L solution led to high quality permeate with a recovery ratio of 81%, and the Rb extraction with recovery ratio of 87% using the granular KCuFC adsorbent. Desorption using 0.2 M NH4Cl solution was suitable for extracting Rb and reusing granular KCuFC.
- Rb recovery with high-quality fresh water from SWRO brine was achieved using the integrated system. Two repeated cycles of integrated submerged MD-adsorption were successfully achieved with granular KCuFC adsorbent.
- CaSO4 crystallization and deposition on the membrane surface and in the reactor was observed when SWRO brine was used as the feed solution. Consequently, the performance of both MD and the adsorbent deteriorated. Hence, elimination of Ca in SWRO brine in the integrated process was recommended.

- The adsorption capacity of KCuFC depended on the size and form of KCuFC adsorbent. The particle form KCuFC (mean size: 0.45 mm) showed higher initial adsorption rate and adsorption capacity (Q_{max}) of 216.17 mg/g (based on Langmuir equation) compared to powder form KCuFC (size: < 100 μm) (135.04 mg/g) and granular form KCuFC (mean size: 2.42 mm) (164.1 mg/g).
- Two production/recovery streams (Rb and fresh water) were simultaneously obtained in the integrated submerged MD-adsorption system. Especially, the recovery of Rb leads to the economic benefits due to its substantial high price (11,180 US$/kg), and it can offset the cost for heating of feed solution in MD part.

CHAPTER 6

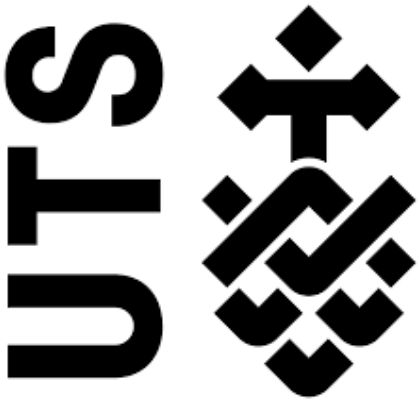

FRACTIONAL-SUBMERGED MEMBRANE DISTILLATION CRYSTALLIZER (F-SMDC) FOR TREATMENT OF HIGH SALINITY SOLUTION

This chapter has been published as: **Y. Choi**, G. Naidu, S. Jeong, S. Lee, S. Vigneswaran, Fractional-submerged membrane distillation crystallizer (F-SMDC) for treatment of high salinity solution, Desalination, 440 (2018) 59-67.

6.1. Introduction

In recent times, simultaneous brine treatment with extraction/production of valuable resources is favored to offset the treatment cost rather than the approach of treatment followed by disposal. The former is also preferred as seawater brine contains a number of valuable elements (Loganathan et al. 2017; Naidu, Jeong, Johir, et al. 2017). In this regard, membrane distillation with crystallizer (MDC) shows promising potential in SWRO brine treatment (Edwie & Chung 2013; Julian et al. 2016; Macedonio & Drioli 2010; Meng, Ye, et al. 2015; Tun et al. 2005). MDC is an integrated process that can achieve high quality fresh water while simultaneously extracting valuable resources from high salinity solution (Julian et al. 2016). MDC is attractive compared to traditional crystallization processes because of the following factors: well-controlled saturation rate, faster nucleation rate and reduction of induction time (Quist-Jensen, Macedonio, et al. 2017). Moreover, the ability to concentrate solution up to a saturation point with minimal flux decline is an added advantage of MDC (Ali et al. 2013; Alkhudhiri et al. 2012; Naidu, Shim, et al. 2017). Cooling crystallization method is widely used in separation processes for solution having different solubility at different temperatures due to its ease of control and maintenance (Lu et al. 2017). However, one of the major limitations is the significant energy consumption due to initial heating (thermal MD operation) followed by cooling for the crystallization.

A number of methods such as submerged MD (SMD) have been evaluated in terms of energy consumption to improve the efficiency over conventional MDC process (Choi et al. 2017; Francis et al. 2015; Meng, Hsu, et al. 2015). For instance, in SMD process, channeling heated feed solution through a pump to the membrane module can be eliminated, which results in lower heat losses through the feed channel (Edwie & Chung 2012; Julian et al. 2016). In this case, the feed tank can also act as a crystallizer (Choi et al. 2017). Nevertheless, several limitations are still present such as challenging saturated feed concentration effect, and fouling caused by crystal formation in the feed tank as well as

on the membrane (Goh et al. 2013; Shin & Sohn 2016; Tijing et al. 2015). Previous studies have shown that at elevated feed concentration levels (Choi et al. 2017), MD performance is affected by flux decline and wetting phenomenon. This decreases the membrane life span, resulting in more frequent membrane replacement, incurring additional operation cost (Choi et al. 2016).

In view of this, fractional submerged MDC (F-SMDC) based on principle of maintaining a feed concentration gradient (CG) and feed temperature gradient (TG) in the reactor was evaluated in this study. Maintaining CG and TG in the feed reactor can positively influence both MD and crystallization. CG and TG in the reactor enables to reduce feed concentration and increase feed temperature at the top portion of the reactor where the submerged membrane is located. This provides additional clean water with minimal membrane fouling. Simultaneously, the bottom portion of the reactor maintains high feed concentration with low feed temperature which enhances crystallization. This is due to the formation of high saturation state at the bottom portion of the reactor where crystals are formed continuously during F-SMDC operation. This setting potentially promises higher water recovery, with reduced membrane scaling issues. Further, the continuous extraction of crystal from the bottom of the reactor is expected to reduce the salt contents in feed solution (Julian et al. 2016).

In this study, the feasibility of F-SMDC for the treatment of highly concentrated and saline feed solution was investigated and compared with conventional submerged membrane distillation crystallization (SMDC). The trend of CG/TG in the feed reactor was examined during the operation. The effect on the flux and crystallization efficiency in the F-SMDC was evaluated. In addition, methods to improve the efficiency of maintaining CG/TG in the feed reactor were investigated.

6.2. Materials and Methods

F-SMDC process with direct contact MD (DCMD) configuration based on GC and TG was used in this study (**Figure 6-1**). The F-SMDC reactor consisted of three cylindrical cells which is equipped with double wall to enable the control of TG as temperature control of feed solution. The partition in the shape of funnel was installed between the top and bottom portion. Feed solution was placed inside the reactor while heating and cooling water was circulated at the outer wall of the reactor with respective heating and cooling units. This enabled the feed solution at the top portion of the reactor to be maintained at 50.0±1.3 °C, while, the feed solution at the bottom portion of the reactor was maintained at 20.0±1.5 °C. Thermometer was placed in each cell to measure the temperature of feed solution in real-time.

Meanwhile, the permeate temperature (T_p) was maintained at 16.5±0.2 °C, and it was measured using temperature sensors placed at the permeate channel. The permeate flow rate of 0.5 L/min was controlled using a gear-pump. Feed solution was fed continuously into the top portion of the reactor by the differential head of water between the reactor and feed tank. Continuous flow of new feed solution to the top portion of reactor enables to maintain a constant feed solution concentration rather than an increasing feed concentration. This systematically minimizes the effect of increased feed concentration on MD performance. The temperature of feed solution in the feed tank (reservoir) was maintained at room temperature (23.2±0.3 °C).

An external crystallizer was used at the last stage of the F-SMDC operation. Upon attaining super-saturation state at the bottom portion of the reactor, the remaining feed solution (mother liquid) was fed to this external reactor. The external reactor was kept at room temperature (23.2±0.3 °C) with constant stirring (50 rpm) of the mother liquid to enhance crystal growth.

The performance of F-SMDC process was first investigated using 120 g/L Na_2SO_4 solution as feed solution. The solubility of Na_2SO_4 in water varies significantly at different temperature (91 g/L @

10 °C, 195 g/L @ 20 °C, and 488 g/L @ 40 °C). A mixed solution containing sodium chloride (NaCl) and Na_2SO_4 was then used to examine an effect of salinity on treatment of high concentration Na_2SO_4 solution. The permeate/fresh water quality was evaluated by measuring the conductivity/total dissolved solids (TDS) value in real-time. All the experiments were duplicated to ensure the reproducibility.

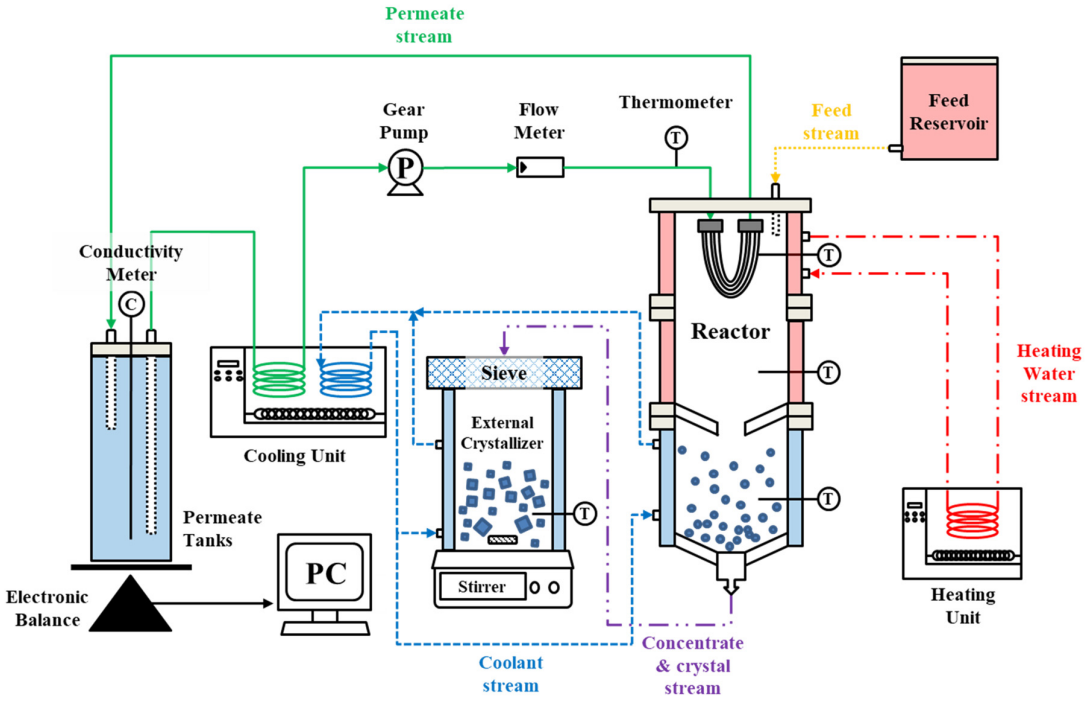

Figure 6-1. Set-up of F-SMDC process: permeate stream (——), stream of continuous feeding to the reactor (feed solution) (·····), stream of concentrate and crystal generated from the reactor to the crystal growth cell (–··–), the stream of heating water for the top portion of the reactor (–·–), stream of coolant water for the bottom portion of the reactor and the crystal growth cell (– – –).

6.3. F-SMDC principle

F-SMDC is a combination of two processes: MD and crystallization in a single feed reactor with a submerged membrane (**Figure 6-2 (a)**). Based on the previous research, submerged-direct contact membrane distillation (S-DCMD) configuration was used for F-SMDC due to higher permeate flux at high concentration and low potential of wetting phenomenon compared to S-VMD configuration (Choi et al. 2017). The submerged membrane module is placed at the top portion of the feed reactor. In F-SMDC, a CG is generated in the feed reactor as a result of difference in solution density. Upon the increase of feed solution concentration (MD part), the density of the feed solution increases, resulting in the gravitation of concentrated feed solution to the bottom of the reactor (**Figure 6-2 (b)**). In S-DCMD, cooling down of feed solution by the cold permeate stream further enhances this factor as water density is higher at low temperature. Accordingly, CG is generated in the reactor. Simultaneously, TG is generated by external heating and cooling of the outer wall (**Figure 3-5**).

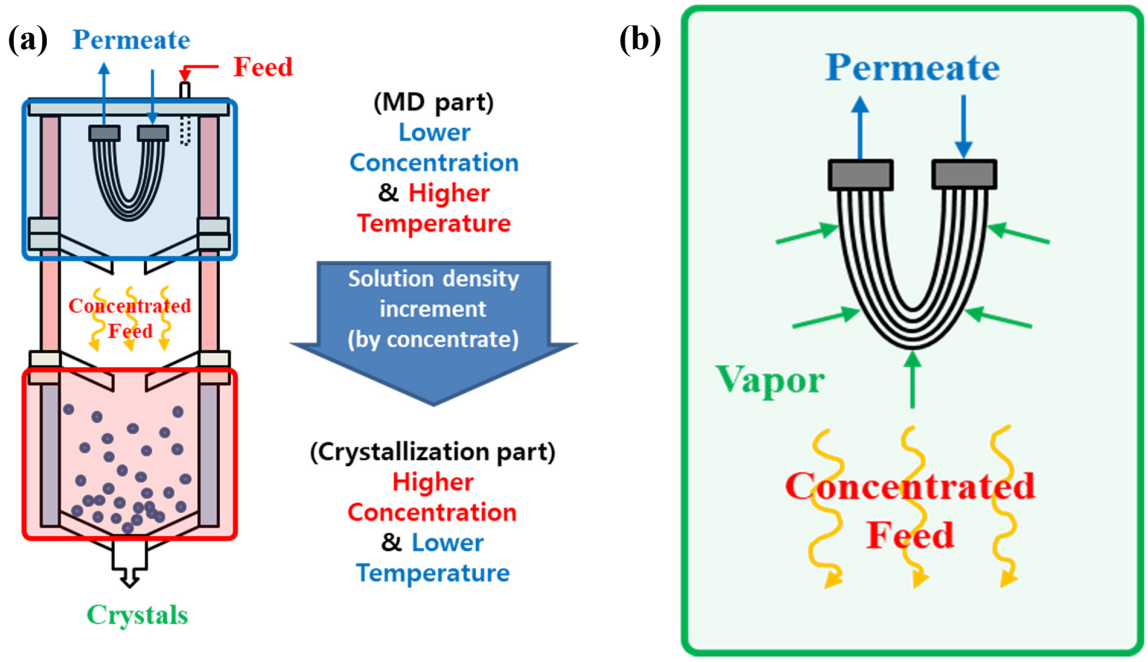

Figure 6-2. Generation of concentration gradient (CG) in feed reactor of F-SMDC: (a) lower feed concentration at the top portion and higher feed concentration at the bottom portion, and (b) concentration effect at the top portion of the reactor containing submerged membrane.

The presence of CG in the feed reactor influences both MD and crystallization efficiency of the F-SMDC process. In MD, dissolved ion concentration in the feed solution is increased as the feed solution in concentrated, resulting in decrease of permeate flux. However, in crystallization process, elevated dissolved ion contents are favorable for attaining saturation degree of targeted compounds. Lower concentration at the top portion of the reactor is suitable for MD operation. Higher concentration at the bottom portion of the reactor is favorable for the formation of crystals since super-saturation (above the limits of metastable zone) of target salt should be reached to get a nucleation of crystals. F-SMDC achieves an increase of feed concentration at the bottom portion of the reactor at a faster ratio compared with theoretical concentration ratio in the whole reactor, and crystals are formed when solution concentration exceeds the limits of metastable zone of solution. Moreover, TG is formed in the reactor by the temperature transfer caused by movement of concentrated feed solution to the bottom portion without additional temperature control (using heating or cooling). Temperature at the top portion is higher than the bottom portion. The maintenance of TG in F-SMDC enhances the crystallization phenomenon.

Convection current in the reactor occurs differently (**Figure 6-3 (a)**). If feed solution is heated up near the reactor wall, its density decreases with its expansion. As a result, it moves towards the upper portion, and the unheated feed solution moves downwards. Moreover, concentrated and cooled (because of the effect of lower permeate temperature (around 16.5±0.2 °C) of S-DCMD) feed solution by membrane operation favors the above effect. As a result, feed solution is mixed, and therefore CG cannot be maintained in the feed reactor. Even though convection current effect on solution mixing does not significantly affect CG, it should still be controlled to ensure that CG is well controlled/maintained throughout the operation. In our design of F-SMDC, the incorporation of a partition in the feed reactor enables to maintain convention current effect within the respective cells (top and bottom portion of the

reactor) (**Figure 6-3 (b)**). The partition prevented the feed solution mixing by convection current, resulting in maintaining CG and TG in the reactor.

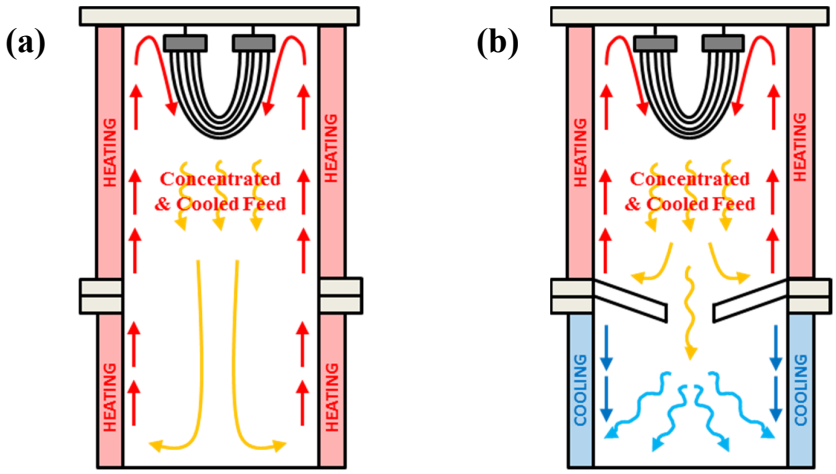

Figure 6-3. Convection current in reactor by heating and cooling of (a) conventional MDC process (reactor without cooling and partition) and (b) F-SMDC process (reactor with cooling and partition).

6.4. Results and discussions

In this study, the feasibility of F-SMDC was examined for the treatment of feed solution containing Na_2SO_4 alone and with NaCl.

6.4.1. Performance comparison of F-SMDC and SMDC

The performance of conventional submerged MDC (SMDC) (reactor without cooling and partitioning) was compared with F-SMDC (reactor with cooling and partitioning) under the same operating conditions (reactor, feed temperature and feed solution) and same sampling points at the top and bottom portion of the reactor. The initial flux of both SMDC and F-SMDC mode was 2.8 and 2.7 LMH respectively. The initial flux of S-MDC was slightly higher than F-SMDC, while the feed solution concentration trend varied. Up to a feed solution VCF 2.5, a similar concentration variation was observed for both SMDC and F-SMDC mode. However, in SMDC, above VCF 2.5, a rapid increase of concentration from VCF 2.5 to 2.8 accompanied by a rapid flux decline was observed (**Figure 6-4**

and **Figure 6-5).** Both processes maintained 99% ion rejection ratio until the end of the experiment. Comparatively, F-SMDC was able to maintain a stable concentrate (without rapid increase) up to VCF 3.0 and sustained the operation up to VCF 3.5. The results indicated that in F-SMDC, the partition between the top and the bottom portion of the reactor prevented the mixing of feed solution by natural convection current, emulating a trap. This enabled to create a CG in the reactor, with a higher concentration at the bottom portion of the reactor. In F-SMDC, the presence of CG in the feed reactor was beneficial for both the MD and crystallization processes. Maintaining a low feed concentration closer to the membrane in F-SMDC enabled to achieve a higher VCF (around VCF 3.5) with smaller flux decline compared to the SMDC (around VCF 2.8). In SMDC, concentrated feed solution interferes with the transportation of vapor through the hydrophobic membrane, decreasing its performance (reduced flux decline).

In F-SMDC, the presence of CG in the feed reactor was well reflected by the CG variation between the top and bottom portion of the reactor (**Figure 6-4**). The CG effect was especially apparent from VCF 1.5 onwards. The feed concentration at the top portion (MD part) of the reactor did not change rapidly while a rapid increase of feed concentration at the bottom portion of the reactor was observed. At the top portion, the feed solution concentration was maintained (range: 171.8±5.1 g/L, 1.4 times of initial feed concentration) below the theoretical feed concentration increment (initial feed concentration × VCF). Above VCF 2.0, feed concentration at the bottom portion of the reactor showed higher increment than the theoretical feed concentration level. Over time, the feed concentration at the bottom portion of the reactor greatly varied to the theoretical feed concentration. The results reflected the capacity of F-SMDC to maintain a stable CG in the feed reactor.

In the F-SMDC mode, higher feed concentration at the bottom portion of the reactor than the top portion made it suitable for the formation of target crystals. Also, lower temperature (around 20.0 ±1.5 °C) at the bottom portion of the reactor, which was generated by the cooling as well as the

movement of concentrated/cooled feed solution from the top portion (heated up) was favorable for the stimulation of crystals.

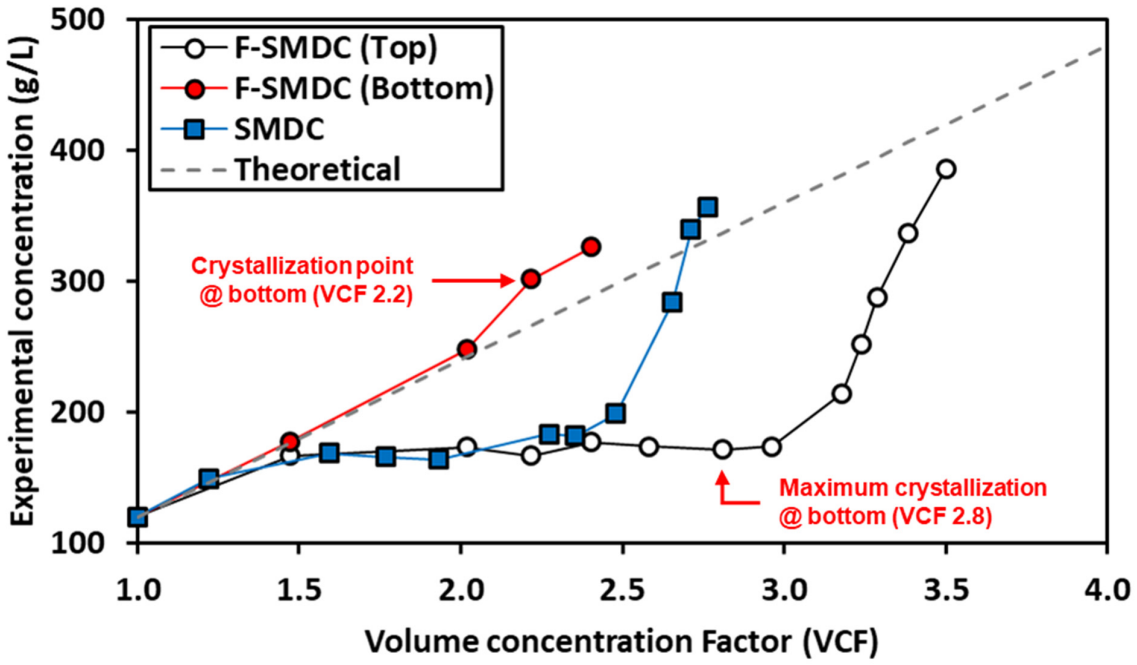

Figure 6-4. Variation of feed concentration in the reactor during the operation in F-SMDC and SMDC modes (feed: 120 g/L Na_2SO_4, T_{Top} = 50.0±1.3 °C, T_{Bottom} = 20±1.5 °C, $T_{permeate}$ = 16.5±0.2 °C).

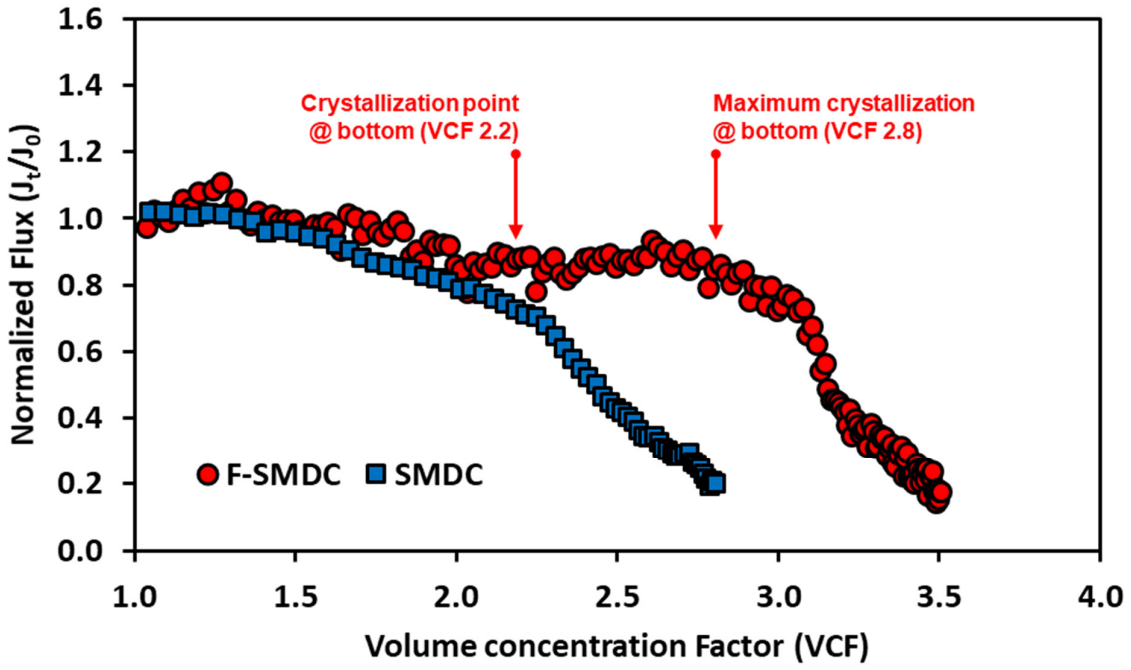

Figure 6-5. Comparison of flux in F-SMDC and SMDC mode (without crystal extraction) (feed: 120 g/L Na_2SO_4, T_{Top} = 50.0±1.3 °C, T_{Bottom} = 20±1.5 °C, $T_{permeate}$ = 16.5±0.2 °C).

The F-SMDC was carried out using S-DCMD configuration. The feasibility of different submerged MD configurations (submerged vacuum direct contact MD called as S-VDCMD) in F-SMDC process was examined under the same operational condition. The motivation for using S-VDCMD is the potential of achieving higher permeate flux. In line with this, S-VDCMD achieved a 25% higher initial permeate flux than S-DCMD. However, the CG in F-SMDC with S-VDCMD configuration was not observed. Higher flux decline was also observed with S-VDCMD compared to F-SMDC with S-DCMD configuration (**Figure 6-6**) with slightly lower feed concentration at the bottom portion than at the top portion of the reactor. This was attributed to the application of vacuum. In a previous S-MD study (Choi et al. 2017), it was found that the deposition and adhesion of crystals on the membrane surface was intensified by the presence of vacuum pressure in the MD, resulting in more prevalent fouling. In S-VDCMD, concentrated ions were captured in the membrane boundary layer due to

stronger driving force (vacuum pressure) compared to S-DCMD (Choi et al. 2017). This restricted the movement of concentrated feed solution, and it stagnated close to the membrane surface. The increase in diffusion potential of concentrated feed solution at the top portion rather than the precipitation downward, resulted in the formation of higher concentration at the top portion than the bottom portion of the reactor. The results highlighted that S-MD using vacuum was not suitable for F-SMDC process.

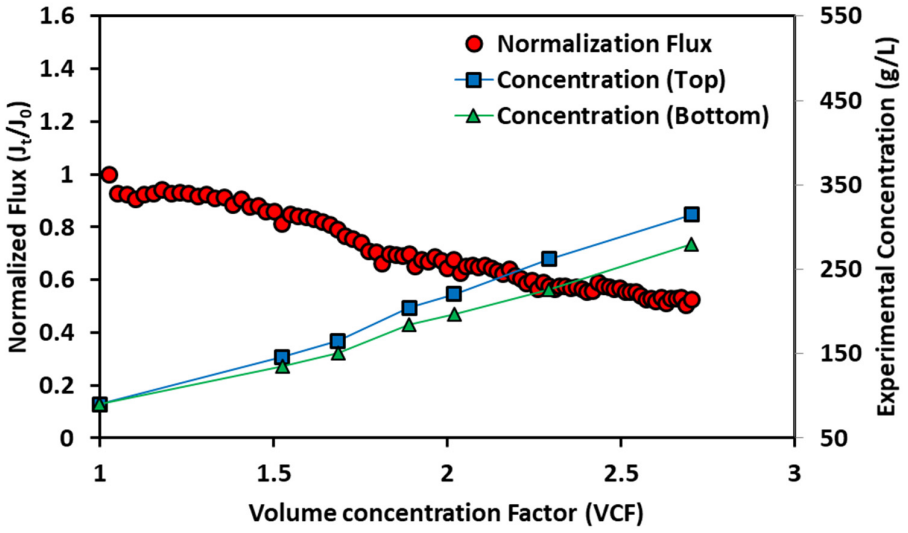

Figure 6-6. Normalized flux and concentration tendency in F-SMDC comparing with S-VDCMD.

6.4.2. Continuous F-SMDC operation

The stability of F-SMDC in treating high concentration solution was examined by carrying out two repeated cycles of operation using the same membrane. At the end of each cycle, used membrane was submerged in DI water and stirred at 200 rpm for 10 mins to rinse/clean the membrane before the subsequent operation.

In S-DCMD configuration, generally, the membrane surface feed temperature is lower compared to bulk feed temperature due to direct contact with cold permeate on the membrane surface. This factor

plays a prevalent role in the solubility of certain crystal salts that are especially influenced by the effect of temperature. One such salt is Na_2SO_4, which exhibits lower solubility at low temperature (91 g/L @ 10 °C, and 195 g/L @ 20 °C) and higher solubility at increased temperature (488 g/L @ 40 °C). This characteristic of Na_2SO_4 can lead to higher saturation state on the membrane surface, and it aggravate the formation of crystals. This results in the non-continuity of MDC process.

The effect of this phenomenon can be mitigated in F-SMDC by creating and maintaining CG in the reactor. The feed concentration (under 195 g/L) was lower at the top portion of the reactor which contains the submerged membrane. Here, the direct contact with the permeate solution (16.5±0.2 °C) lowered the feed solution temperature which was set at 50.0±1.3 °C. Specifically, the feed concentration at the top portion of the reactor was maintained at 171.8±5.1 g/L in cycle 1 and 169.2±3.0 g/L in cycle 2. At these concentration ranges of Na_2SO_4, super-saturation was not reached at 16.5±0.2 °C (feed temperature at bottom portion). As such, salt precipitation followed by crystal deposition on the membrane surface was delayed up to around VCF 3.0 as shown in **Figure 6-7**. In both cycles 1 and 2, fouling on the membrane surface was not detected due to the lower concentration at the top portion. However, in cycle 1, the fouling phenomenon on the membrane surface was detected after VCF 3.0 (**Figure 6-8**). This was due to rapid increase of concentration (214.4 to 385.5 g/L) upon reaching VCF 3.0. Rapid flux decline occurred beyond this point (**Figure 6-7**).

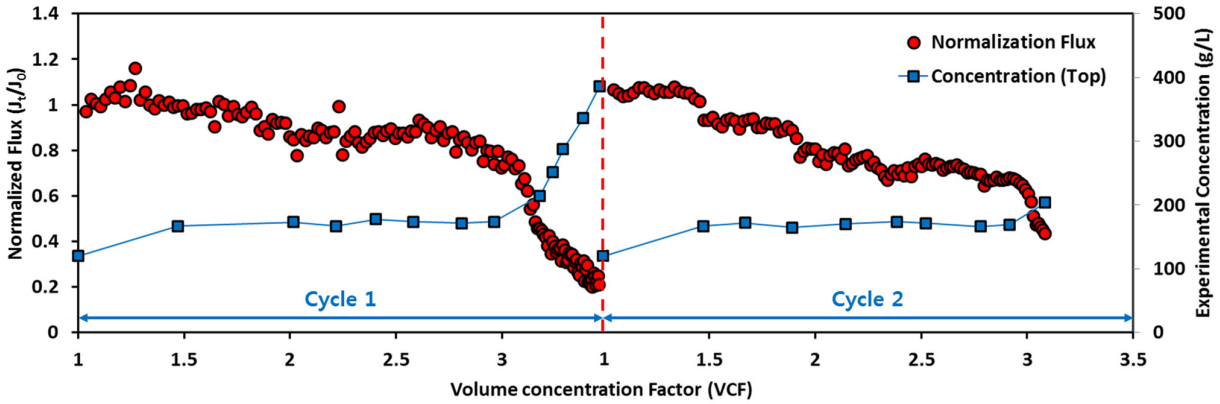

Figure 6-7. Flux and concentration variation in continuous F-SMDC (without crystal extraction until the completion of each cycle).

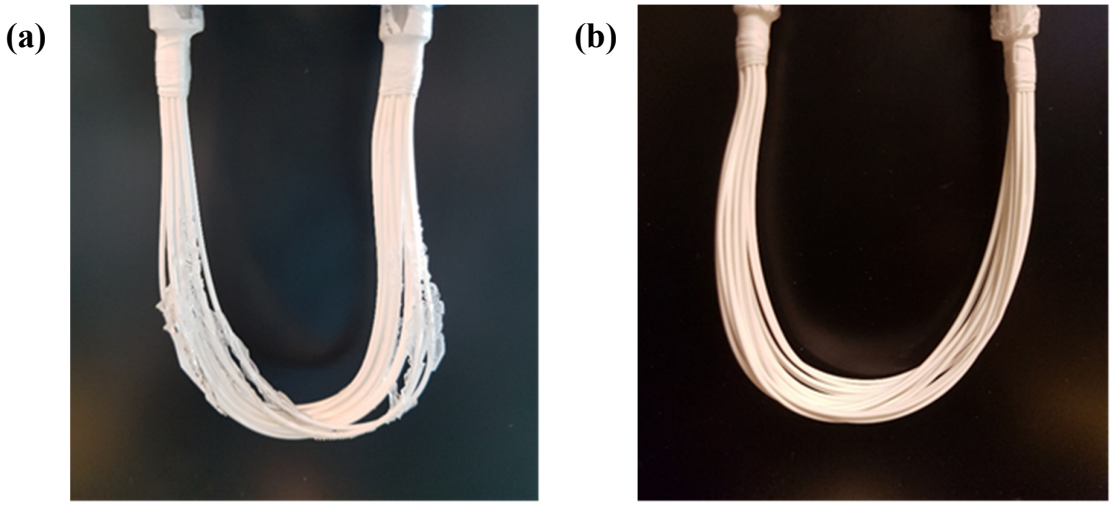

Figure 6-8. Used membrane with Na_2SO_4 treatment at the end of (a) cycle 1, (b) cycle 2.

Initial crystal formation at the bottom portion of the reactor occurred at around VCF 2.2 in both cycles. At VCF 2.8 and above, the bottom portion of the reactor was completely filled with crystals. At this point, the feed concentration at the top portion of the reactor increased rapidly, and CG in the F-SMDC feed reactor was no longer maintained. As such, it is essential to continuously extract crystals generated at the bottom portion of the reactor to maintain a feed concentration gradient in the F-SMDC process. For this reason, an external crystallizer was used in this study as described in **section 6.2**.

At the end of each operation cycle, Na_2SO_4 solution remained at the top and middle portions of the reactor. It must be highlighted that the F-SMDC was carried out in a batch mode. In the scenario of a continuous mode operation, periodic crystal extraction from the bottom portion of the reactor would be possible. This would enable continuous crystal growth simultaneously, while achieving near zero liquid discharge in the reactor. However, in view of the batch mode operation of this study, an external crystallization was used to evaluate the potential of further crystal growth with the remaining Na_2SO_4 solution. This would enable to depict the near zero liquid discharge scenario of a continuous mode. In depth evaluation of F-SMDC operation in a continuous mode will be explored in future studies to establish this scenario.

Upon allowing the reactor to stand at room temperature (23.2±0.3 °C) for 3 days (72 h), further salt crystallization occurred due to its super-saturated state (**Table 6-1**). This step enabled the generation of additional crystals, thereby, increasing the total amount of crystals. Although the initial concentrations in both cycles were different (because of different degree of concentrate: VCF 3.5 in cycle 1 vs. VCF 3.0 in cycle 2), the final concentrations of both cycles were similar. However, the solution volume reduction ratio varied (87% in cycle 1 vs. 47% in cycle 2) (**Table 6-1**). The simple step of allowing the feed solution to remain at room temperature without additional treatment enabled to decrease the feed concentration and volume by 32% and 46% respectively. Further, the small quantity of remaining solution at the top and middle portions of the reactor can be channeled back to the bulk feed tank for a subsequent F-SMDC operation cycle. This indicated that F-SMDC with external crystallization does have the potential to achieve near zero liquid discharge.

Table 6-1. Volume and concentration of feed solution extracted from reactor upon F-SMDC and upon external crystallization (standing at room temperature for 24 - 72 h).

Sample	1st cycle		2nd cycle	
	Concentration (g/L)	Amount (mL)	Concentration (g/L)	Amount (mL)
Final F-SMDC feed (Before crystallization)	329.4±6.1	1140	218.1±2.3	1160
Upon external crystallization	160.4±0.2 (24 h) 149.9±2.3 (72 h)	150	160.4±0.7 (24 h) 147±0.3 (72 h)	620

6.4.3. Crystal production in F-SMDC

In F-SMDC, crystals were generated at the bottom portion of the reactor due to high concentration and lower temperature setting. In this study, the bottom portion of the reactor was cooled down up to 20.0±0.5 °C while the top portion of the reactor was maintained at 50.0±1.3 °C. At the bottom portion of the reactor, the combined condition of higher feed concentration and lower temperature enabled to achieve a faster super-saturation state of Na_2SO_4 compared to the top portion of the reactor. The CG and TG in the F-SMDC (lower concentration and higher temperature at top portion, higher concentration and lower temperature at bottom portion) improved the efficiency of recovering valuable crystals as well as obtaining higher water recovery and better stability (lower scaling) of MD process.

When 120 g/L Na_2SO_4 was treated without using crystals extraction, crystals were generated both at the top and bottom portions of the reactor. The amount of generated crystals formed was directly proportional to the concentration ratio of feed solution (**Table 6-2**). High amount of crystals was generated both during cycle 1 (1169.0 g) and cycle 2 (898.0 g). In the case of cycle 1, F-SMDC operation was carried on beyond the point of rapid flux decline in order to obtain a highly concentrated final solution. The rapid permeate flux decline due to fouling and high feed concentration degraded

the stability of the process. Therefore, it is not recommended to operate F-SMDC beyond the super-saturation state of the feed solution in the future study.

Table 6-2. Crystal and fresh water production by F-SMDC operation (feed: Na_2SO_4).

Sources	1st cycle		2nd cycle	
	Produced crystal (g)	**Produced fresh water (mL)**	**Produced crystal (g)**	**Produced fresh water (mL)**
Bottom portion of the reactor	551.3		541.6	
External crystallizer (containing saturated solution from top and middle portion of the reactor)	617.7	4295.5 (99% ion rejection)	356.4	3561.4 (99% ion rejection)
Total	1169.0		898.0	

The crystal production rate can be increased by factors such as temperature control, crystal size and immersion of crystals into saturated solution. As shown in **Table 6-1**, the volume and concentration of mother liquid decreased due to the formation of Na_2SO_4 crystals with time. For instance, the feed concentration of 160.4±0.2 g/L after 24 h was reduced to 149.9±2.3 g/L after 72 h. This indicated that additional crystals of larger sizes can be produced by the immersion of initial crystals into the mother liquid (**Figure 6-9 (d)**). The morphology of Na_2SO_4 crystals changed from rectangle shape to spherical shape over time (**Figure 6-9 (a), (b)** and **(c)**). Prevalent growth and change in shape of crystals were detected on crystals that were fully immersed in the mother liquid. The results indicated that direct contact with mother liquid would enhance the growth of crystals. It is therefore essential to have enough contact area and immersion time with mother liquid. By doing so, a narrow size distribution of the crystals can be obtained.

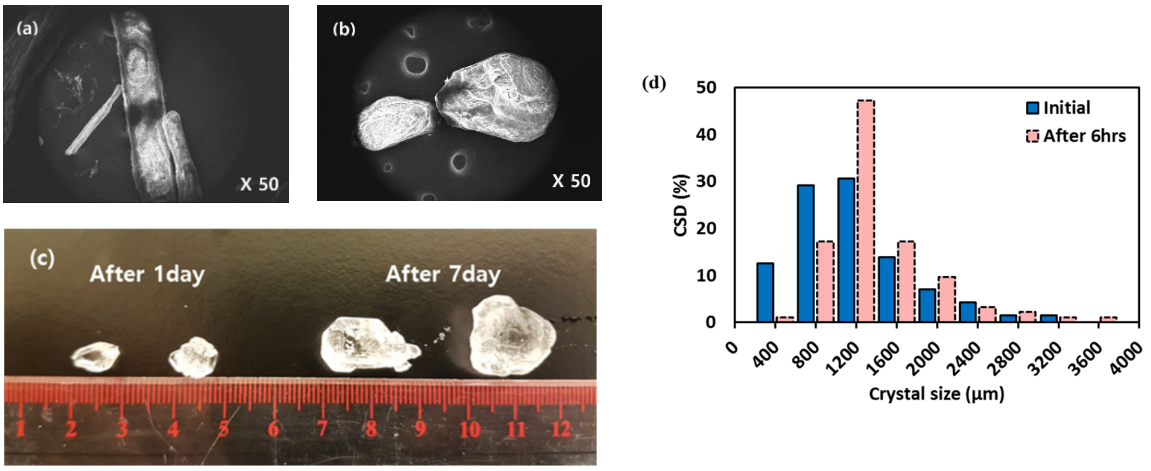

Figure 6-9. Crystal size distribution (CSD) and change in morphology of produced Na_2SO_4 crystals with time. Images of crystals at (a) initial, and after (b) 60min and (c) 1 day and 7 days, and (d) size distribution of Na_2SO_4.

6.4.4. Effect of salinity

The effect of salinity in the treatment of Na_2SO_4 solution was examined by adding NaCl. As shown in **Figure 6-10**, the concentration gradient trend at the initial stage (up to VCF 1.5) was similar with and without the presence of NaCl. In the presence of NaCl, the formation of crystals at the bottom portion of the reactor started from around VCF 1.8, while the concentration at the top portion of the reactor increased (with and without the presence of NaCl), lower VCF was achieved in the presence of NaCl. In the presence of NaCl, from VCF 2.2 onwards, visible presence of crystals was observed. At the same time, rapid flux decline and increase of feed concentration at the top portion of the reactor occurred. This occurrence was associated to the presence of crystals on the membrane surface. The F-SMDC operation condition, namely concentrated feed solution and cooler membrane surface condition (direct contact with cold permeate) enabled the generation of CG. The crystal deposition on the membrane surface reduced the effective membrane area. This decreased the rate of concentration and degree of cooling by permeate, resulting in reduced crystallization of concentrated solution. Therefore,

concentrated solution remained at the vicinity of the membrane boundary layer, and feed concentration at the top portion of the reactor portion increased by diffusion. This caused an increased crystal deposition onto the membrane surface (**Figure 6-10 (b)**).

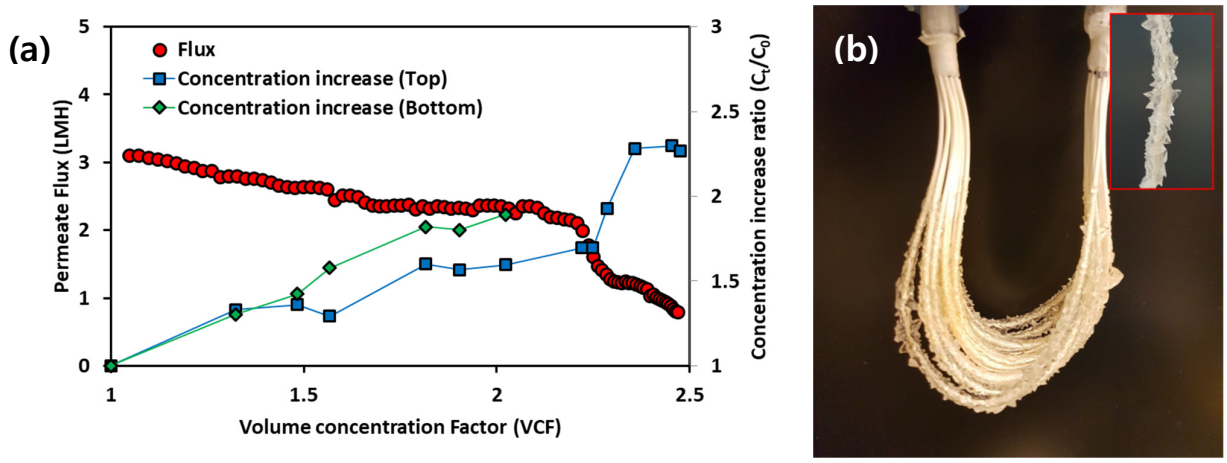

Figure 6-10. F-SMDC with Na_2SO_4 and NaCl: (a) variation of flux and concentration at the top and bottom portion of the reactor, (b) used membrane at the end of the experiment.

The EDX analysis revealed the presence of sodium, oxygen and sulphur elements on the used membrane surface and at the bottom portion of the reactor (**Figure 6-11 (a)** and **(b)**). On the other hand, chloride ion was detected in crystals generated in feed solution of the top and middle portions of the reactor. The results indicated that a separate generation of crystal from solution can be achieved by a control of concentration and temperature at suitable range. In addition, the concentration of sodium ion in solution seems to influence crystallization phenomenon on the membrane surface and at the bottom portion of the reactor. The crystallization on the membrane surface was detected at around VCF 3.3 in the absence of NaCl. The crystals formation on the membrane surface became faster (around VCF 2.2) with NaCl. At this point, the concentrations of sodium ion in both feed solutions with and without NaCl were similar (93.08 g/L without NaCl and 93.28 g/L with NaCl). Also, upon crystal formation at the bottom portion of the reactor, similar amount of sodium ion concentration was

observed in both the feed solutions (without NaCl: 107.78 g/L in cycle 1 / 106.26 g/L in cycle 2, and with NaCl: 106.08 g/L). The difference in the initial point of crystallization on the membrane surface and at the bottom of the reactor was attributed to temperature difference.

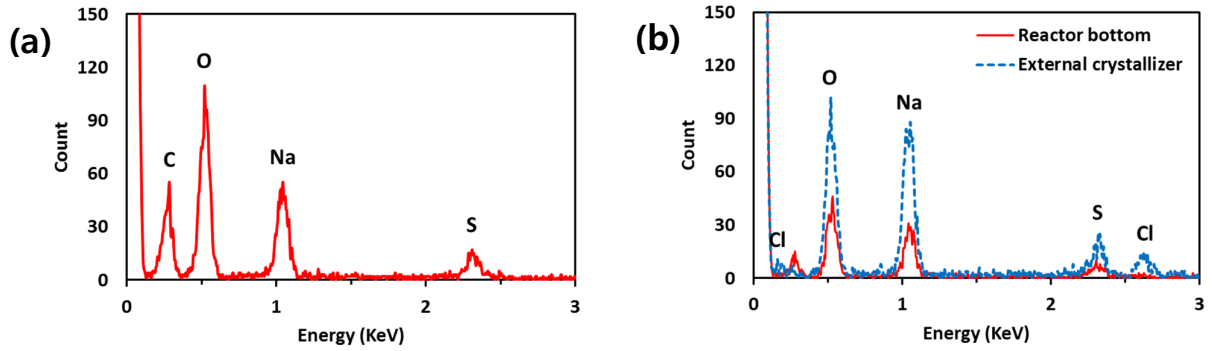

Figure 6-11. EDX analysis of crystals (a) deposited on the used membrane surface, (b) produced from the bottom portion of the reactor and external crystallizer (saturated feed solution from the top and middle portion of the reactor) (feed solution: Na2SO4 and NaCl).

6.5. Summary of this research

The feasibility of fractional submerged membrane distillation-crystallization (F-SMDC) process was evaluated using a feed solution containing high concentration of Na_2SO_4 without and with NaCl. The following conclusions were made from the experimental investigation:

- F-SMDC setting enabled the creation of CG and TG using a partition and double wall heating/cooling in the feed reactor. A lower feed concentration and higher feed temperature was maintained at the top portion of the reactor. Meanwhile, higher feed concentration and lower feed temperature was maintained at the bottom portion of the reactor.
- The presence of CG/TG in F-SMDC enabled to achieve higher water recovery (VCF 3.5) and lower membrane scaling, compared to SMDC mode (VCF 2.9).
- The condition of elevated feed concentration and lower temperature at the bottom portion of the reactor was favourable for high crystal formation in F-SMDC.
- The presence of salt (NaCl) influenced the crystallization of Na_2SO_4 at the bottom portion of the reactor and on the membrane surface, resulting in higher crystallization in both locations.
- F-SMDC was effective in reducing membrane scaling, producing high quality fresh water and valuable crystals (Na_2SO_4).
- The shape and dimension of F-SMDC reactor are essential factors that influence the formation of CG/TG and the overall F-SMCD performance. Further optimization of the reactor configuration is an important factor that must be explored in detail.

CHAPTER 7

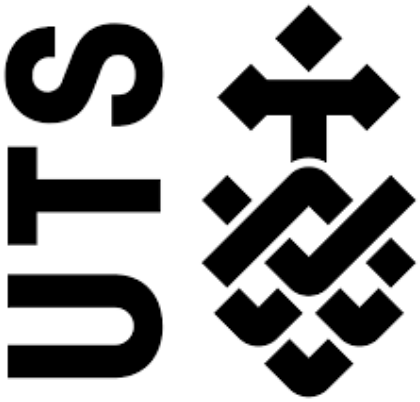

EFFECT OF INORGANIC AND ORGANIC COMPOUNDS ON THE PERFORMANCE OF FRACTIONAL-SUBMERGED MEMBRANE DISTILLATION CRYSTALLIZER

This chapter has been published as: **Y. Choi**, G. Naidu, S. Lee and S. Vigneswaran, Effect of inorganic and organic compounds on the performance of fractional-submerged membrane distillation-crystallizer, Journal of Membrane Science, 582 (2019) 9-19.

7.1. Introduction

Crystallization is a simple and fundamental process for the separation and purification of solid products widely used in the chemicals, pharmaceuticals and food industries as well as for water and wastewater treatments (Chabanon et al. 2016; Kim, Kim, et al. 2017). It is based on a solid-liquid separation process using a control of solubility, in which a pure solid crystal is produced and extracted from the liquid solution (Lu et al. 2017). The solubility of solution can be changed by varying the temperature and/or the solution composition. In spite of the wide application of crystallization, the process still has significant limitations. Almost all the crystallizers are operated in batch mode. The need for a continuous crystallizer is essential, especially for solutions with low concentration of ions (Adler et al. 2000; Chabanon et al. 2016).

The combination of membranes with crystallizers enables to achieve continuous crystallization (Gabelman & Hwang 1999; Gugliuzza et al. 2009; Hermanto et al. 2007). Crystallizer combined with membrane distillation (MD) is especially promising (Quist-Jensen, Macedonio, et al. 2017). This is because, MD is a process driven by a vapor pressure created by temperature difference between the feed and permeate solutions across a microporous hydrophobic membrane (Choi et al. 2017; Naidu, Jeong, Choi, et al. 2017; Naidu, Shim, et al. 2017). More than 90% water recovery can be achieved from highly saline feed solutions by MD (Choi et al. 2017; Ji et al. 2010; Quist-Jensen, Macedonio, et al. 2016). MD can increase the concentration of feed solution to saturation concentration of the target material in solution, and crystallization process can maintain the concentration of feed solution above saturation concentration by the formation of target material in crystal form. The combination of MD with crystallizer improves the individual processes, in terms of achieving higher water recovery, well-controlled saturation ratio, increase of crystallization kinetic, reduction of induction time, low fouling potential, and stable permeate flux (Lu et al. 2017; Quist-Jensen, Macedonio, et al. 2017; Shin & Sohn 2016). The combined system enables the production of freshwater and extraction of valuable resource

from high concentration of feed solution simultaneously especially for challenging solutions such as the seawater brine and wastewater.

MD crystallizer requires both heating (for the thermal MD process) and cooling (for the crystallizer process) (Chen et al. 2014; Edwie & Chung 2013; Kim, Kim, et al. 2017; Kim et al. 2016). A typical MD crystallizer system is a continuous in-line set-up (Curcio et al. 2001; Curcio, Ji, Quazi, et al. 2010). This set-up requires constant and rapid feed solution heating (at the membrane module) and cooling (at the external crystallizer tank). The rapid heating and cooling results in energy losses. Moreover, in an in-line circulation, the short contact time of the feed solution in the crystallizer tank is not sufficient to ensure that salt crystallization occur entirely in the crystallizer tank. Inevitably, the supersaturated feed solution in contact with the membrane (MD process) results in deposition of salt crystals (scaling) on the membrane. This makes the process impractical to achieve high water recovery.

Fractional-submerged membrane distillation crystallizer (F-SMDC), an integrated MD crystallizer in a single reactor helps to mitigate the energy losses through circulation and the contact time limitation of the current in-line MD crystallizer system (Choi et al.). F-SMDC is based on the presence of concentration gradient (CG) and temperature gradient (TG) using a submerged hollow fiber membrane. Here, a double wall reactor enables heating at the top portion of the reactor (containing the submerged membrane) for water recovery and simultaneous cooling at the bottom portion of the reactor for enhancing salt crystallization. This creates a TG in the system. (Choi et al. ; Choi et al. 2017). The increase of feed solution density generated by concentrate (Bayindirli 1992; Bayindirli 1993) in submerged-membrane distillation (S-MD) results in the natural gravitation of the concentrated feed solution moving to the bottom of the reactor. This results in the formation of CG in the reactor. The CG formation in the reactor is essential to maintain the low feed solution concentration at the top portion of the reactor while increasing the feed concentration at the bottom portion until salt super-saturation condition is achieved. This then results in the generation of different saturation levels of the

salts. This phenomenon improves the performance and efficiency of water recovery in the submerged MD and crystallization process. Furthermore, the difference of the saturation level of the solution between the top and bottom portions of the reactor can be enhanced by the TG formed in the reactor.

In this study, the performance of F-SMDC as a treatment process for high salinity feed solution was evaluated. Specifically, the effect of different inorganic and organic compounds on the formation of CG/TG in the F-SMDC reactor were examined. Feed solutions with inorganic compounds of different molecular weight, electronegativity, and solubility variation tendency were used to analyze the effect of these properties on the formation of CG/TG. The effect of organic compounds and its presence in combination with inorganic compounds were also studied.

7.2. Materials and Methods

The fractional-submerged membrane distillation crystallization (F-SMDC) process was based on the concept of formation of CG/TG in the reactor to enhance the performance of both S-MD and crystallization processes (**Figure 3-4**). The feed temperature of solution at the top portion in the reactor was maintained at 50.0 ± 1.2 °C. In order to enhance the degree of crystallization intentionally in the reactor, the temperature at the bottom portion was controlled at a lower temperature of 20.0 ± 1.3 °C using a cooling unit. The temperature of feed solution at each portion was measured by temperature sensors placed along the reactor. The submerged-direct contact membrane distillation (S-DCMD) was placed at the top portion of the F-SMDC.

The feed solution was continuously supplied from feed reservoir to the top portion of the reactor by the head difference of water between the reactor and feed reservoir without any need for pump to provide the feed solution. The feed solution in the reservoir was stirred using a magnetic stirrer and

magnetic stirring bar (50 rpm) to maintain the homogeneous feed concentration. Feed solution in reservoir was maintained at room temperature (23.2 ± 0.3 °C). The permeate temperature was maintained at 16.5 ± 0.3 °C. This temperature was measured using temperature sensors placed at the permeate circulation line prior to the membrane module. A permeate flow rate of 0.8 L/min was maintained by a gear-pump, which was measured using a flow meter. Feed samples were collected regularly along the reactor (the top to bottom portion), in order to evaluate the degree of CG.

In order to examine the effect of properties of different compounds (present in seawater and wastewater brine) on the CG/TG formation in F-SMDC, five different feed solutions were used individually; NaCl, KCl, NH_4Cl, Na_2SO_4, and $MgSO_4$. The feed concentration of each compound was determined as the saturation concentration is reached at VCF 3 (at 20°C) in order to examine the induction time of crystals.

7.3. Results and discussion

7.3.1. F-SMDC principle

F-SMDC is based on the principle of creating and maintaining concentration gradient (CG) and temperature gradient (TG) along the reactor height (top to bottom). The presence of CG and TG is essential in the F-SMDC reactor to enhance the performance of both MD (for better water recovery) and crystallizer (salt production).

In a typical MD process, vapor transfer across the hydrophobic membrane tends to attract ions in the feed solution closer to the membrane boundary layer. As freshwater is produced, the phenomenon of higher ion/concentration density near the membrane boundary layer compared to the feed bulk solution becomes more prevalent (**Figure 7-1**). The higher feed concentration in the membrane boundary layer than the bulk feed concentration affects MD performance. Specifically, the ions in this layer interfere

with the contact of vapor with membrane surface, resulting in the reduction of MD permeate flux. This phenomenon is well established by previous studies (Choi et al. 2017; Martínez-Díez & Vázquez-González 1999; Srisurichan et al. 2006). Likewise, in this study, the similar phenomenon occurred. However, the permeate flux decreased only slightly compared to the initial permeate flux. This was attributed to the downwards movement of concentrated feed solution from the membrane boundary layer (due to higher concentration (density) than the feed bulk solution) (**Figure 7-1**Error! Reference source not found.) (Choi et al.). The concentration gradient (CG) in F-SMDC is generated by the downward movement of concentrated feed solution from a membrane boundary layer to the bottom portion of reactor. It leads to difference in concentration along the height of reactor (lower concentration at the top portion, higher concentration at the bottom portion). Moreover, the temperature of high concentration layer near the membrane boundary layer is reduced by low temperature of permeate stream. The downward movement of concentrated feed solution is enhanced because the density is lower at low temperature. The temperature gradient (TG) in F-SMDC created by the heating of solution at the top portion of the reactor. And, the bottom portion is cooled which it makes TG and CG higher. Moreover, the partition placed in between the top and bottom portion in F-SMDC can further reduce the heat transfer from high temperature solution (at the top portion) to low temperature solution (at the bottom portion). The occurrence of the downward stream of concentrated feed solution is the most important aspect to obtain the advantages of F-SMDC. Detailed principle of each gradient (CG and TG) is discussed in the section below.

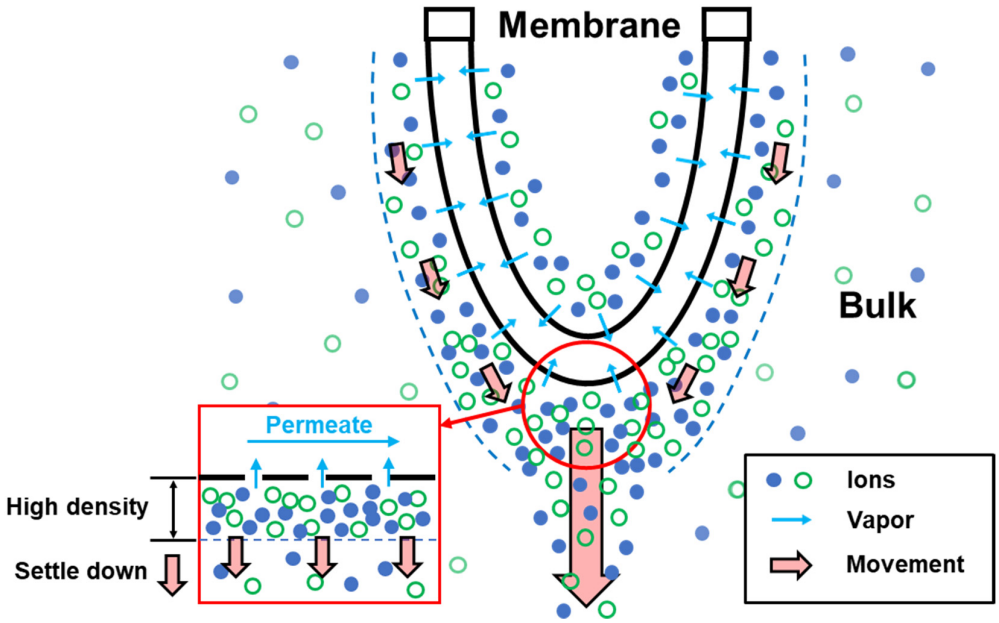

Figure 7-1. Gravitation of concentrated feed solution downwards enabling formation of CG/TG in reactor of F-SMDC.

In F-SMDC, a large height of the top portion results in a weakened downward stream of concentrated feed solution because of the increase of its diffusion potential. In addition, total volume of the reactor in F-SMDC should be minimized to improve total energy efficiency, a larger reactor volume leads to high heat energy requirement and high foot-print.

7.3.1.1. Concentration gradient (CG)

In F-SMDC, the increase of concentration throughout the reactor (the top and bottom portion) was observed during the initial stage. It is attributed to stronger diffusion compared to a driving force for downward stream (as there was insufficient density difference between feed bulk solution and concentrated feed solution near the membrane boundary layer). When enough density difference is created during the operation, the concentrated feed solution moved downward although the diffusion of concentrated feed solution occurred at a lower rate. As a result, the concentration at the top portion

was low, and the downward movement of the concentrated feed solution increased the concentration at the bottom portion during the operation of F-SMDC. The rapid increase in solution concentration at the bottom portion than at the top portion creates a conducive condition to attain saturation state resulting in salt crystal formation within a short operation duration. On the other hand, at the top portion, the maintenance of low feed concentration reduced the adverse effect of ion concentration on MD performance. Further, continuous feeding of feed solution into the top portion helps to maintain low feed concentration and to dilute feed solution concentration at the top portion while increasing the concentration of ions at the bottom portion. In MD process, the variation of concentration of feed solution depends on the volume concentration factor (VCF) because almost all compounds are rejected by the hydrophobic membrane of MD except for volatile compounds. Hence, the theoretical value concentration of feed solution is directly proportional to the concentrate ratio (volume concentration factor (VCF)). For example, the feed solution is concentrated by 3 times at VCF 3. This means the theoretical value is similar value of VCF. In this study, theoretical value and VCF were considered as same due to non-volatile compound were only used as the feed solution. In F-SMDC, a higher concentration factor ratio than the theoretical value is observed, and then the concentration difference between both portions (the top and bottom) of reactor became bigger with a time, which caused by the downward stream of concentrated feed solution.

7.3.1.2. Temperature gradient (TG)

In F-SMDC, alongside the CG, the presence of TG in the reactor is a significant factor for controlling salt solubility. This is because, temperature plays an important role in influencing the solubility/saturation degree of salt compounds in a feed solution. For instance, the solubility of Na_2SO_4 solution of 195 g/L at 20 °C increases dramatically to 450 g/L at 60 °C (Bharmoria et al. 2014). To create TG in F-SMDC, the outer wall of double wall reactor at the top portion is heated up. The heated top portion of the reactor containing the submerged membrane creates a conducive condition for the

MD operation.

For a better understanding of the TG formation tendency in F-SMDC, a baseline study was carried out using deionized (DI) water. The baseline performance was compared with that of concentrated feed solution (80 g/L Na_2SO_4.). Partitions were installed along the reactor to prevent natural fluid convection (Choi et al.) caused by temperature control in the reactor. The feed temperature at the top portion was maintained at 50.2±0.2 °C while the bottom portion was maintained at room temperature (no cooling water circulation in outer wall of reactor).

The temperature distribution (at the top: 50.2±0.2 °C; at the middle :23.3±0.1 °C; and at the bottom portion: 20.1±0.1 °C) of the baseline test (DI water as feed solution), indicated that TG was not formed between the middle and bottom portion. This is because, there was only a small difference in temperature between the middle and bottom portion (temperature difference of around 3 °C) while significant difference occurred between the top and middle portion (difference was around 27 °C). This indicated that the presence of partition restrains the mixing of feed solution caused by natural convection, while mitigating heat transfer, which effectively reduced heat loss as well as mixing of feed solution caused by natural convection. Compared to the baseline test, a significant TG occurred when concentrated Na_2SO_4 was used as feed solution (at the top: 49.8±2.8 °C, at the middle: 35.2 ± 2.3 °C, at the bottom: 26.1 ± 1.0 °C) (**Figure 7-2 (a)**). This result indicated that heat transfer was significantly enhanced in the presence of salt in the feed solution. The movement of concentrated feed solution downward to the bottom portion created additional CG and TG without any additional temperature control at the middle and bottom portion. The TG created in the reactor influenced F-SMDC process performance favorably; crystallization at the bottom portion and reducing fouling by crystals at the top portion. This is because the solubility of crystalline salts is influenced by the temperature of solution.

As shown in **Figure 7-2 (b)**, even if CG was not formed throughout the whole reactor, the solubility of Na_2SO_4 at different portion was different because of the TG along the height of the F-SMDC reactor (**Figure 7-2 (a)** and **(b)**). The higher solubility at the top portion due to higher temperature reduces the potential of crystallization on the membrane surface while the lower solubility at the bottom portion enhances salt crystallization for resource recovery. The decrease of solubility at the bottom portion compared to both the top and middle portion was achieved (reduction of 29.4 – 33.0 %). Moreover, its effect can be enhanced with CG formation. At the middle and bottom portions, feed concentration increased with time, while the concentration at the top portion remained constant. It was also observed that the deviation between the actual feed concentration values at the bottom portion were greater than the theoretical values before the formation of crystal at the bottom portion (**Figure 7-2 (b)**).

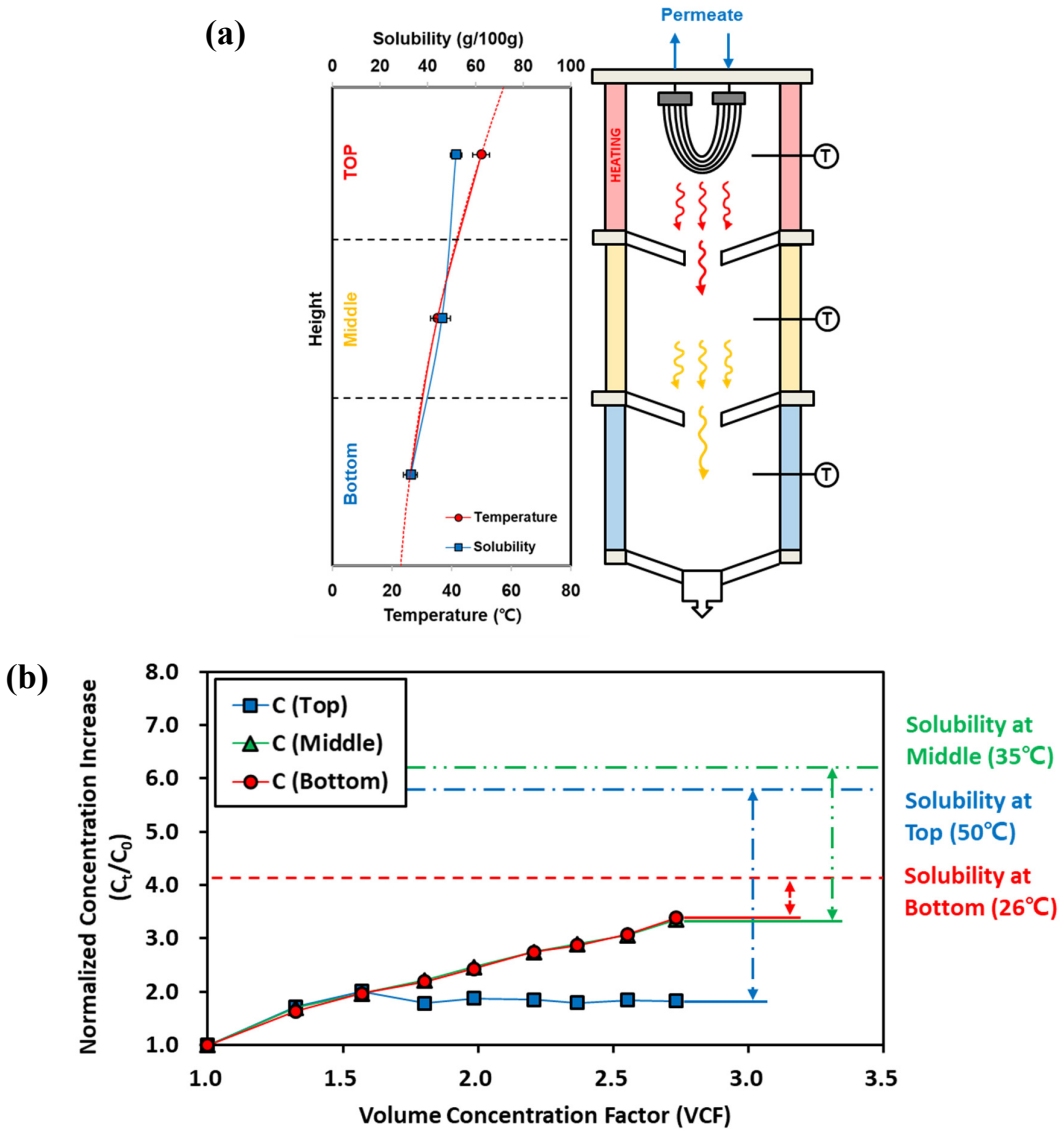

Figure 7-2. The variation of temperature and concentration at each portion in reactor with Na_2SO_4 as feed solution (a) The temperature and solubility along the height of the reactor, and (b) Na_2SO_4 concentration profile (solubility of Na_2SO_4 at different temperature are also shown).

7.3.2. Influence of different inorganic salt on CG/TG

The results in **Section 7.3.1.2** highlighted that the presence of salts such as Na_2SO_4 in the feed solution influenced the temperature distribution of F-SMDC. This implies that the presence of different salts in mixed feed solutions such as in seawater and wastewater brine could play an important role in

controlling the rate and stability of CG/TG. The significance of this factor must be evaluated. Feed solutions containing major salts present in brines, namely sodium sulfate (Na_2SO_4), sodium chloride (NaCl), potassium chloride (KCl), and magnesium sulfate ($MgSO_4$) were used to study their influence on CG/TG in F-SMDC. These different feed solutions enabled a comparative evaluation on CG/TG formation based on factors such as molecular weight, electronegativity of cation and anion, and solubility trend. The initial concentration of each feed solution was different. These initial feed solution concentrations were selected to ensure that each feed solution achieve saturation limit by VCF 3 (20 °C). The CG tendency in the reactor was evaluated using the CG ratio (concentration at the bottom portion (C_{Bottom})/concentration at the top portion (C_{Top})). A CG ratio of over 1 indicated that CG formation was achieved.

7.3.2.1. Molecular weight

Feed concentration increment was the same up to VCF of 1.5 for all these feed solutions at the top portion (**Figure 7-3 (a)** and **(b)**). However, in the case of NaCl, the feed concentration at the top portion increased rapidly after VCF 2.3 although crystals were not formed at the bottom portion (**Figure 7-3 (a)**) and the CG ratio decreased. This led to rapid flux decline from VCF of 2.3 onwards (**Figure 7-3 (c)**). Comparatively, with KCl as feed solution, the feed concentration at the top portion was maintained constantly after VCF of 1.5 with constant increase of CG ratio (**Figure 7-3 (a)** and **(b)**). The presence of salt crystals was observed at the bottom portion of the rector from VCF 2.4 (**Figure 7-4**). In the case of NH_4Cl (which has lower molecular weight than NaCl and KCl), the feed concentration at the top and bottom portion of the reactor showed a gradual increasing trend up to VCF 2.2, and thereafter, the concentration at the top portion remained almost constant with further increase in VCF (**Figure 7-3 (a)** and **(b)**). This is because of crystal formation at the bottom portion at VCF 2.2. This phenomenon was also observed with KCl as feed solution. For 2.3M NH_4Cl, the saturation point at the bottom portion of F-SMDC was at VCF 2.2. It was at VCF 2.4 for 1.5M KCl although theoretical crystallization

(saturation) point was around VCF 3.0. In case of feed solutions containing lower molecular weight compounds (NH_4Cl and NaCl), low CG ratio was observed (between 0.94 to 1.46) although high CG ratio (over 1.51) was observed with KCl. This is attributed to different diffusion coefficient for molecular weight of each compounds (Bodalal et al. 2000; Rard & Miller 1979; Valencia & González 2011). Diffusion coefficient is inversely proportional to the molecular weight of compound (Timachova et al. 2015; Valencia & González 2011). The compounds with higher molecular weight in solution is hard to diffuse because of their lower diffusion coefficient. As a result, high density could be obtained near the membrane boundary layer. This leads to downward movement of concentrated feed solution, and thus CG in the reactor. In F-SMDC process, it is very important aspect to create a favorable condition to obtain downward movement of concentrated feed solution.

At this supersaturation state, continuous crystal formation occurred and the concentration in the reactor remained constant (because of crystal formation). However, fresh water was continuously produced by S-MD with high salt rejection of around 99%. It should be noted that there was a continuous supply of feed into the reactor. At the bottom portion, when the concentration increased by almost three times, crystal formation occurred and thereafter the concentration at the bottom portion was maintained (**Figure 7-4**). When the concentration reached this point, nucleation of salt crystals in the solution occurs (Mitchell & Frawley 2010; Zhang & Liu 2009), and a stable permeate flux was achieved (**Figure 7-3 (c)**). The permeate flux decreased gradually before the formation of crystals at the bottom portion (the saturation point of each chemical) due to the effect of concentration near the membrane surface of S-MD.

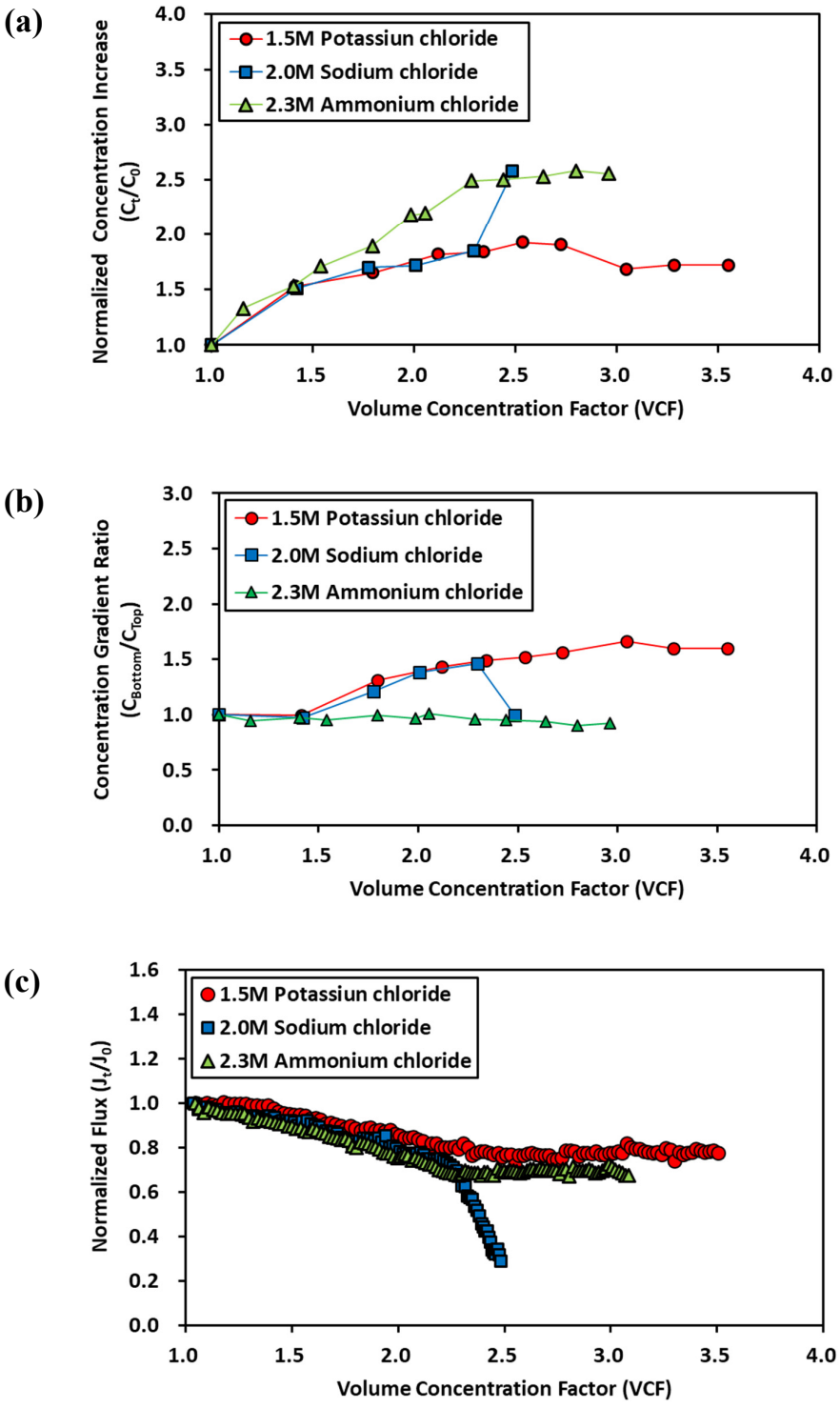

Figure 7-3. The effect of different inorganic salt on F-SMDC: (a) The variation of feed concentration at the top portion (C_t/C_0), (b) The variation of concentration gradient ratio (C_{Bottom}/C_{Top}), and (c) the normalized flux (**T_{Top}** = 50.0±1.2 °C, T_{Bottom} = 20±1.3 °C, $T_{permeate}$ = 16.5±0.3 °C).

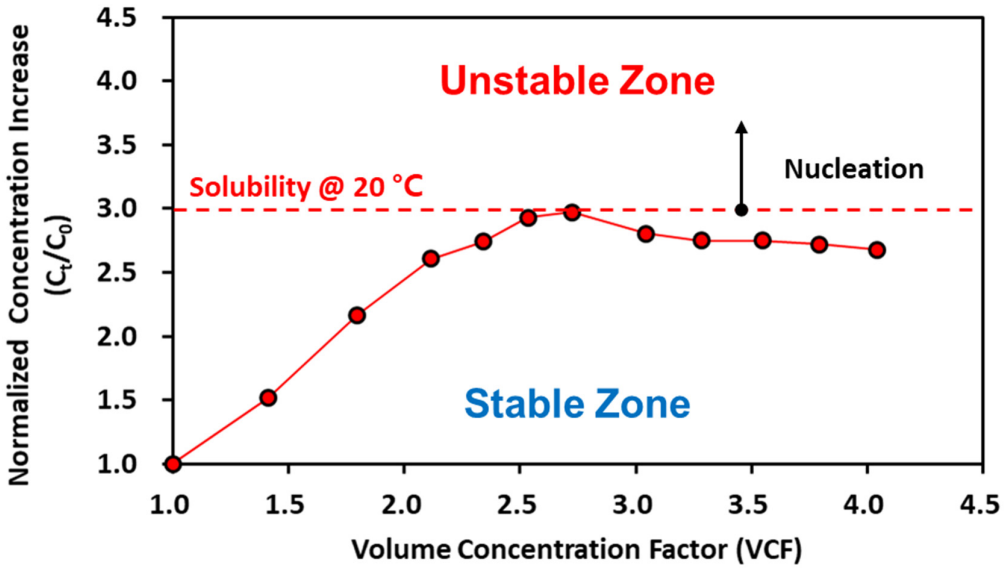

Figure 7-4. The influence of volume concentration factor on solubility of 1.5M KCl at the bottom portion (**T_{Top}** = 50.0±1.2 °C, T_{Bottom} = 20±1.3 °C, $T_{permeate}$ = 16.5±0.3 °C**)**.

CG formation did not occur with NH_4Cl (MW=53.49) compared to NaCl (MW =58.44) and KCl (MW=74.55). This could be attributed to the lower molecular weight of NH_4Cl compared to NaCl and KCl. A prevalent CG formation occurred with feed solution containing compounds with high molecular weight such as KCl, resulting in crystal formation at the bottom portion of the reactor. This revealed that the molecular weight of compounds in the feed solution play an important role in influencing the degree of CG formation as well as permeate flux decline in F-SMDC. This result implies that due to the concentration of crystalline solids at the bottom portion, the saturation level of elements present at low concentrations in seawater reverse osmosis (SWRO) brine, such as lithium, zinc, strontium and rubidium, can be increased, making it possible to selectively recover these elements. This is because the concentration of elements in low concentration increases continuously although the concentration of other components is maintained at the bottom portion (the effect of other ions is maintained) (Naidu et al. 2018; Naidu, Jeong, Johir, et al. 2017).

7.3.2.2. Electronegativity of cation and anion

This study focuses on treating seawater reverse osmosis (SWRO) brine. Major ions in SWRO brine such as sodium, magnesium, and sulfate have been chosen. This was the reason of Na_2SO_4 and $MgSO_4$ were used in this study. The concentration of $MgSO_4$ and Na_2SO_4 used in this study was based on the saturation concentration of each compound. The degree of saturation of each compound could influence the concentrated feed solution's downward stream. Hence, the concentration of compounds was determined in order that saturation of each compounds is reached at the same VCF. The concentration used for each compound reached the saturation concentration at VCF 3 (at 20 °C).

As shown in **Figure 7-5 (a)**, a significant CG formation occurred with Na_2SO_4 (MW=142.04) and $MgSO_4$ (MW=120.37) which have a higher molecular weight than KCl. Comparing Na_2SO_4 and $MgSO_4$ (same anion), the increase in CG ratio (by CG ratio of 1.62 to 1.83) was higher with Na_2SO_4. This was attributed to the smaller electronegativity (Na^+: 0.93, Mg^{2+}: 1.31) (Allred 1961). This may have also influenced the permeate flux. The permeate flux decline rate of Na_2SO_4 was lower (12.56 % flux decline) compared to that of $MgSO_4$ (55.93 % flux decline) (**Figure 7-5 (b)**). This result indicated that the electronegativity of cations influenced the CG generation and the permeate flux variation. The electronegativity is the measure for the tendency of ions to attract a bond pair (Liu et al. 2018). Cations with high electronegativity have stronger attraction towards anions. This would make more ions stay near the membrane boundary layer. This will then influence the downward stream of concentrated feed solution. As a result, a higher increase in concentration was obtained at the top portion. This affected the permeated flux in a negative manner. This result indicated that apart from molecular weight, the electronegativity of ion also influences the formation of CG and permeate flux as well.

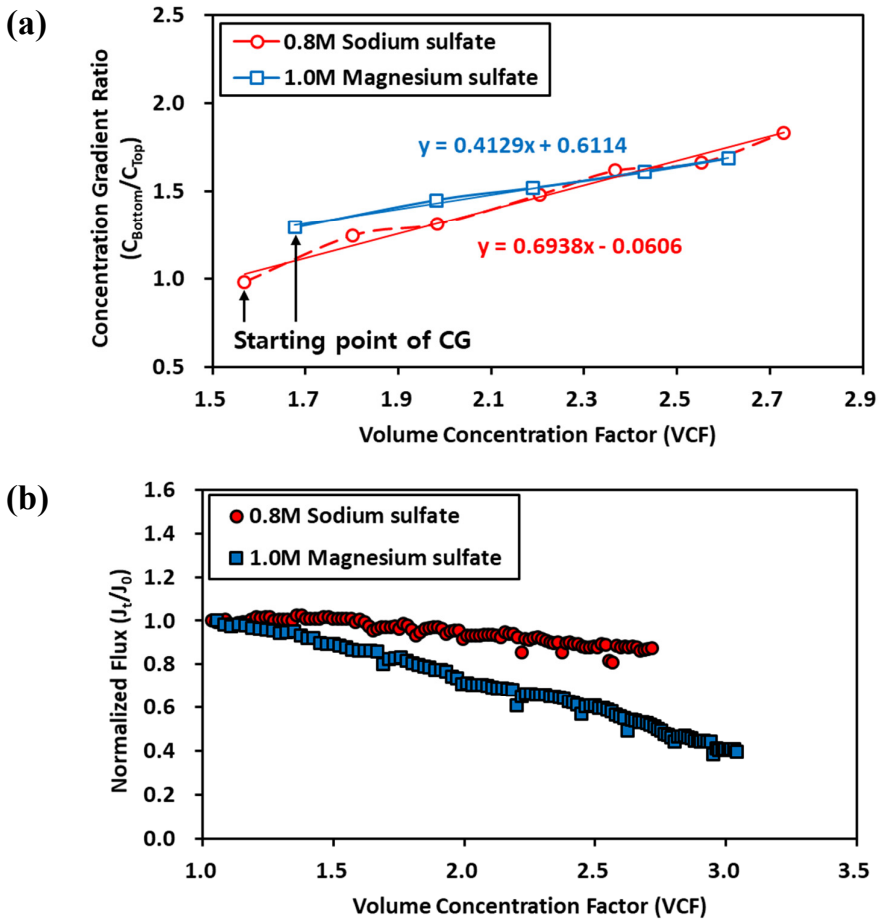

Figure 7-5. The comparison of Na_2SO_4 and $MgSO_4$ as feed solution: (a) the variation of concentration gradient ratio (C_{Bottom}/C_{Top}), and (b) the normalized flux.

7.3.3. TG and CG tendency of organic compounds

In wastewater brines, organic compounds are also present alongside with inorganic compounds. The interference of organic compounds on MD and crystallization phenomenon is therefore inevitable (Naidu, Jeong, Kim, et al. 2014). In order to examine the influence of organic compounds in F-SMDC, two solutions were used; (1) the mixture of organic compounds (humic acid (HA), alginic acid (AA) and bovine serum albumin (BSA) at a concentration of 12.41 ppm (as total organic carbon)), and (2) the mixture of organic compound and inorganic salts of 0.5M Na_2SO_4.

CG was not formed in the feed solution containing only organic compound as feed solution. The concentration at the top and bottom portion of the reactor increased; however, the increase at the top portion was higher than that at the bottom portion (**Figure 7-6**). Comparatively, CG was formed in the feed solution containing organic compound with inorganic salts (Na_2SO_4) (**Figure 7-7**). The CG ratio did not increase up to a VCF of 1.55 (the change ratio compared to average: ±5.29 % DOC). Here, the CG formation of Na_2SO_4 was similar to the CG formation with and without organic compound in the feed solution (**Figure 7-7**). This result suggested that the movement of concentrated inorganic salts downwards in the reactor causes the CG formation of organic compounds, which also helps the movement of organic compound in the feed solution to move downwards. In the absence of the inorganic salts, the lack of downwards movement results in the organic compounds remaining of the top portion of the reactor.

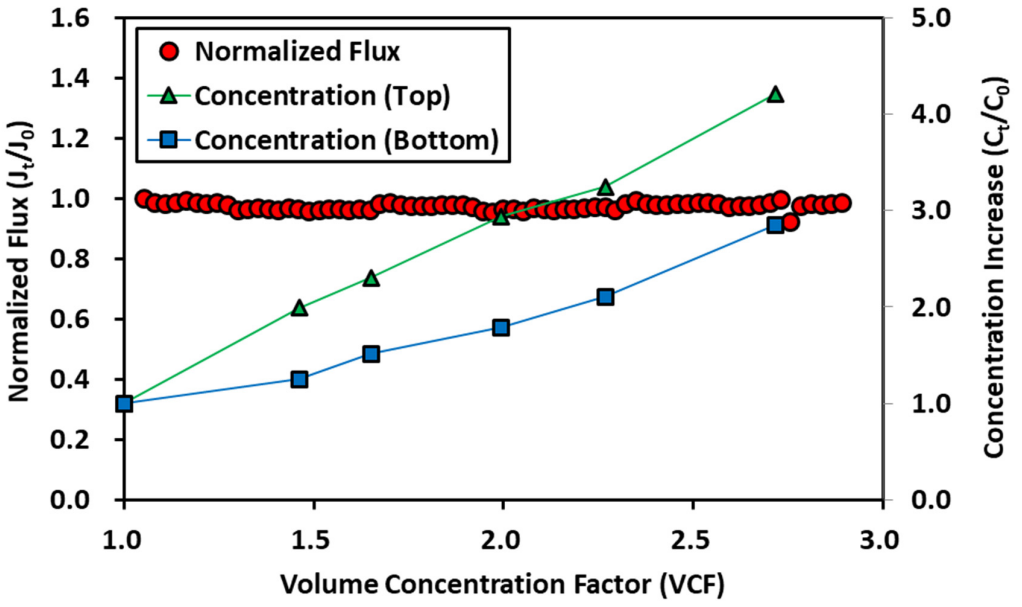

Figure 7-6. The normalized flux and the concentration variation at the top and bottom portion with organic compound alone as feed solution.

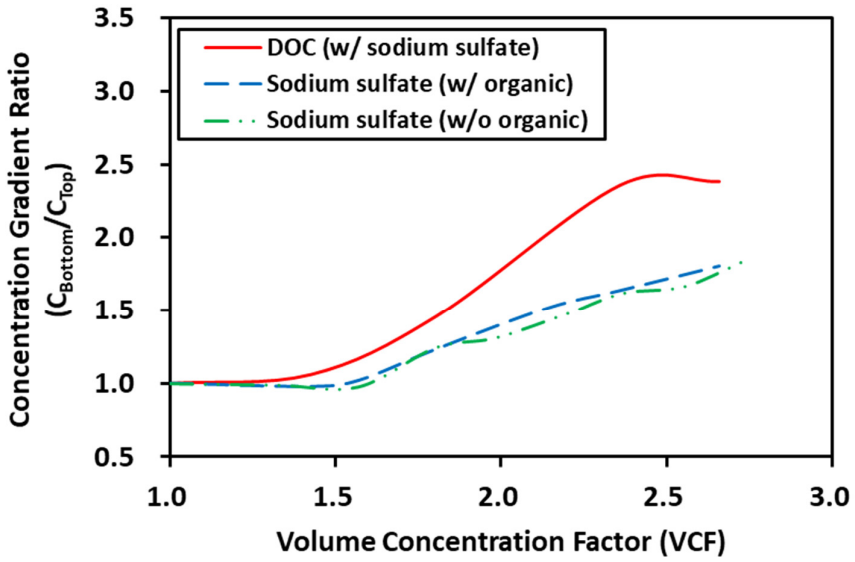

Figure 7-7. The concentration gradient ratio (C_{Bottom}/C_{Top}) with organic compounds alone and with organic compounds and Na_2SO_4 in the feed solution.

The main organic components of concentrated feed solution in the reactor were HOC (hydrophobic), humic substance (HS), building blocks, and LMW organics (**Figure 7-8**). Tendency of bio-polymer is not reported in this study as the low concentration makes it insignificant. As shown in **Figure 7-8 (a)**, the CG was formed for the all components of organic compound as well as inorganic compound. In the case of LMW organics and HOC, their percentage increased with VCF. On the other hand, that of HS and building block decreased (**Figure 7-8 (b)**). Thus, a different downwards movement ratio of each organic component was noticed in the reactor. The concentration increase ratio of HOC and LMW (neutrals) was higher at the bottom layer than other components, resulting in the increase of content percentage of these components. The variation of composition at the bottom portion can influence the crystallization phenomenon (Choi et al. 2018a; Stephen et al. 1993).

The increase of CG ratio was different for each organic component. In particular, the CG ratio of

hydrophobic organic compounds (HOC) was higher, and that of HS and building blocks were lower. The CG formation of organic compounds in the reactor can influence the fouling of S-MD performance. The organic compound present at the top portion of the reactor near the membrane can cause fouling on the membrane surface. The recent studied reported that the HS, which represent up to 80% of total organic carbon in natural water source, are normally disaggregated to low molecular weight (LMW) organic components under thermal condition (in MD) (Jucker & Clark 1994; Naidu, Jeong, Choi, et al. 2017; Naidu et al. 2015) and LMW organic components in the water have been considered as a precursor of biofouling in membrane process. When these organic compounds move downward with concentrated solution, the organic fouling potential and the decrease of membrane hydrophobicity was not increased (Naidu, Jeong, Choi, et al. 2017).

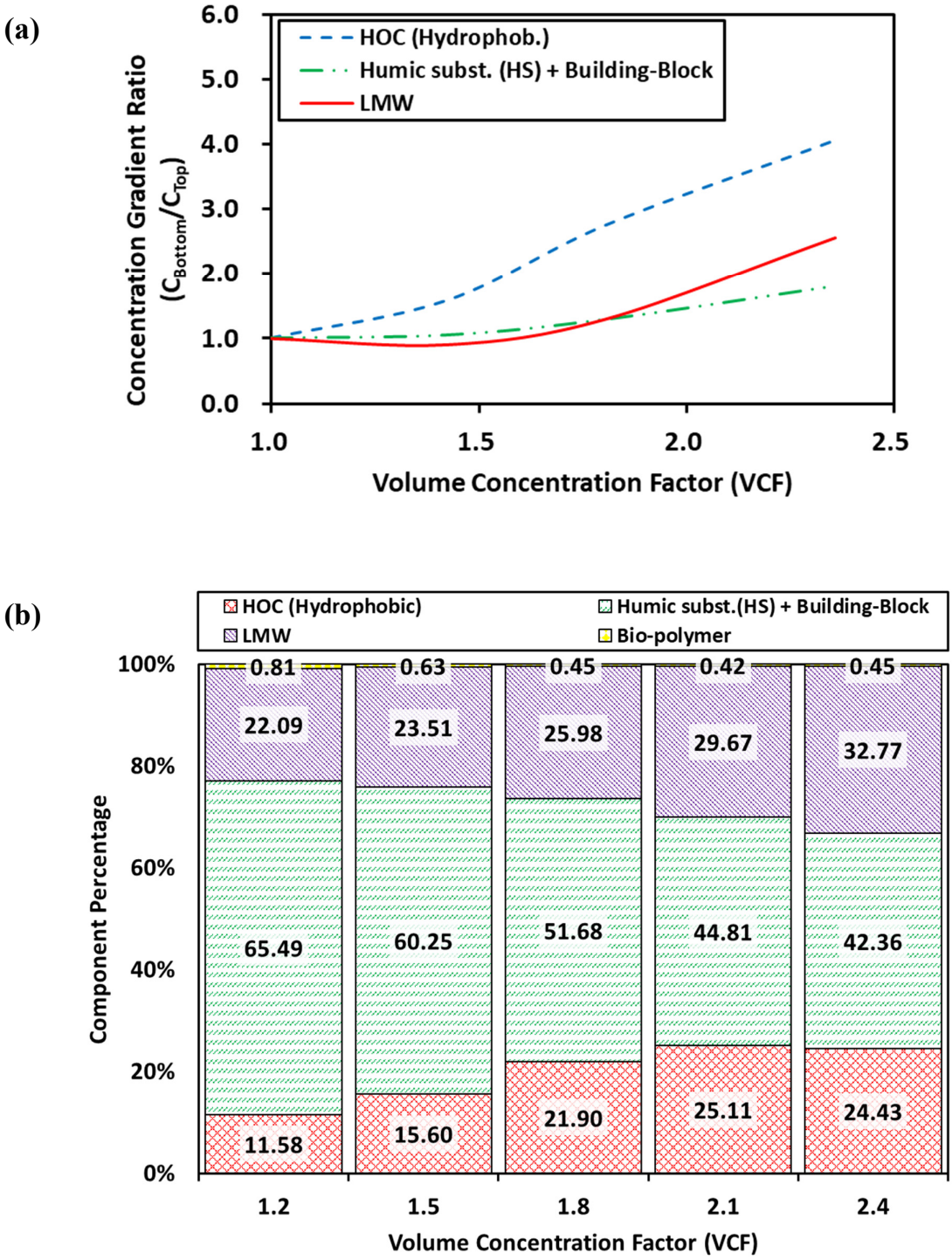

Figure 7-8. The tendency of CG and the percentage difference of the organic compounds during the F-SMDC operation with organic compounds and Na_2SO_4 as feed solution (a) the concentration gradient ratio (C_{Bottom}/C_{Top}), and (b) the comparison of organic components ratio at the bottom portion of the reactor.

7.4. Summary of this research

This study investigated the performance of a novel MD and crystallizer combination, fractional submerged membrane distillation-crystallization (F-SMDC) with feed solutions containing different inorganic and organic compounds. The following conclusions were made based on the experimental results:

- Initial CG/TG was generated in the reactor as the feed solutions attained a higher concentration to its initial concentration values (at around VCF 1.5 onwards). This trend was attributed to the downward movement of concentrated inorganic compounds in the reactor.

- Variation in feed solution solubility in the reactor (the top to bottom) was attributed to the presence of TG along the reactor. For instance, when Na_2SO_4 was used as the feed solution, the lower temperature of 26 °C at the bottom portion of the reactor reduced the solubility of Na_2SO_4 by 67.0 – 70.7 % compared to other portions, enhancing salt crystallization while maintaining a lower feed concentration at the top portion of the reactor. This mitigates the increase of concentration (ion effect) close to the membrane at the top portion of the reactor, enabling to maintain a stable flux throughout the operation.

- At the bottom portion of the reactor, salt crystallization of feed solutions occurred at a faster rate to the theoretically predicted rate (based on salt saturation point). For instance, KCl as a feed solution achieved salt crystals from VCF 2.4 onwards compared to the predicted theoretical salt saturation point of VCF 3.0. This was attributed to the generation and maintenance of high CG ratio (over 1.51) with KCl.

- The properties of inorganic compounds played a significant role in generating and maintaining a high CG ratio. CG was not formed with feed solutions containing compounds

with low molecular weight. For example, in the case of KCl (MW=74.55), $MgSO_4$ (MW=120.37), and Na_2SO_4 (MW=142.04), CG was observed (CG ratio of 1.51 to 1.83). However, in the case of lower molecular weight compounds, NH_4Cl (MW=53.49) and NaCl (MW=58.44), CG was not formed completely (CG ratio of 0.94 to 1.46).

- Apart from molecular weight, electronegativity of cation influenced the CG/TG formation ratio, which in turn influences the flux trend. In the case of Na_2SO_4 with lower cation electronegativity, smaller flux decline (12.56% flux decline) occurred compared to $MgSO_4$ (55.93 % flux decline) (Na^+: 0.93, Mg^{2+}: 1.31).

- The gravitational movement of concentrated inorganic compounds was important to simultaneously create CG and enhance organic compounds present in the feed solution to gravitate downwards to the bottom of the reactor. This phenomenon would potentially mitigate organic deposition on the membrane.

- The subsequent research will be researched for treating the SWRO brines which are synthesised and collected from real SWRO plant in F-SMDC. In this study, the feasibility of F-SMDC on treatment of SWRO brine will be examined, and some issue and recommendation for that will be addressed.

CHAPTER 8

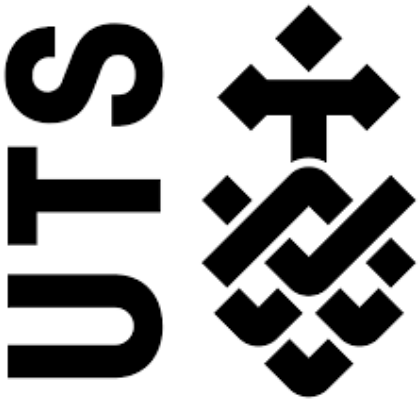

THE RECOVERY OF SODIUM SULFATE FROM SEAWATER REVERSE OSMOSIS (SWRO) BRINE USING FRACTIONAL-SUBMERGED MEMBRANE DISTILLATION CRYSTALLIZER (F-SMDC)

8.1. Introduction

In the MDC process, supersaturation can be achieved faster by controlling the temperature in the crystallizer and continuous (Gabelman & Hwang 1999; Hermanto et al. 2007). The solubility of almost all inorganic components varies according to temperature (Jiang et al. 2016). Commonly, the solubility of inorganic components is poorer at a low temperature, which helps to achieve the target matter being supersaturated. Lower temperature maintained in the crystallizer (i.e. cooling crystallization technique) of an MDC facilitates supersaturation. Also, the extraction of inorganic components as crystals from the solution improves MD performance (Julian et al. 2016). This is because the negative effects of high ion concentration on mass transfer in the MD have been curtailed (Choi et al. 2017). For such reasons, both processes can enhance other ones in the MDC, resulting in enhanced total performance of the MDC. Consequently, the MDC can potentially achieve zero liquid discharge (ZLD) by simultaneous recovery of water and resources.

In simultaneous MDC processes using the cooling crystallization technique (Chen et al. 2014; Kim, Kwon, et al. 2017), a large amount of heating energy is used for re-heating the water in the MD and re-cooling in crystallization. In this study, a fractional-submerged membrane distillation crystallizer (F-SMDC) process was employed to mitigate high energy consumption occurring in a conventional MDC using cooling crystallization. Referring to F-SMDC, the membrane reactor, feed tank and crystallizer are incorporated into a single reactor. F-SMDC provides a favorable condition in which the MD can operate and crystallization as a result of concentration gradient (CG) and temperature gradient (TG) present in the reactor. High temperature and maintenance of a small concentration in the upper section of the reactor provides a favorable scenario for mass/temperature transfer in the MD. Similarly, a continuous increase in the concentration and lower temperature at the bottom portion in the reactor facilitates nucleation and growth of crystals (Choi et al. 2018b).

Sodium sulfate (Na_2SO_4) is widely used as a raw material in the detergent, glass and paper industries (Quist-Jensen, Macedonio, et al. 2017). The extraction of Na_2SO_4 from SWRO brine by F-SMDC does produce economic benefits and reduces the negative effects on the environment. In this study, the feasibility of F-SMDC in recovering Na_2SO_4 from the SWRO brine was examined. The technical issues involved in treating the real SWRO brine in F-SMDC were discussed together with the solutions. A sulfate-rich scenario was created in the reactor so that: firstly, Na_2SO_4 could be extracted; and secondly, adverse outcomes caused by calcium-based crystals were reduced.

8.2. Materials and Methods

In this study, F-SMDC was operated under same conditions and operational parameters as in our earlier F-SMDC experiments. However, the temperature at different locations in the reactor and permeate steam were different. The temperature at the top portion was maintained at 50.0± 0.2 °C by using heating water circulator. The temperature at the bottom portion and in permeate stream were set at 19.8 ± 1.3 and 20.1 ± 0.3 °C, respectively. The flow rate of permeate stream was kept at 0.8 L/min.

The feasibility of F-SMDC in the treatment of SWRO brine was examined using the following three seawater reverse osmosis (SWRO) brine solutions: real SWRO brine, simulated SWRO brine (recovery ratio (R) = 50 %) (**Table 3-1**) and simulated SWRO brine (recover ratio (R) = 50 %) without Ca^{2+}. Further, 1M sodium chloride (NaCl) solution as feed solution was used to examine the influence of low temperature-sensitivity solubility component in F-SMDC.

Sodium sulfate (Na_2SO_4), magnesium sulfate trihydrate ($MgSO_4 \cdot 3H_2O$) and ammonium sulfate ($(NH_4)_2SO_4$) were added into SWRO brine in order to increase the sulfate concentration. In the case of $MgSO_4 \cdot 3H_2O$ and $(NH_4)_2SO_4$, the same amount of chemicals (200 g/L) was added into the synthetic seawater reverse osmosis (SWRO) brine solution. In case of addition of Na_2SO_4, 120 g/L Na_2SO_4 was

used as feed solution till a VCF of 2.5 in order to create of sulfate-rich condition in the reactor prior to feeding of SWRO brine. From VCF 2.5 to the end of operation, only SWRO brine was fed as feed solution.

8.3. Results and discussions

8.3.1. Important issues regarding the treatment of real SWRO brine using F-SMDC

F-SMDC is a suitable process for improving recovery and extraction of valuable resources from high concentration solutions such as SWRO brine. In F-SMDC, concentration gradient (CG) and temperature gradient (TG) are generated by the downward stream of concentrated feed solution via the membrane process (Choi et al. 2018b). Higher temperature at the top section makes the MD's operation ideal. Maintaining a smaller concentration at the top section can reduce the permeate flux decline in the MD. At the bottom section, lower temperature and an increase in salt concentration provide a favorable state for spontaneous nucleation and crystal growth (especially for high temperature-sensitive solubility salts). Moreover, the extraction of water from the feed solution by the MD process (at the top of the reactor) leads to supersaturation of salt. This salt content is then maintained at the saturation level by the extraction of salts generated by crystallization which occurs in the bottom section. As a result, the CG and TG in the reactor play a complementary role between the MD and crystallizer (Choi et al. 2018b).

Firstly, the F-SMDC was operated with real SWRO brine as a feed solution to examine the obstacles encountered by F-SMDC in the treatment of real SWRO brine. An initial permeate flux of 3.37 ± 0.03 L/m^2·h (LMH) was obtained with real SWRO brine as feed solution (**Figure 8-1 (a)**). During the first cycle (C1), the permeate flux decreased gradually (22%) before a rapid flux decline occurred (at VCF 2.21). The $CaSO_4$ crystals on the membrane surface were observed at this point (**Figure 8-2**). These crystals appeared to be growing on the membrane surface and remained on the membrane's

surface. To detach and remove the crystals from the surface, air back-washing was applied when the rapid flux decline was observed. Ninety percent permeate flux was recovered by air back-washing compared to initial permeate flux. Although $CaSO_4$ crystals were detached by air back-washing, a subsequent rapid flux decline was observed following a short VCF because the saturation level of $CaSO_4$ was reached in the feed solution. During C3 and C4, the permeate flux recovery ratio by air-back washing was 80–82%. After C4 the permeate flux was not recovered by air back-washing.

Despite multiple cycles of air back-washing, the concentration gradient (CG) caused by inorganic components in the reactor was predominant and increased periodically and continuously (**Figure 8-1 (a)**). The concentration ratio (C_t/C_0) of inorganic components (measured in terms of conductivity) at the top portion of the reactor was 1.5 when VCF ranged from 1.22 to 2.68 (C1 to C4). After that (C5 and C6), the concentration ratio increased rapidly (i.e. after VCF 3.17). This was attributable to the rapid flux decline caused by deposition and growth of $CaSO_4$ crystals on the membrane surface. It reduced the downward movement of concentrated feed solution from the membrane boundary layer to the bottom section of the reactor. The inorganic concentration here was higher than theoretical concentration (theoretical concentration = initial concentration (C_0) x VCF) during the entire operation.

Variations in concentration of organic components were measured in terms of hydrophobic organic carbon (HOC), and the components in hydrophilic organic carbon, such as humic substance (HS), building-block (BB), and low molecular weight (LMW). They were not stable even after many air-backwashes. The CG of organic components was generated at a later stage as compared to inorganic components (after VCF 1.68). In C1, the CG of three organic components was generated and this increased over time. However, after applying the air back-washing technique, their CG fluctuated significantly (**Figure 8-1 (b)**). The CG of HOC, HS and BB were higher than the standard line of CG (CG ratio of 1) although these fluctuated. However, CG of LMW was lower. Generating the CG

of organic components in the reactor can lead to the membrane experiencing much less organic fouling.

A rapid increase in concentration at the top part was observed at VCF 3.27, and the membrane was damaged by irreversible deposition and growth of $CaSO_4$ crystals on the membrane surface. This resulted in complete cessation of the operation. Consequently, the advantage of CG (formed by both inorganic and organic substances) could not be continued beyond a VCF of 3.27. The presence of Ca^{2+} in the SWRO brine caused continual operational problems in the F-SMDC process. For this reason, the removal of Ca^{2+} or of its reduction is important in treating SWRO brine. Additionally, the stable maintenance of/increase in CG of the organic components above the boundary level of CG is important for mitigating biofouling and reduction of membrane hydrophobicity.

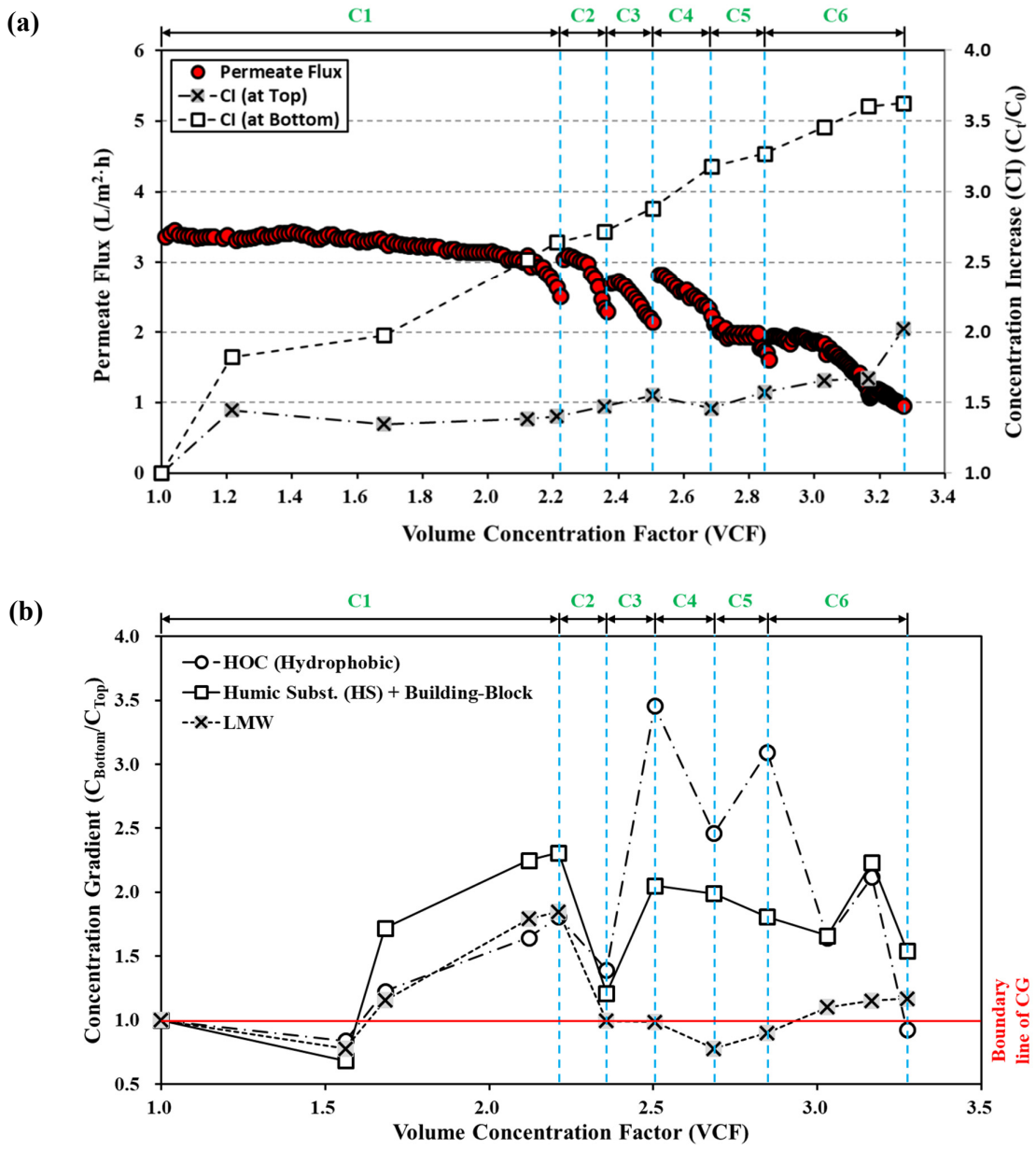

Figure 8-1. The F-SMDC process in the treatment of real SWRO brine: (a) variation of permeate flux, concentration in the reactor (at the top and bottom sections), and (b) concentration gradient ratio of organic components.

Figure 8-2. $CaSO_4$ crystals deposited on the membrane surface after the treatment of SWRO brine.

8.3.2. Treatment of synthetic SWRO brine

8.3.2.1. Reduction of calcium influence

The effect of Ca^{2+} present in the SWRO brine was studied using two different synthetic SWRO brine samples (with Ca^{2+}/without Ca^{2+}) in the absence of organic components. The initial permeate fluxes in SWRO brine with/without Ca^{2+} proved to be similar and they were 3.09 ± 0.02 and 3.12 ± 0.02 $L/m^2 \cdot h$, respectively (**Figure 8-3 (a)**). The presence of Ca^{2+} in the synthetic SWRO brine compromised the performance of F-SMDC and there was a rapid flux decline from VCF 1.76. This decline was around 20% with Ca^{2+} but it was only 9% without Ca^{2+}. At this point, the $CaSO_4$ crystals were observed on the membrane surface for SWRO brine with Ca^{2+} (**Figure 8-4 (a)**). The results indicate that the presence of Ca^{2+} in the SWRO brine triggers a faster decline in the permeate flux when F-SMDC is operating in its early stages. In the case of SWRO brine without Ca^{2+}, the permeate flux decline ratio was less than 10% at VCF 1.94, and it increased gradually by VCF 3.75. A rapid

decline in permeate flux was observed only after a VCF of 3.75. However, crystals were not detected on the membrane surface (as observed by the naked eye).

Maximum CG ratio was also different for synthetic SWRO brine with Ca^{2+} and without Ca^{2+} (with Ca^{2+}: it was 1.15 at VCF 1.84, while without Ca^{2+} it was 2.13 at VCF 3.40) (**Figure 8-3 (a)**). The CG ratio increased with the VCF because of the continuous increase in concentration at the bottom section (although the concentration at the top also remained). The rapid flux decline led to a collapse of CG formation in the reactor (**Figure 8-3 (a)**). When the rapid flux decline was observed, the CG ratio fell as the inorganic concentration in the top part of the reactor rose (**Figure 8-3 (b)**). This was attributed to the downward stream of concentrated feed solution exerting an insufficient driving force. The higher concentration layer generated at the membrane layer led to a favorable condition for spontaneous nucleation (supersaturation state), resulting in the formation and growth of $CaSO_4$ crystals on the membrane surface. However, the active filtration area of the membrane decreased due to the formation of crystals and their growth on the membrane surface.

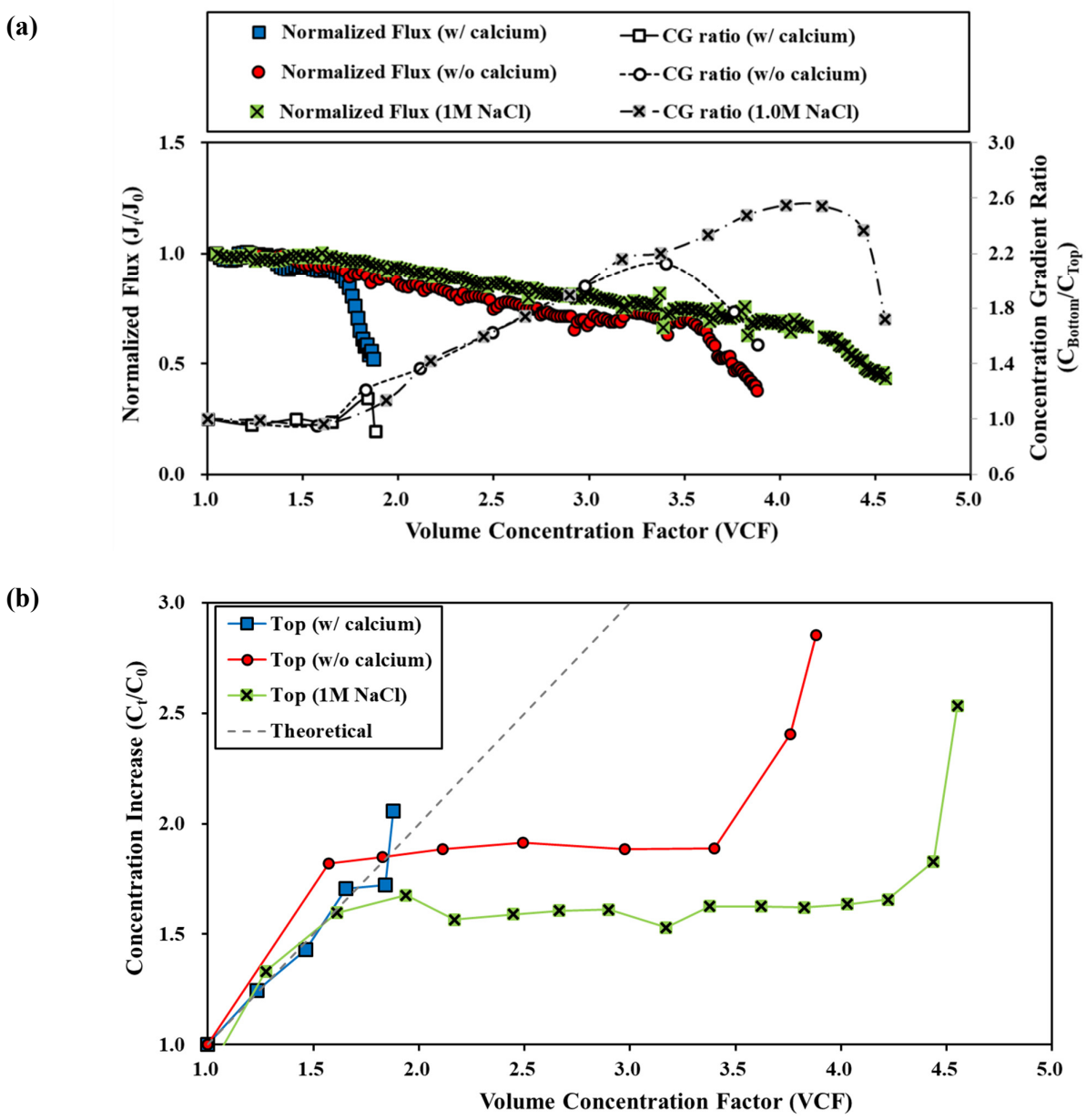

Figure 8-3. Effect of calcium in the feed solution (a) on the permeate flux and CG, and (b) the concentration increase (C_t/C_0) trend during the treatment of low temperature-sensitive solubility brine (consisting of only NaCl).

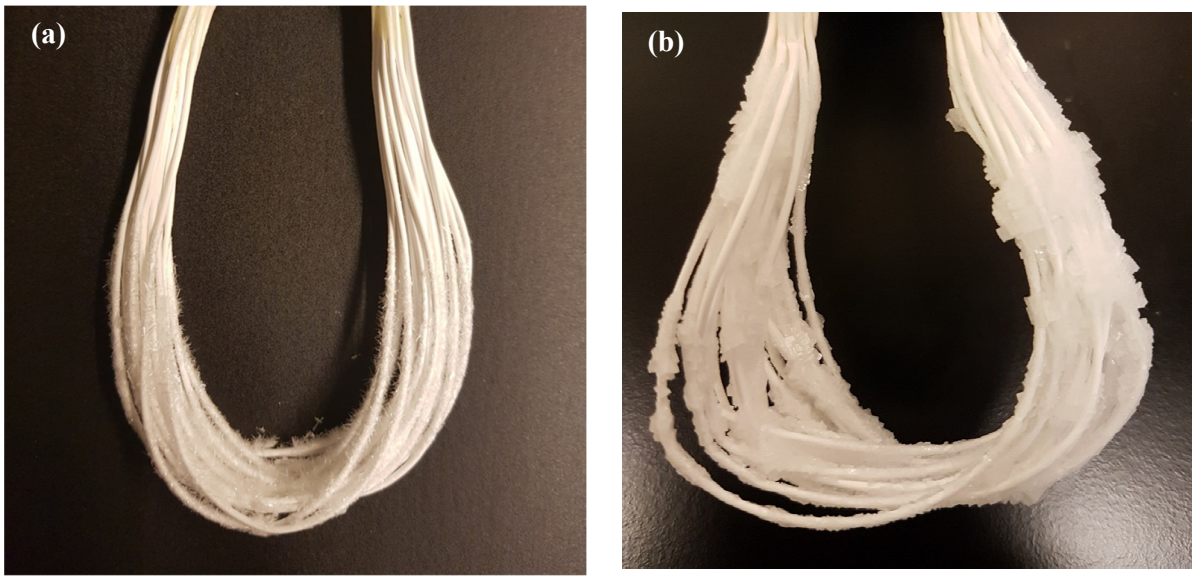

Figure 8-4. Crystal formation on the membrane surface during the treatment of (a) SWRO brine with Ca^{2+}, and (b) 1M NaCl solution.

Calcium-based compounds such as calcium carbonate ($CaCO_3$) and calcium sulfate ($CaSO_4$) are the major foulants in the treatment of SWRO brine (He et al. 2009; Mohammadesmaeili et al. 2010; Nguyen & Lee 2015). These are formed easily during the MD operation because of their low solubility (solubility of $CaCO_3$: 7.75 X 10^{-4} g/100 g at 30 °C, $CaSO_4$: 0.26 g/100 g at 30 °C). It causes the formation of crystals on the membrane surface. As a result, it leads to a rapid flux decline and thus less water being recovered. Moreover, it occurs before the Na_2SO_4 has reached the desired supersaturation level. The removal of Ca^{2+} from the SWRO brine is thus necessary to achieve a higher water recovery ratio and obtain the supersaturation level of Na_2SO_4 in the F-SMDC process. A lime-soda ash softening method is commonly used to remove divalent ions such as Ca^{2+} and Mg^{2+} (Ji et al. 2010; Mohammadesmaeili et al. 2010). In lime-soda ash softening, Ca^{2+} is precipitated using sodium carbonate (Na_2CO_3).

8.3.2.2. Temperature-sensitive soluble components on concentration gradient (CG)

The simulated SWRO brine without Ca^{2+} was used as feed solution to examine the effects of other ions (namely Na^{+}, Mg^{2+}, K^{+}, Cl^{-} and SO_4^{-}) on the F-SMDC process. As shown in **Figure 8-3**, a rapid decline in permeate flux was observed at VCF 3.61 even when SWRO brine without Ca^{2+} was used. The gradual permeate flux decline of 4.71% was observed by VCF 1.41. This followed a flux decline ratio of 15.05%/VCF from VCF 1.41 to 3.60 (flux decline of 34.6% at VCF 3.60). From VCF 3.61 to 3.76, the documented flux decline was 50%. A very high flux decline ratio per VCF (119.75%/VCF) was obtained even though no deposition of crystals was observed on the membrane surface. A similar result was obtained in our previous study utilizing a mixture of Na_2SO_4 and NaCl (Choi et al. 2018b).

In order to investigate the effects of low temperature-sensitive solubility components, NaCl solution (1M NaCl) was used as a sole feed solution at a similar concentration which is found in SWRO brine. In this experiment, a permeate flux decline trend was observed and it was in fact similar to that of simulated SWRO brine without Ca^{2+}.

In the case of simulated SWRO brine, the flux decline occurred early compared to that with 1M NaCl solution (**Figure 8-3**). A permeate flux decline of 4.8% compared to initial flux was observed, followed by the flux then decreasing rapidly from VCF 4.14. The flux decline ratio per VCF of 12.42% was observed from VCF 1.84 to 4.14 (flux decline ratio: 33.3% at VCF 4.14). After that, the flux decline ratio per VCF was 65.88%. This flux decline ratio was lower and it occurred at a higher VCF compared to that of simulated SWRO brine. This is explained by the presence of other elements in the brine. The increase in ion concentration adversely influenced the permeate flux (Choi et al. 2017). At VCF4.14, the deposition of crystals was not observed on the membrane surface. However, the NaCl crystal deposition was observed when the F-SMDC continued to be operated, i.e. when flux decline amounted to 50% (**Figure 8-4 (b)**. This indicates that the main reason for the rapid flux decline was the NaCl concentration and its presence is one of the major problems/obstacles in the F-SMDC process when it

is used for recovering other inorganic compounds from SWRO brine. Our previous research demonstrated that the F-SMDC process is suitable for temperature-sensitive solubility components.

8.3.2.3. Analysis of a sulfate-rich scenario

This study was conducted based on an assumption that the occurrence of Na_2SO_4 crystallization at the bottom part of the reactor prior to rapid flux decline, can minimize the effect of NaCl, resulting in the production of Na_2SO_4 crystals from SWRO brine. If the Na^+ is used for Na_2SO_4 crystallization and its concentration is maintained at the supersaturation degree of Na_2SO_4, the effect of NaCl can be mitigated. However, the concentration of SO_4^{2-} is relatively small for reaching the supersaturation level of Na_2SO_4 compared to Cl^- in the SWRO brine (sulfate ion concentration for Na_2SO_4 crystallization at 20 °C: 131,877 ppm) (**Table 3-1**). Thus, a sulfate-rich scenario in the reactor was created by adding sulfate-based salts. This is one method to accelerate Na_2SO_4 crystallization and avoid the negative influence of NaCl on F-SMDC. At low temperature (in this study, 20 °C was maintained at the bottom section), the solubility of Na_2SO_4 is lower compared to NaCl (Na_2SO_4: 19.5 g/100g as water, NaCl: 36.0 g/100g as water). Thus, if a sulfate-rich scenario is provided at the bottom section of the reactor with enough Na^+ being added for Na_2SO_4 crystallization, the supersaturation level of Na_2SO_4 can be reached and crystallization can be stimulated before rapid flux decline occurs. In regard to Na^+, if the generation and growth of Na_2SO_4 crystals occur, the concentration is maintained because the excess concentration of both Na^+ and SO_4^- over the saturation concentration of Na_2SO_4 is used for the generation/growth of Na_2SO_4 crystals. So, the concentrations of Na^+ and SO_4^{2-} are maintained below the concentration supersaturation level of Na_2SO_4. As a result, the NaCl crystallization does not occur because of the lack of excess Na^+. In this study, the following components were used to provide a sulfate-rich environment in the reactor: sodium sulfate (Na_2SO_4), magnesium sulfate trihydrate ($MgSO_4 \cdot 3H_2O$), and ammonium sulfate ($(NH_4)_2SO_4$). These three are explained in more detail in the following subsections.

8.3.2.3.1. Addition of sodium sulfate (Na_2SO_4)

120 g/L Na_2SO_4 was used to provide both Na^+ and SO_4^- in the solution (up to VCF of 2.5). It provided the reactor with a sodium sulfate-rich environment. The SWRO brine was then added from VCF of 2.5 (**Figure 8-5 (a)**). In other words, after creating a promising situation for Na_2SO_4 crystallization at the reactor's bottom, the simulated SWRO brine served as the feed solution.

The initial permeate flux was 3.25 ± 0.02 L/m^2·h with 120 g/L Na_2SO_4, and it decreased gradually till a VCF of 2.7 (flux decline ratio: 21.63%/VCF) was arrived at. After replacing the feed solution from 120 g/L of Na_2SO_4 to simulated SWRO brine at VCF 2.5, the permeate flux reduced rapidly (flux decline ratio: 1.55%/hr from VCF 2.7 to VCF 2.9). This may have been due to the increase in the concentration at the top section (**Figure 8-5 (a)**). During the operation with a single component of 120 g/L Na_2SO_4 solution (by VCF 2.5), the concentration increase (CI) value at the top part remained in the 1.36–1.50 range. Then, CI started to increase gradually from VCF 2.5 (starting point of the feeding of SWRO brine), resulting in the rapid flux decline (**Figure 8-5**). Na_2SO_4 crystallization was observed at VCF 2.9 at the bottom section. The permeate flux started to recover after crystallization had started. The permeate flux at VCF 2.9 was 42% compared to the initial permeate flux, and it recovered to 63% at VCF of 3.0 compared to initial. After VCF 3.0, it started to decrease again but the rate of decline was smaller (flux decline ratio: 19.87%/VCF).

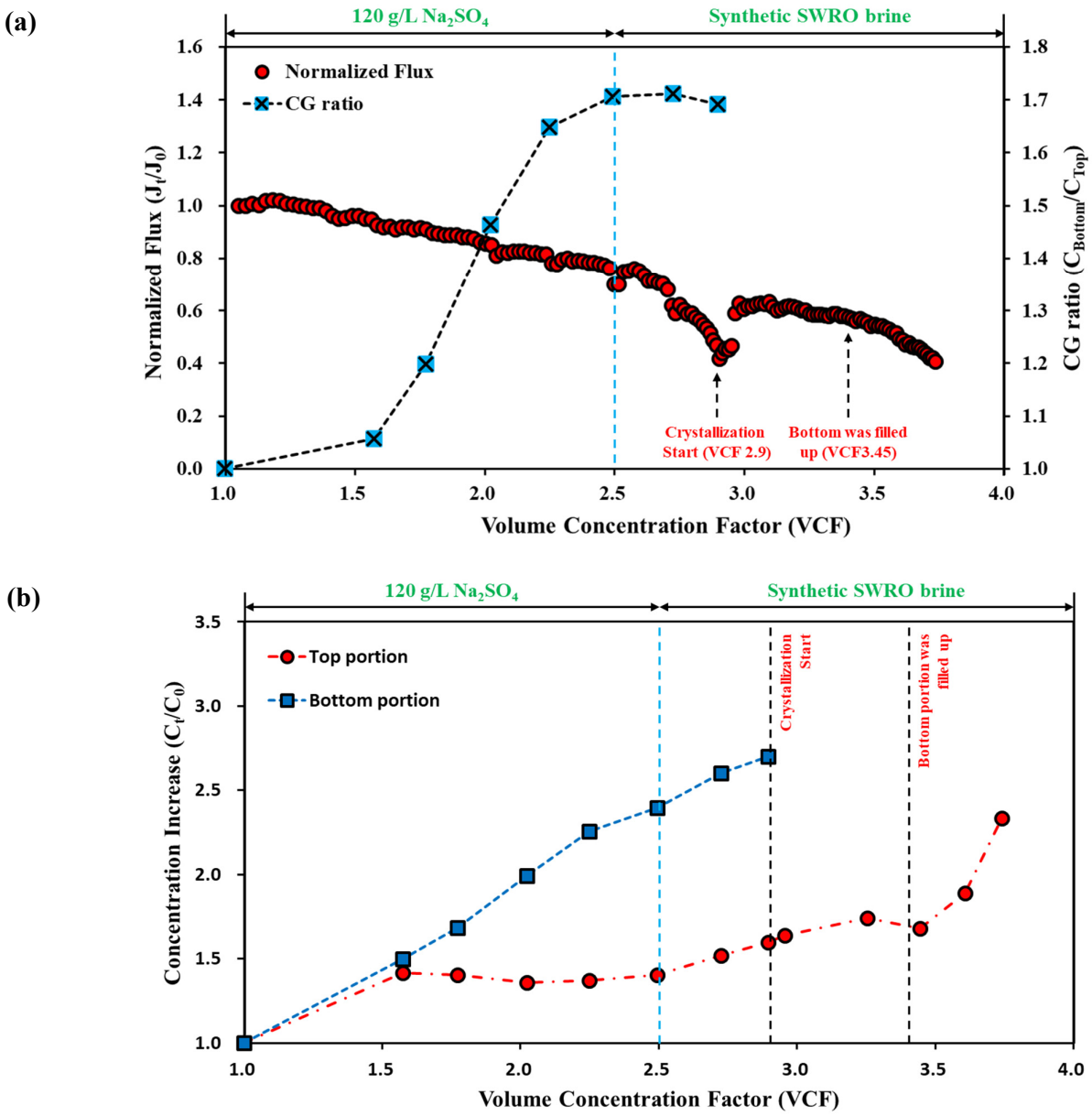

Figure 8-5. Variation of (a) permeate flux and CG ratio, and (b) concentration increase (C_t/C_0) at the top and bottom sections (here Na_2SO_4 solution was added as sole feed solution up to VCF of 2.5; after that synthetic SWRO brine was added).

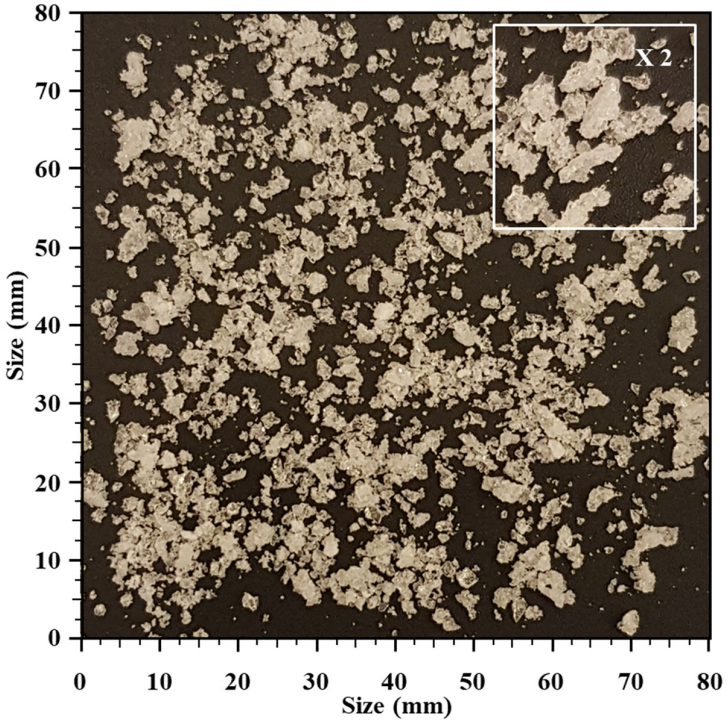

Figure 8-6. Na_2SO_4 crystals generated by the addition of Na_2SO_4.

The Na_2SO_4 extraction from simulated SWRO brine was successfully achieved using the above method. A total amount of 555.2 g Na_2SO_4 crystals (mean size of 2.5 mm (**Figure 8-6**)) and 4.7 L clean water (high water quality with ion rejection of 99.99%) was obtained from the laboratory-scale F-SMDC unit used. After changing the feed solution into SWRO brine, 2.1 L of clean water was produced. Most of the Na_2SO_4 used for providing a viable environment to achieve Na_2SO_4 crystallization was 513 g (reactor volume: 1.71 L). However, the actual extracted amount of Na_2SO_4 crystals from SWRO brine was only 42.2 g. The recovery factor of Na_2SO_4 and water can be significantly increased by using continuous crystal extraction from the bottom of the reactor and providing an appropriate sodium and sulfate-rich condition.

Additionally, the results reveal that of the permeate stream's temperature influenced the induction time of crystallization at the bottom of the reactor. The time required to induce Na_2SO_4 was delayed when

the permeate stream's temperature rose. Na_2SO_4 crystallization at the reactor's bottom was observed at VCF 2.2, when the temperature of the permeate stream was maintained at 16.5 ± 0.2 °C (Choi et al. 2018b) using same concentration of Na_2SO_4 solution. At VCF 2.5, Na_2SO_4 crystallization occurred with the permeate stream temperature being 20.1 ± 0.3 °C. The above results reveal that the crystallization induction time was reduced when the permeate stream was at a lower temperature. This in turn led to a reduction in the temperature of the concentrated solution in the membrane boundary layer, so subsequently its density declined. This facilitated the acceleration of its downward stream, resulting in the desired and faster formation of CG and TG.

8.3.2.3.2. Addition of magnesium sulfate ($MgSO_4$)

Magnesium sulfate trihydrate ($MgSO_4 \cdot 3H_2O$) was used to create a sulfate-rich state in the reactor but without increasing the other cation concentrations (such as Na^+ when adding Na_2SO_4). Prior to the commencement of the experiment, SWRO brine was mixed with a pre-determined amount of $MgSO_4 \cdot 3H_2O$ in the reactor. Then the simulated SWRO brine was used as feed solution without further addition of any chemical. Two concentrations of $MgSO_4 \cdot 3H_2O$ in the mixture (100 and 200 g/L) were chosen to examine its effect on the permeate flux and CG formation in F-SMDC.

The amount of $MgSO_4 \cdot 3H_2O$ added influenced the permeate flux and CG formation in the F-SMDC process. For 200 g/L $MgSO_4 \cdot 3H_2O$, the permeate flux was 8% lower compared to 100 g/L concentration of $MgSO_4 \cdot 3H_2O$ (100 g/L: 3.16 ± 0.08 LMH, 200 g/L: 2.90 ± 0.08 LMH); the flux decline ratio was higher at around VCF 1.8 (**Figure 8-7 (a)**). The formation of CG occurred early when a larger amount of $MgSO_4 \cdot 3H_2O$ of 200 g/L was added (100 g/L: VCF 2.1, 200 g/L: VCF 1.2). As shown in **Figure 8-7 (b)**, for 100 g/L $MgSO_4 \cdot 3H_2O$, the concentration at the bottom of the reactor was smaller than that at the top when VCF ranged from 1.0 to 1.9. This indicates that the downward stream of concentrated feed solution was weaker for the smaller concentration of $MgSO_4 \cdot 3H_2O$. In addition,

although the CG was formed in the reactor, the concentration at the top section increased at a lower ratio than that at the bottom, resulting in a low CG value (**Figure 8-7**). A rapid flux decline was then observed without crystallization at the bottom part of reactor, and the above phenomenon was also observed with the addition of Na_2SO_4. These results suggest that the addition of cations present in the SWRO brine (such as Na^+ and Mg^{2+}) adversely influenced CG formation in F-SMDC. With both concentrations of $MgSO_4 \cdot 3H_2O$, no crystal formation was detected at the bottom section of the reactor.

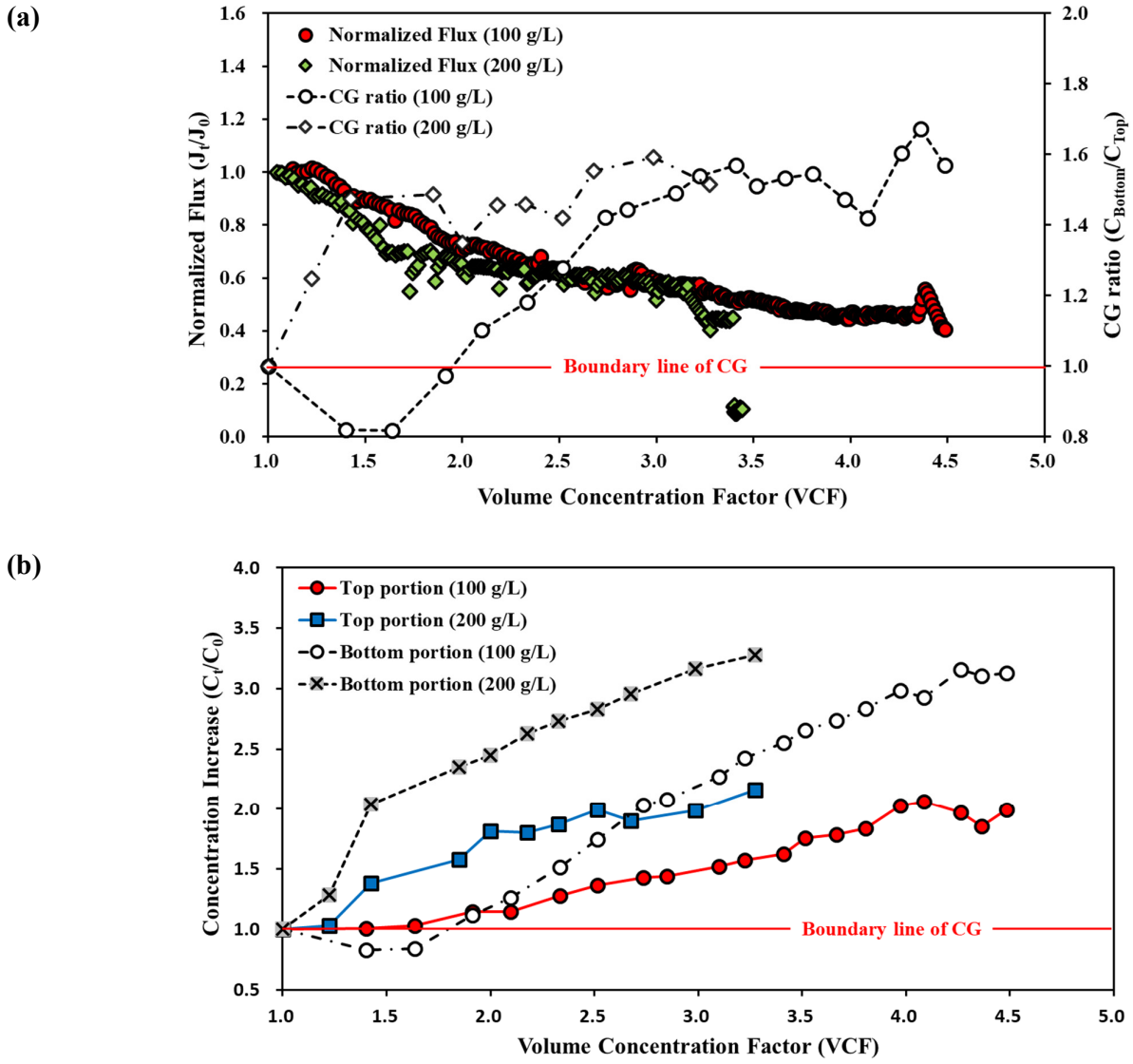

Figure 8-7. Effect of amount of $MgSO_4 \cdot 3H_2O$ on (a) permeate flux and CG ratio, and (b) concentration increase (C_t/C_0) at the top and bottom portion.

8.3.2.3.3. Addition of ammonium sulfate ($(NH_4)_2SO_4$)

As shown above, the addition of Na^+ and Mg^{2+} salts to the WRO brine led to problems for the F-SMDC. Here the sulfate-rich state should be created by using a component containing cations which are not present in SWRO brine at high concentrations. Subsequently, ammonium sulfate ($(NH_4)_2SO_4$) was used to create the sulfate-rich environment. It has higher solubility at low temperature compared to Na_2SO_4, and the mole fraction of sulfate in the $(NH_4)_2SO_4$ is higher than that in Na_2SO_4 and $MgSO_4 \cdot 3H_2O$. For the above reasons, $(NH_4)_2SO_4$ was chosen as the suitable compound for making the sulfate-rich condition. It was mixed with simulated SWRO brine in the reactor in the same way for $MgSO_4 \cdot 3H_2O$.

In this experiment, the CG was observed after VCF 1.42 (CG ratio: 1.9), and the crystallization began at VCF 1.42. A CG of over 2.0 was maintained from VCF 1.62 onward up to VCF 2.72 (**Figure 8-8 (a)**). The permeate flux decreased gradually with the lower flux decline ratio compared to the experiment where Na_2SO_4 and $MgSO_4 \cdot 3H_2O$ were added. The concentration at the top section was maintained from VCF 1.42 to 2.38, while the concentration at the bottom increased continuously. The increase of concentration at the top section was 10-38% from VCF 2.71 to VCF 3.29 (end of cycle 1) (**Figure 8-8 (b)**). Rapid flux decline was observed at VCF 3.11 when the concentration at the top section increased.

In the experiments with SWRO brine (without Ca^{2+}) and single Na_2SO_4 solution, an increase in concentration at the top part and rapid flux decline were observed when the bottom section of the reactor was filled with crystals. This is because the bottom section had an insufficient volume that could retain the concentrated feed solution. However, with the addition of $(NH_4)_2SO_4$ to the SWRO brine, the phenomenon was observed without filling the bottom with crystals. The crystals' deposition on the membrane surface was observed at that time (VCF 3.29) (**Figure 8-9**). They were removed by simple washing using deionized water, which in turn led to the recovery of 82% of the permeate flux

compared to the initial flux. However, the permeate flux decreased again after a few VCF. For the laboratory-scale F-SMDC used in this study, a total of 4.29 L clean water (recovery ratio: 72% from 6 L SWRO brine) and 223.73 g Na_2SO_4 crystals were extracted from simulated SWRO brine.

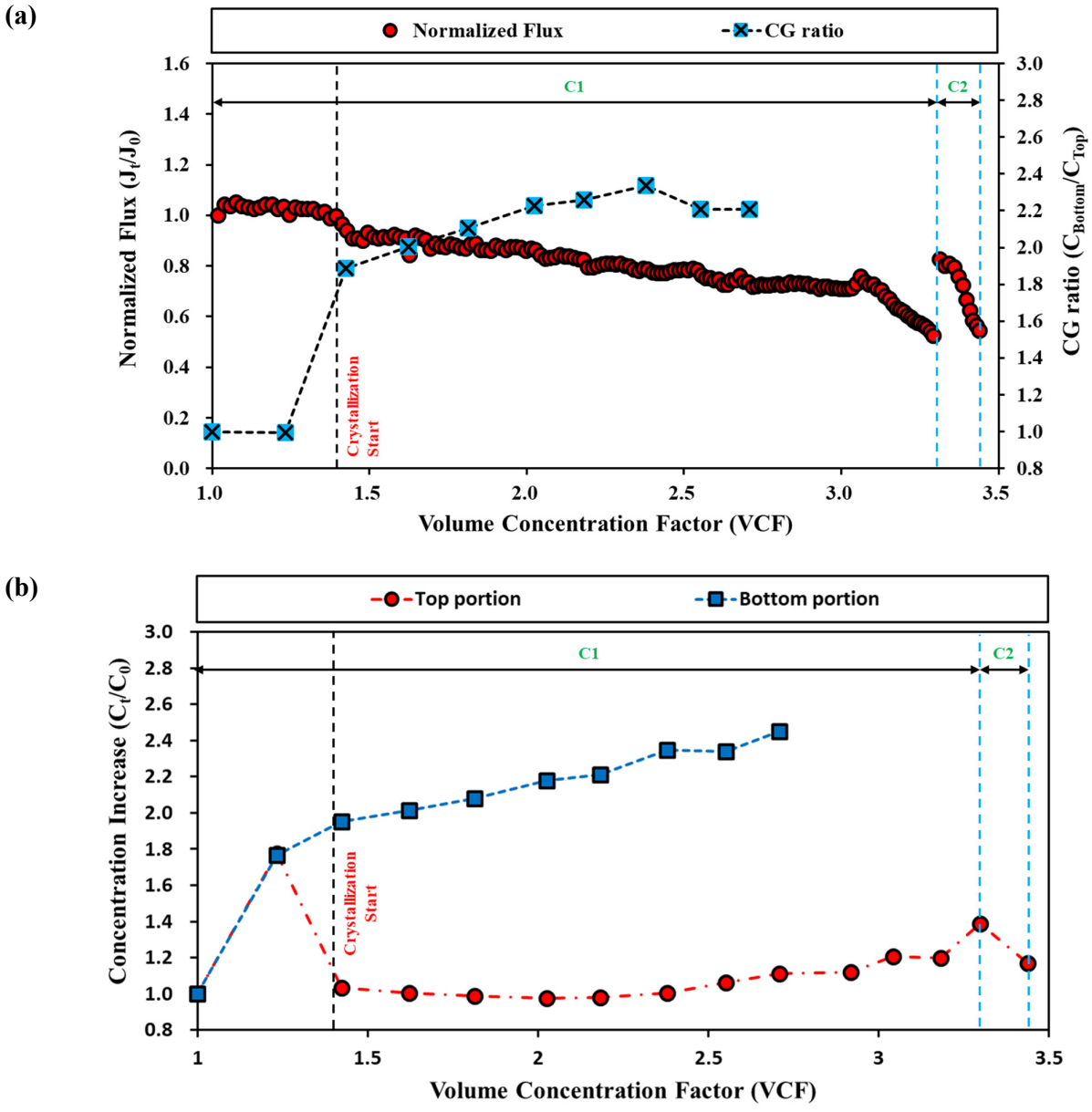

Figure 8-8. Effect of the addition of $(NH_4)_2SO_4$ on (a) permeate flux and CG ratio, and (b) concentration increase (C_t/C_0) at the top and bottom sections of the reactor.

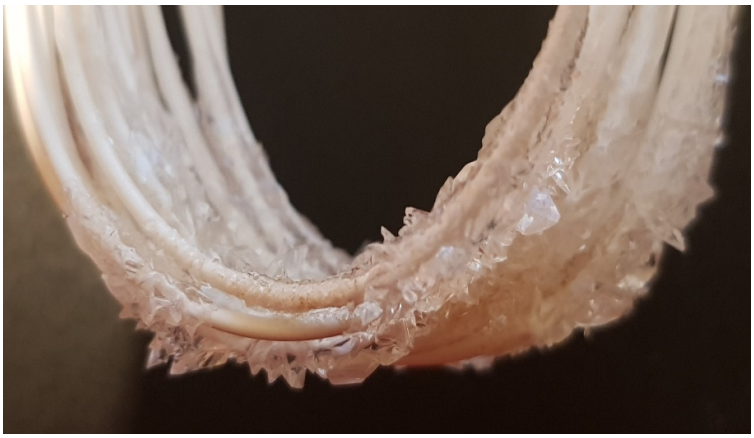

Figure 8-9. Formation of Na_2SO_4 crystals on the membrane surface during the period when rapid flux decline was observed.

8.3.2.3.4. Influence of sulfate-rich scenario on the growth of crystals and nucleation

Referring to the addition of Na_2SO_4, the bottom part of the reactor was filled up with crystals generated in a short period (from 2.90 to VCF 3.45). The crystals' size was smaller compared to that generated from the addition of $(NH_4)_2SO_4$. This outcome indicates that the generation of crystals (nucleation) was much more predominant than the growth of crystals when adding chemicals to create a sulfate-rich context. On the other hand, with $(NH_4)_2SO_4$ addition, crystal growth was observed at the bottom of the reactor as time passed (**Figure 8-10**). This may have been due to the insufficient amount of SO_4^{2-} provided when Na_2SO_4 was used. When Na_2SO_4 was employed to create a sulfate-rich condition, sufficient concentrations of Na^+ and SO_4^{2-} were provided to achieve the supersaturation level of Na_2SO_4 at 20 °C. However, in case of $(NH_4)_2SO_4$, although the SO_4^{2-} was provided continuously, not enough SO_4^{2-} was supplied to reach the supersaturation level of Na_2SO_4. In fact, the SO_4^{2-} concentration in SWRO brine was much lower than Na^+ based on the mole fraction of Na_2SO_4 for nucleation. Thus, a favorable condition (above the metastable zone) was not provided.

A metastable zone is considered to be an ideal one for crystal growth (Mitchell & Frawley 2010). Spontaneous nucleation occurs above the metastable zone. Thus, the growth of crystals was evident

only after first nucleation at the initial stage (VCF 1.42). The generated crystals during the initial stage unction as seed crystals for crystals' growth although SO_4^{2-} was concentrated in the metastable zone. As a result, the larger Na_2SO_4 crystals were obtained with the addition of $(NH_4)_2SO_4$ rather than Na_2SO_4 when considering a sulfate-rich scenario (**Figure 8-6** and **Figure 8-10 (b)**). As well, although a larger CG was formed and maintained the concentration at the top portion of the reactor and deposition/generation of crystals on the membrane surface at VCF 3.29 were caused by insufficient SO_4^- concentration. This insufficient concentration in the reactor led to marked crystal growth, and the consumption of smaller amounts of Na^+ and SO_4^-. In particular, the total concentration of Na^+ in the bulk solution continuously increased over time although Na_2SO_4 crystals did form and grew at the bottom of the reactor. To recover larger amounts of water and other resources, a continuous sulfate-rich environment is required because Na_2SO_4 nucleation occurs in this scenario. Furthermore, the above results show that Na_2SO_4 recovery can be achieved from SWRO brine by providing a sulfate-rich context.

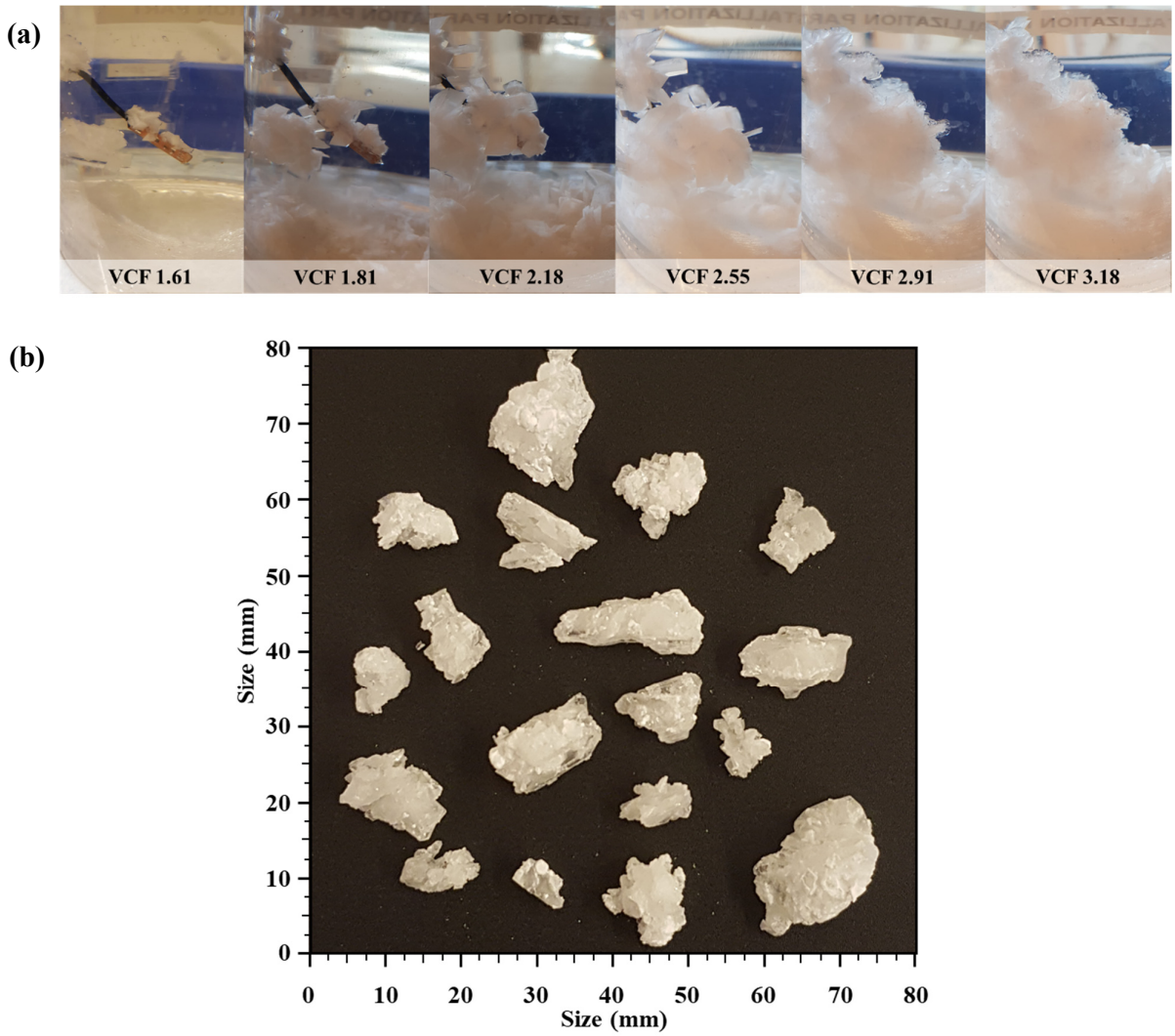

Figure 8-10. Na_2SO_4 crystals generated when $(NH_4)_2SO_4$ was added: (a) variation in morphology with VCF, and (b) when the operation was completed.

8.3.3. Possibility of producing other valuable resources from concentrate

The concentration of other ions such as magnesium (Mg^{2+}), potassium (K^+) and chlorine (Cl^-) also increased proportionally with the concentration factor. These ions affect the effectiveness of the process in the long-term. Chlorine is the one of the primary oxidants and its presence in the reactor at high concentrations actually damages the membrane and other devices due to its strong corrosive properties. It is well demonstrated that chlorine damages the polyamide layer of reverse osmosis (RO)

membrane used in the desalination process (Chae et al. 2015; Gohil & Suresh 2017; Surawanvijit et al. 2016). Also, direct disposal of these ions into the sea is simply toxic to the aquatic eco-system.

A chlorine-rich solution generated from F-SMDC can be used as a source of hypochlorite chemical generation such as sodium hypochlorite (NaOCl) which is also a valuable chemical in the form of disinfectant. Investigations of hypochlorite being created directly from seawater are underway because the current conventional methods of hypochlorite generation using a chlorine gas can lead to major problems in terms of safety (Abdul-Wahab & Al-Weshahi 2009; Casson & Bess 2002; Saleem et al. 2012). Moreover, the NaOCl generated can be used in chemical cleaning of membranes (cleaning in place (CIP)) used in the RO and F-SMDC processes (Puspitasari et al. 2010; Wang et al. 2010). Additionally, Mg^{2+} and K^{+} can be recovered by various methods such as adsorption and precipitation (Glowa et al. 2003; Hardwick et al. 1991; Karidakis et al. 2005; Miyamoto & Pingitore 1992). Mg^{2+} and K^{+} in higher concentrations benefits these processes' adsorption and precipitation performance and efficiency. Recovered Mg^{2+} can be used as a raw material for fertilizer or the production of struvite ($MgNH_4PO_4 \cdot 6H_2O$) from wastewater. Moreover, the concentrate that has been extracted can be used again as a feed solution for the F-SMDC process. The hybrid process for enhanced treatment of SWRO brine is suggested as follows (**Figure 8-11**).

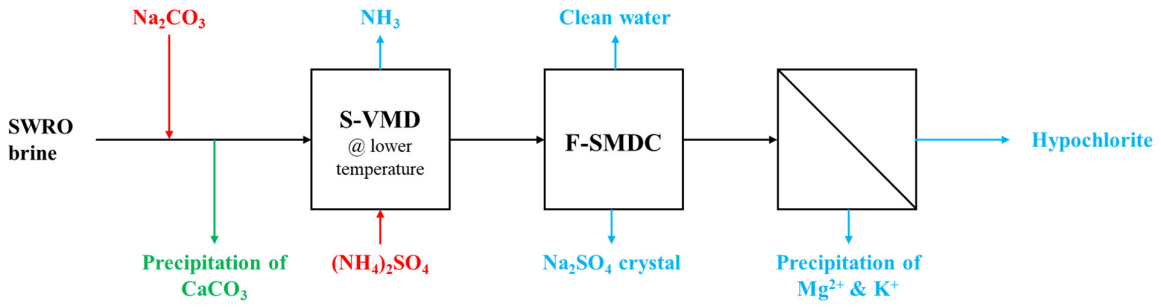

Figure 8-11. Schematic diagram for total SWRO treatment using the hybrid F-SMDC process.

8.4. Summary of this research

The feasibility of fractional-submerged membrane distillation crystallizer (F-SMDC) for the extraction of Na_2SO_4 crystals from seawater reverse osmosis (SWRO) brine was evaluated. The problems that emerged in the treatment of real SWRO brine were examined, and solutions were proposed. Specific conclusions are articulated below:

- Both the deposition of $CaSO_4$ crystals on the membrane surface and the compounds with low sensitivity on solubility with temperature resulted in poor water recovery (water produced: 1.3 L (VCF 1.76)). They also led to crystallization interfering with the target material at the bottom section of the reactor. The removal of Ca^{2+} in the feed solution improved the amount of water recovered (water produced: 4.7 L (VCF 3.75)) and formation of concentration gradient (CG). However, the desired level of supersaturation of Na_2SO_4 was not reached at the bottom part due to rapid flux decline caused by the presence of salts having low sensitivity on solubility **[**with temperature.

- Salts showing low sensitivity on solubility with temperature (NaCl in this study) resulted in rapid flux decline without crystal deposition on the membrane. Na_2SO_4 crystallization at the bottom section can be obtained when a sulfate-rich environment is provided. This could be done when using sodium sulfate (Na_2SO_4), magnesium sulfate trihydrate ($MgSO_4 \cdot 3H_2O$) and ammonium sulfate ($(NH_4)_2SO_4$).

- In the case of adding $MgSO_4 \cdot 3H_2O$, Na_2SO_4 crystallization was not obtained at the bottom section of the reactor. Also, the CG ratio value was low (under 1.6) because of the gradual increase in the concentration at the top section.

- Na_2SO_4 crystallization at the bottom section was observed when Na_2SO_4 and $(NH_4)_2SO_4$ were added and led to the definite formation of CG. The increase in concentration at the top part was observed when Na_2SO_4 and $MgSO_4 \cdot 3H_2O$ were added to create a sulfate-rich environment. On the other hand, in the case of $(NH_4)_2SO_4$ addition, the concentration at the top section did not increase up to VCF 2.38. In both cases where Na_2SO_4 and $(NH_4)_2SO_4$ were added, early crystallization was observed after feeding of SWRO brine.

- Crystal size and recovery ratio varied depending on the kinds of components added. During the initial stage of operation, rapid formation of CG and nucleation were observed with the addition of SO_4^{2-} (i.e. when a sulfate-rich scenario was created). However, crystal growth was predominant compared to nucleation without the continuous creation of a sulfate-rich condition. Results indicated that the provision of continuous sulfate-rich environment is required for stable recovery of Na_2SO_4 and F-SMDC operating for longer when treating SWRO brine.

- The concentrated SWRO brine derived from F-SMDC had high concentrations of Cl^-, Mg^{2+} and K^+ because Na^+ and SO_4^{2-} were extracted as Na_2SO_4. They can also be recovered by other methods and this versatility makes F-SMDC an economical remediation system.

CHAPTER 9

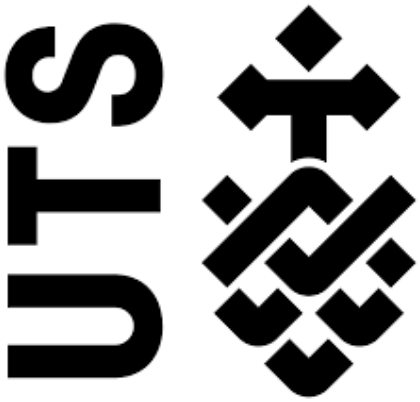

EFFECT OF CHEMICAL AND PHSICAL FACTORS ON THE CRYSTALLIZATION OF CALCIUM SULFATE IN SEAWATER REVERSE OSMMOSIS BRINE

This chapter has been published as: **Y. Choi**, G. Naidu, S. Jeong, S. Lee, S. Vigneswaran, Effect of chemical and physical factors on the crystallization of calcium sulfate in seawater reverse osmosis brine, Desalination, 426 (2018) 78-87.

9.1. Introduction

SWRO brine contains a higher concentration of valuable resources when compared to feed water (seawater). During the crystallization process, salts in the SWRO brine can be separated and used as a valuable resource. However, although these salts may be used as valuable resources, they may display a negative influence at high concentrations and especially when they are treated by using conventional treatment methods (Giwa et al. 2017). The application of MD enables in achieving a highly concentrated brine, and thereby generating a super-saturation state for crystallization (Anisi et al. 2017). Theoretically, MD concentrates the feed solution to create a super-saturated solution to form crystals (Quist-Jensen, Ali, et al. 2016). Meanwhile, the crystallization part of MDC mitigates the scaling phenomenon on membrane surface because salts are continuously removed as solid crystals in the crystallizer (Guan et al. 2012; Shin & Sohn 2016).

Despite the high potential of the MDC, fouling and scaling phenomena are inevitable. These phenomena are more evident with the SWRO brine treatment when compared to the desalination process (Goh et al. 2013; Shin & Sohn 2016). The SWRO brine contains calcium (Ca^{2+}) based crystalline matter at high concentration; calcium sulfate ($CaSO_4$) and calcium carbonate ($CaCO_3$) that possess low solubility (Naidu, Jeong & Vigneswaran 2014). Thus, Ca^{2+} based crystalline matters first precipitate in the form of crystals prior to the reaching of supersaturation of the target material. Hence, the surface and pores of the MD membrane is covered by these sparingly soluble salts (Morillo et al. 2014a). Previous studies investigated the scaling of $CaSO_4$ and $CaCO_3$ in the MD process (Curcio, Ji, Di Profio, et al. 2010; He et al. 2009). The effect of temperature and feed flow velocity on crystallization tendency in a direct contact membrane distillation (DCMD) process was examined (He et al. 2009). The interaction between $CaCO_3$ crystallization and biofouling in a high salinity solution was investigated (Curcio, Ji, Di Profio, et al. 2010).

It is important to understand Ca^{2+} crystallization tendency in terms of the influence of chemical and physical factors. The characteristics of SWRO brine depend on feed water quality, the recovery ratio of the SWRO process, the pre-treatment methods of feed water, and the chemical cleaning of the membrane (Chelme-Ayala et al. 2009; Greenlee et al. 2011; Pérez-González et al. 2012; Squire et al. 1997). The SWRO brine contains various ions and chemical components that were used in the pre-treatment processes and during membrane chemical washing in the RO process. Additionally, the concentration of these ions in the brine is double that in feed water (Chelme-Ayala et al. 2009). The ionic interaction among the ions leads to the crystallization propensity of $CaSO_4$ in the SWRO brine. Therefore, it is important to understand the influence of all ions on the crystallization tendency of $CaSO_4$ for the stable operation of the MDC process. This also obtains reliable information on the ionic interaction for $CaSO_4$ crystallization because it can act as a major foulant in the MD part of MDC process, thereby resulting in the degradation of process performance (Haghtalab & Badizad 2016). Moreover, physical factors, such as agitation (in feed tank) and stirring speed, can affect the extents of crystallization during the MDC process (Akrap et al. 2010).

Thus, the present study investigates the crystallization tendency of $CaSO_4$ in the SWRO brine for different conditions: temperatures (50-80 ºC) and pH values (5-9). The study also examined the effect of (1) NaCl concentration, and chemical agents; (2) organic matters (polysaccharide, protein, and humics); and (3) physical factors (agitation) on the $CaSO_4$ crystallization. The crystal growth was evaluated in terms of the crystal size distribution (CSD) and calcium ion (Ca^{2+}) removal efficiency (variation in the Ca^{2+} concentration before and after the crystallization).

9.2. Materials and Methods

In order to observe $CaSO_4$ crystallization phenomenon in high salinity solution, a synthetic feed solution containing high concentrations of calcium (Ca^{2+}) and sulfate (SO_4^{2-}) ions was prepared. Their concentration were approximately twice as seawater (to represent 50% recovered real SWRO brine) (Waly et al. 2012) (**Table 3-6**). In order to examine the tendency of $CaSO_4$ crystallization in the concentrated brine, batch experiments were conducted under same standard conditions. Each time, a single parameter was changed to examine the effect of that specific parameter on crystal formation. The feed corresponds to a mixed solution of NaCl, Na_2SO_4, and $CaCl_2 \cdot 2H_2O$. Given all the ions that are present, Ca^{2+} and SO_4^{2-} are combined by an ionic electric bond force and precipitation in the form of $CaSO_4$ crystals (**Figure 3-6**). The crystallization phenomenon is influenced by chemical and physical factors. Hence, all experiments were initially conducted at standard condition (heating temperature: 60 °C, pH 7, and stirring speeds: 200 and 50 rpm). The high speed (200 rpm) was provided to the solution homogeneous and lower speed of 50 rpm to facilitate crystallization. The temperature, pH value, and stirring speed conditions were altered to examine each if their effect of them individually on crystallization. In order to examine the effect of temperature on $CaSO_4$ crystallization, feed solutions were heated in a water bath set at the following temperatures: 50 °C, 60 °C, and 80 °C.

Initially, a heating temperature of 60 °C was used. A synthetic standard feed solution (**Table 3-6**) was first used. A 500 mL feed solution was prepared in a beaker with pH adjusted by using 0.1M HCl and 0.1M NaOH. In order to examine the effect of temperature on $CaSO_4$ crystallization, feed solution was heated in a water bath set at temperatures of 50 °C, 60 °C, and 80 °C. Subsequently, feed solutions were mixed at a high speed (200 rpm) in a jar-tester for 2 min to ensure complete mixing. The feed solutions were then allowed to stand for 24 h at a room temperature with slow mixing (50 rpm) to facilitate crystallization. After 24 h, the crystals were separated from the solution by using a glass microfiber filter (Whatman, Grade GF/C, pore: 1.2 µm).

9.3. Results and Discussion

9.3.1. $CaSO_4$ crystal formation

Generally, the $CaSO_4$ crystal has six sides that enable it to grow in six directions as shown in **Figure 9-1** (Linnikov 2000). In the study, for the purposes of simplicity, only growths in two directions were considered, namely [001] and [100]. Directions [001] and [100] are referred to as 'Length' and 'Width', respectively.

Visible salt/crystal formation occurred during the experiment. The SEM-EDX analysis established the formation of $CaSO_4$ crystals (**Figure 9-2 (a)**). Based on the crystal size distribution (CSD) analysis (**Figure 9-2 (b)** and **(c)**), the $CaSO_4$ crystal length was in the range of 50-1000 µm with a width in the range of 10-140 µm. The CSD results indicated that the growth rate and comparative size of the $CaSO_4$ crystals differed in the "Length" and "Width" directions. The growth rate towards the "Length" direction and comparative maximum size was faster and larger than those in the "Width" direction. Based on the initial and final Ca^{2+} concentrations of the solution (initial: 1,620 mg/L, and final: 1,158 mg/L), 28.5% Ca^{2+} removal efficiency was detected. The reduction/removal of Ca^{2+} was attributed to the $CaSO_4$ formation and precipitation.

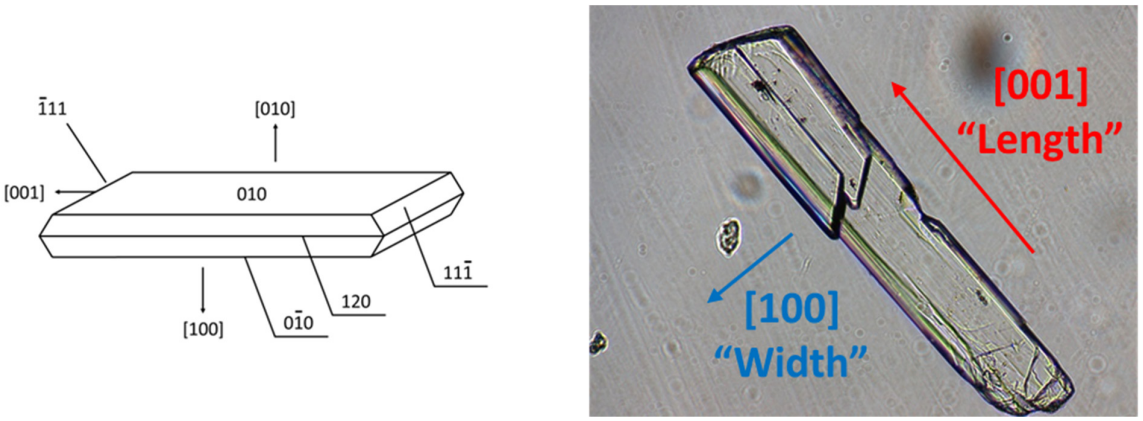

Figure 9-1. Crystal morphology of $CaSO_4$ (Linnikov 2000).

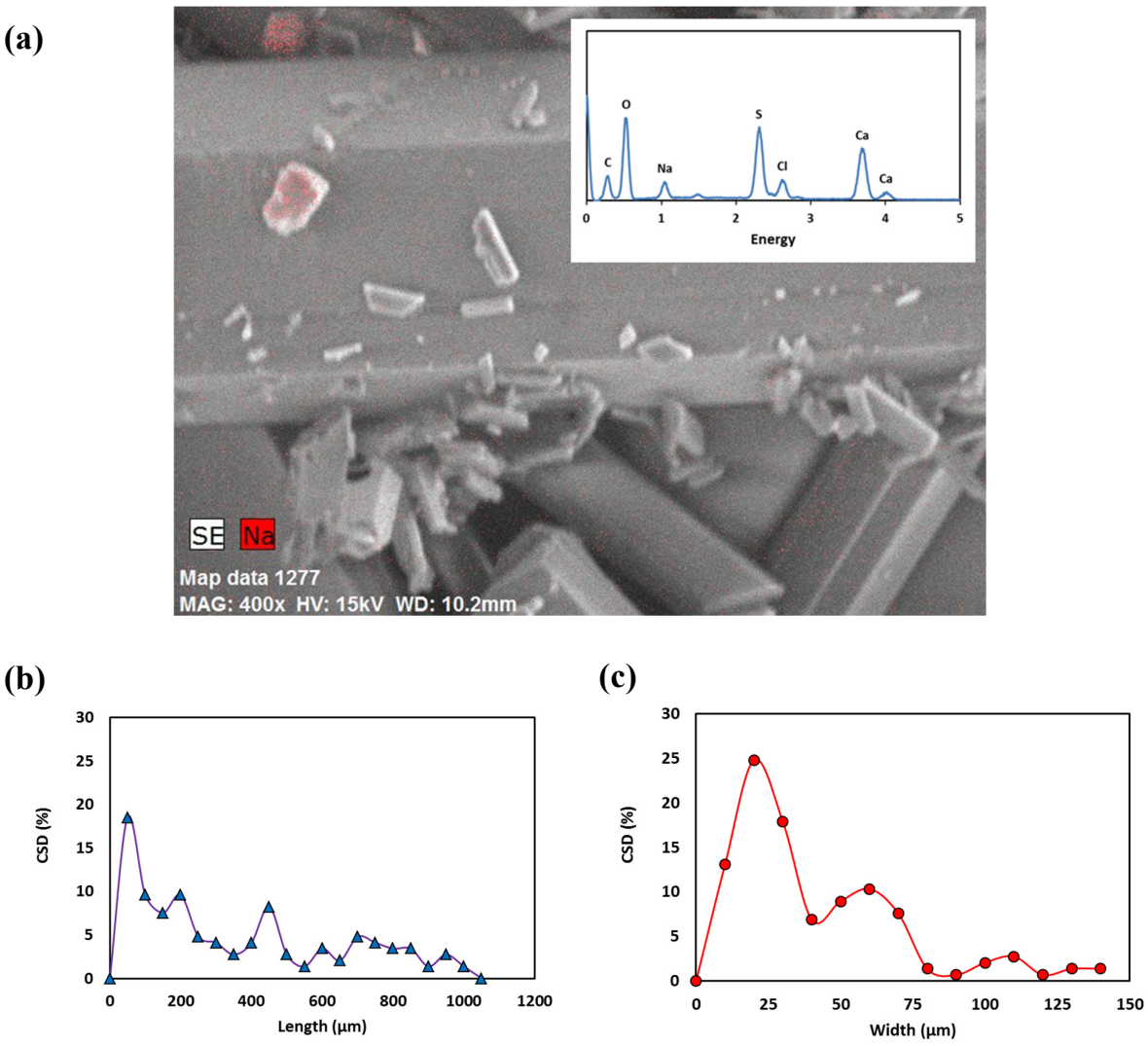

Figure 9-2. $CaSO_4$ crystal that was formed during the batch crystallization experiment: (a) SEM-EDX analysis, (b) CSD of 'Length [001]', and (c) CSD of 'Width [100]'.

9.3.2. Influence of chemical factors

9.3.2.1. pH and Temperature

The influence of solution temperature (50 °C, 60 °C, and 80 °C) and pH (5 to 9) on $CaSO_4$ crystallization was evaluated in terms of crystal CSD as well as the Ca^{2+} crystal formation rate. The results showed that an increase in the heating temperature aided in achieving higher Ca^{2+}

reduction/removal efficiency (**Figure 9-3**). Conversely, there was no distinct trend of Ca^{2+} removal efficiency at different pH ranges (**Figure 9-3**). For example, at 50°C, the Ca^{2+} removal at pH 9 was only 1.5% higher than that at pH 5. The results established that the influence of an increase in the solution temperature on the formation of $CaSO_4$ exceeded that of the solution pH value. This was attributed to the change in solubility with increases in the temperature.

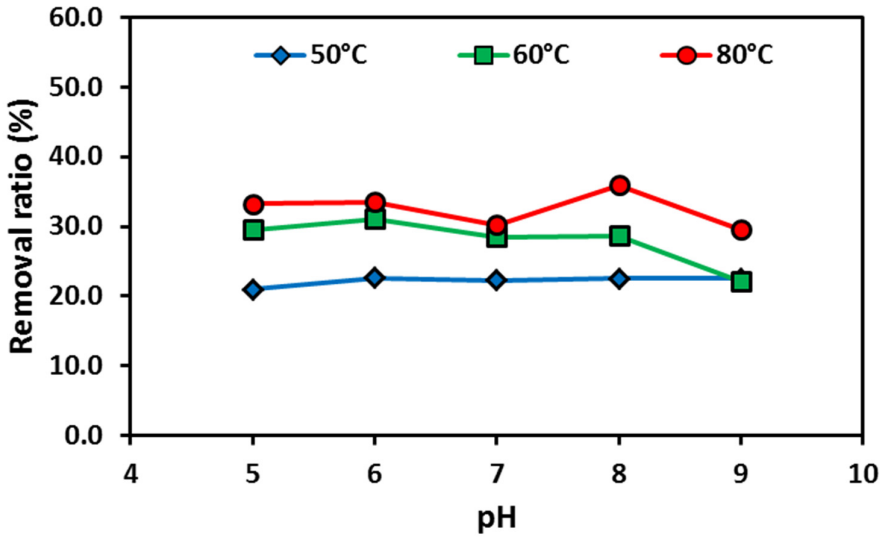

Figure 9-3. Reduction efficiency of calcium ions in the feed solution after crystallization.

A trend of broader CSD was observed at higher temperatures (**Figure 9-4 (a)** and **(b)**). For example, at a heating temperature of 50 °C, CSD was in the range of 50 to 900 µm while it ranged from 50 to 1,400 µm at 80 °C. With the increase in the heating temperature from 50 °C to 80 °C, the average crystal size increased, and the ratio of the small crystal that were formed decreased. This tendency is similar to $CaSO_4$ solubility at different temperatures. Specifically, $CaSO_4$ exhibits a lower solubility at temperatures exceeding 40 °C (Azimi & Papangelakis 2010). It was expected that solubility is an important factor in the formation and growth of $CaSO_4$ crystals. In the case of pH, with respect to high pH values of the feed solution, CSD exceeded the low pH values (**Figure 9-4 (c) and (d)**). This was especially evident in the case of the CSD width. For example, at the same heating temperature of 60 °C,

the CSD width at pH 5 ranged from 50 µm to 650 µm while it ranged from 50 µm to 1150 µm at pH 9. Moreover, the portion of small size crystals at a high pH value was lower than that at a low pH value

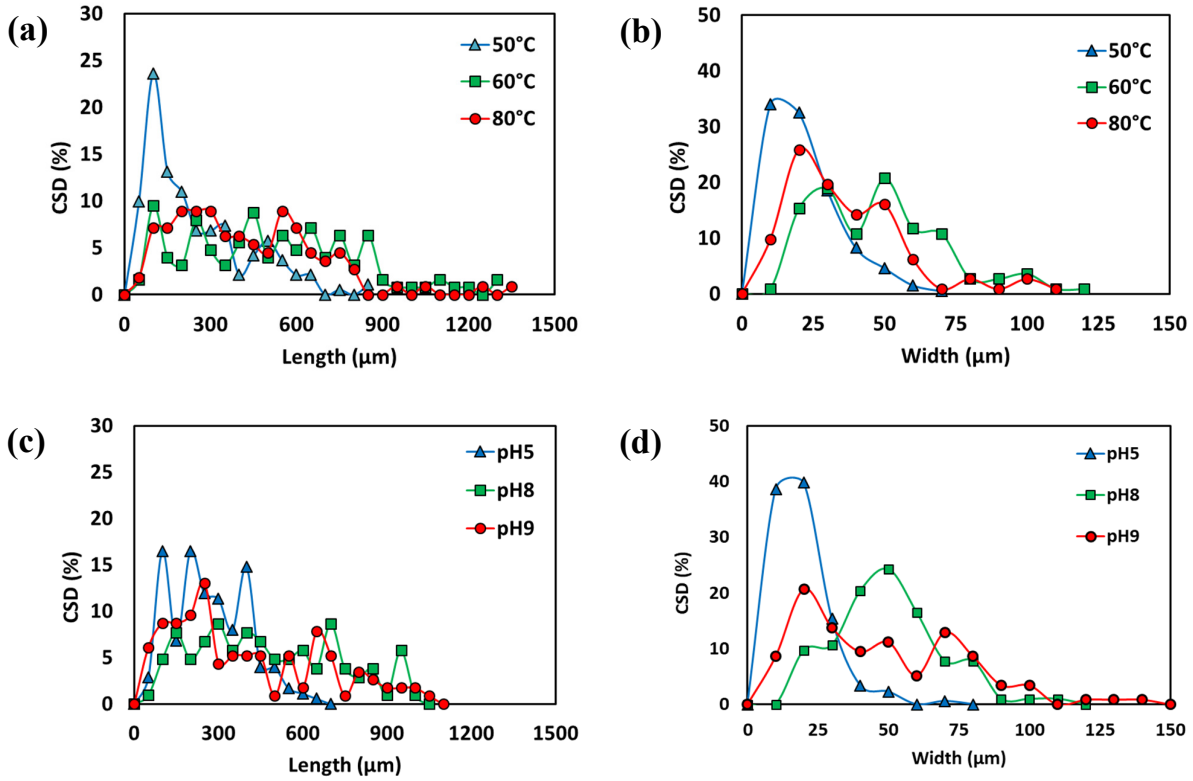

Figure 9-4. Crystal size distribution (CSD) at different heating temperatures and pH values: (a) Length [001] relative to temperature, (b) Width [100] relative to temperature, (c) Length [001] relative to pH, and (d) Width [100] relative to pH.

9.3.2.2. Concentration of NaCl

Actual seawater brine solution is highly saline with a NaCl concentration in the range of 35 g/L to 55 g/L. Thus, it is important to evaluate the influence of salinity on the formation of $CaSO_4$. The tendency of $CaSO_4$ formation in the presence of NaCl (35 g/L and 150 g/L) and in absence of NaCl were examined at a fixed pH of 7 and a temperature of 60 °C.

The presence of salt reduced the formation of the $CaSO_4$ crystal. The solution containing 35 g NaCl/L

to 150 g NaCl/L resulted in 33.1% to 35.3% of Ca^{2+} removal efficiency. Comparatively, Ca^{2+} removal efficiency was 69.7% in the absence of NaCl. The influence of NaCl in reducing the formation of $CaSO_4$ was attributed to the ionic interference of Na^+ and Cl^-.

In terms of CSD, the presence of NaCl increased the size of $CaSO_4$ crystals that were formed. As shown in **Figure 9-5**, in the absence of NaCl in the solution, relatively small crystals were observed (both "Length" and "Width"). In comparison, in the presence of NaCl in the solution, CSD in both directions were higher, and the dominant crystal size increased. Thus, the $CaSO_4$ crystal size increased with increases in the NaCl concentration.

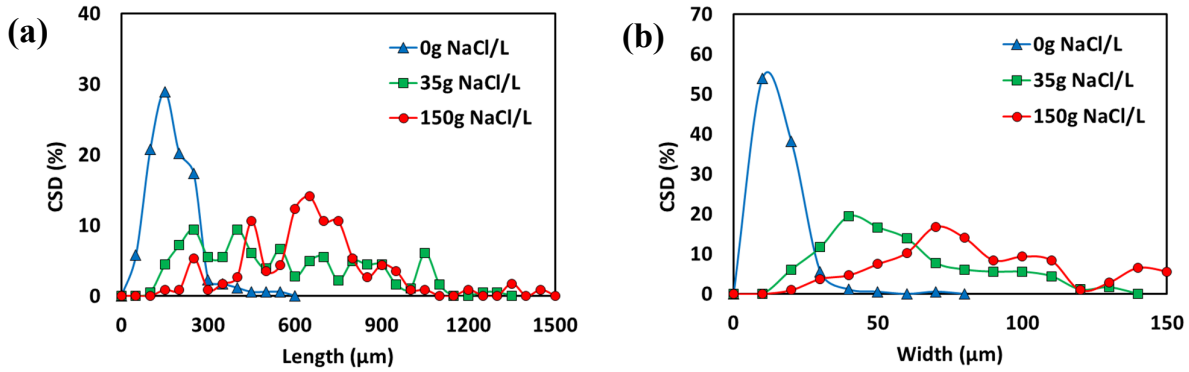

Figure 9-5. Crystal Size Distribution (CSD) with different salt concentrations in the feed solution: (a) Length [001], and (b) Width [100].

9.3.2.3. Effect of inorganic ions.

9.3.2.3.1. Sole ion

The addition of inorganic ions, such as Mg^{2+}, K^+, and HCO_3^-, in the solution led to the growth of other crystals with $CaSO_4$ crystals (**Figure 9-6**). The EDX analysis indicated that Na^+ was detected in the crystals that were formed along with Ca^{2+} and SO_4^{2-} with the addition of Mg^{2+} in the solution (**Figure 9-6 (a)**). Nevertheless, Mg^{2+} peaks were not detected in the EDX spectral. However, the addition of

Mg^{2+} resulted in a significantly reduced Ca^{2+} removal efficiency (19.8±0.2%) when compared to the solution without any ion additions (29.5±0.6%) (**Figure 9-7**). The results implied that Mg^{2+} affected the formation of $CaSO_4$ crystals. Theoretically, Mg^{2+} can also combine with SO_4^{2-} in the solution and precipitate in the form of crystal (magnesium sulfate ($MgSO_4$)). The electronegativity influences a combination of covalent linkages (Boeyens Jan 2008). It is a measure of the tendency of an atom to attract a bonding a pair of electrons. Specifically, the electronegativity of Mg^{2+} exceeds that of Ca^{2+} (Mg^{2+}: 1.31 vs Ca^{2+}: 1.00) (Allred 1961; Boeyens Jan 2008). Hence, the ionic bonding force of Mg^{2+} with electrons exceeds that of Ca^{2+}. Thus, an amount of SO_4^{2-} that can be combined with Ca^{2+} decreased because SO_4^{2-} was attracted by Mg^{2+}. However, Mg^{2+} did not form crystals with SO_4^{2+} due to its much higher solubility when compared with that of a $CaSO_4$ crystal. The solubility of $MgSO_4$ (351 g/L @ 20 °C, 548 g/L @ 60 °C) significantly exceeds that of $CaSO_4$ (2.55 g/L @ 20 °C, 2.44 g/L @ 60 °C) (Marshall 1967; Partridge & White 1929). This is used to account for the reduction in $CaSO_4$ crystals production. Therefore, it is necessary to consider the same since a high quantity of Mg^{2+} presents in the feed (0.22M as Mg^{2+}) simulated the SWRO brine.

The EDX analysis showed that the addition of K^+ to the solution did not change the $CaSO_4$ crystal formation (**Figure 9-6 (b)**). Similarly, the addition of K^+ did not significantly change the Ca^{2+} removal efficiency, and thus the Ca^{2+} removal efficiency remained in the range of 32±1%, and it was closely similar to the solution without any added ions. The presence of K^+ did not significantly influence the $CaSO_4$ formation due to its lower electronegativity (0.82).

Furthermore, when HCO_3^- ions were added to the bulk solution, the other crystals formed in a globular form were observed in conjunction with $CaSO_4$ crystals. The EDX mapping image showed that they did not contain Na^+ and Ca^{2+} in the globular crystals (**Figure 9-6 (c)**). Thus, the crystals with a globular shape were neither NaCl crystals nor $CaSO_4$ crystals. Nevertheless, the addition of HCO_3^- to the solution did not significantly change the Ca^{2+} removal efficiency, and therefore the Ca^{2+} removal

efficiency remained in the range of 30.5±1.7% that was similar to that of the solution without any additional ions (**Figure 9-7**).

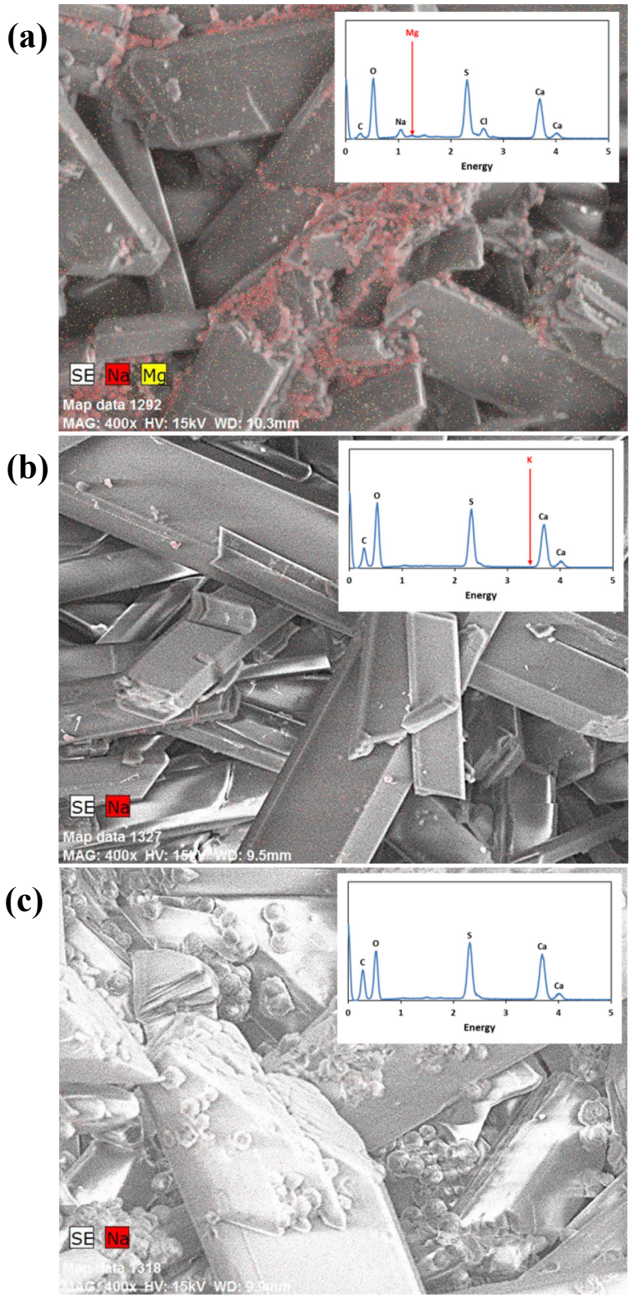

Figure 9-6. SEM-EDX data of crystal shape and components with the addition of ions at 60 °C of (a) Calcium with the addition of magnesium, (b) Calcium with the addition of potassium, and (c) Calcium with the addition of bicarbonate.

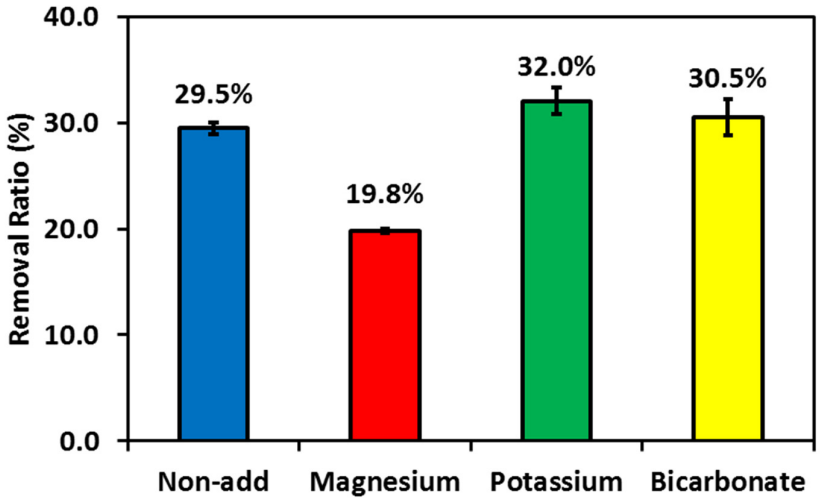

Figure 9-7. The reduction efficiency of calcium ions in the feed solution after crystallization with the addition of inorganic ions.

At the same heating temperature (60 °C), the CSD differed based on the existence of specific ion in the feed solution. The CSD was higher when other ions were not added into the feed solution; and the CSD ranged from 50 µm to 1,200 µm (**Figure 9-9**). However, when K^{+}, Mg^{2+} and HCO_3^{-} were incorporated, the CSD ranged from 50 µm to 800 µm (with K^{+}), from 50 µm to 850 µm (with Mg^{2+}), and from 50 µm to 900 µm (with HCO_3^{-}). This implies that these ions influenced the growth of $CaSO_4$ crystal. Thus, the ions interfere with the growth of $CaSO_4$ crystals.

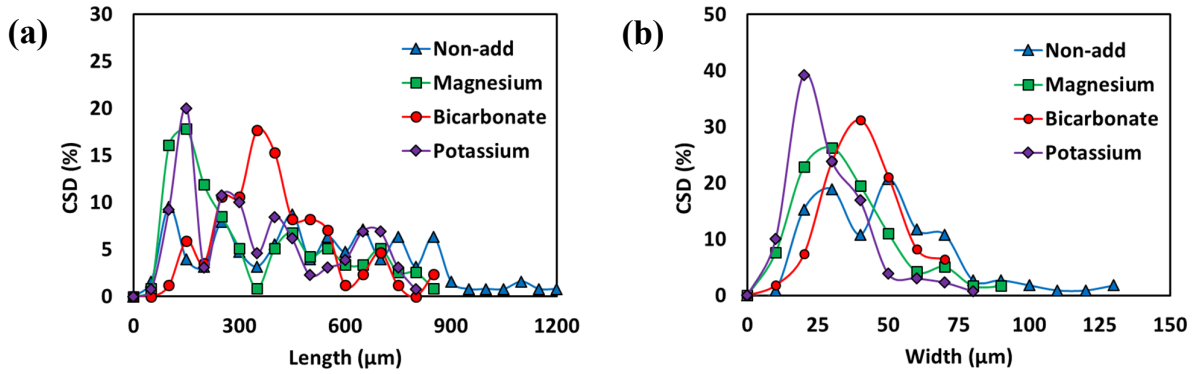

Figure 9-8. Crystal size distribution (CSD) with the addition of inorganic ions: (a) Length [001], and (b) Width [100].

9.3.2.3.2. Chemical washing agents

In the SWRO process, chemical washing agents are employed to remove organic fouling, biofilm, and inorganic scaling (Jeong et al. 2016). The chemicals remain in the wastewater from SWRO process and are subsequently treated together with the SWRO brine. The presence of these chemicals in the SWRO brine may play a role in influencing the growth and size of $CaSO_4$ crystal formation. In the study, the changes in $CaSO_4$ crystal formation in the presence of EDTA chemical washing in the solution and at a fixed temperature of 60 °C and a stirring speed of 50 rpm was evaluated. The pH value of solution changed due to the addition of EDTA (pH 3.82 and 4.71). As shown in **Figure 9-9**, this did not significantly influence the formation and growth of crystals (27.01±0.53%) with addition of EDTA. The CSD and calcium ion rejection were almost similar in the absence and presence of EDTA (26.54%).

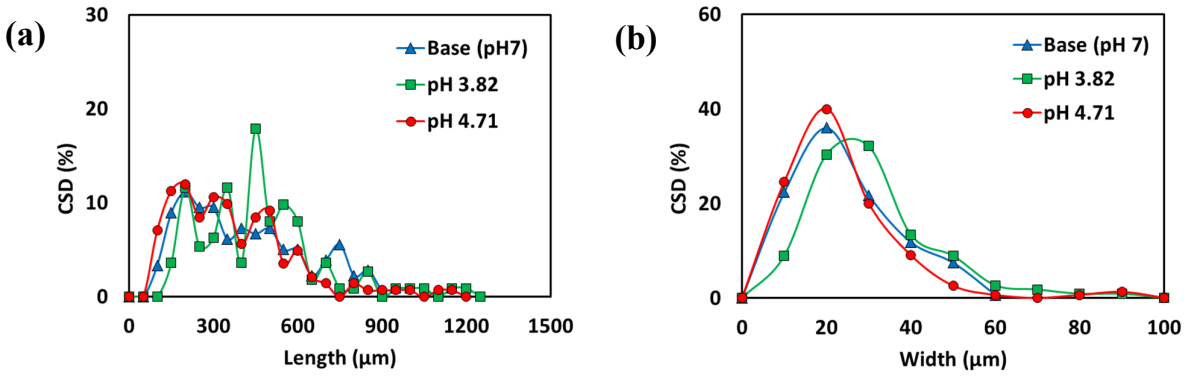

Figure 9-9. Crystal size distribution (CSD) with chemical washing agent: (a) Length [001] with EDTA, and (b) Width [100] with EDTA.

9.3.2.3.3. Coagulation chemicals for pre-treatment

Flocculation is often used as a pre-treatment for RO process to remove colloidal and dissolved organic foulants. $FeSO_4$ and $FeCl_3$ are widely used as coagulants. In the study, the effect of these two coagulants on $CaSO_4$ crystallization was investigated at a fixed pH of 7 and a temperature of 60 °C.

As shown in **Figure 9-10**, the CSD of $CaSO_4$ was affected by the presence of both the coagulants ($FeSO_4$ and $FeCl_3$). In the case of the "Length" direction, the CSD became narrow, and small crystals were detected in presence of coagulants. However, it did not influence the CSD of the "Width" direction. Iron and chloride ions were not detected in the crystals that were formed (**Figure 9-12**). As mentioned above, the added ions can be combined with other ions in the formation of crystals. For example, the addition of Mg^{2+} influences $CaSO_4$ crystal formation (**Figure 9-8**). However, Fe^{2+} did not influence it although iron ions exhibit a higher electronegativity when compared with magnesium and calcium ions (Fe^{3+}: 1.83, Mg^{2+}: 1.31, Ca^{2+}: 1.00). It is expected that concentration of iron ion is not sufficiently high to influence the ionic bond force with sulfate ions (2.0 mM as Fe^{3+} in feed). In case of the magnesium ions, a very high amount of magnesium ions was added into the feed (0.22 M as Mg^{2+}). Additionally, the solubility of $FeSO_4$ and $FeCl_3$ significantly exceeds that of $CaSO_4$ ($FeSO_4$: 256 g/L @ 20 °C, and $FeCl_3$: 920 g/L @ 20 °C).

In terms of the formations of crystal, each coagulant exhibits a different effect. When $FeCl_3$ was added, the amount of calcium that was rejected was almost same (27.9%) as that given the non-addition of coagulant (28.5%). Conversely, the rejection ratio of calcium ions (42.7%) increased when $FeSO_4$ was added. This indicates that $FeSO_4$ simulates the formation of crystals due to the presence of sulfate ions. The results indicated that the addition of sulfate ions influenced the formation of $CaSO_4$ crystal. Increased $CaSO_4$ crystals were formed in the presence of SO_4^{2-} in the feed solution. Overall, both the coagulant chemicals negatively influenced crystal growth in the "Length" direction.

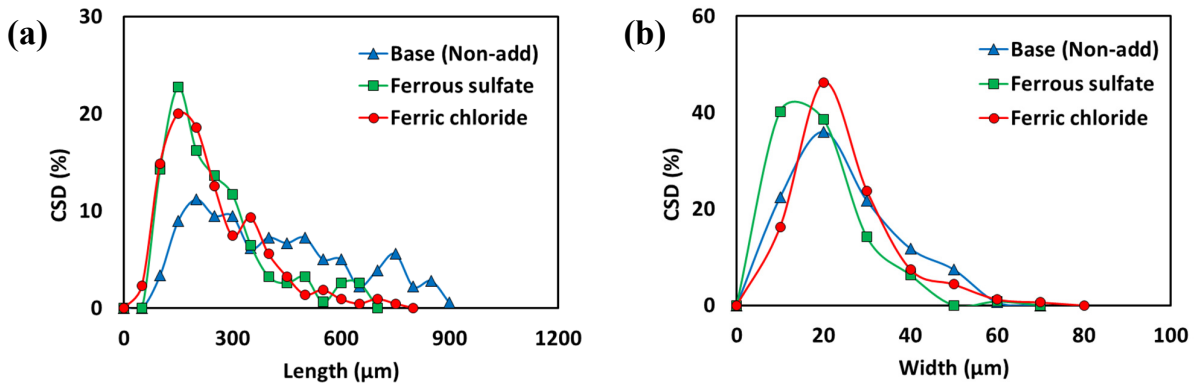

Figure 9-10. Crystal Size distribution (CSD) of $CaSO_4$ in the presence of a coagulant: (a) Length [001], and (b) Width [100].

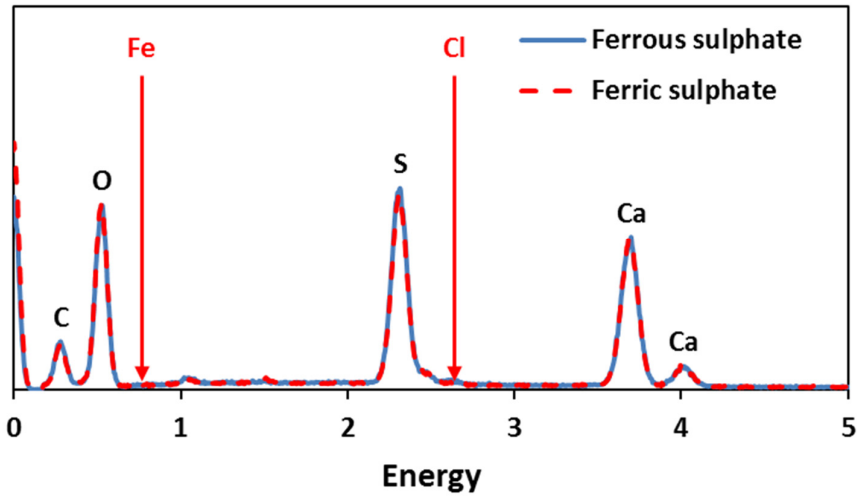

Figure 9-11. EDX data of $CaSO_4$ crystals in the presence of a coagulant.

9.3.3. Effect of organic matter

Organic matters, such as polysaccharide, protein, and humic, are found in seawater and SWRO brine. Here, HA, BSA, and AA represent the humic, proteins, and polysaccharide (the common model organic foulant in brine). As shown in **Figure 9-12**, when organic matters (HA, BSA and AA) are added in a feed solution, the CSD in the "Length" direction became narrower, and the dominant crystals size

became smaller. In contrast, CSD (in "Width" direction) did not change significantly with the addition of organic matters. This revealed that all three organic matters that were used prevented the growth of crystals in the length direction. In the case of the HA addition, the rejection ratio of Ca^{2+} increased to approximately 10% although they did not influence the growth of crystals (Ca^{2+} rejection efficiency: 29.0% @ Non-addition, 38.5% @ addition of HA, 30.8% @ addition of AA, 31.1% @ addition of BSA). This is potentially due to the reduction of electrostatic repulsion between Ca^{2+} (Jermann et al. 2007; Naidu et al. 2015). Additionally, HA possesses a negative charge (Jones & O'Melia 2000). It plays the role of a bridge between Ca^{2+} and HA (bridging effect and/or complexation). Hence, Ca^{2+} adsorbs onto the HA compound. It causes a higher rejection of the Ca^{2+} in a solution than the Ca^{2+} rejection ratio given non-addition (**Table 9-1**).

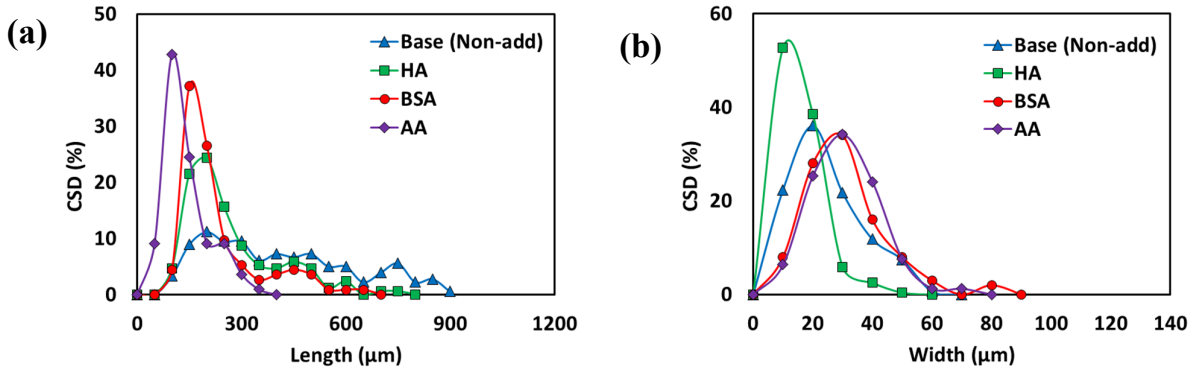

Figure 9-12. Crystal Size Distribution (CSD) in the presence of organic matter: (a) Length [001], and (b) Width [100].

Table 9-1. Calcium ion rejection efficiency in presence of organic matter.

Organic matter	Calcium rejection efficiency (%)
No addition	29.01
Humic acid (HA)	38.45
Alginate (AA)	30.76
Bovine serum albumin (BSA)	31.13

9.3.4. Effect of physical factors

In the submerged membrane process, physical methods, such as agitation, aeration, and vibration are applied to reduce the fouling phenomenon and to agitate (mix) the solution (Ndinisa et al. 2006). Additionally, the crystallization tendency is significantly influenced by physical factors such as agitation speed. Furthermore, it is important to operate the crystallizer at an appropriate agitation speed (Akrap et al. 2010; Shimizu et al. 1999). In this section, three different agitation speeds (0 rpm, 20 rpm (as the lower speed), and 150 rpm (as the higher speed)) were applied.

As shown in **Figure 9-13**, CSD was influenced by the agitation intensity (or mixing speed). The dominant crystals size of CSD increases in the "Length" direction when the agitation intensity increased. This indicates that the hydrodynamic conditions are more suitable for crystal growth at a higher agitation intensity. In this case, a better suspension of crystals was provided by higher agitation intensity. Thus, the surface area that is exposed to the solution for mass transfer between crystal surface and solution increased. As shown in **Figure 9-14**, suspension crystals in the solution were evenly distributed with higher agitation intensity. In comparison, crystals were formed towards the bottom side at a lower agitation intensity. However, in the case of the "Width" direction, the dominant size of

crystal increases at the low mixing speed of 20 rpm although the dominant size decreased at a higher agitation intensity. This may be due to crystal breakage that is caused by collisions between crystals and impeller of jar-tester or wall of batch cell (Akrap et al. 2010). At a higher agitation speed, the probability of collision of crystals increased with increases in the collision power. This can lead to a higher degree of breakage of crystals. A lower dominant size of crystals at higher agitation intensity was detected in the case of the "Width" direction. It is assumed that the crystal side of the "Width" direction (side 120) exhibits a weaker solidity when compared with the dimension of "Length" direction (side īıı) **(Figure 9-1)**. At a high mixing, the increase in the effective surface of the crystal, which is contacted to solution, increases the formation ratio of crystals. However, the formation ratio is not significantly different at lower (20 rpm) and higher (150 rpm) agitation intensities (Ca^{2+} rejection ratio: 11.7% @ 0 rpm, 27.2% @ 20 rpm, and 28.9% @ 150 rpm).

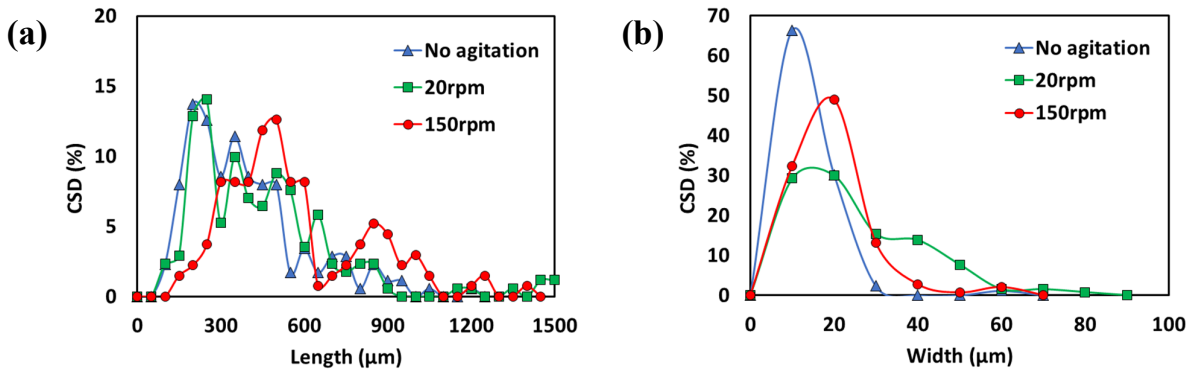

Figure 9-13. Crystal Size Distribution (CSD) at different mixing velocities: (a) Length [001], and (b) Width [100].

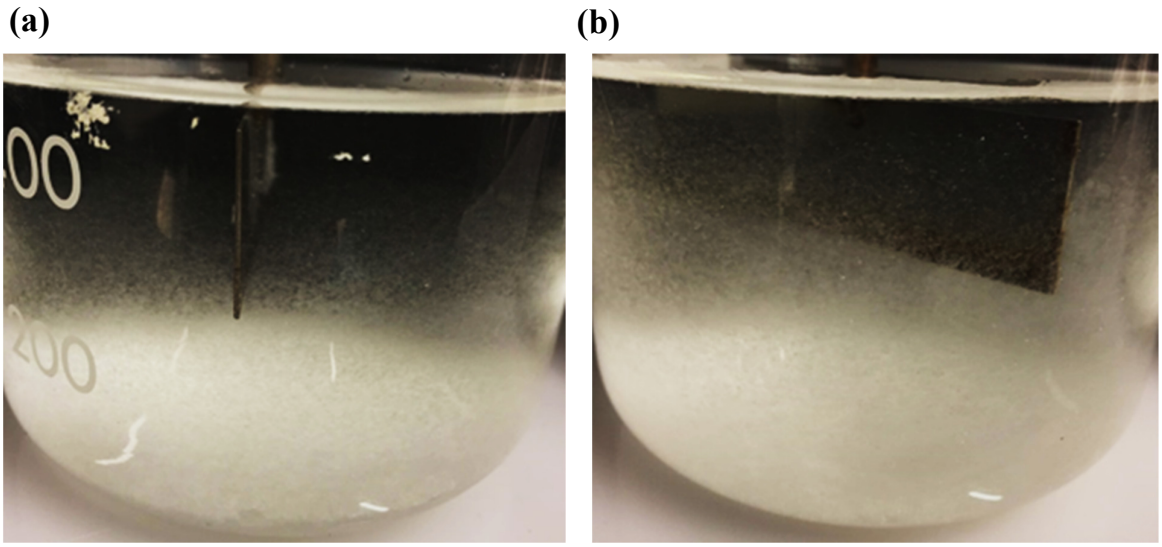

Figure 9-14. Suspension of crystals at different agitation intensities: (a) At lower agitation intensity (20 rpm), and (b) At higher agitation intensity (150 rpm).

9.4. Summary of this research

In this study, the crystallization tendency of $CaSO_4$ in saline solution was examined with different factors at the same standard condition such as chemical factors (temperature, pH, NaCl concentration, and chemical agents), organic matters (AA, HA and BSA) and physical factors (agitation). It is important to possess a good understanding of the suitable control of chemical and physical factors for crystal formation in the MDC process. Crystallization is an effective approach to reduce scaling and fouling and to recover valuable resources from brine. Based on the results of this study, the following conclusions were obtained:

- The size and amount of $CaSO_4$ crystals increased at a higher solution temperature. At the increased solution temperature (80 °C), 32.5±2.6% Ca removal efficiency was achieved when compared to 22.2±0.7% at a lower temperature (50 °C). The pH did not play a significant role in the amount of $CaSO_4$ that was formed but a higher pH enabled an increase in the size of $CaSO_4$ crystals

- The presence of NaCl reduced the formation of $CaSO_4$ and the Ca^{2+} removal efficiency was reduced.
- The presence of Mg^{2+} reduced the Ca^{2+} removal efficiency, and this is attributed to the strong electronegativity of Mg^{2+} when compared to that of Ca^{2+}. The presence of K^+ and HCO_3^- did not play a significant role in the $CaSO_4$ formation. In comparison, $FeSO_4$ stimulates the formation of $CaSO_4$ crystal because it includes a SO_4^{2+}.
- In the presence of organic matter, the CSD in the "Length" direction decreased, and the formation of crystal was slightly improved. In the presence of HA, the Ca^{2+} rejection increased by bridging the effect between Ca^{2+} and HA.
- Agitation positively affects the formation and growth of crystals, and it is controlled by adjusting the agitation intensity. A higher agitation intensity (150 rpm) is suitable because it provides a sufficient suspension of crystals.

CHAPTER 10

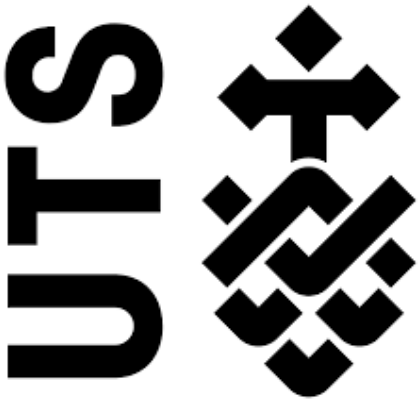

CONCLUSIONS AND RECOMMENDATIONS

10.1. Conclusions

Recently, membrane distillation (MD) and membrane distillation crystallizer (MDC) have been found as potential processes for treatment of high salinity solution, such as SWRO brine. Especially, MDC leads to resource recovery as produces clean water and crystal form resources. Thus, it reduces a waste disposal. However, it is associated with high energy consumption as a result of heating the feed and cooling the permeate streams. It also leads to heat loss in the feed solution side. Thus, this process need to be modified to overcome the above limitations. Thus, this study investigated the performance of submerged MD and on this basis**, developed a novel integrated submerged MD crystallizer process** - fractional-submerged membrane distillation crystallizer (**F-SMDC**) for simultaneously generation fresh water and resource recovery. The following subsections provide specific conclusions from this study. The specific conclusions of each investigations are presented in chapter 4 to 9. This chapter presents the general conclusion. Recommendations are also made for future research on resource recovery from challenging solutions using S-MD and F-SMDC processes.

10.1.1. S-MD process for treatment of SWRO brine

The performance of different S-MD configurations in treating the concentrated brine from SWRO plant was evaluated. The configurations used were submerged-direct contact membrane distillation (S-DCMD), submerged-vacuum membrane distillation (S-VMD) and submerged-vacuum enhanced direct contact membrane distillation (S-VDCMD).

All S-MD configurations showed good performance in treatment of simulated SWRO brine. In the baseline test, S-VMD with vacuum pressure of 50 mbar achieved higher water flux of 40 – 77% compared to S-DCMD and S-VDCMD (with vacuum pressure of 500 and 700 mbar). It is attributed to the different driving force of vapor transfer in different S-MD configurations through a porous hydrophobic membrane. S-VMD was strongly influenced by the concentration of feed solution. The

influence of solution temperature in S-DCMD was the highest because of higher temperature difference between feed and permeate solution. This then led to serious crystallization tendency of calcium sulfate ($CaSO_4$) in the membrane (surface and pores). The $CaSO_4$ crystallization in the membrane caused low water recovery because of pore blocking. The air backwashing effectively removed the crystals deposited on the membrane surface resulting in the recovery of permeate flux. This helped to alleviate the wetting phenomenon of the membrane.

10.1.2. Integrated SMD-adsorption system for rubidium (Rb) recovery

The S-MD process was integrated with adsorption to study its advantage in recovering resources (in this case Rb). S-DCMD configuration was chosen in this integrated system because of its better performance over other S-MD configurations. The performance of integrated submerged MD-KCuFC adsorption was evaluated for simultaneous two recovery of additional clean water and Rb. The adsorption capacity of KCuFC adsorbent was higher in thermal conditions. Hence, the thermal condition in S-MD (55 °C) provided a favorable condition for Rb adsorption by KCuFC without any need for additional heat source. Moreover, the continuous supply of feed solution and adsorbent regeneration enhanced the adsorption capacity because of the provision of sufficient concentration of Rb in the reactor, where the KCuFC was placed in.

The high-quality clean water (permeate conductivity of 1.25 – 1.98 µS/cm, rejection: 99.99 %) and Rb as valuable resource was obtained in the integrated submerged MD-adsorption system. The multiple cycle-operation of this system with regeneration of granular KCuFC adsorbent using 0.2 M NH_4Cl solution led to enhancement of process performance. Based on the two repeated cycle operation, water recovery of 81 % and Rb recovery of 87 % were obtained.

The $CaSO_4$ crystallization caused the degradation of process performance because of crystals deposition on the surface of the membrane and adsorbent. In absence of Ca^{2+} in the feed solution

(simulated SWRO brine), the higher performance was shown in terms of water and Rb recovery. Hence, Ca^{2+} should be removed from the feed solution prior to the application in this process. Furthermore, the size and form of KCuFC adsorbent influenced the adsorption capacity of Rb and the maintenance of adsorbent chemical characteristics. Three different forms of KCuFC adsorbents used in this study (powder form (Size: < 100 μm), particle form (mean size: 0.45 mm) and granular form (mean size: 2.42 mm)) showed different adsorption capacity. The higher initial adsorption rate and adsorption capacity (Q_{max}) of 216.17 mg/g was obtained with the adsorbent in particle form. Furthermore, the high release of adsorbent contents in the solution was observed in powder form KCuFC adsorbent, resulting in the lower adsorption capacity than particle form although its active surface area was bigger in same weight. Superior performance in terms of water recovery and Rb extraction of integrated submerged MD- KCuFC adsorption operation was successfully obtained when single Rb solution and simulated SWRO brine solution were used as feed solution.

10.1.3. F-SMDC process for resource recovery from high salinity solution

Mechanism: The novel F-SMDC developed in this study consist of a single double wall reactor containing a submerged hollow fibre membrane with (i) **a heated top portion** –heated through external wall heating (ii) **a cold bottom portion** – cooled through external wall cooling. This approach enables to generate a feed solution temperature gradient in the reactor. The presence of a **temperature gradient (TG)** creates a favourable condition (heated top condition) for the submerged membrane to continuously produce fresh water (water recovery) while the cold bottom portion of the reactor is favourable for salt crystallisation. Further, water recovery through the membrane on the top portion increases the feed solution concentration. In the reactor, this creates a natural gravitation flow: the concentrated feed solution from the top of the reactor gravitates to the bottom of the reactor. In this way a feed solution **concentration gradient (CG)** generates in the reactor. Further, the cooling condition at the bottom increases the solution density. This natural phenomenon will cause the

concentrated solution to be retained on the reactor bottom, where it will form crystals upon super saturation (away from the membrane). This is designed to act as a mitigation measure for membrane scaling. CG and TG in the F-SMDC reactor is further facilitated by the introduction of a **partition**.

Feasibility: The mechanism of F-SMDC was tested and compared to that of conventional MDC. It was observed that higher water recovery (VCF 3.5) and lower membrane scaling was obtained in F-SMDC compared to submerged MDC mode (VCF 2.9) in the treatment of high salinity sodium sulfate (Na_2SO_4) solution. Compared to MDC, permeate flux decline was lower in F-SMDC due to lower feed concentration at the top portion. Moreover, TG generated in the reactor influenced the Na_2SO_4 solubility in the reactor. The lower temperature at the bottom portion led to the decrease of solubility of Na_2SO_4, enhancing crystallization. The extraction of Na_2SO_4 crystal from the solution at the bottom portion reduced the increase of feed concentration close to the membrane, and therefore, a stable permeate flux was maintained.

Factors influencing CG and TG in F-SMDC: The properties of **inorganic components** in the feed solution play an important role in the generation of high ratio of CG (chapter 7). **Molecular weight and electronegativity of the feed solutions** were important factors for generation of CG. High CG was not observed for inorganic compound with low molecular weight (such as ammonium chloride and sodium chloride (CG ratio range of 0.94 to 1.46)), These compounds did not lead to any crystallization at the bottom portion. On the other hand, high molecular weight components such as potassium chloride, magnesium sulfate and sodium sulfate led to the salt crystals with high CG ratio (range of 1.51 to 1.83). Higher electronegativity led to higher permeate flux decline with an increase of concentration at the top portion of the reactor. For example, with Na_2SO_4 as a feed solution, lower permeate flux decline was observed compared to $MgSO_4$ (electronegativity: Na^+: 0.93, Mg^{2+}: 1.31). The CG generation of **organic component** was induced with the gravitational movement of concentrated inorganic components to the bottom portion in the reactor. This would potentially lead to

the deposition of organic components on the membrane surface, mitigating the fouling potential caused by organic components.

Scaling mitigation: The presence of CG and TG and continuous salt extraction from feed solution leads to the mitigation of scaling on the membrane surface. This enables a continuous operation of F-SMDC and production of high-quality fresh water and valuable crystals (Na_2SO_4). F-SMDC successfully treated feed solution of Na_2SO_4 (120 g/L) and produced of 7.9 L of fresh water and **2.1 kg of crystals, respectively instead of Na_2SO_4 deposition onto the membrane**. However, scaling mitigation mechanism of F-SMDC could not be applied in the presence of calcium as discussed below.

Challenges in F-SMDC: In F-SMDC, because of the low solubility of $CaSO_4$ (sparingly soluble salt), generation and deposition of **$CaSO_4$** crystals on the membrane surface, interferes with the downstream of concentrated feed solution and the subsequent collapse of different concentration layer (CG formation) along the reactor of F-SMDC. This results in the low water recovery ratio (water production: 1.3 L (VCF 1.76)) and no extraction of Na_2SO_4 crystals can be achieved in feed solution containing calcium such as SWRO brine. Likewise, Na_2SO_4 crystallization did not occur in the presence of **NaCl**. This is because, NaCl is a component whose solubility is not correlated to temperature, and therefore, adversely interferes with the CG formation occurring in the feed solution.

Strategies to improve challenges: (i) **$CaSO_4$** - A control of $CaSO_4$ scaling is essential prior to F-SMDC. $CaSO_4$ crystallization phenomenon is influenced by chemicals and physical factors (as discussed in chapter 9), such as chemical washing agent, coagulant, organic components, agitation (stirring), pH and temperature. A larger amount of $CaSO_4$ crystals was obtained at higher solution temperature because $CaSO_4$ is a negative temperature-solubility salt. It led to the increase of crystal size. This is because higher saturation was reached at the high temperature. Such property of $CaSO_4$ can lead to a serious scaling issue in F-SMDC because of the high temperature of the feed solution. However, pH does not play a significant role on the amount of $CaSO_4$ crystal formed, but higher pH

facilitates the growth of $CaSO_4$. The formation of $CaSO_4$ crystallization reduces in the presence of NaCl in the solution. The different electronegativities of the cations attributed to the variation of $CaSO_4$ crystal formation. The presence of Mg^{2+} in the saline solution reduced the formation of $CaSO_4$ although the influence of K^+ and HCO_3^- was not significant. In addition, $CaSO_4$ crystal formation was increased by the provision of SO_4^{2-} using the addition of $FeSO_4$ used as coagulant. Moreover, the presence of organic components and specific agitation speed (150 rpm in this study) improved $CaSO_4$ crystallization. In the **absence of Ca^{2+}**, **higher water recovery** (water production: 4.7 L (VCF 3.75)) and **formation of CG with high CG ratio** (maximum CG ratio of 2.13) were achieved in SWRO brine.

(ii) NaCl - The provision of sulfate-rich condition in the reactor was used via addition of SO_4^{2-} for earlier crystallization of Na_2SO_4 before occurrence of adverse effect of NaCl. It was based on the assumption that adverse impact of NaCl may be mitigated by not reaching saturation of Na^+ for NaCl crystallization, according to the use of Na^+ for Na_2SO_4 crystallization at lower Na^+ concentration than saturation concentration of NaCl. The feasibility of provision of sulfate-rich condition in the reactor was investigated using three different substances: sodium sulfate (Na_2SO_4), magnesium sulfate trihydrate ($MgSO_4 \cdot 3H_2O$), and ammonium sulfate ($(NH_4)_2SO_4$). Addition method of $MgSO_4 \cdot 3H_2O$ and $(NH_4)_2SO_4$ influenced the SO_4^{2-} concentration towards supersaturation of Na_2SO_4 unlike the addition Na_2SO_4. In the case of addition of $MgSO_4 \cdot 3H_2O$, Na_2SO_4 crystallization was not observed with low CG ratio (under 1.6) caused by the gradual increase of concentration at the top portion in the reactor. However, the addition of Na_2SO_4 and $(NH_4)_2SO_4$ both obtained Na_2SO_4 crystals at the bottom portion with enough CG ratio in the reactor. The pre-formation of CG of Na^+ and SO_4^{2-} using Na_2SO_4 solution before feeding the SWRO brine led to attaining supersaturation of Na_2SO_4 in the reactor, and Na_2SO_4 crystals were obtained. However, the concentration increase at the top portion after feeding of SWRO brine was observed as a result of $MgSO_4 \cdot 3H_2O$ addition. In the case of $(NH_4)_2SO_4$ addition, Na_2SO_4 crystallization was achieved without the concentration increase at the top portion up to VCF

2.38. The sulfate-rich condition at the initial stage of operation led to early nucleation. The crystal size and recovery ration were dependent on the component added and addition method because of different of provision ratio of Na^+ and SO_4^{2-}. The addition method which is not feeding continuously did not provide the sulfate-rich condition compared to Na^+ concentration. It is because of the much lower concentration of SO_4^{2-} in the SWRO brine than Na^+, resulting in the increase of Na^+ with high concentration ratio in bulk solution. As a result, the crystal growth predominated over nucleation of Na_2SO_4. This result indicated that the continuous provision of sulfate during the operation of F-SMDC is required for continuous crystallization of Na_2SO_4. The concentrated brine from F-SMDC also includes Cl^-, Mg^{2+} and K^+ at high concentrations compared to Na^+ and SO_4^{2-}. Thus, it can be used as a source for recovery of other products which can improve the economic efficiency of F-SMDC.

10.2 Recommendations

Based on the results, the S-MD hybrid processes can be alternative process for zero liquid discharge (ZLD) in the treatment of SWRO brine because of its simultaneous production of clean water and resources in for of crystals. Especially, F-SMDC showed the benefits compared to conventional MDC process. However, there are some issues remain which have to be solved for sustainable operation of F-SMDC process. More studies are required on MDC process to optimize the resource recovery from the challenging feed solutions (**Figure 10-1**). Following are some recommendations based on the present research:

- SWRO brine consists of many cations (Na^+, Mg^{2+}, K^+) and anions (SO_4^{2-}, Cl^-) present. When a specific inorganic component is extracted in the form of crystal, its ionic concentration is maintained near supersaturation. However, concentration of other ions increases continuously, resulting in reaching supersaturation of other inorganic components. This results in a reduction of selective separation capacity in MDC process. Hence, techniques for simultaneous and selective crystallization should be developed to improve the MDC performance. Simultaneous treatment of multi component solution (real challenging feed solution) should be developed and investigated. In case of conventional crystallization process, the application of multi-crystallizer in same line can be option for simultaneous recovery of each crystal separately. In F-SMDC, a concept of multi-vertical layered portion can be considered for selective crystallization. In the current study on F-SMDC, two portions (top and bottom) were used. The multi-vertical layered portion suggested refers to additional installation of multiple portions vertically. Each portion can play a role of individual crystallizer to crystallize different inorganic component separately. The seed crystal technology can be used for making favorable condition for crystal growth.

- The adverse issues in conventional MDC in terms of energy consumption can be addressed by applying the adaptive crystallization techniques. In MDC process, the combination with cooling crystallization technique has weakness in terms of consumption of high heat energy and recovering negative temperature-solubility salt. It leads to low efficiency. To overcome this, the reaction crystallization and drowning-out crystallization techniques may be used instead of cooling crystallization because these do not need a control of solution temperature for reaching supersaturation. It also improves energy efficiency in MDC compared to conventional simultaneous MDC process with cooling crystallization.
- The shape and dimension of the reactor in F-SMDC process is essential factor as it influences the formation of CG and TG and its overall performance. The CG/TG formation can be improved by enhancing the downward stream of concentrated feed solution from the membrane surface to the bottom portion. There are two strategies to achieve this: (i) modification of the shape and the dimension of each portion (top and bottom) of the reactor, and (ii) the partition shape. The top portion of F-SMDC reactor should be heated up only for MD operation. A lager dimension of the top portion causes higher energy consumption to heat the bulk solution. Moreover, the reduction of the dimension of the top portion leads to the reduction of diffusion of concentrated feed solution from the membrane surface to bulk solution at the top portion. It enhances the formation of a concentrated feed solution layer near the membrane boundary layer, resulting in the stimulation of its downward movement. In addition, a faster concentration rate can be obtained. This leads to a faster reaching of the supersaturation degree in the bottom portion. On the other hand, a larger dimension of the bottom portion can provide higher possibility of contact between crystalline (concentrated) solution and crystal formed, resulting in an increase of crystal growth.

- The modification of partition shape is another option for enhancing the downward stream of concentrated solution.
- The periodic extraction of crystals formed is necessary for a continuous operation of F-SMDC. The bottom portion plays a role for storage of concentrated feed solution. If it is filled up by crystals, there will be no space for the concentrated feed solution. This in turn will result in the increase of concentration at the top portion. It is thus important to preserve enough space at the bottom portion.
- The combination of F-SMDC and valuable resource adsorption can improve the process operational and economic efficiency because it causes three production stream: fresh water, crystal production and extraction of valuable resource ion. Higher concentration at the bottom portion of reactor in F-SMDC provides favorable condition for adsorption. The optimization of design and parameter should be studied.

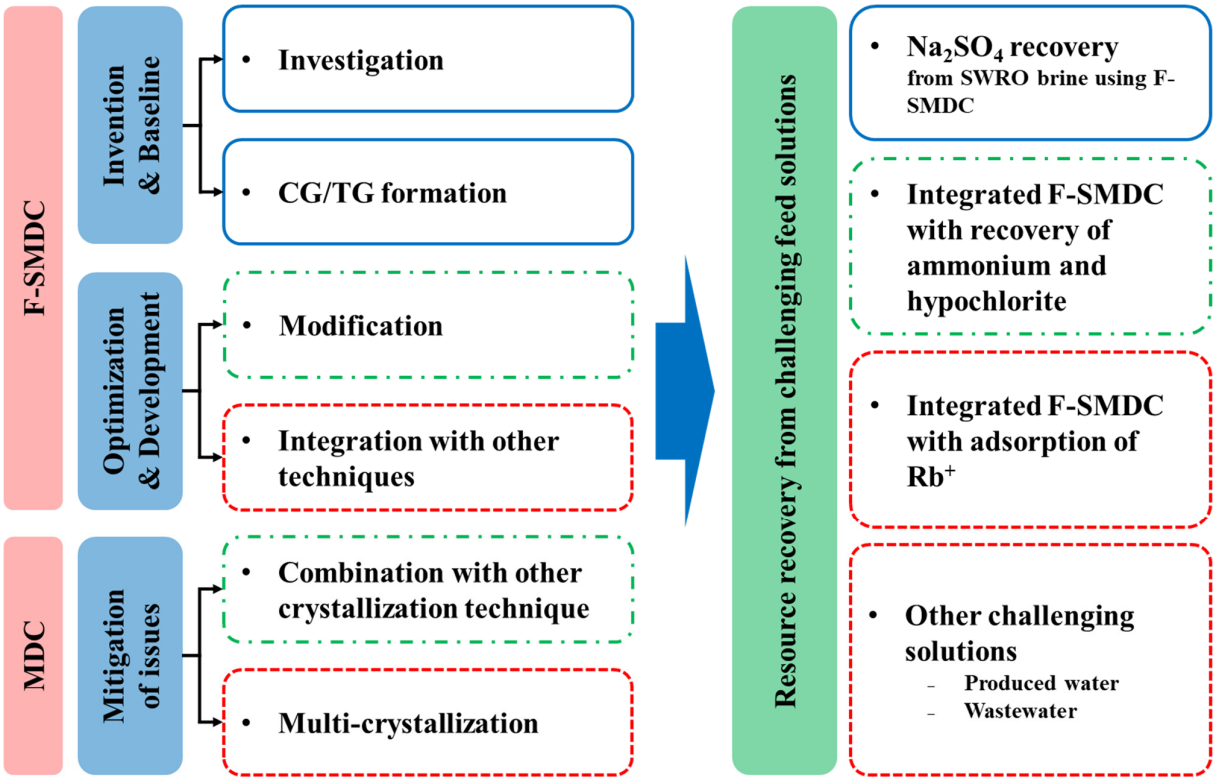

Figure 10-1. Diagram of the research scope and future research gaps to be addressed: research completed (——), on-going research (—·—), and future research (------).

REFERENCES

Å, S.B.L. & C., R.Å.K. 1992, 'Semibatch reaction crystallization of benzoic acid', *AIChE Journal*, vol. 38, no. 3, pp. 328-42.

Abdul-Wahab, S.A. & Al-Weshahi, M.A. 2009, 'Brine Management: Substituting Chlorine with On-Site Produced Sodium Hypochlorite for Environmentally Improved Desalination Processes', *Water Resources Management*, vol. 23, no. 12, pp. 2437-54.

Abdulwahab, M., Majeed, N.S. & Issa, S.Y. 2013, 'Water recovery from brine solution by forward osmosis process', *J. Eng*, vol. 19, no. 8, pp. 1019-30.

Abu Bakar, M.R., Nagy, Z.K., Saleemi, A.N. & Rielly, C.D. 2009, 'The Impact of Direct Nucleation Control on Crystal Size Distribution in Pharmaceutical Crystallization Processes', *Crystal Growth & Design*, vol. 9, no. 3, pp. 1378-84.

Adler, S., Beaver, E., Bryan, P., Robinson, S. & Watson, J. 2000, *Vision 2020: 2000 separations roadmap*, EERE Publication and Product Library.

Afrasiabi, N. & Shahbazali, E. 2011, 'RO brine treatment and disposal methods', *Desalination and Water Treatment*, vol. 35, no. 1-3, pp. 39-53.

Ahmed, M., Shayya, W.H., Hoey, D., Mahendran, A., Morris, R. & Al-Handaly, J. 2000, 'Use of evaporation ponds for brine disposal in desalination plants', *Desalination*, vol. 130, no. 2, pp. 155-68.

Akrap, M., Kuzmanić, N. & Prlić-Kardum, J. 2010, 'Effect of mixing on the crystal size distribution of borax decahydrate in a batch cooling crystallizer', *Journal of Crystal Growth*, vol. 312, no. 24, pp. 3603-8.

Ali, A., Macedonio, F., Drioli, E., Aljlil, S. & Alharbi, O.A. 2013, 'Experimental and theoretical evaluation of temperature polarization phenomenon in direct contact membrane distillation', *Chemical Engineering Research and Design*, vol. 91, no. 10, pp. 1966-77.

Ali, A., Quist-Jensen, C.A., Drioli, E. & Macedonio, F. 2017, 'Evaluation of integrated microfiltration and membrane distillation/crystallization processes for produced water treatment', *Desalination*, vol. 434, pp. 161-8.

Ali, A., Quist-Jensen, C.A., Macedonio, F. & Drioli, E. 2015, 'Application of Membrane Crystallization for Minerals' recovery from produced water', *Membranes*, vol. 5, pp. 772-92.

Alkhudhiri, A., Darwish, N. & Hilal, N. 2012, 'Membrane distillation: A comprehensive review', *Desalination*, vol. 287, pp. 2-18.

Allred, A.L. 1961, 'Electronegativity values from thermochemical data', *Journal of Inorganic and Nuclear Chemistry*, vol. 17, no. 3, pp. 215-21.

Anisi, F., Thomas, K.M. & Kramer, H.J.M. 2017, 'Membrane-assisted crystallization: Membrane characterization, modelling and experiments', *Chemical Engineering Science*, vol. 158, pp. 277-86.

Azimi, G. & Papangelakis, V.G. 2010, 'The solubility of gypsum and anhydrite in simulated laterite pressure acid leach solutions up to 250 °C', *Hydrometallurgy*, vol. 102, no. 1–4, pp. 1-13.

Barata, P.A. & Serrano, M.L. 1998, 'Salting-out precipitation of potassium dihydrogen phosphate (KDP): IV. Characterisation of the final product', *Journal of Crystal Growth*, vol. 194, no. 1, pp. 109-18.

Bayindirli, L. 1992, 'MATHEMATICAL ANALYSIS of VARIATION of DENSITY and VISCOSITY of APPLE JUICE WITH TEMPERATURE and CONCENTRATION', *Journal of Food Processing and Preservation*, vol. 16, no. 1, pp. 23-8.

Bayindirli, L. 1993, 'DENSITY and VISCOSITY of GRAPE JUICE AS A FUNCTION of CONCENTRATION and TEMPERATURE', *Journal of Food Processing and Preservation*, vol. 17, no. 2, pp. 147-51.

Beltrán, J.M.n. 1999, 'Irrigation with saline water: benefits and environmental impact', *Agricultural water management*, vol. 40, no. 2-3, pp. 183-94.

Berry, D.A., Dye, S.R. & Ng, K.M. 1997, 'Synthesis of drowning-out crystallization-based separations', *AIChE Journal*, vol. 43, no. 1, pp. 91-103.

Bharmoria, P., Gehlot, P.S., Gupta, H. & Kumar, A. 2014, 'Temperature-Dependent Solubility Transition of Na2SO4 in Water and the Effect of NaCl Therein: Solution Structures and Salt Water Dynamics', *The Journal of Physical Chemistry B*, vol. 118, no. 44, pp. 12734-42.

Bodalal, A., Zhang, J.S. & Plett, E.G. 2000, 'A method for measuring internal diffusion and equilibrium partition coefficients of volatile organic compounds for building materials', *Building and Environment*, vol. 35, no. 2, pp. 101-10.

Boeyens Jan, C.A. 2008, 'The Periodic Electronegativity Table', *Zeitschrift für Naturforschung B*, vol. 63, no 2, p. 199, viewed 2017-04-18t14:08:00.348+02:00, <//www.degruyter.com/view/j/znb.2008.63.issue-2/znb-2008-0214/znb-2008-0214.xml>.

Bolter, E., Turekian, K.K. & Schutz, D.F. 1964, 'The distribution of rubidium, cesium and barium in the oceans', *Geochimica et Cosmochimica Acta*, vol. 28, no. 9, pp. 1459-66.

Bouchrit, R., Boubakri, A., Hafiane, A. & Bouguecha, S.A.-T. 2015, 'Direct contact membrane distillation: Capability to treat hyper-saline solution', *Desalination*, vol. 376, pp. 117-29.

Bush, J.A., Vanneste, J. & Cath, T.Y. 2016, 'Membrane distillation for concentration of hypersaline brines from the Great Salt Lake: Effects of scaling and fouling on performance, efficiency, and salt rejection', *Separation and Purification Technology*, vol. 170, pp. 78-91.

Çakmakce, M., Kayaalp, N. & Koyuncu, I. 2008, 'Desalination of produced water from oil production fields by membrane processes', *Desalination*, vol. 222, no. 1, pp. 176-86.

Casson, L. & Bess, J. 2002, *Conversion to on-site sodium hypochlorite generation: water and wastewater applications*, CRC Press.

Cath, T.Y., Adams, V.D. & Childress, A.E. 2004, 'Experimental study of desalination using direct contact membrane distillation: a new approach to flux enhancement', *Journal of Membrane Science*, vol. 228, no. 1, pp. 5-16.

Chabanon, E., Mangin, D. & Charcosset, C. 2016, 'Membranes and crystallization processes: State of the art and prospects', *Journal of Membrane Science*, vol. 509, pp. 57-67.

Chae, H.-R., Lee, J., Lee, C.-H., Kim, I.-C. & Park, P.-K. 2015, 'Graphene oxide-embedded thin-film composite reverse osmosis membrane with high flux, anti-biofouling, and chlorine resistance', *Journal of Membrane Science*, vol. 483, pp. 128-35.

Chelme-Ayala, P., Smith, D.W. & El-Din, M.G. 2009, 'Membrane concentrate management options: a comprehensive critical reviewA paper submitted to the Journal of Environmental Engineering and Science', *Canadian Journal of Civil Engineering*, vol. 36, no. 6, pp. 1107-19.

Chen, G., Lu, Y., Krantz, W.B., Wang, R. & Fane, A.G. 2014, 'Optimization of operating conditions for a continuous membrane distillation crystallization process with zero salty water discharge', *Journal of Membrane Science*, vol. 450, pp. 1-11.

Chernyshov, M.N., Meindersma, G.W. & de Haan, A.B. 2003, 'Modelling temperature and salt concentration distribution in membrane distillation feed channel', *Desalination*, vol. 157, no. 1, pp. 315-24.

Choi, Y., Naidu, G., Jeong, S., Lee, S. & Vigneswaran, S., 'Fractional-submerged membrane distillation crystallizer (F-SMDC) for treatment of high salinity solution', *Desalination*.

Choi, Y., Naidu, G., Jeong, S., Lee, S. & Vigneswaran, S. 2018a, 'Effect of chemical and physical factors on the crystallization of calcium sulfate in seawater reverse osmosis brine', *Desalination*, vol. 426, pp. 78-87.

Choi, Y., Naidu, G., Jeong, S., Lee, S. & Vigneswaran, S. 2018b, 'Fractional-submerged membrane distillation crystallizer (F-SMDC) for treatment of high salinity solution', *Desalination*, vol. 440, pp. 59-67.

Choi, Y., Naidu, G., Jeong, S., Vigneswaran, S., Lee, S., Wang, R. & Fane, A.G. 2017, 'Experimental comparison of submerged membrane distillation configurations for concentrated brine treatment', *Desalination*, vol. 420, pp. 54-62.

Choi, Y., Vigneswaran, S. & Lee, S. 2016, 'Evaluation of fouling potential and power density in pressure retarded osmosis (PRO) by fouling index', *Desalination*, vol. 389, pp. 215-23.

Creusen, R., van Medevoort, J., Roelands, M., van Renesse van Duivenbode, A., Hanemaaijer, J.H. & van Leerdam, R. 2013, 'Integrated membrane distillation–crystallization: Process design and cost estimations for seawater treatment and fluxes of single salt solutions', *Desalination*, vol. 323, pp. 8-16.

Creusen, R.J.M., van Medevoort, J., Roelands, C.P.M. & Duivenbode, J.A.D.v.R.v. 2012, 'Brine Treatment by a Membrane Distillation-crystallization (MDC) Process', *Procedia Engineering*, vol. 44, no. Supplement C, pp. 1756-9.

Curcio, E., Criscuoli, A. & Drioli, E. 2001, 'Membrane Crystallizers', *Industrial & Engineering Chemistry Research*, vol. 40, no. 12, pp. 2679-84.

Curcio, E. & Drioli, E. 2005, 'Membrane Distillation and Related Operations—A Review', *Separation & Purification Reviews*, vol. 34, no. 1, pp. 35-86.

Curcio, E., Ji, X., Di Profio, G., Sulaiman, A.O., Fontananova, E. & Drioli, E. 2010, 'Membrane distillation operated at high seawater concentration factors: Role of the membrane on CaCO3 scaling in presence of humic acid', *Journal of Membrane Science*, vol. 346, no. 2, pp. 263-9.

Curcio, E., Ji, X., Quazi, A.M., Barghi, S., Di Profio, G., Fontananova, E., Macleod, T. & Drioli, E. 2010, 'Hybrid nanofiltration–membrane crystallization system for the treatment of sulfate wastes', *Journal of Membrane Science*, vol. 360, no. 1, pp. 493-8.

Dammak, I., Neves, M., Isoda, H., Sayadi, S. & Nakajima, M. 2016, 'Recovery of polyphenols from olive mill wastewater using drowning-out crystallization based separation process', *Innovative Food Science & Emerging Technologies*, vol. 34, pp. 326-35.

Deng, L., Liu, Y., Huang, T. & Sun, T. 2016, 'Fluoride removal by induced crystallization using fluorapatite/calcite seed crystals', *Chemical Engineering Journal*, vol. 287, pp. 83-91.

Di Profio, G., Curcio, E. & Drioli, E. 2005, 'Trypsin crystallization by membrane-based techniques', *Journal of Structural Biology*, vol. 150, no. 1, pp. 41-9.

Ding, D., Zhao, Y., Yang, S., Shi, W., Zhang, Z., Lei, Z. & Yang, Y. 2013, 'Adsorption of cesium from aqueous solution using agricultural residue – Walnut shell: Equilibrium, kinetic and thermodynamic modeling studies', *Water Research*, vol. 47, no. 7, pp. 2563-71.

Ding, Z., Liu, L., Liu, Z. & Ma, R. 2010, 'Fouling resistance in concentrating TCM extract by direct contact membrane distillation', *Journal of Membrane Science*, vol. 362, no. 1, pp. 317-25.

Drioli, E., Criscuoli, A. & Curcio, E. 2002, 'Integrated membrane operations for seawater desalination', *Desalination*, vol. 147, no. 1, pp. 77-81.

Drioli, E., Curcio, E., Criscuoli, A. & Profio, G.D. 2004, 'Integrated system for recovery of CaCO3, NaCl and MgSO4·7H2O from nanofiltration retentate', *Journal of Membrane Science*, vol. 239, no. 1, pp. 27-38.

Drioli, E., Curcio, E., Di Profio, G., Macedonio, F. & Criscuoli, A. 2006, 'Integrating Membrane Contactors Technology and Pressure-Driven Membrane Operations for Seawater Desalination: Energy, Exergy and Costs Analysis', *Chemical Engineering Research and Design*, vol. 84, no. 3, pp. 209-20.

Drioli, E., Di Profio, G. & Curcio, E. 2012, 'Progress in membrane crystallization', *Current Opinion in Chemical Engineering*, vol. 1, no. 2, pp. 178-82.

Drioli, E., Wu, Y. & Calabro, V. 1987, 'Membrane distillataion in the treatment of aqueous solutions', *Journal of Membrane Science*, vol. 33, no. 3, pp. 277-84.

Duong, H.C., Cooper, P., Nelemans, B., Cath, T.Y. & Nghiem, L.D. 2016, 'Evaluating energy consumption of air gap membrane distillation for seawater desalination at pilot scale level', *Separation and Purification Technology*, vol. 166, pp. 55-62.

Duong, H.C., Duke, M., Gray, S., Cooper, P. & Nghiem, L.D. 2016, 'Membrane scaling and prevention techniques during seawater desalination by air gap membrane distillation', *Desalination*, vol. 397, pp. 92-100.

Edwie, F. & Chung, T.-S. 2012, 'Development of hollow fiber membranes for water and salt recovery from highly concentrated brine via direct contact membrane distillation and crystallization', *Journal of Membrane Science*, vol. 421–422, pp. 111-23.

Edwie, F. & Chung, T.-S. 2013, 'Development of simultaneous membrane distillation–crystallization (SMDC) technology for treatment of saturated brine', *Chemical Engineering Science*, vol. 98, pp. 160-72.

Effler, S.W., Brooks, C.M., Auer, M.T. & Doerr, S.M. 1990, 'Free Ammonia and Toxicity Criteria in a Polluted Urban Lake', *Research Journal of the Water Pollution Control Federation*, vol. 62, no. 6, pp. 771-9.

El-Bourawi, M.S., Ding, Z., Ma, R. & Khayet, M. 2006, 'A framework for better understanding membrane distillation separation process', *Journal of Membrane Science*, vol. 285, no. 1, pp. 4-29.

El-Dessouky, H.T. & Ettouney, H.M. 2002, *Fundamentals of salt water desalination*, Elsevier.

Fakhru'l-Razi, A., Pendashteh, A., Abdullah, L.C., Biak, D.R.A., Madaeni, S.S. & Abidin, Z.Z. 2009, 'Review of technologies for oil and gas produced water treatment', *Journal of Hazardous Materials*, vol. 170, no. 2, pp. 530-51.

Fath, H., Sadik, A. & Mezher, T. 2013, 'Present and Future Trend in the Production and Energy Consumption of Desalinated Water in GCC Countries', *Int. J. of Thermal & Environmental Engineering*, vol. 5, no. 2, pp. 155-65.

Francis, L., Ghaffour, N., Al-Saadi, A.S. & Amy, G.L. 2015, 'Submerged membrane distillation for seawater desalination', *Desalination and Water Treatment*, vol. 55, no. 10, pp. 2741-6.

Gabelman, A. & Hwang, S.-T. 1999, 'Hollow fiber membrane contactors', *Journal of Membrane Science*, vol. 159, no. 1, pp. 61-106.

García-Payo, M.C., Izquierdo-Gil, M.A. & Fernández-Pineda, C. 2000, 'Wetting Study of Hydrophobic Membranes via Liquid Entry Pressure Measurements with Aqueous Alcohol Solutions', *Journal of Colloid and Interface Science*, vol. 230, no. 2, pp. 420-31.

Garrett, D.E. 1996, 'Sylvinite, Other Potash Ore Processing', in D.E. Garrett (ed.), *Potash: Deposits, Processing, Properties and Uses*, Springer Netherlands, Dordrecht, pp. 325-402.

Gianluca, D.P., Carmen, S., Antonella, C., Efrem, C. & Enrico, D. 2009, 'Antisolvent membrane crystallization of pharmaceutical compounds', *Journal of Pharmaceutical Sciences*, vol. 98, no. 12, pp. 4902-13.

Giwa, A., Dufour, V., Al Marzooqi, F., Al Kaabi, M. & Hasan, S.W. 2017, 'Brine management methods: Recent innovations and current status', *Desalination*, vol. 407, pp. 1-23.

Glowa, K., Arocena, J. & Massicotte, H. 2003, 'Extraction of potassium and/or magnesium from selected soil minerals by Piloderma', *Geomicrobiology Journal*, vol. 20, no. 2, pp. 99-111.

Goh, S., Zhang, J., Liu, Y. & Fane, A.G. 2013, 'Fouling and wetting in membrane distillation (MD) and MD-bioreactor (MDBR) for wastewater reclamation', *Desalination*, vol. 323, pp. 39-47.

Gohil, J.M. & Suresh, A.K. 2017, 'Chlorine attack on reverse osmosis membranes: Mechanisms and mitigation strategies', *Journal of Membrane Science*, vol. 541, pp. 108-26.

Gostoli, C. & Sarti, G.C. 1989, 'Separation of liquid mixtures by membrane distillation', *Journal of Membrane Science*, vol. 41, pp. 211-24.

Greenlee, L.F., Testa, F., Lawler, D.F., Freeman, B.D. & Moulin, P. 2010, 'Effect of antiscalants on precipitation of an RO concentrate: Metals precipitated and particle characteristics for several water compositions', *Water Research*, vol. 44, no. 8, pp. 2672-84.

Greenlee, L.F., Testa, F., Lawler, D.F., Freeman, B.D. & Moulin, P. 2011, 'Effect of antiscalant degradation on salt precipitation and solid/liquid separation of RO concentrate', *Journal of Membrane Science*, vol. 366, no. 1-2, pp. 48-61.

Gryta, M. 2002, 'Concentration of NaCl solution by membrane distillation integrated with crystallization', *Separation Science and Technology*, vol. 37, no. 15, pp. 3535-58.

Gryta, M. 2005, 'Long-term performance of membrane distillation process', *Journal of Membrane Science*, vol. 265, no. 1, pp. 153-9.

Gryta, M. 2016, 'The study of performance of polyethylene chlorinetrifluoroethylene membranes used for brine desalination by membrane distillation', *Desalination*, vol. 398, pp. 52-63.

Gryta, M. & Barancewicz, M. 2010, 'Influence of morphology of PVDF capillary membranes on the performance of direct contact membrane distillation', *Journal of Membrane Science*, vol. 358, no. 1, pp. 158-67.

Guan, G., Wang, R., Wicaksana, F., Yang, X. & Fane, A.G. 2012, 'Analysis of Membrane Distillation Crystallization System for High Salinity Brine Treatment with Zero Discharge Using Aspen Flowsheet Simulation', *Industrial & Engineering Chemistry Research*, vol. 51, no. 41, pp. 13405-13.

Guan, G., Yang, X., Wang, R., Field, R. & Fane, A.G. 2014, 'Evaluation of hollow fiber-based direct contact and vacuum membrane distillation systems using aspen process simulation', *Journal of Membrane Science*, vol. 464, pp. 127-39.

Gugliuzza, A., Aceto, M.C. & Drioli, E. 2009, 'Interactive functional poly(vinylidene fluoride) membranes with modulated lysozyme affinity: a promising class of new interfaces for contactor crystallizers', *Polymer International*, vol. 58, no. 12, pp. 1452-64.

Gupta, V.K., Agarwal, S. & Saleh, T.A. 2011, 'Synthesis and characterization of alumina-coated carbon nanotubes and their application for lead removal', *Journal of Hazardous Materials*, vol. 185, no. 1, pp. 17-23.

Haghtalab, A. & Badizad, M.H. 2016, 'Solubility of gypsum in aqueous NaCl + K2SO4 solution using calcium ion selective electrode-investigation of ionic interactions', *Fluid Phase Equilibria*, vol. 409, pp. 341-53.

Hardwick, L.L., Jones, M.R., Brautbar, N. & Lee, D.B. 1991, 'Magnesium absorption: mechanisms and the influence of vitamin D, calcium and phosphate', *The Journal of nutrition*, vol. 121, no. 1, pp. 13-23.

Hash, J. & Okorafor, O.C. 2008, 'Crystal size distribution (CSD) of batch salting-out crystallization process for sodium sulfate', *Chemical Engineering and Processing: Process Intensification*, vol. 47, no. 4, pp. 622-32.

He, F., Sirkar, K.K. & Gilron, J. 2009, 'Studies on scaling of membranes in desalination by direct contact membrane distillation: CaCO3 and mixed CaCO3/CaSO4 systems', *Chemical Engineering Science*, vol. 64, no. 8, pp. 1844-59.

Hermanto, M.W., Chiu, M.-S., Woo, X.-Y. & Braatz, R.D. 2007, 'Robust optimal control of polymorphic transformation in batch crystallization', *AIChE Journal*, vol. 53, no. 10, pp. 2643-50.

Ho, J.S., Ma, Z., Qin, J., Sim, S.H. & Toh, C.-S. 2015, 'Inline coagulation–ultrafiltration as the pretreatment for reverse osmosis brine treatment and recovery', *Desalination*, vol. 365, pp. 242-9.

Holaň, J., Ridvan, L., Billot, P. & Štěpánek, F. 2015, 'Design of co-crystallization processes with regard to particle size distribution', *Chemical Engineering Science*, vol. 128, pp. 36-43.

Holmbäck, X. & Rasmuson, Å.C. 1999, 'Size and morphology of benzoic acid crystals produced by drowning-out crystallisation', *Journal of Crystal Growth*, vol. 198-199, pp. 780-8.

Hou, D., Wang, Z., Li, G., Fan, H., Wang, J. & Huang, H. 2015, 'Ultrasonic assisted direct contact membrane distillation hybrid process for membrane scaling mitigation', *Desalination*, vol. 375, pp. 33-9.

Huang, H., Xiao, D., Pang, R., Han, C. & Ding, L. 2014, 'Simultaneous removal of nutrients from simulated swine wastewater by adsorption of modified zeolite combined with struvite crystallization', *Chemical Engineering Journal*, vol. 256, pp. 431-8.

Hutnik, N., Kozik, A., Mazienczuk, A., Piotrowski, K., Wierzbowska, B. & Matynia, A. 2013, 'Phosphates (V) recovery from phosphorus mineral fertilizers industry wastewater by continuous struvite reaction crystallization process', *Water Research*, vol. 47, no. 11, pp. 3635-43.

Jeong, S., Naidu, G., Vollprecht, R., Leiknes, T. & Vigneswaran, S. 2016, 'In-depth analyses of organic matters in a full-scale seawater desalination plant and an autopsy of reverse osmosis membrane', *Separation and Purification Technology*, vol. 162, pp. 171-9.

Jeppesen, T., Shu, L., Keir, G. & Jegatheesan, V. 2009, 'Metal recovery from reverse osmosis concentrate', *Journal of Cleaner Production*, vol. 17, no. 7, pp. 703-7.

Jermann, D., Pronk, W., Meylan, S. & Boller, M. 2007, 'Interplay of different NOM fouling mechanisms during ultrafiltration for drinking water production', *Water Research*, vol. 41, no. 8, pp. 1713-22.

Ji, X., Curcio, E., Al Obaidani, S., Di Profio, G., Fontananova, E. & Drioli, E. 2010, 'Membrane distillation-crystallization of seawater reverse osmosis brines', *Separation and Purification Technology*, vol. 71, no. 1, pp. 76-82.

Jia, F., Li, J. & Wang, J. 2017, 'Recovery of boric acid from the simulated radioactive wastewater by vacuum membrane distillation crystallization', *Annals of Nuclear Energy*, vol. 110, no. Supplement C, pp. 1148-55.

Jiang, X., Lu, D., Xiao, W., Ruan, X., Fang, J. & He, G. 2016, 'Membrane assisted cooling crystallization: Process model, nucleation, metastable zone, and crystal size distribution', *AIChE Journal*, vol. 62, no. 3, pp. 829-41.

Jones, K.L. & O'Melia, C.R. 2000, 'Protein and humic acid adsorption onto hydrophilic membrane surfaces: effects of pH and ionic strength', *Journal of Membrane Science*, vol. 165, no. 1, pp. 31-46.

Jucker, C. & Clark, M.M. 1994, 'Adsorption of aquatic humic substances on hydrophobic ultrafiltration membranes', *Journal of Membrane Science*, vol. 97, no. Supplement C, pp. 37-52.

Julian, H., Meng, S., Li, H., Ye, Y. & Chen, V. 2016, 'Effect of operation parameters on the mass transfer and fouling in submerged vacuum membrane distillation crystallization (VMDC) for inland brine water treatment', *Journal of Membrane Science*, vol. 520, pp. 679-92.

Julian, H., Ye, Y., Li, H. & Chen, V. 2018, 'Scaling mitigation in submerged vacuum membrane distillation and crystallization (VMDC) with periodic air-backwash', *Journal of Membrane Science*, vol. 547, pp. 19-33.

Karidakis, T., Agatzini-Leonardou, S. & Neou-Syngouna, P. 2005, 'Removal of magnesium from nickel laterite leach liquors by chemical precipitation using calcium hydroxide and the potential use of the precipitate as a filler material', *Hydrometallurgy*, vol. 76, no. 1-2, pp. 105-14.

Katzir, L., Volkmann, Y., Daltrophe, N., Korngold, E., Mesalem, R., Oren, Y. & Gilron, J. 2010, 'WAIV-Wind aided intensified evaporation for brine volume reduction and generating mineral byproducts', *Desalination and Water Treatment*, vol. 13, no. 1-3, pp. 63-73.

Kezia, K., Lee, J., Weeks, M. & Kentish, S. 2015, 'Direct contact membrane distillation for the concentration of saline dairy effluent', *Water Research*, vol. 81, pp. 167-77.

Khaing, T.-H., Li, J., Li, Y., Wai, N. & Wong, F.-s. 2010, 'Feasibility study on petrochemical wastewater treatment and reuse using a novel submerged membrane distillation bioreactor', *Separation and Purification Technology*, vol. 74, no. 1, pp. 138-43.

Khayet, M. 2011, 'Membranes and theoretical modeling of membrane distillation: A review', *Advances in Colloid and Interface Science*, vol. 164, no. 1, pp. 56-88.

Kile, V. & Ajy, G. 2005, 'Disposal of membrane reject water at four Florida water treatment facilities', pp. 6-9.

Kim, J., Kim, J. & Hong, S. 2017, 'Recovery of water and minerals from shale gas produced water by membrane distillation crystallization', *Water Research*, vol. 129, pp. 447-59.

Kim, J., Kwon, H., Lee, S., Lee, S. & Hong, S. 2016, 'Membrane distillation (MD) integrated with crystallization (MDC) for shale gas produced water (SGPW) treatment', *Desalination*.

Kim, J., Kwon, H., Lee, S., Lee, S. & Hong, S. 2017, 'Membrane distillation (MD) integrated with crystallization (MDC) for shale gas produced water (SGPW) treatment', *Desalination*, vol. 403, pp. 172-8.

Kimura, S., Nakao, S.-I. & Shimatani, S.-I. 1987, 'Transport phenomena in membrane distillation', *Journal of Membrane Science*, vol. 33, no. 3, pp. 285-98.

Lawson, K.W. & Lloyd, D.R. 1997, 'Membrane distillation', *Journal of Membrane Science*, vol. 124, no. 1, pp. 1-25.

Lee, S., Choi, J.-S. & Lee, C.-H. 2009, 'Behaviors of dissolved organic matter in membrane desalination', *Desalination*, vol. 238, no. 1–3, pp. 109-16.

Lee, S., Choi, J., Park, Y.-G., Shon, H., Ahn, C.H. & Kim, S.-H. 2018, 'Hybrid desalination processes for beneficial use of reverse osmosis brine: Current status and future prospects', *Desalination*.

Lee, S., Kim, J. & Lee, C.-H. 1999, 'Analysis of CaSO4 scale formation mechanism in various nanofiltration modules', *Journal of Membrane Science*, vol. 163, no. 1, pp. 63-74.

Li, B. & Sirkar, K.K. 2005, 'Novel membrane and device for vacuum membrane distillation-based desalination process', *Journal of Membrane Science*, vol. 257, no. 1–2, pp. 60-75.

Li, C.Y., Li, W.G., Wang, G.Z. & Wang, K. 2010, 'The Preparation and the Research of Copper-Chelex Chitosan for Removal Ammonia-Nitrogen from the Drinking Water', *Advanced Materials Research*, vol. 113-116, pp. 1166-9.

Li, L. & Sirkar, K.K. 2017, 'Studies in vacuum membrane distillation with flat membranes', *Journal of Membrane Science*, vol. 523, pp. 225-34.

Lian, L., Guo, L. & Guo, C. 2009, 'Adsorption of Congo red from aqueous solutions onto Ca-bentonite', *Journal of Hazardous Materials*, vol. 161, no. 1, pp. 126-31.

Linnikov, O.D. 2000, 'Investigation of the initial period of sulphate scale formation Part 2. Kinetics of calcium sulphate crystal growth at its crystallization on a heat-exchange surface', *Desalination*, vol. 128, no. 1, pp. 35-46.

Liu, J., Tennessen, E., Miao, J., Huang, Y., Rondinelli, J.M. & Heinz, H. 2018, 'Understanding Chemical Bonding in Alloys and the Representation in Atomistic Simulations', *The Journal of Physical Chemistry C*, vol. 122, no. 26, pp. 14996-5009.

Liu, S., Papageorgiou, L.G. & Gikas, P. 2012, 'Integrated Management of Non-conventional Water Resources in Anhydrous Islands', *Water Resources Management*, vol. 26, no. 2, pp. 359-75.

Loganathan, P., Naidu, G. & Vigneswaran, S. 2017, 'Mining valuable minerals from seawater: a critical review', *Environmental Science: Water Research & Technology*, vol. 3, no. 1, pp. 37-53.

Lokare, O.R., Tavakkoli, S., Wadekar, S., Khanna, V. & Vidic, R.D. 2017, 'Fouling in direct contact membrane distillation of produced water from unconventional gas extraction', *Journal of Membrane Science*, vol. 524, pp. 493-501.

Lu, H., Wang, J., Wang, T., Wang, N., Bao, Y. & Hao, H. 2017, 'Crystallization techniques in wastewater treatment: An overview of applications', *Chemosphere*, vol. 173, pp. 474-84.

Luis, P., Van Aubel, D. & Van der Bruggen, B. 2013, 'Technical viability and exergy analysis of membrane crystallization: Closing the loop of CO2 sequestration', *International Journal of Greenhouse Gas Control*, vol. 12, pp. 450-9.

Macedonio, F., Curcio, E. & Drioli, E. 2007, 'Integrated membrane systems for seawater desalination: energetic and exergetic analysis, economic evaluation, experimental study', *Desalination*, vol. 203, no. 1, pp. 260-76.

Macedonio, F. & Drioli, E. 2010, 'Hydrophobic membranes for salts recovery from desalination plants', *Desalination and Water Treatment*, vol. 18, no. 1-3, pp. 224-34.

Macedonio, F., Quist-Jensen, C.A., Al-Harbi, O., Alromaih, H., Al-Jlil, S.A., Al Shabouna, F. & Drioli, E. 2013, 'Thermodynamic modeling of brine and its use in membrane crystallizer', *Desalination*, vol. 323, pp. 83-92.

Mansourizadeh, A., Ismail, A.F. & Matsuura, T. 2010, 'Effect of operating conditions on the physical and chemical CO2 absorption through the PVDF hollow fiber membrane contactor', *Journal of Membrane Science*, vol. 353, no. 1, pp. 192-200.

Marshall, W.L. 1967, 'Aqueous systems at high temperature. XX. Dissociation constant and thermodynamic functions for magnesium sulfate to 200.degree', *The Journal of Physical Chemistry*, vol. 71, no. 11, pp. 3584-8.

Martínez-Díez, L. & Vázquez-González, M.I. 1999, 'Temperature and concentration polarization in membrane distillation of aqueous salt solutions', *Journal of Membrane Science*, vol. 156, no. 2, pp. 265-73.

Masindi, V., Osman, M.S. & Abu-Mahfouz, A.M. 2017, 'Integrated treatment of acid mine drainage using BOF slag, lime/soda ash and reverse osmosis (RO): Implication for the production of drinking water', *Desalination*, vol. 424, pp. 45-52.

Meng, S., Hsu, Y.-C., Ye, Y. & Chen, V. 2015, 'Submerged membrane distillation for inland desalination applications', *Desalination*, vol. 361, pp. 72-80.

Meng, S., Ye, Y., Mansouri, J. & Chen, V. 2015, 'Crystallization behavior of salts during membrane distillation with hydrophobic and superhydrophobic capillary membranes', *Journal of Membrane Science*, vol. 473, pp. 165-76.

Mericq, J.-P., Laborie, S. & Cabassud, C. 2010, 'Vacuum membrane distillation of seawater reverse osmosis brines', *Water Research*, vol. 44, no. 18, pp. 5260-73.

Mezher, T., Fath, H., Abbas, Z. & Khaled, A. 2011, 'Techno-economic assessment and environmental impacts of desalination technologies', *Desalination*, vol. 266, no. 1–3, pp. 263-73.

Mickley, M. 2001, *Membrane Concentrate Disposal: Practices and Regulation, Final Report*, US Department of the Interior, Bureau of Reclamation, Technical Service Center, Water Treatment Engineering and Research Group.

Min, M.-k., Cho, J., Cho, K. & Kim, H. 2000, 'Particle size and alloying effects of Pt-based alloy catalysts for fuel cell applications', *Electrochimica Acta*, vol. 45, no. 25, pp. 4211-7.

Mitchell, N.A. & Frawley, P.J. 2010, 'Nucleation kinetics of paracetamol–ethanol solutions from metastable zone widths', *Journal of Crystal Growth*, vol. 312, no. 19, pp. 2740-6.

Miyamoto, S. & Pingitore, N. 1992, 'Predicting calcium and magnesium precipitation in saline solutions following evaporation', *Soil Science Society of America Journal*, vol. 56, no. 6, pp. 1767-75.

Mohammadesmaeili, F., Badr, M.K., Abbaszadegan, M. & Fox, P. 2010, 'Byproduct Recovery from Reclaimed Water Reverse Osmosis Concentrate Using Lime and Soda-Ash Treatment', *Water Environment Research*, vol. 82, no. 4, pp. 342-50.

Morillo, J., Usero, J., Rosado, D., El Bakouri, H., Riaza, A. & Bernaola, F.-J. 2014a, 'Comparative study of brine management technologies for desalination plants', *Desalination*, vol. 336, pp. 32-49.

Morillo, J., Usero, J., Rosado, D., El Bakouri, H., Riaza, A. & Bernaola, F.-J. 2014b, 'Comparative study of brine management technologies for desalination plants', *Desalination*, vol. 336, no. Supplement C, pp. 32-49.

Mostafa Nowee, S., Abbas, A. & Romagnoli, J.A. 2008, 'Antisolvent crystallization: Model identification, experimental validation and dynamic simulation', *Chemical Engineering Science*, vol. 63, no. 22, pp. 5457-67.

Mullin, J.W. 2001, *Crystallization*, Fourth edn, Butterworth-Heinemann, Oxford.

Naeimi, S. & Faghihian, H. 2017, 'Performance of novel adsorbent prepared by magnetic metal-organic framework (MOF) modified by potassium nickel hexacyanoferrate for removal of Cs+ from aqueous solution', *Separation and Purification Technology*, vol. 175, pp. 255-65.

Naidu, G., Jeong, S., Choi, Y., Song, M.H., Oyunchuluun, U. & Vigneswaran, S. 2018, 'Valuable rubidium extraction from potassium reduced seawater brine', *Journal of Cleaner Production*, vol. 174, pp. 1079-88.

Naidu, G., Jeong, S., Choi, Y. & Vigneswaran, S. 2017, 'Membrane distillation for wastewater reverse osmosis concentrate treatment with water reuse potential', *Journal of Membrane Science*, vol. 524, pp. 565-75.

Naidu, G., Jeong, S., Johir, M.A.H., Fane, A.G., Kandasamy, J. & Vigneswaran, S. 2017, 'Rubidium extraction from seawater brine by an integrated membrane distillation-selective sorption system', *Water Research*, vol. 123, pp. 321-31.

Naidu, G., Jeong, S., Kim, S.-J., Kim, I.S. & Vigneswaran, S. 2014, 'Organic fouling behavior in direct contact membrane distillation', *Desalination*, vol. 347, pp. 230-9.

Naidu, G., Jeong, S. & Vigneswaran, S. 2014, 'Influence of feed/permeate velocity on scaling development in a direct contact membrane distillation', *Separation and Purification Technology*, vol. 125, no. Supplement C, pp. 291-300.

Naidu, G., Jeong, S. & Vigneswaran, S. 2015, 'Interaction of humic substances on fouling in membrane distillation for seawater desalination', *Chemical Engineering Journal*, vol. 262, pp. 946-57.

Naidu, G., Jeong, S., Vigneswaran, S., Hwang, T.-M., Choi, Y.-J. & Kim, S.-H. 2016, 'A review on fouling of membrane distillation', *Desalination and Water Treatment*, vol. 57, no. 22, pp. 10052-76.

Naidu, G., Loganathan, P., Jeong, S., Johir, M.A.H., To, V.H.P., Kandasamy, J. & Vigneswaran, S. 2016, 'Rubidium extraction using an organic polymer encapsulated potassium copper hexacyanoferrate sorbent', *Chemical Engineering Journal*, vol. 306, pp. 31-42.

Naidu, G., Shim, W.G., Jeong, S., Choi, Y., Ghaffour, N. & Vigneswaran, S. 2017, 'Transport phenomena and fouling in vacuum enhanced direct contact membrane distillation: Experimental and modelling', *Separation and Purification Technology*, vol. 172, pp. 285-95.

Narducci, O. & Jones, A.G. 2012, 'Seeding in Situ the Cooling Crystallization of Adipic Acid using Ultrasound', *Crystal Growth & Design*, vol. 12, no. 4, pp. 1727-35.

Ndinisa, N.V., Fane, A.G. & Wiley, D.E. 2006, 'Fouling Control in a Submerged Flat Sheet Membrane System: Part I – Bubbling and Hydrodynamic Effects', *Separation Science and Technology*, vol. 41, no. 7, pp. 1383-409.

Nguyen, Q.-M. & Lee, S. 2015, 'Fouling analysis and control in a DCMD process for SWRO brine', *Desalination*, vol. 367, pp. 21-7.

Oh, H.-J., Choung, Y.-K., Lee, S., Choi, J.-S., Hwang, T.-M. & Kim, J.H. 2009, 'Scale formation in reverse osmosis desalination: model development', *Desalination*, vol. 238, no. 1, pp. 333-46.

Ohlinger, K.N., Young, T.M. & Schroeder, E.D. 2000, 'Postdigestion Struvite Precipitation Using a Fluidized Bed Reactor', *Journal of Environmental Engineering*, vol. 126, no. 4, pp. 361-8.

Partridge, E.P. & White, A.H. 1929, 'THE SOLUBILITY OF CALCIUM SULFATE FROM 0 TO 200°', *Journal of the American Chemical Society*, vol. 51, no. 2, pp. 360-70.

Pérez-González, A., Urtiaga, A.M., Ibáñez, R. & Ortiz, I. 2012, 'State of the art and review on the treatment technologies of water reverse osmosis concentrates', *Water Research*, vol. 46, no. 2, pp. 267-83.

Phattaranawik, J., Fane, A.G., Pasquier, A.C.S. & Bing, W. 2008, 'A novel membrane bioreactor based on membrane distillation', *Desalination*, vol. 223, no. 1, pp. 386-95.

Phattaranawik, J., Fane, A.G., Pasquier, A.C.S., Bing, W. & Wong, F.S. 2009, 'Experimental Study and Design of a Submerged Membrane Distillation Bioreactor', *Chemical Engineering & Technology*, vol. 32, no. 1, pp. 38-44.

Phuong, N.T.N. & Kwang-Joo, K. 2011, 'Transformation of hemipentahydrate to monohydrate of risedronate monosodium by seed crystallization in solution', *AIChE Journal*, vol. 57, no. 12, pp. 3385-94.

Poling, B.E., Prausnitz, J.M. & O'connell, J.P. 2001, *The properties of gases and liquids*, Fifth edn, The McGraw-Hill, New York.

Profio, G.D., Caridi, A., Caliandro, R., Guagliardi, A., Curcio, E. & Drioli, E. 2010, 'Fine Dosage of Antisolvent in the Crystallization of l-Histidine: Effect on Polymorphism', *Crystal Growth & Design*, vol. 10, no. 1, pp. 449-55.

Puspitasari, V., Granville, A., Le-Clech, P. & Chen, V. 2010, 'Cleaning and ageing effect of sodium hypochlorite on polyvinylidene fluoride (PVDF) membrane', *Separation and Purification Technology*, vol. 72, no. 3, pp. 301-8.

Quist-Jensen, C.A., Ali, A., Mondal, S., Macedonio, F. & Drioli, E. 2016, 'A study of membrane distillation and crystallization for lithium recovery from high-concentrated aqueous solutions', *Journal of Membrane Science*, vol. 505, pp. 167-73.

Quist-Jensen, C.A., Macedonio, F. & Drioli, E. 2016, 'Membrane crystallization for salts recovery from brine—an experimental and theoretical analysis', *Desalination and Water Treatment*, vol. 57, no. 16, pp. 7593-603.

Quist-Jensen, C.A., Macedonio, F., Horbez, D. & Drioli, E. 2017, 'Reclamation of sodium sulfate from industrial wastewater by using membrane distillation and membrane crystallization', *Desalination*, vol. 401, pp. 112-9.

Quist-Jensen, C.A., Sørensen, J.M., Svenstrup, A., Scarpa, L., Carlsen, T.S., Jensen, H.C., Wybrandt, L. & Christensen, M.L. 2017, 'Membrane crystallization for phosphorus recovery and ammonia stripping from reject water from sludge dewatering process', *Desalination*, vol. 440, pp. 150-60.

Rahman, M.M., Liu, Y., Kwag, J.-H. & Ra, C. 2011, 'Recovery of struvite from animal wastewater and its nutrient leaching loss in soil', *Journal of Hazardous Materials*, vol. 186, no. 2, pp. 2026-30.

Rahman, M.M., Salleh, M.A.M., Rashid, U., Ahsan, A., Hossain, M.M. & Ra, C.S. 2014, 'Production of slow release crystal fertilizer from wastewaters through struvite crystallization – A review', *Arabian Journal of Chemistry*, vol. 7, no. 1, pp. 139-55.

Rard, J.A. & Miller, D.G. 1979, 'The mutual diffusion coefficients of Na2SO4−H2O and MgSO4−H2O at 25°C from Rayleigh interferometry', *Journal of Solution Chemistry*, vol. 8, no. 10, pp. 755-66.

Richard, L., G., V.N., Herman, K., Peter, J. & Johan, G. 2011, 'Application of ultrasound for start-up of evaporative batch crystallization of ammonium sulfate in a 75-L crystallizer', *AIChE Journal*, vol. 57, no. 12, pp. 3367-77.

Roberts, D.A., Johnston, E.L. & Knott, N.A. 2010, 'Impacts of desalination plant discharges on the marine environment: A critical review of published studies', *Water Research*, vol. 44, no. 18, pp. 5117-28.

Rubio, J. & Tessele, F. 1997, 'Removal of heavy metal ions by adsorptive particulate flotation', *Minerals Engineering*, vol. 10, no. 7, pp. 671-9.

Ruiz Salmón, I., Janssens, R. & Luis, P. 2017, 'Mass and heat transfer study in osmotic membrane distillation-crystallization for CO2 valorization as sodium carbonate', *Separation and Purification Technology*, vol. 176, no. Supplement C, pp. 173-83.

S., T.N. 1989, 'Micromixing limits in an MSMPR crystallizer', *Chemical Engineering & Technology*, vol. 12, no. 1, pp. 1-11.

Saffarionpour, S., Tam, S.-Y.S., Van der Wielen, L.A.M., Brouwer, E. & Ottens, M. 2019, 'Influence of ethanol and temperature on adsorption of flavor-active esters on hydrophobic resins', *Separation and Purification Technology*, vol. 210, pp. 219-30.

Saleem, M., Chakrabarti, M.H., Hasan, D.u.B., Islam, M.S., Yussof, R., Hajimolana, S.A., Hussain, M.A., Khan, G.M.A. & Ali, B.S. 2012, 'On site electrochemical production of sodium hypochlorite disinfectant for a power plant utilizing seawater', *International Journal of Electrochemical Science*, vol. 7, no. 5, pp. 3929-38.

Sanmartino, J.A., Khayet, M., García-Payo, M.C., El Bakouri, H. & Riaza, A. 2016, 'Desalination and concentration of saline aqueous solutions up to supersaturation by air gap membrane distillation and crystallization fouling', *Desalination*, vol. 393, pp. 39-51.

Saripalli, K.P., Sharma, M.M. & Bryant, S.L. 2000, 'Modeling injection well performance during deep-well injection of liquid wastes', *Journal of Hydrology*, vol. 227, no. 1, pp. 41-55.

Schofield, R.W., Fane, A.G. & Fell, C.J.D. 1987, 'Heat and mass transfer in membrane distillation', *Journal of Membrane Science*, vol. 33, no. 3, pp. 299-313.

Schofield, R.W., Fane, A.G., Fell, C.J.D. & Macoun, R. 1990, 'Factors affecting flux in membrane distillation', *Desalination*, vol. 77, pp. 279-94.

Shim, W.G., He, K., Gray, S. & Moon, I.S. 2015, 'Solar energy assisted direct contact membrane distillation (DCMD) process for seawater desalination', *Separation and Purification Technology*, vol. 143, pp. 94-104.

Shimizu, K., Takahashi, K., Suzuki, E. & Nomura, T. 1999, 'Effect of baffle geometries on crystal size distribution of aluminum potassium sulfate in a seeded batch crystallizer', *Journal of Crystal Growth*, vol. 197, no. 4, pp. 921-6.

Shin, Y. & Sohn, J. 2016, 'Mechanisms for scale formation in simultaneous membrane distillation crystallization: Effect of flow rate', *Journal of Industrial and Engineering Chemistry*, vol. 35, pp. 318-24.

Sivaraj, R., Namasivayam, C. & Kadirvelu, K. 2001, 'Orange peel as an adsorbent in the removal of Acid violet 17 (acid dye) from aqueous solutions', *Waste Management*, vol. 21, no. 1, pp. 105-10.

Sluys, J.T.M., Verdoes, D. & Hanemaaijer, J.H. 1996, 'Water treatment in a Membrane-Assisted Crystallizer (MAC)', *Desalination*, vol. 104, no. 1, pp. 135-9.

Soare, A., Dijkink, R., Pascual, M.R., Sun, C., Cains, P.W., Lohse, D., Stankiewicz, A.I. & Kramer, H.J.M. 2011, 'Crystal Nucleation by Laser-Induced Cavitation', *Crystal Growth & Design*, vol. 11, no. 6, pp. 2311-6.

Sodaye, H., Nisan, S., Poletiko, C., Prabhakar, S. & Tewari, P.K. 2009, 'Extraction of uranium from the concentrated brine rejected by integrated nuclear desalination plants', *Desalination*, vol. 235, no. 1, pp. 9-32.

Squire, D., Murrer, J., Holden, P. & Fitzpatrick, C. 1997, 'Disposal of reverse osmosis membrane concentrate', *Desalination*, vol. 108, no. 1, pp. 143-7.

Srisurichan, S., Jiraratananon, R. & Fane, A.G. 2006, 'Mass transfer mechanisms and transport resistances in direct contact membrane distillation process', *Journal of Membrane Science*, vol. 277, no. 1, pp. 186-94.

Stephen, M., Douglas, D.A., Jon, M.D., Trevor, D., Brigid, R.H., Fiona, C.M. & Nicholas, J.R. 1993, 'Crystallization at Inorganic-organic Interfaces: Biominerals and Biomimetic Synthesis', *Science*, vol. 261, no. 5126, pp. 1286-92.

Summers, E.K., Arafat, H.A. & Lienhard, J.H. 2012, 'Energy efficiency comparison of single-stage membrane distillation (MD) desalination cycles in different configurations', *Desalination*, vol. 290, pp. 54-66.

Surawanvijit, S., Rahardianto, A. & Cohen, Y. 2016, 'An Integrated approach for characterization of polyamide reverse osmosis membrane degradation due to exposure to free chlorine', *Journal of Membrane Science*, vol. 510, pp. 164-73.

Suzuki, K., Tanaka, Y., Osada, T. & Waki, M. 2002, 'Removal of phosphate, magnesium and calcium from swine wastewater through crystallization enhanced by aeration', *Water Research*, vol. 36, no. 12, pp. 2991-8.

Tait, S., Clarke, W.P., Keller, J. & Batstone, D.J. 2009, 'Removal of sulfate from high-strength wastewater by crystallisation', *Water Research*, vol. 43, no. 3, pp. 762-72.

Tijing, L.D., Woo, Y.C., Choi, J.-S., Lee, S., Kim, S.-H. & Shon, H.K. 2015, 'Fouling and its control in membrane distillation—A review', *Journal of Membrane Science*, vol. 475, pp. 215-44.

Timachova, K., Watanabe, H. & Balsara, N.P. 2015, 'Effect of Molecular Weight and Salt Concentration on Ion Transport and the Transference Number in Polymer Electrolytes', *Macromolecules*, vol. 48, no. 21, pp. 7882-8.

Tomaszewska, M. & Białończyk, L. 2013, 'Production of ethanol from lactose in a bioreactor integrated with membrane distillation', *Desalination*, vol. 323, pp. 114-9.

Tong, T. & Elimelech, M. 2016, 'The Global Rise of Zero Liquid Discharge for Wastewater Management: Drivers, Technologies, and Future Directions', *Environmental Science & Technology*, vol. 50, no. 13, pp. 6846-55.

Tünay, O., Kabdasli, I., Orhon, D. & Kolçak, S. 1997, 'Ammonia removal by magnesium ammonium phosphate precipitation in industrial wastewaters', *Water Science and Technology*, vol. 36, no. 2-3, pp. 225-8.

Tun, C.M., Fane, A.G., Matheickal, J.T. & Sheikholeslami, R. 2005, 'Membrane distillation crystallization of concentrated salts—flux and crystal formation', *Journal of Membrane Science*, vol. 257, no. 1–2, pp. 144-55.

Tung, H.-H., Paul, E.L., Midler, M. & McCauley, J.A. 2009, *Crystallization of organic compounds: an industrial perspective*, John Wiley & Sons.

U.S. Department of the Interior: U.S. Geological Survey. Mineral Commodity Summaries, <http://minerals.usgs.gov/minerals/pubs/mcs/index.html (Accessed: 31 January 2019)>.

Ulrich, J. & Frohberg, P. 2013, 'Problems, potentials and future of industrial crystallization', *Frontiers of Chemical Science and Engineering*, vol. 7, no. 1, pp. 1-8.

Ulrich, J. & Jones, M.J. 2004, 'Industrial Crystallization: Developments in Research and Technology', *Chemical Engineering Research and Design*, vol. 82, no. 12, pp. 1567-70.

Valencia, D.P. & González, F.J. 2011, 'Understanding the linear correlation between diffusion coefficient and molecular weight. A model to estimate diffusion coefficients in acetonitrile solutions', *Electrochemistry Communications*, vol. 13, no. 2, pp. 129-32.

Veeken, A.H.M., Akoto, L., Hulshoff Pol, L.W. & Weijma, J. 2003, 'Control of the sulfide (S2−) concentration for optimal zinc removal by sulfide precipitation in a continuously stirred tank reactor', *Water Research*, vol. 37, no. 15, pp. 3709-17.

Voutchkov, N. 2011, 'Overview of seawater concentrate disposal alternatives', *Desalination*, vol. 273, no. 1, pp. 205-19.

Waly, T., Kennedy, M.D., Witkamp, G.-J., Amy, G. & Schippers, J.C. 2012, 'The role of inorganic ions in the calcium carbonate scaling of seawater reverse osmosis systems', *Desalination*, vol. 284, pp. 279-87.

Wang, P., Wang, Z., Wu, Z., Zhou, Q. & Yang, D. 2010, 'Effect of hypochlorite cleaning on the physiochemical characteristics of polyvinylidene fluoride membranes', *Chemical Engineering Journal*, vol. 162, no. 3, pp. 1050-6.

Wang, W., Han, H., Yuan, M., Li, H., Fang, F. & Wang, K. 2011, 'Treatment of coal gasification wastewater by a two-continuous UASB system with step-feed for COD and phenols removal', *Bioresource Technology*, vol. 102, no. 9, pp. 5454-60.

Weingaertner, D.A., Lynn, S. & Hanson, D.N. 1991, 'Extractive crystallization of salts from concentrated aqueous solution', *Industrial & Engineering Chemistry Research*, vol. 30, no. 3, pp. 490-501.

Wen, X., Li, F. & Zhao, X. 2016, 'Removal of nuclides and boron from highly saline radioactive wastewater by direct contact membrane distillation', *Desalination*, vol. 394, pp. 101-7.

Wendt, K., Petersen, S. & Ulrich, J. 2015, 'Influence of seeding on concentration distribution within pastilles drop formed out of binary melts', *Chemical Engineering Science*, vol. 133, pp. 70-4.

Wu, Q. & Bishop, P.L. 2004, 'Enhancing struvite crystallization from anaerobic supernatant', *Journal of Environmental Engineering and Science*, vol. 3, no. 1, pp. 21-9.

Wu, Y., Kong, Y., Liu, J., Zhang, J. & Xu, J. 1991, 'An experimental study on membrane distillation-crystallization for treating waste water in taurine production', *Desalination*, vol. 80, no. 2, pp. 235-42.

Yamamoto, O. 2001, 'Influence of particle size on the antibacterial activity of zinc oxide', *International Journal of Inorganic Materials*, vol. 3, no. 7, pp. 643-6.

You, W.-T., Xu, Z.-L., Dong, Z.-Q. & Zhang, M. 2015, 'Vacuum membrane distillation–crystallization process of high ammonium salt solutions', *Desalination and Water Treatment*, vol. 55, no. 2, pp. 368-80.

Younos, T. 2005, 'Environmental Issues of Desalination', *Journal of Contemporary Water Research & Education*, vol. 132, no. 1, pp. 11-8.

Yu, R., Geng, J., Ren, H., Wang, Y. & Xu, K. 2013, 'Struvite pyrolysate recycling combined with dry pyrolysis for ammonium removal from wastewater', *Bioresource Technology*, vol. 132, pp. 154-9.

Zhang, T., Ding, L., Ren, H. & Xiong, X. 2009, 'Ammonium nitrogen removal from coking wastewater by chemical precipitation recycle technology', *Water Research*, vol. 43, no. 20, pp. 5209-15.

Zhang, T.H. & Liu, X.Y. 2009, 'Nucleation: What Happens at the Initial Stage?', *Angewandte Chemie International Edition*, vol. 48, no. 7, pp. 1308-12.

Zijlema, T.G., Geertman, R.M., Witkamp, G.-J., van Rosmalen, G.M. & de Graauw, J. 2000, 'Antisolvent Crystallization as an Alternative to Evaporative Crystallization for the Production of Sodium Chloride', *Industrial & Engineering Chemistry Research*, vol. 39, no. 5, pp. 1330-7.

Zuo, G., Guan, G. & Wang, R. 2014, 'Numerical modeling and optimization of vacuum membrane distillation module for low-cost water production', *Desalination*, vol. 339, pp. 1-9.

Zuo, J., Chung, T.-S., O'Brien, G.S. & Kosar, W. 2017, 'Hydrophobic/hydrophilic PVDF/Ultem® dual-layer hollow fiber membranes with enhanced mechanical properties for vacuum membrane distillation', *Journal of Membrane Science*, vol. 523, pp. 103-10.

Zuoliang, S., Qiuxiang, Y. & Jianxin, C. 2013, 'Industrial Crystallization: Trends and Challenges', *Chemical Engineering & Technology*, vol. 36, no. 8, pp. 1286-.